Neutrophil Extracellular Traps (NETs) in Thermal and Traumatic injuries

Ali Asiri

A thesis submitted to the University of Birmingham for the degree of DOCTOR OF PHILOSOPHY

Supervisors
Dr Paul Harrison
Dr Alexander Brill

The Department of Inflammation and Ageing,
College of Medicine and Health,
University of Birmingham
October 2024

Abstract

Severe thermal injuries and trauma result in considerable immunological and haemostatic disturbances, increasing the risk of sepsis, disseminated intravascular coagulation (DIC) and multiple organ failure (MOF). The formation of neutrophil extracellular traps (NETs), an essential innate response to infection and tissue damage, leads to elevated circulating levels of NET-derived chromatin and cell-free DNA (cfDNA), which act in defence but also as a trigger for immunothrombosis. Our research indicates that post-burn and trauma cfDNA primarily consists of nucleosome fragments (~150 bp), with higher molecular weight nucleosome oligomers (i.e., ~ 300 and 450 bp) in ultra-early samples (< 1 hour) obtained from trauma patients. However, absence or low nucleosome levels in the majority of admission samples in burns were confirmed along with the presence of increased levels of large undegraded NET-derived chromatin captured using microfluidic chips. CfDNA levels also correlate with neutrophil activation and the extended neutrophil parameter Y (NEUT-Y). The breakdown of NETs into circulating cfDNA in the form of nucleosomes, increased NEUT-Y levels with production of Immature Granulocytes (IG) are potential early biomarkers for predicting sepsis in burns.

Moreover, high levels of IL-8 are released and are major mediators of NET formation in burns. Haematological studies demonstrated classical post-injury nadir and recovery patterns in platelet counts following thermal injury. Severe burns also led to high significant impairment of high shear platelet function in the early days after the injury (e.g. day 3) and were associated with reduced *ex vivo* thrombus formation. Additionally, post-injury high levels of VWF and low levels of ADAMTS13 although not correlated with platelet function correlated

with NET biomarkers, NEUT-Y and cfDNA, providing a further important contribution to NETosis.

This thesis illustrates the importance of the mechanisms and dynamics of NET production and breakdown as biomarkers, therapeutic targets and in the pathogenesis of post-injury sepsis, DIC, and MOF.

COVID-19 MITIGATION STATEMENT

The COVID-19 pandemic significantly impacted the research originally planned for this thesis. I began my PhD program on March 2nd, 2020. The first COVID-19 lockdown lasted from March 17th, 2020, until the end of June 2020. During this time, I was evacuated to Saudi Arabia at the beginning of June 2020. I returned to the UK at the end of October 2020 and underwent self-isolation for two weeks. Shortly after, a second lockdown began in November 2020, lasting for a month, followed by a third lockdown from January 2021 until the end of March 2021. The first year of my research was therefore extremely affected by the COVID-19 crisis, with my research delayed due to limited access to the laboratory. This thesis focuses on neutrophil extracellular traps in burns and trauma. However, no burns and trauma patients were recruited in our studies during the three lockdown periods. Additionally, patient recruitment during the COVID-19 crisis was limited based on the results of COVID-19 tests. Furthermore, there were several implications of COVID-19 on access to training, limited working hours, a shortage of healthy donors, and self-isolation periods, all of which contributed to delayed research required for this thesis between March 2020 and May 2021.

Acknowledgements

First and foremost, I would like to express my deepest gratitude to my supervisor, Dr Paul Harrison, whose guidance and support have been invaluable throughout my PhD journey. His encouragement, advice, and unwavering belief in me, especially during the moments when I felt lost in my research, have been crucial. I am deeply grateful for his care and friendship, which have been constant sources of strength. I would also like to extend my sincere thanks to Dr Alexander Brill, Professor Naiem Moiemen, and Professor Janet Lord for their insightful advice during my research.

A special thank you goes to Dr Jon Hazeldine, whose help in the lab has been immense. He has not only been a tremendous colleague but also a close friend, making the time in the lab enjoyable with his humour, including his signature "sterile tips." His suggestions based on my results were always thoughtful. Some I embraced, while others I managed to dodge! Dr Jon’s support has been invaluable in shaping my work.

I would also like to thank Dr Joshua Price and Dr Kirsty McGee for their help at the beginning of my PhD, particularly in training me and allowing me to feel settled in the lab environment. Dr Joshua's joyful spirit and music always created a positive and vibrant atmosphere in the lab, making it a great place to work. My gratitude extends to both Dr Jon Bishop and Dr Joshua Price for their invaluable assistance with data analysis. A sincere thank you to the great Dr Yung-Yi for her kindness and help throughout my research. I will never forget my bench neighbours, Dr Amanda Veiga Sardeli and Feras Almujalli, for their companionship and sharing tools. A special mention goes to Amanda for the fun time playing footvolley. I wish I had continued playing, as it gave a much-needed balance between work and relaxation.

I would like to extend my appreciation to the Royal Embassy of Saudi Arabia Cultural Bureau and King Fahad Security College for their generous funding and support of my PhD studies.

Finally, I wish to express my profound gratitude to my wife, Tahani Aldahman, and my daughters, Mayar and Mela, for their unwavering love, patience, and kindness during all the challenging times. To my father, my dear mothers, and my brothers and sisters, your support has been my foundation, and I am incredibly proud of each of you. Without your love and encouragement, I would not have reached this stage.

Thank you

Disclosures

All work presented in this thesis was performed as part of The Scientific Investigation of the Biological Pathways Following Thermal Injury- 2 (SIFTI-2) and Golden Hour (GH) studies and is therefore part of a collaboration between a number of investigators. Credit has been attributed to those responsible for data creation cooperation when applicable. All data presented in this thesis was evaluated and compiled by Ali Asiri.

Publications arising from this thesis

1. **Asiri A.**, Hazeldine J., Moiemen N. and Harrison P., *IL-8 Induces Neutrophil Extracellular Trap Formation in Severe Thermal Injury.* Int J Mol Sci, 2024. **25**(13).
2. **Asiri A.**, Price J., Hazeldine J., Mcgee K., Sardeli A. V., Chen Y. Y., Sullivan J., Moiemen N. S, and Harrison P., *Measurement of Platelet Thrombus formation in patients following Severe Thermal Injury.* Platelets, 2024, In Press
3. Tullie S., Nicholson T., Bishop J. R. B., Mcgee K. C., **Asiri A.**, Sullivan J., Chen Y. Y., Sardeli A. V., Belli A., Harrison P., Moiemen N. S., Lord J. M. and Hazeldine J., *Severe thermal and major traumatic injury results in elevated plasma concentrations of total heme that are associated with poor clinical outcomes and systemic immune suppression.* Front Immunol, 2024. **15**: p. 1416820.

Publications in Preparation

1. Tullie S., **Asiri A**., Acharjee A., Moiemen N. S., Lord J. M., Harrison P., and Hazeldine J., *Day 1 cell-free DNA levels as an objective prognostic marker of mortality in major burns patients.* Manuscript in preparation.
2. **Asiri A.**, Hazeldine J., Bishop J. R. B., Moiemen N. S, Sakuma M., Irimia D. and Harrison P., *Qualitative and Quantitative Analysis of Circulating NET Derived Nucleic Acid after Severe Thermal Injury.* Manuscript in preparation
3. **Asiri A.**, Almujalli F., Hazeldine J., Bishop J. R. B., Mcgee K., Amirize E., Abdulsalam A., Kankam H., Tullie S., Price J., Sardeli A. V., Chen Y. Y., Sullivan J., Sardeli A. V., Yung-Yi Chen, Jack Sullivan, Lord J. M., Moiemen N. S, and Harrison P., *Novel Haematological and Neutrophil Parameters in Severe Thermal Injur*y. Manuscript in Preparation

Conferences

1. European Burn Association Annual Meeting, Turin, September 2022

a. Asiri A., Hazeldine J., Moiemen N. and Harrison P. Characterisation of Neutrophil-derived Cell Free DNA (cf-DNA) In Burns and Trauma (Poster).

2. British Burns Association, Dublin, June 2023

a. Ali Asiri, Joshua Price, Jon Hazeldine, Amanda Sardeli, Yung-Yi Chen, Kirsty McGee, Jack Sullivan, Jon RB Bishop, Janet M. Lord, Naiem Moiemen, Paul Harrison. Measurement of Platelet Thrombus formation in Severe Thermal Injury (oral). Won second best talk prize at meeting.

b. Ali Asiri, Jon Hazeldine, Jon RB Bishop, Kirsty McGee, Ezekwe Amirize, Abdulrazak Abdulsalam, Hadyn Kankam, Joshua Price, Amanda Sardeli, Yung-Yi Chen, Jack Sullivan, Janet M. Lord, Naiem S. Moiemen, Paul Harrison. Novel Haematological and Neutrophil Parameters in Severe Thermal Injury (oral).

c. Asiri A., Hazeldine J., Moiemen N. and Harrison P. Characterisation of Neutrophil-derived Cell Free DNA (cf-DNA) In Burns (Poster).

3. British Burns Association (BBA)/The International Society for Burn Injuries (ISBI), Birmingham, August 2024

a. Asiri A., Hazeldine J., Moiemen N. and Harrison P., IL-8 Induces Neutrophil Extracellular Trap Formation in Severe Thermal Injury (oral).

Table of contents

List of Tables

List of Figures

Abbreviations

ABA	American Burn Association
ABSI	A Body Shape Index
ACCP/SCCM	The American College of Chest Physicians/Society of Critical Care Medicine
ADM	Adrenomedullin
aPTT	Activated partial thromboplastin time
ARDS	Acute respiratory distress syndrome
ATP	Adenosine triphosphate
AUC	Area Under the Curve
AUROC	Under the receiver operating characteristic curve
Baux	A burn mortality prediction system
Bcl-XL	Bcl-2 protein members anti-apoptotic
BM	Bone marrow
BSA	Bovine serum albumin
CARS	Compensatory anti-inflammatory response syndrome
CD35	CR1 receptor
CD88	C5aR
CIs	Confidence intervals
CitH3	Citrullinated histone 3
CRP	C-reactive protein
CXCR2	CXC chemokine receptor 2
DAMPs	Damage-associated molecular patterns
DAPI	4′,6-Diamidino-2-phenylindole dihydrochloride

DIC	Disseminated intravascular coagulation
DNase	Deoxyribonuclease
DNase1L3	DNase1-like 3
DVT	Deep vein thrombosis
ECGM	Endothelial cell growth medium MV
EDTA	Ethylenediaminetetraacetic acid
ELISA	Enzyme linked immunosorbent assay
FBC	Full blood count
FMLP	Formyl-methionyl-leucyl-phenylalanine
FT	Full-thickness
GH	Golden Hour
GM-CSF	Granulocyte-macrophage colony-stimulating factor
GTP	Guanosine triphosphate
H1	Histone 1
H2A	Histone 2A
H2B	Histone 2B
H3	Histone 3
H4	Histone 4
HBSS	Hanks' Balanced Salt Solution
HMGB1	High-mobility group protein 1
HNA-3	Human neutrophil antigen-3
IBID	Injury Database
ICU	Intensive care unit
IFN	Interferon-gamma

IGs	Immature granulocytes
IL	Interleukin
IL-1	Interleukin-1
IL-10	Interleukin-10
IL-13	Interleukin-13
IL-22	Interleukin-22
IL-4	Interleukin-4
IL-6	Interleukin-6
IL-8	Interleukin-8
INR	International normalised ratio
IPF	Immature platelet fraction
ISS	Injury severity score
LBP	Lipopolysaccharide-binding protein
LDGs	Low density granulocytes
LDNs	Low density neutrophils
LFA-1	Lymphocyte function-associated antigen-1
LL-37	Antimicrobial peptide LL-37
LPS	Lipopolysaccharide
LTA	Lipoteichoic acid
MAC-1	Macrophage-1 antigen
MIF	Migration inhibitory factor
MNase	Micrococcal nuclease
MODS	Multiple organ dysfunction syndrome
MOF	Multiple organ failure

MPO	Myeloperoxidase
MPV	Mean platelet volume
MR-proADM	Mid-regional proadrenomedullin
NADPH	Nicotinamide adenine dinucleotide phosphate
NE	Neutrophil elastase
NETs	Neutrophil extracellular traps
NEUTs	Neutrophils
NEUT-GI	Neutrophil granularity intensity
NEUT-RI	Neutrophil reactive intensity
NEUT-X	Neutrophil X parameter
NEUT-Y	Neutrophil Y parameter
NEUT-Z	Neutrophil Z parameter
NIHR	National Institute for Health Research
NF-κB	Nuclear factor kappa B
NOX-2	NADPH oxidase 2
NuQ. H3.1	Nucleosome histone 3.1
OR	Odds Ratio
OST	Occlusion Start Time
OT	Occlusion Time
PAD4	Peptidyl arginine deiminase 4
PBMCs	Peripheral blood mononuclear cells
PBS	Phosphate buffered saline
PCT	Procalcitonin
PI3K	Phosphatidylinositol-3-kinase

PFP	Platelet-free plasma
PICS	Persistent inflammation, immunosuppression, and catabolism syndrome
PLT-F	Platelet fluorescence
PLT-I	Platelet impedance count
PLT-O	Platelet optical count
PMA	Phorbol 12-Myristate 13-Acetate
PSGL-1	P-selectin glycoprotein ligand-1
RA	Rheumatoid arthritis
rBaux	Revised Baux indication
RBC	Red blood cells
ROS	Reactive oxygen species
ROTEM	Rotational thromboelastometry
SFL	Fluorescence signals
SIFTI-1	Scientific Investigation of the Biological Pathways Following Thermal Injury-1
SIFTI-2	Scientific Investigation of the Biological Pathways Following Thermal Injury-2
SIRS	Systemic inflammatory response syndrome
SLC44A2	Solute Carrier Family 44 Member 2
SLE	Systemic lupus erythematosus
SNP	Single nucleotide polymorphism
SOFA	Sequential organ failure assessment
T-TAS	Total Thrombus-formation Analyser System

t-PA	Tissue-type plasminogen activator
TBSA	Total body surface area
TEG	Thromboelastography
TF	Tissue factor
TGF-β	Transforming growth factor-β
TIC	Trauma-induced coagulopathy
TLR	Toll-like receptors
TMB	3,3',5,5'-Tetramethylbenzidine
TNF	Tumour necrosis factor
TPO	Thrombopoietin
VDBP	Vitamin D-binding protein
VT	Venous thrombosis
VTE	Venous thromboembolism
VWF	Von Willebrand factor
WB	Whole blood
WBC	White Blood cells

Chapter 1:

Introduction

1 Introduction

1.1 Traumatic and thermal injury

Traumatic and Thermal injuries are major health issues that are associated with significant morbidity and mortality [1, 2]. Trauma is a tissue injury that occurs to the body and is caused by accidents or violence [3]. According to a World Health Organization update in 2022, there are approximately 4.4 million deaths every year worldwide caused by traumatic injuries. Out of these, one-third are a result of road traffic accidents, one-sixth are due to suicide, one-ninth are caused by homicide, and about one-sixtieth is due to war and conflict [4]. In multi-trauma centers in England, the mortality rate for traumatic patients younger than 16 years was reported to be approximately 2.5%. This rate was higher for adult patients aged 16 to 24 years, with a mortality rate of around 4.9% [5]. The majority of deaths caused by trauma have also been reported to occur before hospital admission [6], especially if associated with severe blood loss [7]. Traumatic brain injury is especially life-threatening as only 10% of patients with penetrating brain injury survive to be treated in hospital. Even then mortality within hospital remains high and there is also significant morbidity caused by ongoing neurological problems [8].

Thermal injuries can be defined by exposure of skin to a high temperature that causes burns which include exposure to heat, bruising, chemicals, or gas inhalation [9]. Interestingly, the actual mortality rate among patients with thermal injuries is also high [10]. According to National Centre Data for injury prevention and control in the United States, in 2006 it was reported that every year 1.2 million burn injuries occur as a result of fires, of which nearly 100,000 burn patients are severe, thus requiring hospital care and resulting in 5000 deaths [11]. Burn patients are also more prone to infection due to significant skin barrier loss [12].

There are three main types of systemic responses following severe trauma and burns; 1) A cardiovascular response that occurs immediately after injury, 2) Immunological and Inflammatory responses which occur immediately but can persist for days after injury, and 3) Metabolic responses, which are physiological changes that occur in response to injury to meet increased energy demands. These responses include hypermetabolism, which raises resting energy expenditure, and hypercatabolism, which significantly breaks down muscle proteins. While these processes are crucial for recovery and rehabilitation, they can persist for months or even years after the injury [13, 14]. Significant pathological effects include impaired immune and uncontrolled metabolic responses that can contribute to poor prognosis and outcomes [15].

Despite advancements in burn care that improve patient outcomes, mortality from sepsis and its prevalence remain a significant issue [16, 17]. The prevalence of sepsis was reported to differ, with trauma patients exhibiting fewer occurrences (2.4%–16.9%) compared to burn patients (8%–42.5%) [17]. Sepsis is defined as a “life threatening organ dysfunction caused by a dysregulated host response to infection” [18]. Sepsis causes a complex reaction of host pro- and anti-inflammatory mechanisms that promote both morbidity and mortality by weakening the immune system [19]. The response of organs to sepsis can cause multiple organ dysfunction syndrome (MODS), which is often the major cause of death in those patients who survive resuscitation [18].

Therefore, investigations into mechanisms of the morbidity and mortality of trauma and thermal injuries are highly relevant to not only improve the health care of patients but to decrease severe outcomes.

1.2 Pathophysiology of trauma

Severe traumatic injuries result in physiological and immunological changes that often predispose to infection, coagulopathy, organ dysfunction and eventual multiple organ failure (MOF) [20, 21]. The initial phase occurs hours post-trauma, marked by haemorrhage from vascular injury, potentially causing hypovolaemic shock. The later phase presents trauma-induced coagulopathy (TIC), characterised by extensive microvascular bleeding due to endothelial damage and dysregulated coagulation [22]. The complex pathophysiology of trauma involves haemorrhage, shock, and coagulopathy. Significant blood loss triggers systemic reactions, including glycocalyx shedding and inflammation, activating protein C and increasing fibrinolysis and platelet dysfunction, leading to Acute Traumatic Coagulopathy (ATC). Resuscitation factors such as dilution and depletion of coagulation factors, hypothermia, and metabolic acidosis exacerbate this condition, resulting in TIC, which involves decreased coagulation factor production and fibrinogen levels, heightening the risk of lethal haemorrhage. Early identification and targeted treatment of coagulopathy are crucial for improving outcomes in trauma patients (Figure 1.1) [23].

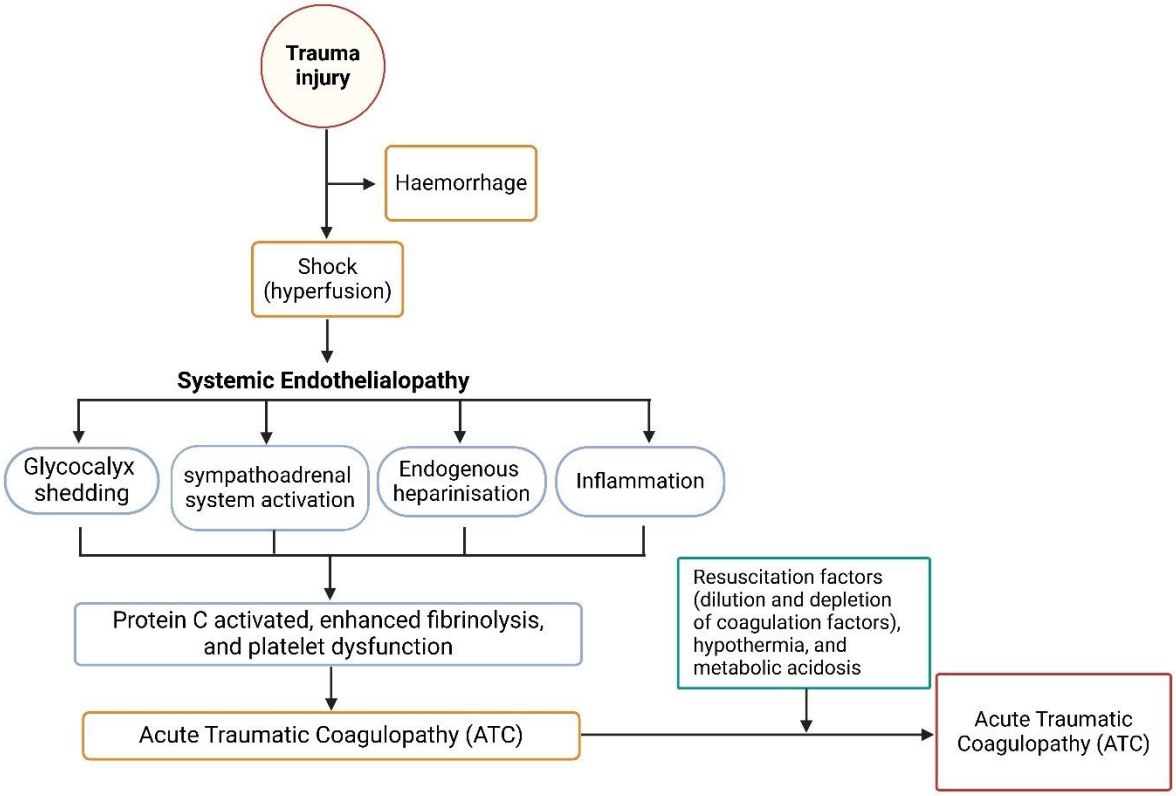

Figure 1.1: Pathophysiology of trauma-induced coagulopathy. Following trauma, haemorrhage and blood loss can lead to shock and systemic hypoperfusion, initiating a condition of systemic endothelialopathy, which includes the shedding of the glycocalyx, activation of the sympathoadrenal system, endogenous heparinisation, and inflammation, promoting the activation of protein C pathways, fibrinolysis, and platelet dysfunction. These changes result in acute traumatic coagulopathy, which is worsened by resuscitation-related factors such as dilution of coagulation factors, metabolic acidosis, hypothermia, and reduced levels of fibrinogen. The cumulative effects of these accelerate trauma-induced coagulopathy, which is characterised by poor clot formation and dysregulated haemostasis. The figure is modified using BioRender Software based on Figure 1 of " Update on the pathophysiology and management of acute trauma hemorrhage and trauma-induced coagulopathy based upon viscoelastic testing" by Maegele et al. [23].

According to Lord et al. (2014), the response to injuries involves interactions across the neurological, haemostatic and endocrine systems (Figure 1.2) [24]. These interactions contribute to endothelial cell activation, resulting in inflammatory cell recruitment and adhesion, increased cellular permeability, and tissue oedema, persistent Inflammation, Immunosuppression, and Catabolism Syndrome (PICS). PICS is a disorder characterised by extended systemic inflammation, immunological impairment, and muscle and fat depletion (catabolism) [25]. Increasing the risk of of sepsis, systemic inflammatory response syndrome (SIRS) and MOF. The pattern and response to trauma depends on the type of tissue injury, stress, degree of haemorrhage, and pain [14]. In severe trauma, the immune systemic response also results in immunoparesis characterised by a functional impairment or partial suppression of the immune system, which increases the risk of infection and sepsis which further drives activation of inflammation [24]. The inflammatory response results in changes in immunological, metabolic and hormonal components that are associated with the size of tissue injury [26]. This response is normally temporary but required for the benefit of normal tissue healing and repair with an expected balance between pro-inflammatory and anti-inflammatory responses. In patients with severe trauma, prolonged excessive pro-inflammatory and anti-inflammatory responses have been observed that lead to further complications [26].

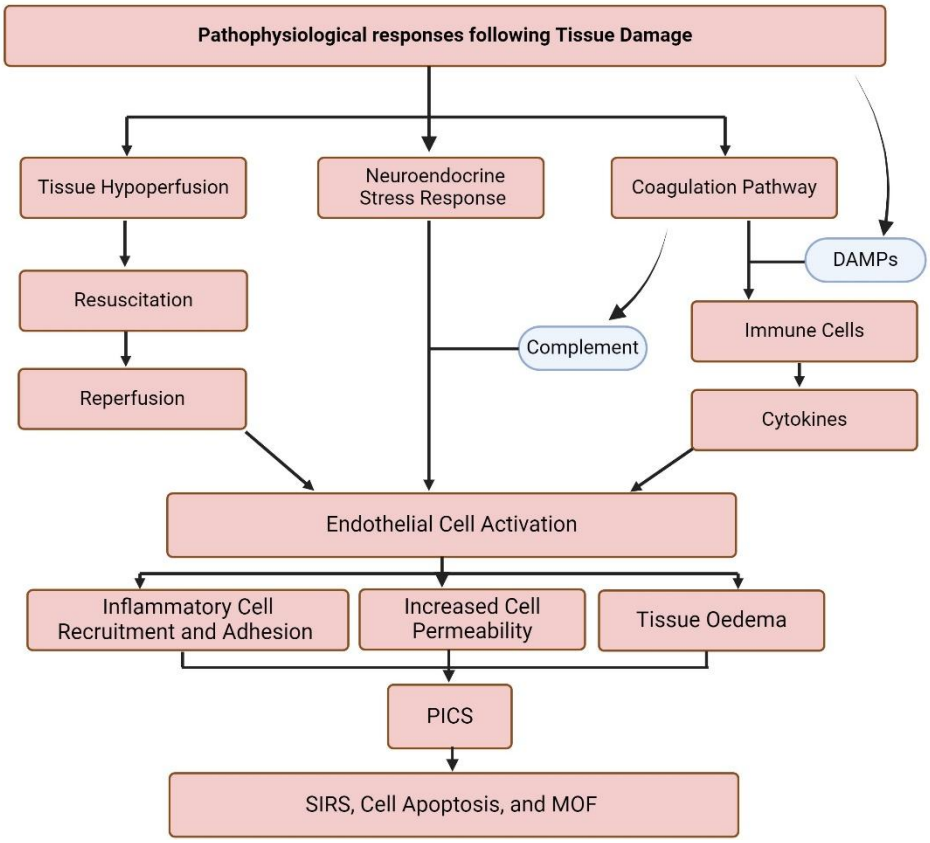

Figure 1.2: Pathophysiological responses following traumatic injuries include tissue hypoperfusion, neuroendocrine stress response and coagulation. Systemic pathways that lead to SIRS and MOF after trauma. Activated endothelium also loses its integrity as a result of tissue hypoperfusion resulting in increased vascular permeability and oedema. Activation of neuroendocrine and coagulation pathways results in dissemination of the response through release of cellular and humoral factors. PICS: persistent inflammation, immunosuppression, and catabolism syndrome. DAMPs: damage-associated molecular patterns. The figure is modified using BioRender Software based on Figure 1 of "The systemic immune response to trauma: an overview of pathophysiology and treatment" by Lord et al. [24].

1.3 Pathophysiology of thermal injury

Understanding skin anatomy and physiology is essential for the clinical assessment of emergency burns. Figure 1.3 illustrates a schematic representation of layers of the

skin and its relationship to burn injury depth [11]. The skin consists of ectoderm and mesoderm and has two kinds of layers. The outer layers are epidermis which are nonvascular layers of various thickness depending on the surface site of the body. Dermis layers are the inner layers and also known as corium. Dermis layers are larger than the epidermis and made of collagen and include the microcirculation which consists of venules, arterioles and capillaries. Both of the layers are bound to each other by complex mechanisms involving the distribution of epidermal appendages throughout the dermal layer that include hair follicles, sweat and sebaceous glands. In addition, the centre of epidermal appendages are padded with epithelial cells, so new cells can be produced if lost during tissue injury of the skin. Nerve endings and pain receptors are also in both skin layers which can mediate extreme pain in burn injuries. The severity of burn injuries of the skin can be sub-classified: - A) First degree burns which affect the epidermis.; B) Second degree burns which are deeper and can be either superficial or deep depending if they reach into the bottom dermis layers.; C) Third degree burns which crosses the epidermis and epidermis and into the subcutaneous fat [11].

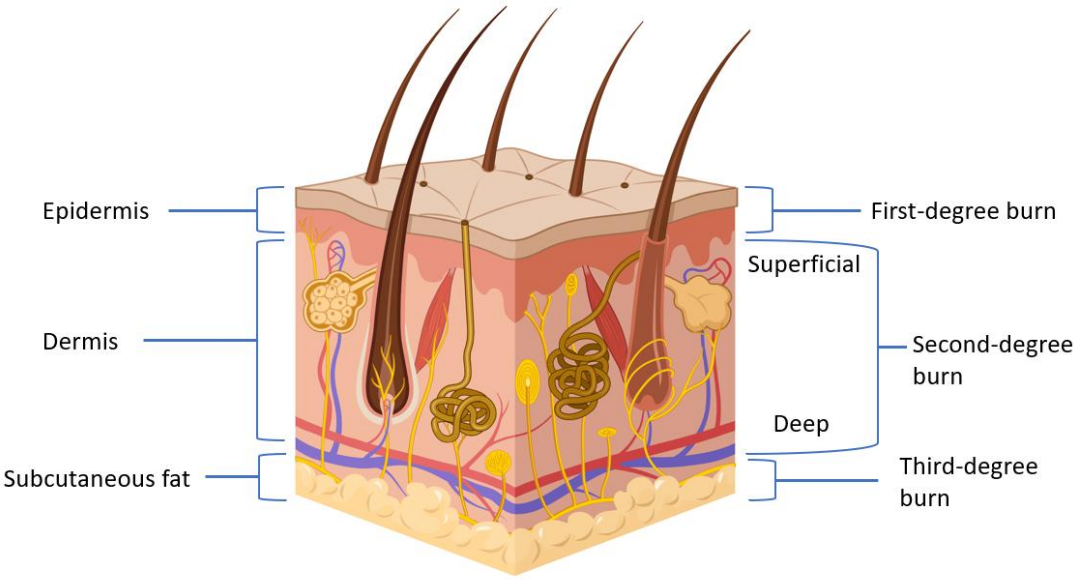

Figure 1.3: Skin layer anatomy and its relationship to the burn depth. The skin consists of two layers, the epidermis and dermis. The dermis is thicker than the epidermis and includes the microcirculation. Injury depth is helpful for the classification of injury severity; 1) A first-degree burn is a condition where only the superficial cells of the epidermis are injured.; 2) A second-degree burn is also called a partial thickness burn and occurs when the first layer and some of the second layer are burned and 3) A third-degree burn destroys the epidermis, dermis and subcutaneous fat. The figure is modified using BioRender Software based on Figure 1 of "Burn Wound Infections." By Church, Elsayed et al. [11].

In 1947, Jackson described three distinct areas or zones for burn injuries (Figure 1.4) [27]: The zone of coagulation, which is the maximum area of damage. In this zone, irreversible tissue loss occurs because of coagulation and tissue ischaemia/necrosis. The zone of stasis surrounds the coagulation zone and is where the tissue can be salvageable but is still characterised by low tissue perfusion. Burn resuscitation (fluid replacement therapy) can improve the perfusion and prevent irreversible damage to the tissue. The zone of hyperaemia is the outer zone of the burn with increased tissue perfusion that will be maintained unless there is infection or spreading of prolonged hypoperfusion.

These burn zones are not static and dynamically change post-injury e.g. the zone of stasis can change resulting in the deepening and widening of the wound [28].

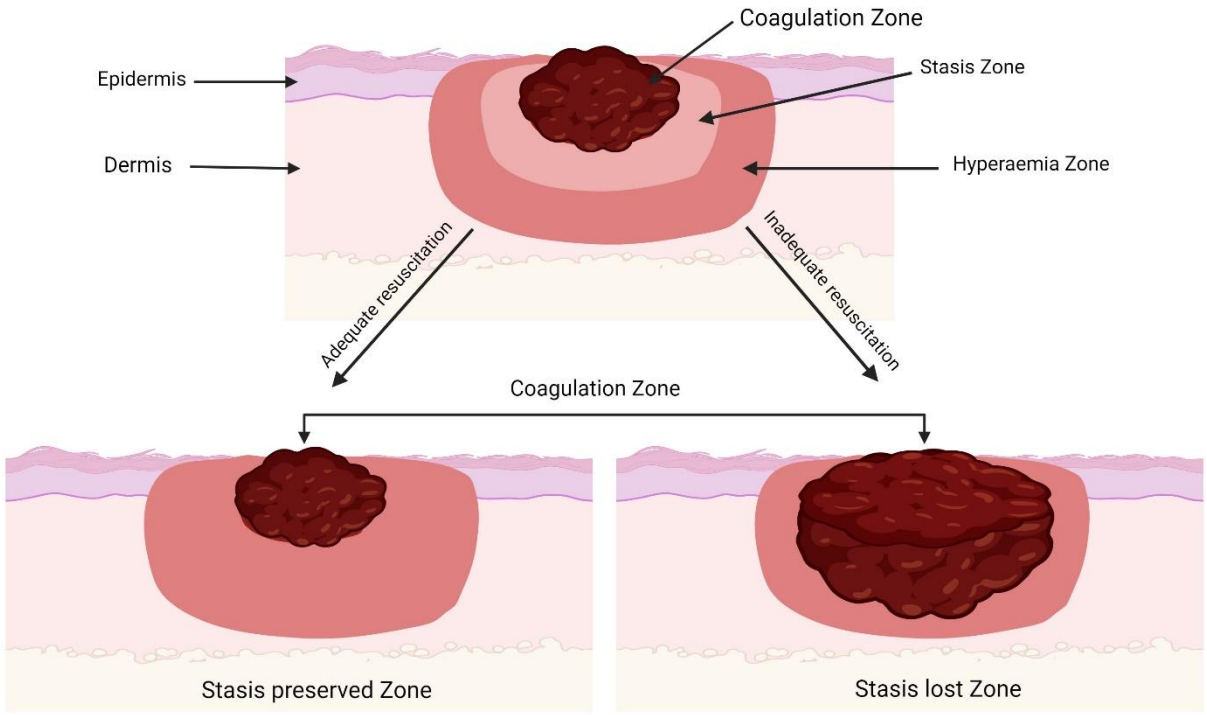

Figure 1.4: Jackson's description of the burn wound zones. The burn wound consists of three zones that represent the response to the injury which are the zones of coagulation, stasis, and hyperaemia. Inadequate resuscitation can result in an increase in the zone of coagulation. The figure is modified using BioRender Software based on Figure 2 of "ABC of burns Pathophysiology and types of burns" by Shehan and Peter [28].

1.4 Shock in trauma and burns

Shock is an irregular and life-threating physiological condition that occurs in severe trauma and thermal injuries, characterised by a reduction in intravascular volume, pulmonary artery occlusion, pressure decreases, elevation of vascular system resistance and depletion of myocardial contractility that results in serious derangement

of organ perfusion and cardiovascular function [29, 30]. Burns shock is classified into various categories that involve hypovolaemic, haemorrhagic, cardiogenic, septic, distributive, and obstructive shock [31, 32]. Hypovolaemia is a state of reduced blood or plasma volume. Hypovolaemic shock occurs immediately within few hours after severe injury and it is characterised by a significant intravascular volume loss leading to decrease loading blood and, stock volume, cardiac output, urine output, and increased systemic volume resistance [33]. In severe burns with severe blood loss, serving adequate blood volume to most critical organs is very important to preserve the patient's life. For example, heart and the brain perfusion is maintained preferentially resulting in insufficient supply to other main organs such as the kidney and the liver which could ultimately result in MOF [34]. The severity of hypovolaemic shock is depending on changes in the vital signs, for instance blood pressure and heart tachypnoea, and pallor [34]. Haemorrhagic shock is a pathologic condition following severe bleeding after injury results in impaired intravascular volume and insufficient oxygen delivery that causes tissue hypoxia, organ dysfunction, and inflammation [35].

Septic shock is a subcategory that increases the mortality risk substantially and characterised by the presence of hypotension and abnormalities of perfusion leading to organ dysfunction with dysregulation of the response to infection [18, 36]. When septic shock occurs, the systemic mean of blood pressure is less than 60 mm Hg, or less than 80 mm Hg if there is previous hypertension after appropriate fluid resuscitation and/or there is requirement of a vasopressor to maintain the circulation [37]. Distributive shock is an aberrant condition of peripheral circulation due to septic shock, while obstructive shock is associated with defects in vascular obstructive that includes pericardial tamponade, pulmonary embolism, haemothorax, hydrothorax, and

ascites [31]. Once any of the burn shock categories are present, appropriate management is required immediately to prevent any further complications and MOF.

1.5 Improvements in management of trauma and burns

Despite the significant mortality and morbidity of burns, modern management techniques have resulted in significant improvements in outcomes in the past recent decades [38]. A study of the international Burn Injury Database (IBID) for England and Wales has illustrated the distribution and outcomes of the burn injuries in 81,181 patients receiving burn care between 2003 and 2011. Although the mortality rate in hospital among all burn patients was 875 (1.51%), the risk of death dramatically decreased with half the number of deaths in the last study year compared to the first two years of the study [39]. This clearly demonstrates that the development of modern treatment strategies has clearly had an impact on saving burn patients' lives [39].

1.5.1 Fluid resuscitation

Adequate fluid management in burns is required to improve the survival of burns patients. Rapid fluid accumulation occurs in the burn wounds so without treatment hypovolaemic shock will develop especially if the burn covers more than 15-20% of total body surface area (TBSA) [40]. A delay of fluid resuscitation for more than two hours post-injury increases the risk of mortality [41]. So, the primary aim of fluid resuscitation is to prevent an occurrence of burn shock and to reduce the disruption of physiological parameters during the post-injury hormonal and cellular responses [42].

1.5.2 Inhalation injury

Inhalation injuries are associated with thermal injury and have been seen to increase the mortality rate in burns patients [43]. The pathophysiology of Inhalation injuries can cause obstruction of the upper airway within the first 12 hours and is caused by thermal injury or chemical irritation [44]. Gases produced during burns or other chemical materials such as carbon monoxide exhibit a high affinity for haemoglobin which can result in oxygen insufficiency in the tissues. Leading to the gradual development of oedematous tracheobronchial mucosa after the first 24 hours post-injury characterised by damaged mucous membranes banding the upper airways, trachea and bronchi associated with possible complications of upper airways swelling and obstruction [45, 46]. In addition, Inhalation injuries can result in a significant decrease in pulmonary performance by approximately 50% of normal [47]. Therefore, extravascular lung fluid and flow of pulmonary lymph are increased as a result of the perfusion mismatch [44]. In severe injuries, the risk of bacterial infections is increased with subsequent sepsis and pneumonia that increase the risk of mortality and morbidity among patients with inhalation injuries [48]. Patients with inhalation injuries require treatment and management to get improve prognosis and to avoid other complications and death [49].

1.5.3 Burn wound care

Injury progression and depth of burns is a complicated issue that also needs to be assessed in the treatment, management, and the morbidity of burns [50]. Wound inflammation is normally helpful in successful healing and resolution, as inflammatory mediators provide immune signals that induce macrophages and leukocytes to migrate into the wound to promote healing and eventual resolution of inflammation

[51]. Early excision and skin grafting normally begin from the first 24 hours to 7 days following injury [52] to prevent or reduce the morbidity and mortality in burns patients [53]. A delay of excision is usually associated with many complications that include increasing length of hospital stay, delays in wound healing, with an increase in the rate of infection and sepsis [52]. Patients with increased extensive burns require temporary but appropriate dressings which transiently protect the wounds and promotes wound healing. Coverage of the wounds can also be performed by use of xenografts, allografts, dermal analogues, or skin substitutes [51]. In addition, topical appropriate antibiotics are required in burn patients especially with a deep wound to prevent wound infection [54]. Improved knowledge of the pathophysiology of burns are required to improve the management, treatment, and to reduce other complications in burn patients.

1.5.4 Systemic inflammatory response syndrome (SIRS)

Severe trauma and thermal injuries result in immune system activation with promotion of a massive inflammatory response which is known as SIRS [55, 56]. SIRS was defined in 1992 as the systemic inflammatory response with at least two of the following criteria ; 1) hypothermia or hyperthermia, 2) tachypnea or hyperventilation, 3) tachycardia, 4) leukopenia or leucocytosis (Table 1.1) [57].

Table 1.1: Criteria for SIRS [58].	
Temperature	Hypothermia: Less than 36°C. Hyperthermia: More than 38°C.
Respiratory	Tachypnea: More than 20 breaths per minute Hyperventilation: The CO_2 less than 4.3 KPa
Heart rate	Tachycardia: More than 90 beats/minute.
WBC count	Leukopenia: Less than 4×10^9/L Leucocytosis: More than 12×10^9/L

SIRS is the initial response to injury through the increase of inflammatory mediators into the circulation through the release of cytokines from the immune cells within the tissue injured site. A massive increase of these mediators increases the risk of organ damage or MODS [59].

In addition, as mentioned above severe injuries are associated with SIRS, it is reported that this response begins as early as thirty minutes after major injury due to the damaged tissue or the large loss of blood [24]. Damage-associated molecular patterns (DAMPs) are endogenous factors or alarm molecules released during tissue injury that not only initiate pro-inflammatory activity, but attract immune cells (e.g. phagocytes) to the wound and with subsequent infections will enhance the amplitude of the inflammatory response [60]. SIRS is therefore initiated through immune system stimulation by infectious and non-infectious diseases, tissue injury and surgery [61].

In severe trauma, the systemic response results in a lower ability in defending against infection and can therefore promote the risk of sepsis [24]. Many complications are also associated with SIRS including renal failure, acute respiratory distress syndrome (ARDS), hyperglycaemia, coagulopathy and acute hepatic failure [62].Also, in severe

burns and trauma, it was thought that the SIRS response was followed by the compensatory anti-inflammatory response syndrome (CARS). Recent evidence suggests that SIRS and CARS responses are not only simultaneous and not sequential but that the amplitude of the response is associated with ongoing SIRS and immunosuppression increasing the risk of sepsis and subsequent mortality from organ failure [61, 63].

1.6 Damage associated molecular patterns (DAMPS)

DAMPS are molecules released by cell death or stress and act by immunosuppression and promoting inflammation [64]. DAMPs are derived from intracellular components which can be classified based on their intracellular origins to nuclear DAMPs (e.g., high-mobility group box 1 protein (HMGB1), DNA, histones), mitochondrial DAMPs (e.g., mitochondrial DNA, cardiolipin), cytoplasmic DAMPs (e.g., ATP, S100 protein family, such as S100A8 and S100A9), plasma membrane-derived DAMPs (e.g., heat shock proteins,), and endoplasmic reticulum DAMPs (e.g., calreticulin) (Table 1.2) [65-69]. DAMPs act in modulating the immune system and the function of antigen-presenting cells (APCs), neutrophils, eosinophils, and mast cells [65]. Burns and trauma contribute to the occurrence of cellular stress through the release of DAMPs [70, 71]. Released DAMPs from cellular injury after burns and trauma, such as HMGB1, DNA, histones, mitochondrial DNA and ATP, are detected by pathogen recognition receptors (PRRs) such as toll-like receptors (TLRs), which lead to activation of the innate immune system, resulting in SIRS, inflammation, MODS, and inflammatory complications, for example, ARDS [65, 67]. Importantly, increased levels of nuclear DAMPs, such as DNA and histones, in burn and trauma patients, are associated with worse outcomes, including severe inflammation, MODS, and higher

mortality rates [72-74]. Understanding the relationship between DAMPs and the complications of inflammation and mortality may help in finding appropriate therapy for trauma and burns patients.

Table 1.2: DAMPs released post-severe burns and traumatic injuries [65-69, 75].

Category	**DAMPs**
Nucleic Acids	Cell-free DNA (cfDNA)
	Histones
	Mitochondrial DNA (mtDNA)
	High Mobility Group Box 1 (HMGB1)
Lipids	Phosphatidylserine
	Oxidised Phospholipids
	Cardiolipin
Cytoplasmic DAMPs	ATP
	S100 Proteins
Plasma Membrane-Derived DAMPs	Heat Shock Proteins
Endoplasmic Reticulum DAMPs	Calreticulin

1.7 Sepsis

Sepsis is an observed complication in severe trauma and burns, which leads to an increase in the risk of morbidity and mortality among patients [76]. Sepsis is defined as a life-threatening organ dysfunction caused by a dysregulated host response to infection [77]. In 2007, the American Burn Association (ABA) defined the diagnostic criteria for sepsis, specifically in burn patients. It is essential to understand these criteria in order to evaluate septic patients using appropriate diagnostic methods and to prevent the misuse of antibiotic treatments. According to the ABA, a diagnosis of sepsis in burn patients is defined by the presence of at least three of the following criteria, which are detailed in Table 1.3 [78].

Table 1.3: Criteria for the diagnosis of sepsis [78].

Temperature	Hypothermia: Less than 36.5°C. Hyperthermia: More than 39.5°C.
Respiratory	Tachypnea: More than 25 breaths per minute Hyperventilation: More than 12 L/min
Heart rate	Tachycardia: More than 110 beats/minute.
WBC count	Leukopenia: Less than 4×10^9/L Leucocytosis: More than 12×10^9/L
Platelet count	Thrombocytopenia: Less than 100,000/µl
Blood Glucose (In case of absence of pre-existing diabetes mellitus)	Hyperglycaemia: • More than 200 mg/dl for untreated plasma glucose • More than 7 units of insulin/hour intravenous drip • Significant insulin resistance (Increase Insulin demand more than 25% within 24 hours).
Feeding	Incapability to continue enteral feedings for more than 24 hours due to abdominal distension or high gastric residuals with a feeding rate of two times or massive diarrhoea more than 2500 ml/day

Additionally, in 2016, sepsis was defined as sepsis-3, underscoring the evaluation of the Sequential Organ Failure Assessment (SOFA) score, wherein an elevation of two or more points indicates sepsis [79].

The difference between sepsis and septic shock is that septic shock is a serious condition subset of sepsis. It is characterised by significant circulatory, cellular, and metabolic disruptions that increase mortality risk compared to sepsis alone. A diagnosis of septic shock is made in patients who require vasopressors to maintain a mean arterial pressure of at least 65 mm Hg, along with a serum lactate level above 2 mmol/L (greater than 18 mg/dL), even after adequate fluid resuscitation. These criteria are associated with a hospital mortality rate exceeding 40% [79].

Sepsis is a result of a harmful systemic response to infections [57]. This harmful response includes SIRS, coagulation activation, and altered fibrinolysis [80]. Severe sepsis is associated with a combination of multiple organ dysfunction with hypotension or hyperperfusion [57] that requires health care interventions [81]. The majority of patients with severe sepsis exhibit cardiac, lung, and renal dysfunction [80].

Despite the medical developments in treating and managing burns patients, the prevalence of sepsis remains high [82]. Sepsis is highly prevalent at a frequency of 300 per 100,000 persons globally [83]. The mortality rate of sepsis in traumatic and burns patients' is approximately 28.0% and 34.4%, respectively [84-86]. The total incidence of severe sepsis in the UK is around 1530 cases per million of the population with up to 50 % mortality in hospitals [87]. Moreover, a study of paediatric severe sepsis among patients younger than 18 years old in 26 countries gave an incidence of 8.21% with the most infectious sites being the lungs and the circulation. The mortality was also high at 25% with 67% diagnosed with MODS [82]. Understanding sepsis pathophysiology is important for clinical management. Heterogeneity occurs in

inflammatory responses of patients with sepsis with either hyper-inflammation and/or immuno-suppression [88]. Stimulation of the over-production of the cytokine tumour necrosis factor (TNF) occurs which increases the risk for deaths among septic patients [89]. Elevations in other inflammatory cytokines are also observed in septic patients including interleukin-6 (IL-6) [88]. An example of harmful immuno-suppression is the inhibition of T lymphocyte proliferation due to the response to mitogenic stimuli, including anti-CD3 antibodies and concanavalin A (ConA). This suppression is partially attributable to elevated interferon-gamma (IFN-γ) production, which stimulates macrophage-derived nitric oxide (NO). Increased NO levels obstruct T cell signalling pathways, resulting in diminished proliferation following mitogenic activation [90]. Moreover, sepsis modifies T cell subpopulations and disturbs cytokine balance, hence undermining T cell responses to mitogens [91].

In addition, sepsis affects coagulation pathways, resulting in microvascular thrombosis and altered fibrinolysis, exacerbating organ failure and contributing to disseminated intravascular coagulation (DIC) [93, 94]. These processes frequently result in MODS, which significantly elevates morbidity and death in individuals with sepsis [94]. Other significant cellular function changes during sepsis, such as activation of neutrophils and induction of apoptosis in lymphocytes. Also, the presence of metabolic changes in septic patients such as hyperglycaemia require close monitoring especially in patients with insulin resistance [88].

1.8 Biomarkers of sepsis

Sepsis is a condition of microbial invasion from the site of infected tissue to the bloodstream, which also can be called bacteraemia, that subsequently results in MOF [130]. An appropriate and early diagnosis of sepsis is important for receiving optimal and timely therapeutic interventions, such as antibiotics, fluid resuscitation, and organ support. Both sepsis and SIRS present a significant diagnostic challenge because they imitate each other clinically [131]. Blood culture provides a laboratory test to specifically identify the presence of microbes in blood. However, testing is time consuming and It has been demonstrated that the blood cultures can sometimes not only give positive results in patients with SIRS but also give negative results in septic patients [130]. The accurate differentiation between SIRS and sepsis is therefore very important for providing the correct therapeutic strategies, including antibiotic stewardship [131]. For example, every hour delay in treating septic patients with antibiotics results in an increase of mortality by 7.6% [132]. Therefore, the recommendations of the current guideline for sepsis therapy is to ensure that both antibiotic or surgical treatments are given as early as possible to improve outcomes [133].

Initiation of antibiotic therapy is also required in the approach of management of sepsis. Consideration of the infection site is important as antibiotics have different sensitivity depending on the locality and type of infection [134]. Unsuccessful determination of an infection source will subsequently result in mis-identification of the pathogen and is also associated with high mortality [135]. Antimicrobial-resistant bacteria will also affect the antibiotic therapy performance especially when using a normal selection of antibiotic therapies [136]. Pathogen resistance to antibiotics in sepsis therefore significantly contributes to increased mortality [137]. Recently,

biomarkers have been also been incorporated into the evaluation of sepsis evaluation which could help in monitoring host response characteristics and the presence or loss of infection [138]. Several Biomarkers have therefore been investigated for predicting sepsis and their advantages in the sepsis diagnostic strategies evaluated.

1.8.1 Cytokines and chemokines

Cytokines described as immune response regulators to infection, play important roles in trauma and inflammation, and are broadly divided into; 1) pro-inflammatory cytokines that stimulate systemic inflammation; 2) anti-inflammatory cytokines that have a role in inflammation resolution and enhancement of healing [139]. Both the levels of pro- and anti-inflammatory cytokines have been observed to begin to synchronize with the onset of septic shock [140]. For example, the level of cytokines is often higher in serum from sepsis compared to non-septic patients [141]. TNF-α, IL-6, Interleukin-1 beta (IL-1β), and IL-8 are pro-inflammatory cytokines and have been reported to increase in patients with sepsis. They also initiate immune system responses and cause fever, endothelial cell activation and recruitment of circulating neutrophils [130, 139]. Anti-inflammatory cytokines such as IL-4, IL-10, IL-13, IL-22, and transforming growth factor-β (TGF-β) are also secreted at higher levels in sepsis [142]. In 2013, a study on neonatal sepsis has demonstrated that IL-6 has high sensitivity and specificity in differentiation between septic and non-septic neonates and therefore seems to be useful for the diagnosis of sepsis. Furthermore, these high levels also significantly declined 24 hours after taking antibiotics and can be used to potentially monitor treatment responsiveness and predict clinical outcomes [143]. Alsabani et al. (2022) who also demonstrated that IL-6 & IL-8 can distinguish between SIRS & Sepsis in adult ICU patients [144].However, it is well known that cytokine levels

can also be elevated due to other reasons such as SIRS caused by injury or surgery and various immune diseases [130].

1.8.2 Lipopolysaccharide-binding protein (LBP)

LBP is a protein made in the liver that binds to lipopolysaccharide (LPS), which is the prominent component of the outer membrane of gram-negative bacteria, resulting in the LPS-LBP complexes [130, 145]. This complex acts according to the LBP level, in the enhancement or inhibition of LPS signals [130]. Increasing serum LBP levels of up to 2-3-fold normal levels have been demonstrated in septic patients than in non-septic patients [146]. Sakr et al. (2008) have illustrated that in the ICU, the concentration of LBP was also increased in septic patients with MOF [147]. However, the study also suggested that LBP could not discriminate between sepsis patients without MOF and non-septic patients.

1.8.3 C-reactive protein (CRP)

CRP is a protein released by the liver as an acute-phase protein and regulated by IL-6. CRP levels are elevated in inflammation, tissue damage, infection, stroke and cardiovascular disease [148, 149]. CRP has been illustrated as a valuable marker in infection diagnosis and monitoring of antibiotic medication [150]. Also, the CRP plasma concentration has been reported to correlate with the severity of infection [151]. A large multicentre study was performed within 891 patients diagnosed with sepsis in the ICU. CRP gave significant results on day 3 in response to antibiotic medication and could differentiate between survivors and non-survivor patients over 5 days [152]. However, CRP levels cannot early distinguish between survivors and non-

survivors in septic patients [153]. Li et al. (2022) demonstrated that CRP levels were elevated in septic burns but were not statistically distinguishable from those in non-septic burns [155]. Additionally, high levels of CRP are found in patients after major operations and with no signs of sepsis. CRP elevation therefore does not specifically reflect the occurrence of sepsis [154]. Although CRP can be a useful marker in daily monitoring for studying antibiotic therapy efficacy within patients with sepsis, since CRP can be elevated after major surgery, it is non-specific and unreliable for diagnosing sepsis.

1.8.4 Procalcitonin

Procalcitonin (PCT) is a precursor protein of calcitonin that has been described as a biomarker of sepsis and is secreted from many different organs during an infection including the liver, kidney, lungs, spleen and colon [130]. PCT production occurs in response to infection which also dramatically decrease during recovery [156]. Wacker et al. (2013) illustrated that PCT is a helpful marker in early sepsis diagnosis with good sensitivity and specificity of 77% and 79% respectively [157].

PCT has been reported as a more specific marker than CRP with a closer correlation with infectious severity and MOF [158]. Furthermore, PCT measurement can distinguish between survivors and non-survivors of sepsis. Tschaikowsky et al. (2002) have illustrated that PCT levels showed a more pronounced and consistent decline in survivors of sepsis compared to CRP levels, making PCT a potentially more reliable biomarker for monitoring septic patients [154]. Consequently, PCT is being used more and more as a supplementary or substitute indicator for CRP, especially in the medical evaluation of patients who are suspected or confirmed to have bacterial infections [159].

1.8.5 Lactate

Serum lactate has also been associated as a marker of severe sepsis [160]. It has been demonstrated that serum lactate reflects both anaerobic metabolism and hypo-perfusion of tissues in septic patients. Septic patients with liver and kidney failure results in the elevation of serum lactate levels due to the inability of clearance of lactate [161]. Anaerobic metabolism can influence the lactate concentration due to tissue hypoperfusion and anaerobic glycolysis [162]. In 2009, high serum lactate levels were associated with increased risk of mortality in severe sepsis [161]. In contrast, Nguyenet et al. (2004) demonstrated that early lactate clearance resulted in good prognosis for patients with severe sepsis [160]. Therefore, monitoring serum lactate can be a potential marker for the risk of mortality in sepsis.

1.8.6 Mid-regional proadrenomedullin (MR-proADM)

MR-proADM is a new hormone biomarker which is claimed to behave in a similar fashion to cytokines during inflammation and infection [163]. Adrenomedullin (ADM) consists of 52 amino acids, is synthesised in the adrenal medulla, secreted during stress and has several biological actions, including vasodilation, antimicrobial and anti-inflammation effects [130]. Although ADM levels have been reported to be increased during sepsis, measurement is associated with technical challenges due to its rapid clearance from the circulation [164]. MR-proADM is a peptide derived from ADM and has also been shown to reflect the ADM level in the plasma of septic patients [165]. Christ-Crain et al. (2005) demonstrated that proADM concentration is significantly higher in patients with severe sepsis and patients with septic shock. Also, the study could distinguish between patients with SIRS and severe sepsis [164] suggesting that it could be a useful biomarker.

1.8.7 Angiopoietin

Angiopoietin is an endothelial vascular growth factor that plays a role in the maintenance, development, and repair of blood vessels. There are four sub-types; Ang-1, Ang-2, Ang-3 and Ang-4 [166]. Ang-1 acts to stabilise endothelium, while Ang-2 disrupts endothelial integrity to promote vascular leakage [130]. Ricciuto et al. (2011) described that measurement of Ang-1 and Ang-2 levels are associated with the mortality risk of septic patients. Ang-1 levels were low in contrast to high Ang-2 levels in non-surviving patients [167] suggesting it is an informative biomarker for monitoring septic patients.

1.8.8 High-mobility group box 1 protein (HMGB1)

HMGB1 is a nuclear protein that has several biological actions both in and outside the cells depending on its location, binding status, and molecular redox condition [168]. HMGB1 is considered to be a cytokine mediator as it can be secreted by either macrophages, monocytes, platelets or by necrotic cells [169]. HMGB1 has been reported as a late mediator in severe systemic inflammation in mice [170]. HMGB1 serum and tissues levels increase during sepsis [171]. Sunden-Cullberg et al. (2005) assessed HMGB1 in patients with sepsis, severe sepsis, and septic shock. The study outcomes show a delay in the HMGB1 kinetics but with a sustained high concentration during the period of the study. However, there was no correlation between HMGB1 levels and sepsis severity, in which there were significant lower HMGB1 levels in non-survivors compared to survivors [172]. The study of Karlsson et al. (2008) illustrates HMGB1 levels could not be used to discriminate between survivors and non-survivors [173].

1.8.9 Macrophage migration inhibitory factor (MIF)

MIF is defined as a cytokine that has a critical role in immune responses during sepsis [174]. MIF concentrations have been reported to be high in patients with severe sepsis and can distinguish between non-survivors and survivors [175].

1.8.10 Biomarkers of complement proteins in sepsis

The complement system is part of the innate immune system that rapidly recognises and eliminates infection [176]. Complement plays a key role against infection by generating several proteins that participate in innate system recognition of foreign organisms by opsonisation and chemotaxis as well as causing direct lysis [177]. Activation of the complement system is initiated through three pathways; 1) Classical pathway; 2) Lectin pathway; 3) Alternative pathway (Figure 1.5) [178]. Sepsis is associated with activation of complement factors 3 and 5 (C3a and C5a) [179]. C3a and C5a regulate the inflammatory response by increasing vascular permeability, and promoting the extravasation and chemotaxis of leukocytes [177]. C3b and C5b enhance phagocytosis through opsonisation [180]. In a mouse model of sepsis, the three pathways of complement are all activated resulting in increased levels of C5a [180]. Increased C5a levels have been reported in patients with severe sepsis [181].

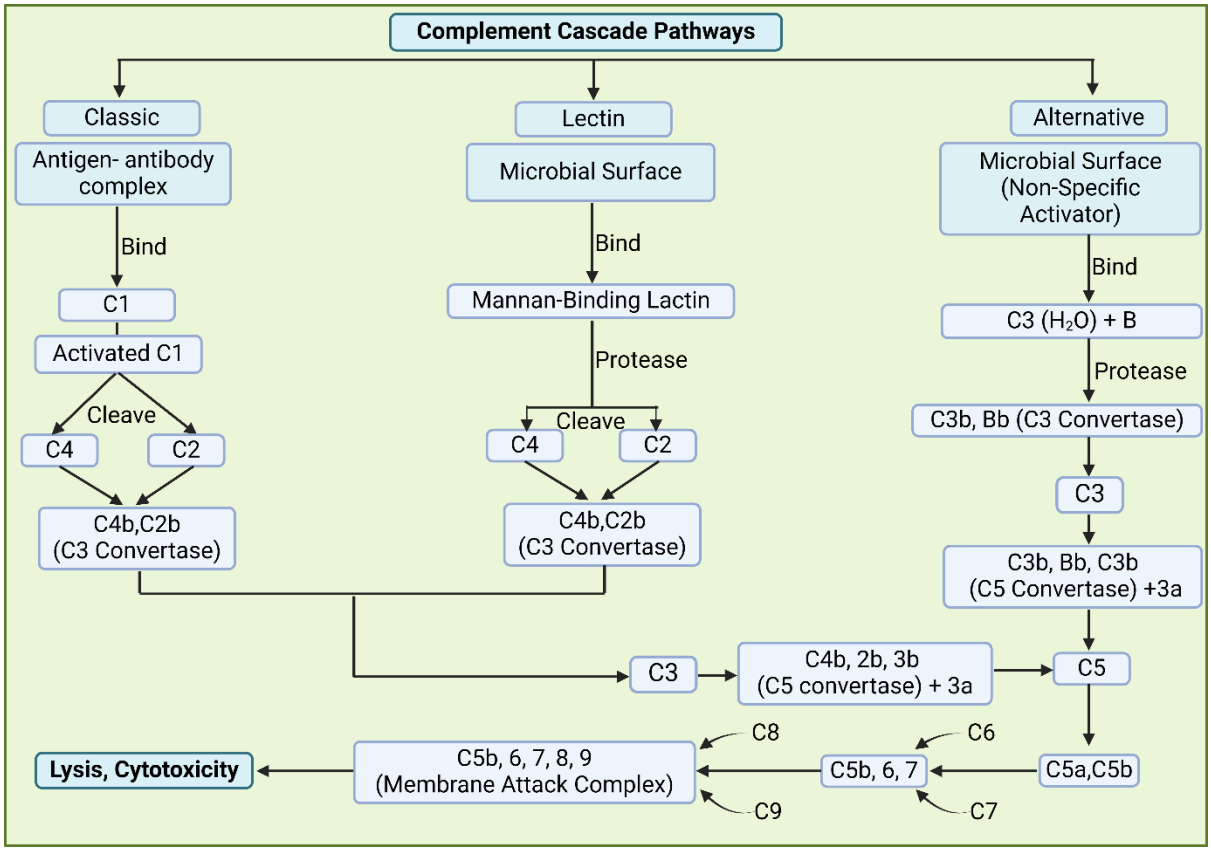

Figure 1.5: The complement cascade. Complement is activated via the classical pathway through antigen-antibody complexes or through the alternative and lectin pathways by non-immunological substances like endotoxin. In both of the classic and lectin pathways, C3 convertase cleaves C3 to form C5 convertase (C2b, C4b, C3b complex). In the alternative pathway, C3 convertase cleaves C3 to form the complex (C3b, Bb, C3b plus C3a). C5 convertase cleaves C5 to C5a, and C5b. C5b binds to C6 and C7. The complex of C5b,6,7 binds to C8, and C9 to form C5b,6,7,8,9 complex which is known as membrane attack complex that results in microbial lysis and cytotoxicity. The figure has been modified using BioRender Software based on Figure 1 of " Bench-to-bedside review: The role of C1-esterase inhibitor in sepsis and other critical illnesses" By Singer et al. [178].

1.9 Disseminated intravascular coagulation (DIC)

Disseminated intravascular coagulation (DIC) is an acquired disease characterized by systemic coagulation activation [95]. DIC results in widespread vascular thrombosis that leads to insufficient blood supply to the body organs thereby significantly contributing to organ dysfunction and failure. Subsequently, because of ongoing coagulation activation, platelet and coagulation protein depletion can occur which can then induce severe bleeding from different sites in the tissues [95]. A key precursor to DIC is sepsis-induced coagulopathy (SIC), which is defined by a combination of sepsis-related organ dysfunction and abnormalities in coagulation tests, including prolonged prothrombin time and a reduced platelet count. SIC criteria provides identify patients at risk of progressing to overt DIC [96].

Furthermore, sepsis is a significant factor in promoting DIC [97], which has an incidence of 35% in severe sepsis [98]. Traumatic and thermal injuries are significant contributors to DIC, primarily by releasing tissue-derived substances, such as thromboplastin, into the bloodstream. Thromboplastin, also known as tissue factor (TF), is a transmembrane glycoprotein that is a major activator of the extrinsic coagulation pathway. It is produced by injured tissues following burns or trauma, leading to excessive thrombin production and widespread coagulation [99-101]. Also, DIC is considered as a contributor to MODS due to thrombosis causing insufficient blood supply [103]. The diagnostic criteria for overt DIC are defined by the International Society on Thrombosis and Haemostasis (ISTH) scoring system defines overt DIC using platelet count, prothrombin time, fibrinogen levels, and D-dimer concentrations. A score ≥5 indicates overt DIC, while a score <5 suggests non-overt DIC, requiring continuous monitoring(Table 1.4) [104].

Table 1.4: The ISTH criteria for DIC diagnosis		
Parameter	**Criteria**	**Points**
Platelet Count	>100 × 10^9/L	0
	50–100 × 10^9/L	1
	<50 × 10^9/L	2
Fibrin-Related Marker	No increase	0
	Moderate increase	2
	Strong increase	3
Prothrombin Time (PT)	<3 seconds	0
	3–6 seconds	1
	>6 seconds	2
Fibrinogen Level	>1 g/L	0
	≤1 g/L	1

1.9.1 Coagulation in thermal and traumatic injuries

Coagulation is the process of blood clotting, essential for preventing bleeding during vascular injuries [106]. Coagulation factors regulate this process, which are proteins involved in haemostasis, divided into pro-coagulation factors that promote clotting and anti-coagulation factors that inhibit it. They act sequentially to form a blood clot, with careful regulation to prevent excessive clotting. These factors also interact with platelets and blood vessel walls to create a stable clot, minimising bleeding [107].

The process of blood clot formation involves a series of managed steps to control haemostasis and prevent excessive clotting. In the coagulation cascade, both intrinsic and extrinsic pathways converge on factor X, activating various clotting factors. Tissue injury and the release of TF activate factor VII in the extrinsic pathway. Meanwhile,

damage to the endothelium activates factors XII, XI, IX, and VIII in the intrinsic pathway. Both pathways ultimately activate factor X, where the complex of activated factors X and V converts prothrombin into thrombin. Thrombin is a key enzyme in coagulation, as it transforms fibrinogen into fibrin, leading to the formation of the blood clot (Figure 1.6) [108, 109].

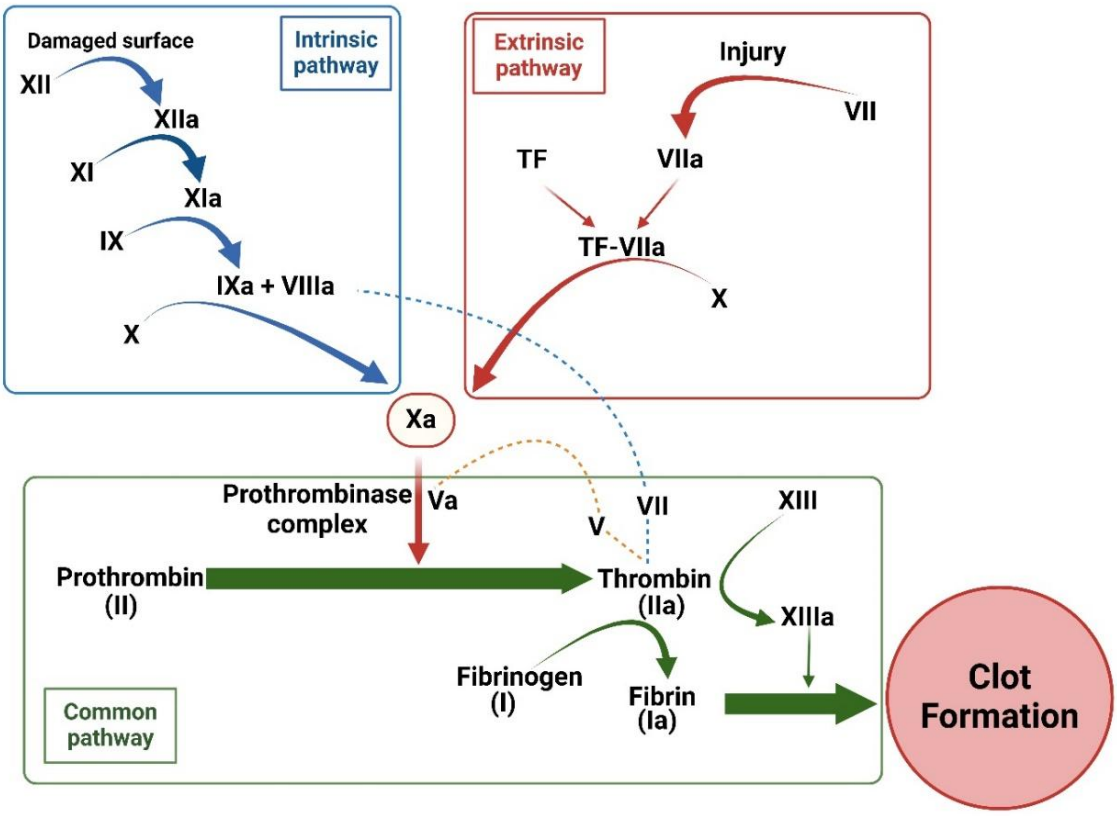

Figure 1.6: Coagulation cascade and clot formation process. The coagulation cascade consists of three interconnected pathways: the intrinsic pathway, extrinsic pathway, and common pathway, all converging to produce a stable fibrin clot. The intrinsic pathway is initiated by damage to the endothelial surface, leading to the sequential activation of factor XII (XIIa), factor XI (XIa), and factor IX (IXa), which combines with activated factor VIIIa to activate factor X. The extrinsic pathway begins with tissue injury, where TF binds to and activates factor VII (VIIa), which also activates factor X. Both pathways converge in the common pathway, where activated factor Xa, in complex with activated factor Va (prothrombinase complex), converts prothrombin (factor II) into thrombin (IIa). Thrombin subsequently cleaves fibrinogen (factor I) into fibrin (Ia). Factor XIIIa stabilises the fibrin strands, forming a cross-linked fibrin clot. The figure is modified using BioRender Software based on “The Therapeutic Potential of Anticoagulation in Organ Fibrosis” By Oh et al. (2022) [182].

Pro-coagulation factors like fibrinogen, thrombin, and TF work through intrinsic, extrinsic, and common pathways to form a fibrin mesh stabilising the platelet plug. Anticoagulant factors, including antithrombin III, protein C, and protein S, regulate clotting by inhibiting excessive thrombin activity and coagulation factor cleavage. This balance ensures that clots form only at sites of vascular injury, preventing unnecessary clotting in healthy vessels [109].

The coagulation cascade collaborates with platelets and the walls of blood vessels to form a stable clot that helps to stop bleeding. When a blood vessel is injured, platelets adhere to the subendothelial matrix by interacting with von Willebrand factor (VWF) and collagen, both of which are essential for clot formation. Activated platelets release granules that contain pro-coagulation substances such as ADP, thromboxane A2, and fibrinogen, promoting platelet aggregation and attracting more platelets to the injury site. Additionally, thrombin plays a crucial role by activating more platelets and stabilising the clot through Factor XIII-mediated fibrin crosslinking, reinforcing the haemostatic plug [109, 110].

In burns and trauma, coagulation pathways are disrupted due to extensive tissue injury and the systemic inflammatory response. Released TF from injured tissues initiates the extrinsic coagulation pathway by activating factor VII, creating the TF-VIIa complex, leading to thrombin production and fibrin clot formation [110, 111]. Burn injuries result in significant endothelial damage, exposing subendothelial collagen and VWF, hence enhancing platelet adhesion and aggregation. Concurrently, pro-inflammatory cytokines, including IL-6 and TNF-α, enhance coagulation by elevating TF expression on monocytes and endothelial cells [112]. These pathways create a hypercoagulable state that encourages microvascular thrombosis. In trauma, hypoperfusion and acidosis further enhance thrombin production while inhibiting

anticoagulation, particularly the protein C pathway. This imbalance promotes clot formation and can lead to DIC in severe trauma [113, 114].

1.9.2 Fibrinolysis in burns and trauma

Fibrinolysis is the physiological process that prevents fibrin clots' formation after controlled haemorrhage. This process ensures that the coagulation mechanism does not remain constant, preserving vascular patency in balance with coagulation [115]. Plasmin is a serine protease that plays a crucial role in fibrinolysis by degrading fibrin polymers. As a result, fibrin degradation products provide feedback inhibition on the coagulation process [116].

In burns and trauma, fibrinolysis is often dysregulated, shifting between hyperactivation and inhibition. Initially, fibrinolysis is increased due to elevated levels of plasminogen activator, which leads to excessive degradation of blood clots. However, as the condition progresses, a shutdown of fibrinolysis commonly occurs, marked by higher levels of plasminogen activator inhibitor-1 (PAI-1) [117-119].

In burns, endothelial damage and systemic inflammation drive fibrinolytic imbalance. High circulating levels of D-dimer, a fibrin degradation product, indicate ongoing fibrinolysis but also serve as a marker of excessive thrombin generation and clot turnover [120]. Similarly, trauma-induced coagulopathy features a hyperfibrinolytic phase during the initial injury, followed by fibrinolytic suppression due to PAI-1 overexpression, which promotes microvascular thrombosis and contributes to MOF [22, 121].

Burn and trauma patients experience poorer outcomes due to fibrinolytic shutdown, which exacerbate DIC and impairs tissue perfusion. Blood flow to important organs is

further compromised and the risk of MODS and MOF increases due to the persistence of fibrin-rich thrombi, which is caused by decreased fibrinolysis [21, 122].

1.10 Multiple organ failure (MOF)

MOF is considered a major cause of mortality in patients with trauma and burns [123, 124]. Organ failure has been demonstrated within one or many of the pulmonary, adrenal, cardiac, haematological, hepatic, renal, central nerve system, gastrointestinal, and vasomotor systems [125]. It has been demonstrated that MOF causes 10.5% of total mortality amongst traumatic patients [123]. Also, a retrospective study in severe burns patients between 1999 and 2005 in Finland demonstrated 40% mortality was caused by MOF [124]. In 2019, research examining data from a database, including patients from six burn centres in the United States between 2003 and 2009, revealed that 30% of 322 adult patients with severe burns developed MOF [126].. The mechanism of occurring MOF is also poorly understood. Some studies have suggested that DIC is an independent factor that significantly contributes to MOF [128]. It has been demonstrated that the presence of thrombi in vessels of patients with severe sepsis leads to organ dysfunction [129]. Other studies show that reactive oxygen species, neutrophil enzymes and cytokine elevation might also play important roles in MOF, especially in patients with severe sepsis [128]. Understanding the pathophysiology of MOF in traumatic and burns patients with severe sepsis may provide not only useful biomarkers but potentially aid in the therapeutic management of MOF.

1.11 Neutrophils

1.11.1 Background/overview

Neutrophils play a crucial role in the response to burns and trauma injuries, acting as the initial responders to injury and infection. After an injury occurs, neutrophils rapidly recruited to the affected site, providing a first line of defence against pathogens [183, 184]. In patients who developed sepsis, the dysregulation of neutrophils can exacerbate inflammation, impair the clearance of bacteria, and lead to immunosuppression due to excessive degranulation or release of neutrophil extracellular traps (NETs) [185].

Neutrophils are the main subtype of leukocytes of the innate immune system characterised by a multi-lobular nucleus and are synthesised by the bone marrow (BM) through a process that is controlled by granulocyte colony (G-CSF) and inflammatory cytokines such IL-6, and released into the blood downstream as mature terminally differentiated cells [186, 187]. The circulation lifespan of neutrophil is very short at about 8 hours in humans [181]. Neutrophil function is an important part of the innate immune response for the rapid elimination of pathogens [188]. The attraction of neutrophils to infected sites is essential in preventing bacterial and fungal infections [189]. Neutrophils consist of different subsets, including high-density neutrophils (HDNs) and low-density neutrophils (LDNs). These subsets can arise in situations such as burns and sepsis. HDNs are known for their strong ability to kill and eliminate bacteria, while LDNs, which are linked to severe inflammation and sepsis, leading to immunosuppression that can lead to further complications and poor outcome [185].

Neutrophils induce pathogen killing through either phagocytosis, degranulation, or generation of neutrophil extracellular traps (NETs) (Figure 1.7) [188]. Neutrophil phagocytosis engulfs and eliminates pathogens via intracellular killing in the

phagosome through generation of reactive oxygen species (ROS) [190]. Degranulation releases neutrophil granules that contain enzymes, such as elastase, gelatinase B, and myeloperoxidase, with high effectiveness in bacteria killing [191]. Neutrophils can also release their chromatin, composed of DNA and histones, and antimicrobial proteins such as myeloperoxidase and neutrophil elastase to form NETs to ensnare trap and kill infections [192].

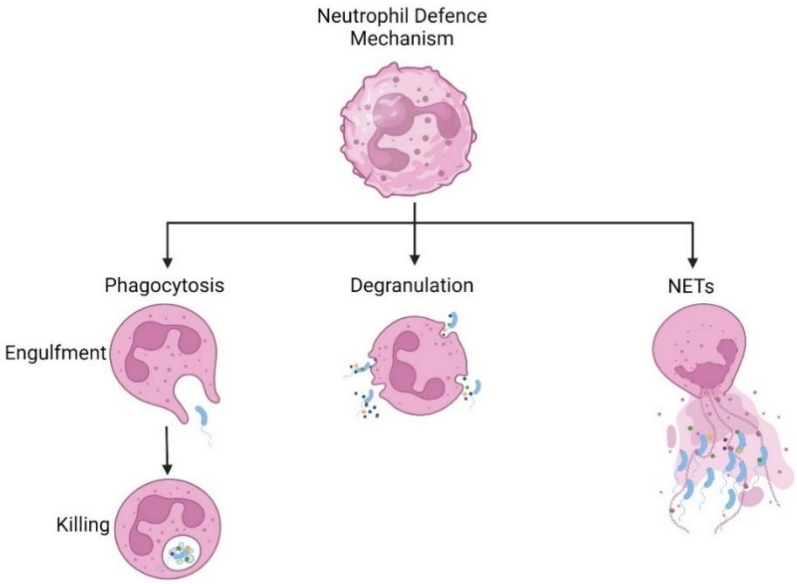

Figure 1.7: The three major killing mechamisims mediated by neutrophils. Phagocytosis is the process of engulfing and killing pathogens. Degranulation causes the release of the neutrophil granules. Neutrophil extracellular traps (NETs) are released and contain chromatin and antimicrobial agents to ensnare and kill pathogens. The figure is modified using BioRender Software based on “Neutrophil recruitment and function in health and inflammation” By Kolaczkowska et al. [189].

1.11.2 Chemotaxis

Neutrophil chemotaxis is the process of migration to the infected site of the tissue [193]. Normally, neutrophils do not interact with the vessel wall. However, during tissue infection, adhesion of neutrophils to the endothelial cells of blood vessels occurs due to the interaction between the adhesion receptors of neutrophils and endothelial cell ligands, followed by activation of neutrophils and extravasation and migration to the infected site through the basement membrane (Figure 1.8) [194]. Selectins are glycoprotein molecules known as surface adhesion molecules and include E-selectin which is expressed on activated endothelial cells, L-selectin that is expressed on leukocytes, and P-selectin which is expressed on both activated platelets and endothelial cells [195]. Chemokines and inflammatory mediators that are produced at the infected site, such as TNF-α, IL-8, C5a and others, induce transient neutrophil adhesion via inducing selectin expression, and results in neutrophil rolling [196, 197]. Also, cytokines and chemokines control the activation and migration of neutrophils to the specific locality within the infected tissue [198]. Activated neutrophils enhance the expression and function of β1 and β2 integrins to mediate firm adhesion. Firm adhesion is mediated by several proteins of β2 integrin family such as Lymphocyte function-associated antigen-1 (LFA-1 or CD11a/CD18) and macrophage-1 antigen (Mac-1 or CD11b/CD18) that contributes to arrest of neutrophil rolling on endothelial cells [199, 200]. CD11b/CD18 expression has been indicated to be increased during inflammation in traumatic and thermal injuries as it has an important role in mediating firm adhesion of neutrophils to the endothelium [201].

Moreover, CXC chemokine receptor 2 (CXCR2) is a transmembrane G protein–coupled receptor that is multi-functional in promoting neutrophil function including degranulation, phagocytosis, integrin activation, phagocytosis, respiratory burst, cell

movement, and transmigration [202]. CXCR2 is a key chemokine receptor that therefore promotes neutrophil adhesion [203].

Neutrophils transmigrate from venules into the narrow pathways between endothelial cells to the infected site, which is induced and controlled by chemokines and cytokines [197]. Neutrophil transmigration also requires chemoattractants that promote the process successfully. Formyl– methionyl–leucyl–phenylalanine (FMLP), C5, IL-8, and leukotriene B4 are involved in transmigration via stimulation of chemokine receptors that are expressed on the neutrophils [83]. Furthermore, C5aR (CD88) and CR1 receptor (CD35) on neutrophils are complement receptors and have a critical role in neutrophil chemotaxis, degranulation, and microbe recognition during inflammation. [204].

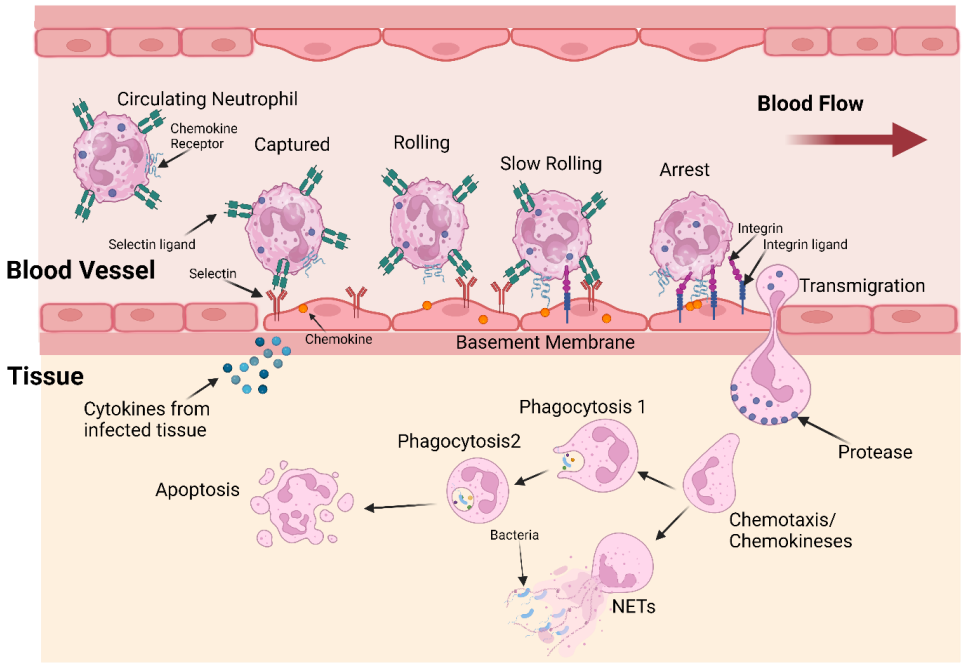

Figure 1.8: Neutrophil chemotaxis occurs in response to infection. Cytokines, chemokines, and lipid mediators activate vascular endothelial cells that lead to expression of chemokines and selectins on their surfaces. Activated neutrophils bind to selectins by their ligands and start rolling on the endothelial cells through their interaction with selectins. The rolling of neutrophils is slowed down by integrins, which are stimulated by chemokines and selectins, until neutrophils become arrested. Also, integrins mediate neutrophil crawling through endothelial cells and the vascular basement membrane. Then, neutrophil transmigration begins at the junction of endothelial cells. Neutrophils release protease enzymes that enable them to transmigrate to the extravascular space. After that, the neutrophils track a chemoattractant gradient until they reach the infected tissue site and initiate attacking pathogens through phagocytosis and NETs release. Pathogens are killed by granulocyte contents and by released ROS. Finally, the neutrophils are eliminated by apoptosis. The figure has been modified using BioRender Software based on Figure 1 of “Re-Examining Neutrophil Participation in GN” By Caster et al. [205].

1.11.3 Phagocytosis and Exocytosis

Phagocytosis is an essential function of neutrophils that contributes to killing bacteria [206]. Neutrophils can kill bacteria very fast within minutes. Furthermore, a single neutrophil can kill more than 50 bacteria [207]. Neutrophil antimicrobial killing can be

performed by direct engulfment of bacteria or by releasing of neutrophil enzymes in order to kill bacteria [208]. Neutrophils have the ability to identify and recognise pathogens through toll-like receptors (TLR) which are expressed on their surface, such as TLR-2 and TLR-4 that recognise gram-positive and gram-negative bacteria respectively [209]. Also, Neutrophils express Fc receptors (such as CD16, and CD32) and complement receptors (for example; CD35, and CR3) which enhance phagocytosis [210].

The process of phagocytosis after engulfment delivers the pathogen to the phagosomal lumen to initiate killing. At the phagosomal lumen wall, the nicotinamide adenine dinucleotide phosphate (NADPH) oxidase allows the production of ROS, creating a toxic medium for the engulfed pathogen [199]. The neutrophil pH also regulates the phagocytosis process and enzyme activity including Myeloperoxidase (MPO), cathepsin G, and elastase [211, 212].

Degranulation (exocytosis) occurs when the neutrophils translocate their granules to the plasma membrane resulting in their expression on the cell surface or release into the local environment [208]. Exocytosis is activated by various mediators such as immunoglobulin G (IgG), N-formyl-methionyl-leucyl-phenylalanine (FMLP), Ca^{2+}, guanosine triphosphate (GTP), and hydrolysis of adenosine triphosphate (ATP) [213, 214]. Upon exocytosis, neutrophils release antimicrobial proteins, enzymes (such as elastase), and ROS for the purpose of the extracellular killing of pathogens [214].

1.11.4 Apoptosis

Aged neutrophils can also undergo apoptosis or programmed cell death, in the absence of either pathogen agents or cytokines, before their removal by macrophages [215]. Neutrophil apoptosis prevents the uncontrolled release of cytotoxic components

of neutrophils to the extracellular environment [216]. Death of neutrophils occurs spontaneously within hours to days through apoptosis and their lifespan can be extended or shorted by modulating apoptosis agents [217]. Neutrophil apoptosis is influenced by several inflammatory modulating agents such as LPS, GM-CSF, and TNF-α that have a capacity in increasing the tyrosine phosphorylation for various proteins that regulate the extracellular signals [215]. Also, neutrophil apoptosis can be stimulated by either extrinsic (such as TNF-α) or intrinsic pathway stimuli (such as ROS or release of cytochrome C into the cytosol) [218, 219]. Apoptotic neutrophils are subsequently phagocytosed by macrophages for the benefit of eliminating inappropriate inflammatory responses [220].

Bcl-2 protein members such as anti-apoptotic (Mcl-1, Bcl-XL) and proapoptotic (Bad, Bax) agents are involved in neutrophil apoptosis regulation [221]. Mcl-1 has a dynamic function in the control neutrophil apoptosis [222]. Mcl-1 expression prevents apoptosis and extends the lifespan of neutrophils during infection and immune response status [223]. Also, other Bcl-2 members such as the proapoptotic Bax-α and the antiapoptotic Bcl-XL can regulate neutrophil apoptosis [217]. Inappropriate neutrophil apoptosis could result in negative outcomes and promote disease.

1.11.5 Neutrophil action in sepsis during trauma and burns

Neutrophils migrate in response to the infection through the coordinated process that has been outlined above. Upon neutrophil arrival to the infected site, neutrophils perform a variety of defence mechanisms for killing and eliminating pathogens. Microbes are recognized by the neutrophil receptors, followed by producing inflammatory chemokines and cytokines, oxidant generation, and initiating killing of microbes by phagocytosis, degranulation, and NET generation [197].

Neutrophil morphological changes have been indicated after trauma that includes increases in cell size, membrane flexibility, and shape modification that led neutrophils to be elongated [183]. Neutrophil transmigration within blood vessels toward the infected site involve interactions between the neutrophil and different components on endothelial cells and pericytes in the presence of mediators also leading to changes in neutrophil morphology [224]. For example, activated complement C5a has been demonstrated to contribute to neutrophil morphological changes through increase the cell membrane elasticity and the cell size by cytoskeleton polymerization, thus regulating neutrophil migration to the infected site [225].

However, migration of neutrophils to the tissues in trauma and burns is associated with rapid granulopoiesis resulting in changes in neutrophil heterogeneity that is characterized by either low density neutrophils (LDNs), immature granulocytes (IGs) low density granulocytes (LDGs), granulocytic-myeloid derived suppressor cells (GMDSCs), or immunosuppressive neutrophils [226]. Neutrophil heterogeneity also causes impaired defence and immune function. For instance, LDNs which are mononucleated neutrophils can be found during trauma and expresses arginase activity at a high level that could link to the function of T-cells leading to impaired immunity [226, 227].

In septic burns and trauma, neutrophils have a dual function in the pathophysiology of sepsis, acting as essential mediators of antimicrobial defence while also contributing to organ dysfunction. Dysregulated neutrophil activity in sepsis may trigger adverse effects on host tissues by releasing proteases and pro-inflammatory mediators, exacerbating systemic inflammation [228]. Impaired neutrophils function by disrupting their ability to perform critical processes such as phagocytosis, chemotaxis, ROS production, and the formation of NETs, limiting pathogen clearance, increasing the risk

of secondary infections and exacerbating immunological dysregulation [229, 230]. Impaired neutrophils exhibit a reduced chemotactic distance and a lower number of cells capable of responding to signals, which hinders their ability to reach injured sites [231]. Furthermore, neutrophil accumulation of diverse organs during the initial phase of the burn indicates that they may serve as a source of ROS. The generation of ROS subsequent to a severe burn may inflict compromise on peripheral organs. The inflammation caused by a burn injury is also present in uninjured tissues, disrupting the balance between ROS generation and elimination, thus leading to oxidative stress that exacerbates endothelial damage, induces microvascular thrombosis, and impairs tissue perfusion [232]. Dysregulated neutrophil function can transition from protective to pathogenic, resulting in systemic inflammation, coagulopathy, and MOF. Furthermore, dysregulated neutrophil hyperactivation and excessive NET formation might facilitate immunothrombosis, coagulopathy and DIC [233].

1.11.6 Neutrophil dysfunction in trauma and burns

Multiple neutrophil abnormalities have been reported in patients with burns and trauma in the immune response to the infection site but also in the attacking and killing bacteria mechanisms [234]. Neutrophil dysfunction is therefore a problem that may impact upon immune dysfunction in trauma and burns.

1.11.6.1 Dysregulation of Chemotaxis

Adhesion abnormalities of activated neutrophils during migration have been observed in septic patients due to impaired expression of adhesion molecules or chemotaxis signalling that can lead to neutrophil paralysis [235]. Subsequently, these paralysed

neutrophils can reverse migrate and reflow into the circulation resulting in organ damage of internal organs such as the liver, kidneys, and lungs [236]. The causes of neutrophil paralysis are not fully understood. The occurrence of neutrophil paralysis and dysfunction of adhesion could also be due to successful bacterial immune evasion mechanisms through disruption of the orientation of activated neutrophils away from infected site [234]. CXCR2 has been observed to be reduced in patients with severe sepsis [237]. Tarlowe et al. (2005) illustrated that downregulation of CXCR2 during severe inflammation leads to hyporesponsiveness to IL-8 in traumatic patients [238]. This suggests that reduced CXCR2 can affect neutrophil adherence which contribute to MOF [239].

1.11.6.2 Dysregulation in ROS generation

Dysregulation of the immune response in sepsis in the presence of cytokines and ROS released by circulating activated neutrophils at distal sites to the main infected tissue can also lead to MOF [239]. In addition, neutrophils produce immunosuppressive phenotypes in states of immaturity and altered expression of cytokines [204]. It is being considered that the immunosuppression that is induced by sepsis is now a clinical syndrome for survivor patients, with increased risk of recurrent hospital admissions and mortality [240].

The phosphatidylinositol-3-kinase (PI3K) pathway plays a critical role in regulating several cellular processes that include cell proliferation, differentiation, and inflammatory responses [241]. PI3K is an intracellular signalling in neutrophils and contributes to their chemotaxis and accumulation at the infected site [242]. During severe sepsis, activated PI3K pathway signalling leads to suppression of nuclear factor kappa-light-chain-enhancer of activated B cells (NF-κB) proinflammatory

mediators' responses such as the production of cytokines, respiratory burst, and enhancement of apoptosis resistance [241]. Activation of the PI3K family member (PI3K-Akt) pathway has been reported as a negative regulator. It acts on the suppression of LPS and TNF-α production and nitric oxide synthase induction [243].

ROS is normally released by cells including neutrophils as a defence response and promotes dysfunction of endothelium by oxidation of cellular signalling proteins, for example, tyrosine phosphatases [244]. Uncontrolled and overproduction of ROS results in organelle and cell membrane damage that causes metabolic and structural dysfunction of neutrophils [244]. It has been reported that burns and traumatic patients with sepsis produce abnormal ROS levels in contrast to healthy volunteers as controls [245]. Therefore, uncontrolled ROS production increases mortality risk as it contributes to neutrophil dysfunction and organ dysfunction [234].

Furthermore, excessive levels of ROS lead to tissue injuries, which can be through peroxidation of the lipid membrane and induce acute organ inflammation [246]. Ogawa et al. (2008) have reported that spontaneous production and circulated ROS are higher in elderly patients than in younger patients, which could reflect changes in age-associated immune dysregulation [247].

1.12 Neutrophil Extracellular Traps (NETs)

1.12.1 NETs Structure and Function

NETs are extracellular fibres generated by activated neutrophils and are composed of granular and nuclear components [248]. Brinkmann et al. (2004) first described the unique structure of NETs consisting of smooth fibres with a diameter of 15-17 nm and globular domains between 25 and 28 nm. The fibres consist of neutrophil DNA with embedded proteins such as elastase, cathepsin G, and myeloperoxidase from the

primary granules and lactoferrin and gelatinase from the secondary and tertiary granules, respectively. The major component of NET structure is chromatin or DNA, as the structures can be disintegrated by treatment with deoxyribonuclease (DNase). In addition, nuclear histones (H1, H2A, H2B, H3, and H4) are also important structural components that have role in DNA packaging and compaction [249]. As the main function of the neutrophils is the first line of defence in microbe elimination, NETs are a newly described method for ensnaring and killing infections [250].

1.12.2 Molecular basis of NET generation

During inflammation, NET generation is stimulated in response to different agents that include pro-inflammatory mediators such as IL-8 and LPS, and microbes such as bacteria or fungi [251]. The formation of NETs is activated by several mediators that induce NETosis by several processes. MAC-1 integrin has been indicated as an initial mediator by changing cytoskeletal morphology of the neutrophil as a prelude to facilitating the breakdown both of nuclear and plasma membranes for releasing NETs [252]. ROS also contributes to NET formation as an initial mediator. Fuchs et al. (2007) have illustrated that activated neutrophils generate a high level of ROS by activation through NADPH oxidase resulting in the release of NETs [253]. Activated neutrophils also become flat and adhere to the substratum [254]. After that, the nucleus chromatin undergoes de-condensation mediated by the actions of NE and MPO destroying the core histones linkages such as H1 and H3 [255]. This allows the outer and inner membranes to separate gradually from each other [254]. Finally, the nuclear membrane is subsequently damaged which leads to chromatin expansion and then extracellular ejection which will be then mixed with granular antimicrobial factors. [250].

NETosis is the term that is used for describing neutrophil cell death by NET generation as a host defence mechanism [256]. NETosis has been described as the disruption of the nuclear membrane through the mechanism of cell death that is termed “Suicidal NETosis” [257]. However, it has been demonstrated that NET formation is not caused by necrotic or apoptotic mechanisms [258]. NETs can also be formed with maintenance of normal neutrophilic functions that include chemotaxis and phagocytosis and this is termed “Vital NETosis” [259].

Mitochondrial NETosis is a recent discovered NETosis pathway that highlights the involvement of mitochondria in NET generation [260]. The creation of ROS in the mitochondria and the release of mitochondrial DNA (mtDNA) are essential for the formation of extracellular traps in this pathway [261]. All mechanisms of vital, suicidal, and mitochondrial NETosis play an important role in the elimination of microorganisms [259, 262].

1.12.2.1 Vital NETosis

The vital NETosis pathway can be triggered by stimuli such as LPS from Gram-negative bacteria and lipoteichoic acid (LTA) from Gram-positive bacteria, IL-8, TNF-α, granulocyte-macrophage colony-stimulating factor (GM-CSF), macrophage inflammatory protein (MIP) and through platelet-neutrophil interaction. These stimuli cause changes in the structure of the cell's cytoskeleton in neutrophils, without activating NADPH oxidase. This results in vesicle generation that contain antimicrobial proteins and chromatin [263-265]. LPS stimulates host recognition receptors to induce rapid vital NETosis [266].Toll-like receptors (TLR) such as TLR4 have been described molecular patterns that induce vital NETosis formation [267]. Neutrophils can distinguish between LPS serotypes from different bacterial sources due to structural

variations of lipid A in the LPS. These differences influence the activation of TLR4 and initiate various signalling pathways, including the mitogen-activated protein kinase (MAPK) pathway. As a result, neutrophils release NETs that are unique to specific bacterial serotypes. However, platelets enhance this response by boosting neutrophil activation through P-selectin interactions. This amplifies LPS-induced NET formation and strengthens the immune defence against particular pathogens [268]. Vital NETosis also facilitates rapid effective defence against microbes in the bloodstream and tissues [263]. Vital NETosis is characterised by rapid NET formation occurring between 5 and 60 minutes [266, 269]. Pilsczek et al. (2010) demonstrated that NETs can form within 10 minutes when neutrophils are stimulated by staphylococcus aureus [269]. This rapid process of vital NETosis requires efficient trafficking of the DNA from the intracellular (nucleus) to the extracellular environment [266].

1.12.2.2 Suicidal NETosis

NET formation has described as suicidal NETosis that is distinct from both necrosis and apoptosis [253]. NETs formation occurs by changing the morphology of the nucleus through decondensation and eventual release and externalisation of chromatin [266]. Suicidal NETosis is a NADPH oxidase-dependent pathway that can be induced by pathogens, cytokines, inflammatory mediators and phorbol 12-myristate 13-acetate (PMA). These stimuli trigger the activation of NADPH oxidase, an enzyme complex responsible for generating ROS within the neutrophil promoting chromatin decondensation and the breakdown of nuclear and granular membranes [253, 269, 270]. Suicidal NETosis is caused by the nuclear translocation of NE and MPO causing histone degradation that leads the decondensation of the chromatin and ending with membrane disruption and NET release [271]. PMA has been reported as an in vitro

stimulating agent for NET generation [253]. PMA and IL-8 also contribute to NETosis with the DNA covered with histones and neutrophil elastase (NE) [263]. Interestingly, Abrams et al. (2019) have demonstrated that high levels of IL-8 plasma in patients with trauma significantly contribute in NET generation when incubated with purified neutrophils, and NET formation is substantially blocked by inhibiting IL-8 [272].

NADPH oxidase produces ROS as an initial mediator that leads to chromatin decondensation, NE and MPO degradation of histones linkages which facilitate the web of DNA to be mixed with the granules, followed by releasing of NETs through the membrane to the extracellular environment. The suicidal NETosis process requires between 120 to 140 minutes to be occur which takes significantly longer than vital NETosis [266].

1.12.2.3 Mitochondrial NETosis

Mitochondria are organelles located within cells that carry out a range of vital functions and main sources of cellular energy and also produce many biosynthetic intermediates such as lipids, and amino acids [273]. Additionally, they play a role in cellular stress responses, including apoptosis, innate immunity, and hypoxia. In addition to its intracellular functions, mitochondria can also impact an organism's physiology by controlling communication between cells and organs [274].The initiation of mitochondrial NETosis generally involves the stimulation of neutrophils by pathogens, inflammatory cytokines, stress within the mitochondria, or tissue damage, among other stimuli. NETosis initiation is the result of a sequence of intracellular events triggered by activation signals [262, 274, 275].

Mitochondrial NETosis refers to mitochondrial DNA (mtDNA) being released along with other components of NETs [261]. While classical NETosis is mainly dependent

on the expulsion of nuclear DNA, additional studies have shown that mitochondria can also play a role in the formation of NETs under specific circumstances [261, 264, 276]. Activated neutrophils undergo metabolic reprogramming, increasing mitochondrial ROS generation, which is essential for mitochondrial NETosis. High mitochondrial ROS levels can damage and permeabilise the mitochondrial membrane. This releases mtDNA into the cytoplasm. NET-related proteins such as histones, elastase, MPO interact with mtDNA in the cytoplasm. These interactions help mtDNA bind to neutrophil chromatin and other granular proteins [277]. In essence, two distinct mechanisms of mtDNA exteriorization are suggested: (A) an initial release into the cytosol, followed by vesicle fusion with the plasma membrane, wherein the DNA is externalised; and (B) fusion between the plasma membrane and mitochondria, resulting in the direct release of the DNA content into the extracellular environment. The second mechanism has not been conclusively demonstrated [278]. The differences between vital, suicidal, mitochondrial NETosis pathways in NET formation are illustrated in Figure 1.9 and Table 1.5.

The mechanisms governing the development of NETosis pathways in injured patients remain incompletely understood. However, evidence suggests that NETosis is influenced by the type and severity of stimuli, the immunological microenvironment, and the phase of the immune response. Vital NETosis occurs during the early stages of infection or inflammation, enabling neutrophils to release NETs while maintaining their viability [263, 279, 280]. In contrast, suicidal NETosis mostly been triggered by chemical stimulants such as PMA. Despite this, suicidal NETosis was observed in advanced stages of infection or inflammation, characterized by neutrophil death to release NETs, typically triggered during severe inflammatory conditions such as chronic granulomatous disease (CGD) and preeclampsia [253, 280, 281]. Finally,

mitochondrial NETosis promotes NET formation and maintains neutrophil functionality by releasing mitochondrial DNA. This process is linked to mitochondrial stress and is crucial in chronic inflammatory diseases and autoimmune disorders like systemic lupus erythematosus (SLE), as well as in elderly trauma patients [282-284].

Table 1.5: Comparisons between vital, suicidal, and mitochondrial NETosis [261, 263, 266, 278].

Properties of NETs	Vital NETosis	Suicidal NETosis	Mitochondrial NETosis
The nature of stimulus	LPS, LTA, TNF-α, and GM-CSF	PMA, IL-8	pathogens, inflammatory cytokines, and stress
Formation time	Minutes (5-60 minutes)	Hours (120-140 minutes)	15 minutes to 3 hours
The mechanism employed for NETs releasing	Needs to smuggle the DNA to the extracellular environment by DNA vesicular trafficking from nuclear envelope, cross through the cytoplasm and the plasma membrane.	Requires NADPH oxidase, MPO and NE mediators to complete the NETs formation process	High mitochondrial ROS levels
Fate and Function	Maintain the integrity of membrane and can still capture bacteria	Cell Death	Maintain the integrity of membrane

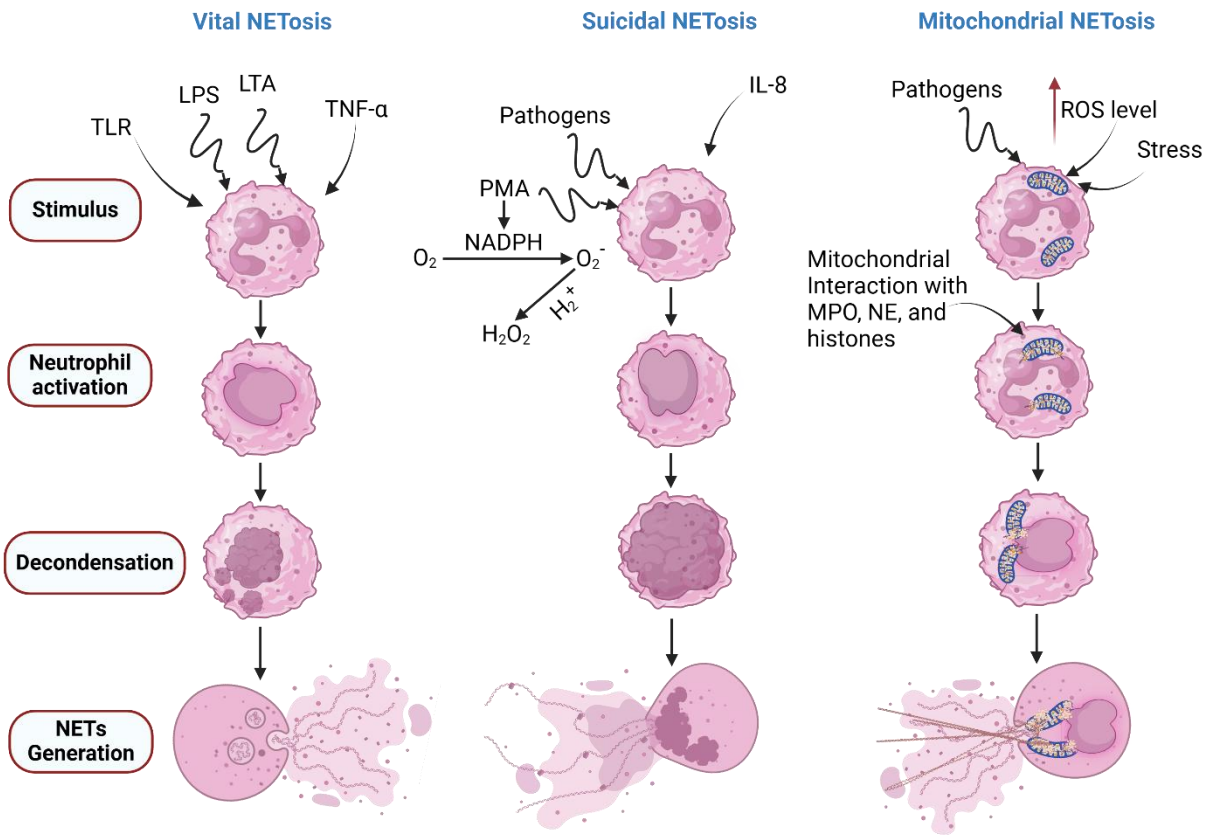

Figure 1.9: NET formation pathways. NETS generation can occur through three different pathways; vital, suicidal, and mitochondrial NETosis. Vital NETosis can occur either by released LPS or LAT from bacteria, released TNF-α, or by the interaction between TLR4 activation of platelets and subsequent binding with CD11a on neutrophils, or activation of TLR2 and CR3 in the presence of pathogens such as E. coli and staphylococcus aureus. The nucleus loops become aggregated, becoming round in shape and then decondensed DNA and vesicles are formed. Finally, NETs are released via nuclear budding of vesicles and the neutrophil still maintains its outer membrane for the purpose of capture bacteria. Suicidal NETosis pathway is initiated by either PMA, IL-8, or pathogens. NADPH oxidase acts in releasing NETs. Translocation of NE, MPO, and cathelicidin antimicrobial peptides (LL-37) lead to chromatin decondensation, and nuclear membrane disruption. The nucleus contents are mixed with granular proteins. NETs are extracellularly released through the outer membrane rupture and neutrophil cell death subsequently occurs. Mitochondrial NETosis caused by either neutrophils response to infection or stress within mitochondria. ROS Levels increase lead to mitochondrial membrane rapture and mtDNA release to the cytoplasm. Interactions occur between mtDNA and histones, MPO, and NE help to bind with other granules protein, followed by mtDNA and vesicle fusion through the plasma membrane. The figure has been modified using BioRender software from Figure 2 of " How Neutrophil Extracellular Traps Become Visible " by de Buhr et al. [257] and Figure 6 of “New Perspectives on the Importance of Cell-Free DNA Biology” by Bronkhorst et al. [285].

1.12.3 Histones

Histones are proteins with a cationic charge and consist of four subgroups which are H1 as a linker histone, H2 (H2A, and H2B), H3, and H4 [286]. Histones play an important role in DNA packaging and compaction [287]. Mostly, the DNA of eukaryotes are super-coiled by the histones that leads to formation of nucleosomes in which histones regulate DNA replication, transcription, and repair [288]. Approximately 147 base pairs of the DNA is wrapped twice around a histone core (H2A, H2B, H3, and H4) [289]. H1 is the linker that binds the entry and exit points for the wrapped DNA with histone core [290]. All histones have N-terminal tails that are extended from the core structure and rich in residues of the amino acids of lysine and arginine. These amino acids are characterized by flexibility that undergoes post translation modifications such as methylation that regulates chromatin function, ubiquitination, acetylation and phosphorylation that play a role in gene regulation and replication [291]. Although, histones are important in the packaging of DNA into the nucleus, extracellular histones exhibit significant immunostimulatory and toxicity effects. When histones are released during tissue injuries, extracellular histones contribute to cellular damage and can cause organ dysfunction [292].

1.12.4 The Role of Histone Modifications in NET Formation

Histone modifications regulate de-condensation of chromatin during NETosis. Histone citrullination is considered to facilitate de-condensation of chromatin during the process of NETosis [293]. For example, citrullination of H3 (CitH3) facilitates the rapid de-condensation of chromatin [294]. As histone modification regulates chromatin structure, it also controls nuclear functions. Peptidyl arginine deiminase 4 (PAD4) is a

nuclear enzyme that mediates gene expression through controlling arginine citrullination and methylation in histones [295]. PAD4 converts the histone's arginine residues to citrulline, lead to extensive de-condensation of chromatin resulting in dismantling and swelling of the nucleus through NETosis [296]. Histones have been considered to be highly toxic extracellularly to the surrounding space of released NETs and have the ability to enhance thrombosis [297]. Interestingly, CRP has been shown to neutralize histones. CRP binds to histones, which leads to the prevention of histone-induced calcium influx into cells, thereby reducing histone cytotoxicity [298]. In inflammation, NETs are produced in response to microbes which also can release histones during NETosis [292]. Extracellular histones can also be released from necrotic cells and contribute to endothelial cell dysfunction, organ failure, and mortality [299]. In addition, it has been reported that histones play a role in enhancing sterile inflammation through overproduction of cytokines by TLRs [300]. Extracellular histones can also prevent extracellular DNA degradation resulting in autoimmune stimulation, and formation of anti-nuclear antibodies [291]. Furthermore, it has been suggested that PAD-4 crucially contributes to the pathological events of venous thrombosis [297].

1.12.5 Cell Free Deoxyribonucleic Acid (cfDNA)

CfDNA are small fragments of DNA found circulating in the blood plasma or serum [301]. CfDNA can be released through several cellular processes, including necrosis, apoptosis, and by NETosis [302]. As NETs are composed of DNA, high levels of circulating cfDNA/NETs have been observed in septic patients [73]. Hampson et al. (2017) have shown that plasma and serum cfDNA levels were significantly elevated in burns patients with sepsis at days 7 and 14 postburn comparing with healthy

volunteers and non-septic patients. The study suggested that cfDNA could be used as a diagnostic/prognostic biomarker for sepsis in patients with burns [74]. The average level of cfDNA has been reported in healthy individuals between 42.1 and 111.5 ng/ml. In contrast, in septic patients cfDNA levels were significantly higher by more than 10 fold (between 1160 and 2240 ng/ml) [240]. Additionally, Meng et al. (2012) and Altrichter et al. (2012) have demonstrated that the cfDNA levels are elevated after major trauma and burns and are persistently high for all measured time points up to days 7-10 post-injury, respectively [73, 303]. This suggests that cfDNA can be a potential marker in determining the severity of inflammation among traumatic and burns patients.

1.12.6 NETs in trauma and burns

NETs are one of the key neutrophil defence mechanisms in killing and eliminating microbes. NETs are often released during severe trauma and burns as a response to sterile injury and subsequent infection [73, 304]. It has been reported that NETs can be generated within < 60 minutes at the local site of sterile injury and inflammation [305]. However, high cfDNA levels might increase the mortality risk in patients with burns and trauma. Margraf et al. (2008) have illustrated that patients with multiple trauma have been observed with a significant high level of cfDNA, and those who were diagnosed with more than 800 ng/ml of cfDNA have subsequently correlated with sepsis, MOF, and death [306]. Additionally, Altrichter et al. (2010) have shown that 7 of 37 patients with severe burns died during the first month of burns injuries, where they have been evaluated with significantly high cfDNA levels [73]. Despite the importance of NETs in fighting microbes, NETs can also contribute to further complications such as DIC and MOF, particularly through excessive NETosis. To

mitigate the pathogenic consequences of NETs, recombinant human deoxyribonuclease I (DNase I), commonly known as dornase alfa, has been utilised to degrade extracellular DNA. By breaking down NETs in pulmonary secretions, dornase alfa has shown promise in clinical trials for reducing mucus viscosity in patients with cystic fibrosis. This therapeutic approach highlights the potential of DNase-based treatments for managing NET-related complications in various inflammatory disorders [307].

1.12.7 Excessive NETosis

Despite the improvement in survival rate in burns and traumatic patients, sepsis and MOF remain a significant problem for increasing mortality. Regardless of the primary function of NETs in defence against microbes, excessive NETosis can also play a negative role within infected patients. Excessive NETosis has been shown to induce MODS in several conditions [308]. Excessive NETosis contributes negatively to several diseases including ARDS and cystic fibrosis, and can also induce immunothrombosis, diabetes, SLE, and Rheumatoid arthritis (RA) [309]. Excessive NETosis results in circulating cfDNA that could be directly associated with the occurrence of main organ failure. Tanaka et al. (2014) have illustrated that cfDNA is not only elevated in plasma but increased in the lung pulmonary capillaries and postcapillary venules of hepatic sinusoids [311]. NET-released chromatin within capillary plexi within organs has been suggested to not only disturb blood flow but also cause tissue hypoxia and MOF [312]. Czaikoski et al. (2016) have shown evaluated the correlation between NET levels in blood and MODS occurrence in septic patients and mice. Elevated NET levels in the blood contribute to the pathological complications that leads to MODS. NET degradation using recombinant DNase

reduces organ failure and endothelial cell damage [308]. Although previous studies have illustrated the significant importance of cfDNA in monitoring sepsis and inflammation severity, measuring circulated large fragments of cfDNA in whole blood is also important for evaluating excessive NETosis post-injury and understanding their contribution to MODS and DIC. Otawara et al. (2018) demonstrated circulating NET chromatin derived from neutrophils in blood circulation after major burns in rat models using a microfluidic assay [313]. Moreover, Sakuma et al. (2022) demonstrated the presence of circulating large chromatin fragments in treated whole blood with PMA *in vitro* using a microfluidic assay designed to capture circulating NETs [314]. It is therefore important to understand NET complexity and distinguish its formation and function in healthy and in pathological inflammatory responses, and as a potential biomarker of sepsis and poor outcomes.

1.12.8 Platelet-neutrophil interactions

Although neutrophils and platelets play important roles in inflammation and host defence, platelets can form complexes with neutrophils when stimulated appropriately. Platelet-neutrophil interactions can be measured in several conditions, including inflammation and sepsis [315]. Platelets have also been recently demonstrated as a key stimulator of NET formation in which platelet TLR4 contributes to NET generation to ensnare pathogens [258]. Platelets promote vital NETosis by acting as immune sentinel cells for infections. Stimulation of platelet TLR4 by LPS induces platelet activation to promote platelet-neutrophil complexes by binding of platelet P-selectin to neutrophil P-selectin glycoprotein ligand-1 (PSGL-1). The interaction is further stabilised through platelet glycoprotein Ibα interactions with neutrophil MAC-1 [315].

In addition, other platelet receptors, including CD40 ligand (CD40L) and glycoprotein αIIbβ3, facilitate platelet interactions with neutrophils, promoting NETosis [316, 317]. However, platelet neutrophil interactions have also been indicated by significantly contributing to the initiation of thrombosis through NET generation. NETs that are formed in vasculature can also further interact with circulating platelets, leading to platelet adhesion and activation, which causes thrombosis [318]. In addition, NETs can also promote thrombus formation through binding of tissue factor (TF), FXII, and VWF [315]. Savchenko et al. (2014) have investigated patients diagnosed with venous thromboembolism (VTE) including deep vein thrombosis (DVT) and pulmonary embolism (PE). The study indicates that NET accumulation with the presence of histone H3 enhances the organisation and formation of thrombi [319]. Furthermore, degrading NETs has been reported in thrombolysis in mice by the action of DNase [320]. It has illustrated that DNase I promotes NET degradation and thrombolysis [321]. Although it is clear that NETs have a positive effect on the defence against microbes, they are double-edged swords and excessive or untimely NETosis may promote venous thromboembolism and/or MODS/MOF. This opens up the possibility of using anti-NET therapies e.g., DNase to treat DVT and MOF.

1.12.9 Solute Carrier Family 44 Member 2 (SLC44A2)

Solute Carrier Family 44 Member 2 (SLC44A2) is a choline transporter protein and represents the human neutrophil antigen-3 (HNA-3 antigen) as a target for alloantibodies in transfusion medicine [322]. The location of SLC44A2 is on chromosome 19p13.2 and involves 22 exons but with two isoforms SLC44A2-1 and SLC44A2-2 that differ from each other by an amino acid substitution at the position 461 of exon 7, in which the genetic code substitution of Arg154 represents SLC44A2-

1 (HNA-3a) and Gln154 represents SLC44A2-2 (HNA-3b) [323]. Structurally, SLC44A2 consists of 10 domains spanning the membrane, with interconnected intracellular and extracellular loops [324]. Furthermore, the incidence of the single nucleotide polymorphism (SNP) indicative of both SLC44A2-1 and SLC44A2-2 alleles have been measured in several populations, including African American, Caucasian, Han Chinese, Thai, Japanese, Brazilian, and Tunisian etc [323].

The function of SLC44A2 is yet to be fully defined. However, its deficiency causes spiral ganglion degeneration, loss of hair and hearing in mice [325]. Also, SLC44A2 deficiency has been associated with transfusion-related acute lung injury and Meniere disease in humans [324].

Moreover, several studies have explored the potential role of SLC44A2 in thrombosis. Tilburg et al. (2018) have evaluated the role of SLC44A2 in haemostasis using mice lacking SLC44A2 (SLC44A2-/-) and SLC44A2-positive mice (SLC44A2+/+). They induced vascular damage in muscle arterioles using laser damage and observed impaired fibrin accumulation in SLC44A2-/- mice, particularly those with an FVB background. Additionally, SLC44A2-/- mice with a B6 background exhibited diminished platelet accumulation and impaired response to injury compared to SLC44A2+/+ mice. These findings suggest SLC44A2 may play a role in the haemostatic response to injury [322].

Similarly, Zhi et al. (2020) assessed 18 SNPs in 2,655 individuals, finding SNP rs2288904 of SLC44A2 significantly associated with heightened risk of post-orthopaedic surgery DVT. This SNP, expressed in multiple tissues, correlated significantly with SLC44A2 expression levels, highlighting its potential role in DVT susceptibility [326]. Tilburg et al. (2020) further explored the role of SLC44A2 in VTE using SLC44A2-deficient mice in two separate VTE models: a hypercoagulability

model induced by small interfering ribonucleic acid (siRNA) and a flow restriction (stenosis) model. In the hypercoagulability model, SLC44A2 deficiency did not affect initial VTE outcomes but led to decreased plasma fibrinogen and VWF levels alongside increased blood neutrophils compared to wild-type mice. In the stenosis model, SLC44A2-deficient mice exhibited significantly smaller thrombi, suggesting a potential role for SLC44A2 in VTE pathogenesis, particularly in neutrophil-dependent mechanisms [327].

Regarding the previous studies, several possibilities that involved SLC44A2 in thrombosis. It is suggested that SLC44A2 is associated with the risk of DVT and VTE, while lacking SLC44A2 might be contribute to thrombosis defective upon injuries. It has been suggested that the risk of SLC44A2 for VTE could be due to platelet-neutrophils interactions [327]. The glycoprotein αIIbβ3 is an integrin family member present on the platelet plasma membrane as a transmembrane protein [328]. αIIbβ3 is the major integrin expressed on platelet membrane and plays an important action in platelet aggregation and clotting [329]. αIIbβ3 is activated by, thrombin, adenosine diphosphate (ADP), and thromboxane A2 through signalling pathways of G protein-coupled receptors [330]. Constantinescu-Bercu et al. (2020) found that VWF binding to platelets primes them to facilitate platelet-neutrophil interactions via αIIbβ3 activation on the platelet surface subsequently binding to SLC44A2 on neutrophils. This process leads to neutrophil extracellular trap (NET) formation, increasing blood clot size. Blocking αIIbβ3 reduces platelet-neutrophil interactions, while anti-SLC44A2 antibodies hinder neutrophil binding to platelets. Additionally, a mutation in SLC44A2 (SNP rs2288904-A) weakens its binding to αIIbβ3 [331]. These findings describe the critical key role of αIIbβ3 and SLC44A2 in platelet-neutrophil interactions, which could

be a novel therapeutic target to prevent thrombosis in burns and traumatic injury patients.

Furthermore, Bennett et al. (2020) explored the association between SLC44A2 and VTE. Their study revealed that SLC44A2 is expressed on human and mouse platelets and plays a role in VTE, regulated by platelet mitochondrial energy. SLC44A2 mediates choline transport into mitochondria, essential for ATP generation, with platelets lacking SLC44A2 showing reduced ATP production upon activation. The study suggests that defects in SLC44A2 may lead to low choline metabolism, potentially contributing to thrombosis. However, the exact function of SLC44A2 in thrombosis remains incompletely understood, necessitating further investigation into its role in haemostasis, NET formation, and thrombosis [332].

1.12.10 NETs Degradation

Once NETs are formed, it is important that they are cleared effectively through natural degradation mechanisms to prevent their dissemination and continued presence in the blood. DNase is found in the body fluids including serum and urine and acts to degrade DNA including NETs [303]. In vitro, incubation of NETs with DNase I results in the degradation of the majority of NETs (nearly 90%) [333]. Fuchs et al. (2010) have illustrated the dynamics of NET degradation by DNase 1. Incubation of NETs with DNase 1 in specific conditions release histones to the culture supernatant which indicate that DNase 1 separates the histones from the chromatin fibres resulting in the liberation of cfDNA. In addition, DNase 1 has been shown to inhibit platelet aggregation to the NETs [318]. However, patients with DNase 1 deficiency or impaired NETs degradation can suffer from the persistence of NETs that contribute to tissue damage and autoimmune diseases [334]. Impaired NET degradation have been

indicated in a group of patients with SLE, illustrating the presence of DNase I inhibitors [335]. It has been observed that circulating NETs are increased after burns and trauma injuries with reduced DNase activity. Also, it has been shown that treating the blood samples with excess DNase significantly degrades NETs [303, 313].

Moreover, DNase1-like 3 (DNase1L3) is a DNase member that play a role in apoptosis mechanisms through chromatin cleavage as described *in vitro* [336, 337]. DNase1L3 is produced and secreted mainly by macrophages in tissues and dendritic cells [338]. Lazzaretto et al. (2019) have shown that DNase1L3 has capability to degrade NETs in vitro [339]. In addition, Jimenez-Alcazar et al. (2017) have evaluated the role of DNase1 and DNase1L3 in NET degradation in a mice model. The study shows that NET formation led to intravascular clot formation in the absence of both DNase1 and DNase1L3 that subsequently led to occurrence of MOF and mortality [340].

Moreover, macrophages also have an important role in NET degradation through uptake and digestion [341]. Macrophages are distributed around the body tissues and recognised as effector cells in repairing tissue and for the resolution of inflammation [342]. Macrophages can be stimulated by endocrine and paracrine signals or directly stimulated through tissue surface receptors or immune cells during injuries [343]. Although DNase is important in NET degradation and can prevent intravascular thrombi formation by NETs, macrophages have also been described with a significant capability for NET degradation [344]. Haider et al. (2020) examined the role of macrophages in NET degradation by using human blood samples in vitro and murine models *in vivo*. The study shows that macrophages are able to degrade NETs dramatically and can be inhibited by preventing micropinocytosis [341]. DNase I has therapeutic advantages in the degradation of NETs and the mitigation of related

inflammation, considering that clinical use demands critical evaluation of its limits and possible harmful effects [307, 345]

1.12.11 Actin

Actin is abundant in the cytoskeleton and plays an important function in eukaryotic cell functions through maintenance of cell morphology, endocytosis and exocytosis trafficking, movement, motility, and cell division [346]. Actin can be found in two main states which are globular actin (G-actin) and filamentous actin (F-actin) that represent monomeric and helical polymer forms, respectively [347]. G-actin gathers into the polymers of F-actin, in which this form is highly regulated with an equilibrium depending on ATP [348]. Many complex activities of cells depend on G-actin and F-actin beside other proteins [349]. Binding of actin with ATP, the polymerisation results in G-actin to F-actin conversion and activates adenosine triphosphatase (ATPase) that activates the actin filament for motility [350]. Filaments also support internal mechanical mechanisms, intracellular material movement and cell motility [349].

However, the release of actin filaments into the circulation acts as a DAMP and is associated with several complications including hepatic necrosis, respiratory distress syndrome, and septic shock [351]. In addition, extracellular actin contributes to vascular dysfunction during tissue trauma [352]. Released actin is normally regulated by actin scavenging proteins which are vitamin D-binding protein (VDBP) and gelsolin that work together to remove actin from the circulation [351]. Major tissue damage following severe burns can release circulating actin excessively, in which this released actin from necrotic and damaged cells inhibits DNase I directly [353]. Thereby, DNase I activity can be protected or controlled by the actin scavenging system [354]. Bareyre et al. (2001) have illustrated that following brain trauma, actin is shown to be contribute

to DNase I inhibition [348]. Recently, Dinsdale et al. (2019) have shown that cfDNA accumulation following thermal injuries is due to the effect of actin on reducing DNase activity and that the scavenging system can also protect DNase 1 activity to prevent excessive NETosis and MOF [353].

The actin scavenging system consists of gelsolin and VDBP that have a critical role in rapid actin depolymerization and clearance of actin filaments from the circulation [355]. Gelsolin is an actin modulating protein that plays an important role in cytosolic transition through reducing the distribution of actin filaments [356]. Circulating gelsolin levels in healthy individuals are between 174 and 278 µg/mL and are decreased during severe injuries and inflammation [357] including in major trauma and burns [358]. It is suggested that reduced or depleted gelsolin is due its binding to extracellular actin after cell damage following major trauma and burns [359].

VDBP also called Gc globulin is a plasma protein that binds and transport vitamin D but is also involved in the actin scavenging system [360]. The normal circulating VDBP level is between 137 and 559 µg/mL [361]. VDBP levels can be increased due to pregnancy or decreased due to increased binding to actin in patients with liver failure, trauma, septic shock, and MODS [362, 363]. The role of gelsolin and VDBP is important in the clearance of extracellular actin through the mechanism of the actin scavenging system [364].

Lee et al. (1992) have described the role of actin scavenging system (Figure 1.10). The function of actin scavenging system is initiated by forming complexes of monomeric actin and gelsolin. The severing process begins through binding of gelsolin to F-actin which results in breakdown of the filaments to two separated fragments. Within the same time capping process is begun by gelsolin binding to the barbed ends of actin filaments. Both severing and capping processes depolymerize F-actin and

inhibit of additional monomers to F-actin. Then, it is followed by trapping actin monomers by VDBP within high affinity complex and cleared mainly by the liver, kidneys and spleen [351].

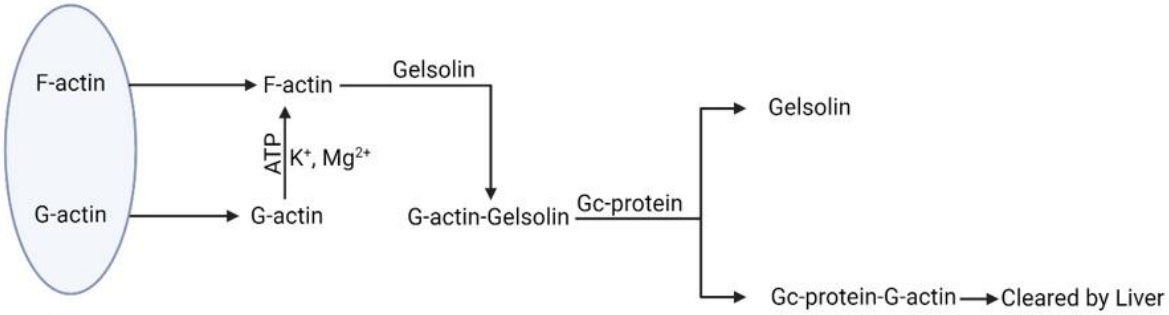

Figure 1.10: The actin scavenging system. Extracellular actin consists of filaments (F-actin) and monomers (G-actin). The scavenging system process is initiated by binding gelsolin to F-actin to liberate G-actin forming G-actin-gelsolin complexes. The G-actin-gelsolin complex interacts with VDBP (Gc-protein). Then, Gelsolin is liberated and VDBP traps G-actin to be removed by the liver. The scheme has been modified using BioRender software from Figure 1 of " The extracellular actin scavenger system in trauma and major surgery " By Benny Dahl [365].

1.13 Platelets in burns

Platelets are small blood cells generated from megakaryocytes in the bone marrow, playing a crucial role in sustaining haemostasis by promptly reacting to vascular damage, aggregating at the injured vascular site and promoting clotting to prevent and stop blood loss [366]. In addition to their function in haemostasis, platelets are essential for wound healing and the modulation of immunological responses. Platelets facilitate tissue repair and regulate inflammation at the injury site through the release of cytokines and growth factors [367, 368].

Following vascular injury, platelet activation constitutes a crucial initial phase in haemostasis, facilitating prompt stopping of haemorrhage and tissue repair. The endothelial disruption exposes subendothelial matrix proteins, including collagen and VWF, which promote platelet adhesion [369]. Upon adhesion, platelets experience activation, marked by morphological alterations, degranulation, and the activation of surface integrins such as αIIbβ3, facilitating platelet aggregation [370, 371]. The release of agonists from platelet granules, such as ADP, thromboxane A2, and serotonin, enhances this process by recruiting more platelets to the injury site, accelerating the conversion of prothrombin to thrombin and facilitating the formation of fibrin and the stabilisation of the platelet plug [372]. However, platelet hyperactivation in response to severe injuries can lead to thrombotic complications, coagulation dysfunction, thrombocytopenia and prolonged inflammation [24, 373, 374].

1.13.1 Platelet dysfunction

Platelet dysfunction is a significant consequence after severe burns and trauma, characterised by the impairment of platelets to execute their essential haemostatic function, such as adhesion, aggregation, and secretion. This dysfunction is characterised by compromised platelet activation, diminished aggregation ability, and irregular interactions with the coagulation cascade and vascular endothelium [375-377].

Additionally, released DAMPs post severe thermal and trauma injuries such as HMGB1, DNA, histones, and S100A8/A9 contribute to inducing platelet dysfunction post injuries [373, 375]. Platelet dysfunction often manifests early after burns and trauma injuries as a result of the initial inflammatory response and mechanical injury

[100, 375]. Platelet dysfunction after injuries is characterised by platelet exhaustion (hyperactivation) mainly by the role of released VWF, TF, and DAMPs, impaired platelet adhesion due to elevated proteases post-injury, such as thrombin and plasmin, and impaired platelet aggregation as a result of low circulating fibrinogen [375, 378-380]. Complications related to platelet dysfunction encompass an elevated risk of microvascular thrombosis, DIC, extended bleeding, thrombocytopenia, impaired wound healing, and cardiovascular disease (CVD), leading to poor clinical outcomes and increased mortality risk [22, 374, 381, 382].

1.13.2 Thrombocytopenia

Thrombocytopenia is characterised by a reduction in platelet count, which is a prevalent consequence after severe injury and trauma. Following an acute injury, the systemic inflammatory response to the endothelial damage cause high consumption of platelets, leading to low circulating platelet levels [373]. This process is frequently exacerbated by the activation of coagulation pathways, which promote further platelet consumption during clot formation. Furthermore, trauma-induced thrombocytopenia correlates with poor clinical outcomes, such as extended hospitalisation, elevated death rates, and incidence of bleeding and infection [383]. Thrombocytopenia in burns is usually observed within the first 24 to 48 hours post-injury, followed by a rebound thrombocytosis and a gradual restoration to normal levels over a period of 2 to 4 months [100].

Platelet hyperactivation induced by systemic inflammation, results in both platelet consumption and functional impairment, hence sustaining thrombocytopenia during the healing phase [384]. Moreover, the sequestration of platelets in the spleen and the reduction of bone marrow activity due to the inflammatory response lead to further

diminish platelet production and availability [385]. Patients with burns and trauma exhibit platelet depletion and dysfunction, complicating their clinical treatment and frequently necessitating platelet transfusions and measures to reduce the risks of bleeding and thrombosis [386]. Glas et al. (2024) have illustrated that thrombocytopenia serves as an early indicator of serious complication and a predictor of poor outcomes in severe burns, which is also associated with established poor prognostic indicators such as degree of burn, ABSI score, inhalation injury and the incidence of sepsis [387]. Previously, Cato et al. (2018) illustrated that early thrombocytopenia is a useful biomarker for indicating sepsis and mortality. Additionally, reduced peak levels of platelet counts are strongly associated with 50-day mortality [388]. The early decreases in platelet counts and lower peak levels are key indicators of sepsis risk and mortality in burn and trauma patients, highlighting the importance of platelet monitoring for predicting adverse outcomes.

1.13.3 Clotting Dysfunction (Coagulopathy)

Coagulopathy is characterised by procoagulant and antifibrinolytic alterations, as well as impaired activity of the natural anticoagulant systems which is observed in patients shortly after a burn injury. This is also observed in patients with sepsis after severe traumatic injury [389]. Coagulopathy represents a critical complication in the management of severe thermal and traumatic injuries, contributing significantly to thromboembolic complications, MOF, morbidity and mortality [121, 390]. The pathogenesis of coagulopathy involves complex processes, such as systemic inflammatory reactions, damage to the endothelial cells, and imbalances in the levels of pro-coagulant and anti-coagulant substances [109]. Coagulopathy is classified into two phases: the early or acute phase, which occurs in early admission days post

thermal or traumatic injuries, and the late stage, which occurs much later in both burns and trauma patients [389, 391].

In trauma the acute coagulopathy phase frequently occurs due to the rapid activation of the protein C pathway and systemic hypoperfusion. This leads to hyperfibrinolysis and the fast depletion of coagulation components [392]. The acute trauma-induced coagulopathy (TIC) is a condition that occurs as a result of a combination of reduced blood flow, tissue damage, and inflammation. This condition leads to both bleeding and the formation of blood clots [393]. TIC occurs early following trauma injuries, with the prevalence of TIC increasing with the severity of the injury, affecting approximately 38% of severe trauma patients [383, 394]. Acute coagulopathy in trauma can also occur due to secondary variables such as acidosis, hypothermia, and hemodilution [395]. However, in thermal injuries, tissue-type plasminogen activator (t-PA) levels are frequently elevated during the acute phase, which occurs immediately following injury and is characterised by substantial fibrinolysis and coagulation activation, often resulting in a hypercoagulable state [389]. The late phase of coagulopathy in thermal and trauma patients is primarily caused by severe sepsis or surgical procedures. Coagulopathy following an injury is marked by alterations that promote blood clotting and hinder fibrinolysis. This can result in the development of DIC and MOF [389, 396]. Premature procoagulant changes distinguish acute burn-induced coagulopathy, compromised fibrinolytic systems, and dysfunction of platelets [397]. The criteria of acute coagulopathy in burn and trauma patients were defined by prolonged activated partial thromboplastin time (aPTT) and international normalised ratio (INR) levels with > 60 seconds and >1.5, respectively [389, 398]. However, the inaccuracy of standard plasmatic clotting tests further adds to the clinical challenges of characterising coagulopathy in burn patients. Newer viscoelastic techniques, such as

thromboelastography (TEG) and rotational thromboelastometry (ROTEM), provide better diagnostic tools by allowing for real-time evaluation of fibrinolysis and blood clotting activities. It is well-known that most patients with severe burns arrive at the hospital in a hypercoagulable condition. However, a lot of variation is probably related to the severity of the damage [397]. According to a 2018 study by Huzar et al., who analysed 65 burn patients with TBSA levels of more than 15%, 60% of the patients were associated with hypercoagulopathy at admission, whereas 24% were diagnosed with hypocoagulopathy [399]. Additionally, Wiegele et al. (2019) examined 20 patients admitted with severe burns (>20% TBSA) and found that all of them were diagnosed with hypocoagulopathy based on ROTEM and thrombin-generating tests [400]. Moreover, Pusateri et al. used TEG in 115 patients within 4 hours of thermal injury and found three admission fibrinolytic phenotypes: high fibrinogen levels or fibrinolytic shutdown (30% of burns); normal fibrinogen levels or physiologic (60%); and low fibrinogen levels or hyperfibrinolytic (9%). Burns with fibrinogen levels or hyperfibrinolytic had more severe burns (TBSA > 20%). Admission hyperfibrinolysis was linked to a roughly 13-fold increased mortality risk and a 5-fold quicker time to death compared to individuals with normal fibrinogen [120]. A frequent consequence of severe burns, can lead to late coagulopathy, especially whether it develops early or late in the clinical course, such as sepsis and surgery with burn wound excisions that could cause considerable blood loss and coagulopathy [389].

VWF is a substantial contributor to the coagulopathy that is observed in patients who have experienced burns or trauma. Elevated levels of VWF are suggestive of endothelial damage and contribute to the development of a hypercoagulable state in the context of severe burns. As a consequence of endothelial injury and systemic inflammation, VWF increases, facilitating platelet aggregation and adhesion, thereby

exacerbating coagulopathy [401]. VWF is regulated by the metalloprotease ADAMTS13, which cleaves and prevents spontaneous VWF–platelet interactions [402]. Several studies have observed significantly high VWF levels and decreased ADAMTS13 following inflammation and tissue damage compared to healthy controls [403-405].

1.13.4 Aims and Hypothesis

Our research hypothesises that excessive NETs and neutrophil-derived cfDNA contribute to further complications in burns and trauma, playing a significant role in the development of immunothrombosis, leading to DIC and MOF. Released soluble factors post-injury, particularly IL-8, are likely major mediators of this response, contributing to neutrophil activity and can trigger NET formation. This cascade leads to sustained inflammation and immune dysregulation, thereby heightening the risk of complications associated with excessive NETosis. We also hypothesise that high MW VWF levels will be increased post-burn injury with consumption of ADAMTS13. This will cause consumption of platelets and trigger further NET generation, increasing risk of immunothrombosis in response to injury and infection.

The aims of the study are: -

- Provide a comprehensive analysis of circulating NET-derived chromatin in patients with burns and trauma, focusing on both the quantitative and qualitative aspects of cfDNA generation and degradation.
- Investigating circulating large chromatin structures derived from NETs in whole blood in patients with burns.
- Determine the potential role of IL-8 in NET generation in patients with burns.
- Investigate haematological and neutrophil parameters in severe thermal injury using an automated haematological analyser/flow cytometer.
- Investigate the classical changes in platelet count dynamics following severe burn injury and measure platelet physiological thrombus formation *in vitro* using the T-TAS system with both AR and HD chips.
- Investigate the relationship between post-burn injury VWF and ADAMTS13 levels with platelet function and NET formation.

Chapter 2: Materials and Methods

2 Materials and Methods

2.1 Study design and ethical approval

2.1.1 Study design

This research includes data from two observational studies: The Scientific Investigation of the Biological Pathways Following Thermal Injury-2 (SIFTI-2), and the Golden Hour (GH) Study targeting trauma patients.

SIFTI-2 is an ongoing observational cohort study at Queen Elizabeth University Hospital Birmingham enrolling patients with moderate-to-severe burn injuries: ≥15% and ≥20% of the total body surface area (TBSA) in adults and children, respectively [406]. Patients are admitted and recruited through the major trauma and burns centres at the Queen Elizabeth Hospital Birmingham. Daily blood samples are collected from patients from hospital admission to day 14 post-burn, as well as at day 28, and months 3, 6, 12 and 24 post-injury. Clinical data are collected and held in anonymous databases that contain clinical assessments, injury severity and key biomarkers. Sepsis was diagnosed according to classical ABA criteria [78].

This study was approved by the research ethics committee (REC reference:16/WM/0217) [406].

The GH study was initiated in 2014 and supported by the National Institute for Health Research (NIHR). The GH study enrols adult patients (≥18 years old) in the pre-hospital setting who have sustained a traumatic injury with a suspected injury severity score (ISS) >8. Blood samples are obtained immediately (pre-hospital by emergency care teams) within 1 hour of injury (T0) and at two subsequent in-hospital timepoints; 4-12 hours (T4-12) and 48-72 hours (T48-72) following injury [407]. The study received

ethical approval from the North Wales Research Ethics Committee - West (REC reference: 13/WA/0399, Protocol Number: RG_13–164).

Clinical evaluations, assessment of damage severity, and important biomarkers are all included in the anonymised clinical data stored in databases for both SIFTI-2 and GH studies.

2.1.2 Patient cohorts

A total of 96 burn patients were included in the in SIFTI-2 study. The median age of patients was 49 years (range 16–84 years), and the median burn size was 32% total body surface area (TBSA) (range 15–85%). The incidence of sepsis was 51.2% and mortality was 20.8%. Septic status was not determined for 12 patients due to early mortality from non-septic causes or study withdrawal. Detailed patient demographics are displayed in Table 2.1.

The GH study enrolled 147 adult trauma patients. The most common cause of injury was a road traffic collision (53.1%). Their ages ranged from 18 to 95 years, and their average ISS was 25 (ranging from 9 to 66) (Table 2.2). The average duration of the blood sample before hospitalisation was 42 minutes following injury, with a range of 13-60 minutes.

Table 2.1: Burn patients demographics	
Characteristic	**Burns patients (n=96)**
Age, years (range)	49 (16-84)
Gender, (M:F)	74:22
% TBSA (range)	32 (15-85)
% FT TBSA (range)	11 (0-80)
Inhalation injury (Y: N)	39:57
Mechanism of injury Flash, n (%) Flame, n (%) Flame and flash, n (%) Electrical, n (%) Scald, n (%)	 7 (7.29) 79 (82.29) 5 (5.20) 1 (1.04) 4 (4.17)
ABSI (range)	8 (2-14)
Baux (range)	80 (34-143)
rBaux (range)	89 (39-160)
SOFA	6 (0-17)
Sepsis Y:N (%)	43:41(51.2)
Mortality Y: N, (%)	20:76 (20.83)

Abbreviations: TBSA (total body surface area), FT (Full-thickness), ABSI (A Body Shape Index), Baux (a burn mortality prediction system), rBaux (revised Baux indication), SOFA (Sequential Organ Failure Assessment).

- Baux is a prediction system for burn-related mortality that calculates the probability of death by adding the patient's age to the percentage TBSA.

- rBaux is modified Baux score accounting for inhalation injury with improvement in death prediction.
- SOFA score is a clinical tool for organ function and failure rate assessment.

Table 2.2: GH patients demographics	
Characteristic	Trauma patients (n=147)
Age, years (range)	42 (18–95)
Gender, (M:F)	126:21
Time to pre-hospital sample, minutes post-injury (range)	41 (13–60)
ISS (range)[#]	25 (9–66)
NISS (range)[#]	37 (9–75)
Admission GCS score (range)	10 (3–15)
Mechanism of injury	
Fall, n (%)	30 (20)
A/P, n (%)	33 (22)
Blunt, n (%)	6 (5)
RTC, n (%)	78 (53)
ICU-free days (range)	19 (0–30)
Hospital-free days (range)	7 (0–29)
Mortality, n (%)	24 (16.3)

Data are expressed as mean (range) unless otherwise stated. # Information relating to ISS and NISS was available for 137 patients. A/P, Assault/Penetrating; GCS, Glasgow coma scale; ICU, Intensive care unit; ISS, Injury severity score; NISS, New injury severity score; RTC, Road traffic collision.

2.2 Blood sampling

Blood samples were collected from the SIFTI-2 cohort of 96 thermally injured patients with TBSA ≥15% at multiple time points: days 1 to 14, day 28, and months 3, 6, 12 and 24 post-injury. The samples were drawn into BD Vacutainers® (BD Biosciences, UK) containing either tri-sodium citrate or Z-serum clotting activator, which were utilised to prepare platelet-free plasma (PFP) and serum, respectively. For patients enrolled in the GH study, additional blood samples were collected at three specific post-injury time points: pre-hospital (≤1 hour), 4–12 hours, and 48–72 hours post-injury. In pre-hospital settings, samples were obtained either during intravenous cannulation or via venepuncture. The vacutainers were stored at room temperature during transport to the hospital. Upon arrival, samples were processed within 1 hour by a single researcher who provided 24/7 coverage. In parallel, blood samples were also collected from 20 healthy controls (HCs) who voluntarily participated in the study, providing baseline samples for comparison and control analyses.

2.3 Whole blood analysis

A full blood count was immediately performed on each sample using the Sysmex-XN1000 analyser (Sysmex, Milton Keynes, UK), with blood collected in vacutainers containing sodium citrate or EDTA as the anticoagulant. Quality control material (XN check, Sysmex UK) was measured daily to ensure instrument performance throughout the study. The instrument is also enrolled into a monthly national external quality assurance scheme to further validate instrument performance in comparison with all clinical laboratories across the UK and within and between different instrument groups (UKNEQAS, Watford, UK).

2.4 Whole Blood Parameters measured

Analysed Full blood count (FBC) data for burn patients enrolled in the SIFTI-2 study, as well as healthy controls (HC; N=20), were directly collected from the XN1000 instrument. The FBC analysis encompassed a comprehensive evaluation of key haematological parameters, including platelet counts and white blood cell (WBC) subtypes, such as neutrophils, lymphocytes, monocytes, eosinophils, and immature granulocytes (IGs). In addition to these standard FBC metrics, extended parameters were collected to analyse further insights into the functionality and characteristics of these cell types.

3 different platelet counts were measured including the platelet impedance count (PLT-I), the platelet optical count (PLT-O) and fluorescent platelet (PLT-F) count along with mean platelet volume (MPV) and the Immature platelet fraction (IPF). In addition, the instrument provides extended WBC parameters for the morphology, functionality, and maturity of all leukocyte populations. Neutrophil and monocyte extended parameters provide changes in cell function and maturity, offering valuable information about the immune system's reaction to infection and inflammation. Neutrophil and monocyte X illustrate cell granularity and internal complexity. by side scatter diffraction in the Sysmex analyser, which reflects the cytoplasmic structure of the cell. The neutrophil and monocyte Y parameters measure the fluorescence intensity, and the nuclear maturity. It provides insights into the cell RNA/DNA content and overall cellular activity. Neutrophil and monocyte Z parameters provide a comprehensive evaluation of cells by integrating X and Y parameters, expressing the width of dispersion in cell size. Furthermore, Neutrophil reactive intensity (RI) evaluate cell activation state by assessing fluorescence intensity, reflecting cells reactive changes, while neutrophil granularity index (GI) evaluates cell granularity. Lymphocyte extended parameter RE

(reactivity) evaluate the cellular reactivity, while lymphocyte AS (antibody-synthesising lymphocytes) measure the levels of antibody synthesis activity particularly in B lymphocytes. For ex *vivo* investigation, neutrophil parameters were also being measured and data collected for treated and untreated whole blood and isolated neutrophils with ionomycin as described in sections 2.9.1 and 2.9.2.

2.5 Preparation of platelet free plasma

Tri-sodium citrate vacutainers were centrifuged at 2000 x g for 20 minutes at 4°C to obtain platelet-poor plasma (PPP). Following this initial centrifugation, the PPP was carefully separated and subjected to a second centrifugation at 13,000 x g for an additional 20 minutes at 4°C to ensure the removal of any residual platelets. The resulting platelet-free plasma (PFP) was aliquoted into appropriate storage tubes and stored at -80°C for future analysis.

2.6 Preparation of serum

Serum was prepared by allowing z-serum clotting activator vacutainers to sit at room temperature for 30 minutes, followed by centrifugation at 1,620 x g for 10 minutes at room temperature. The serum was aliquoted and stored at -80°C.

2.7 Platelet function measurement

Platelet function was measured using the Total Thrombus-formation Analyser System (T-TAS) (Zacros, Fujimori Kogyo Co. Ltd., Tokyo, Japan). The instrument uses chips

stored at 4^0C to maintain stability with the same batches of each chip were used throughout this study. The AR chip is coated with collagen and tissue factor within an 80 µm depth flow chamber measured at 600 s^{-1} and is dependent on platelet count. The HD chip is also coated with collagen and tissue factor but within a 50 µm thick flow chamber measured at 1200 s^{-1} and can be used to measure thrombocytopenic samples. To perform the test, chips were prewarmed to room temperature and 20 µl CaCTI reagent (Corn-derived trypsin inhibitor and $CaCl_2$) was added to gently mixed citrated whole blood (480 µl) immediately prior to testing to inhibit activation of the coagulation contact pathway. Treated blood was then tested within both AR and HD chips in parallel both incubated within the instrument at 37^0C. The test activated both primary and secondary haemostasis resulting in thrombus formation and occlusion of blood flow in the chips. The following parameters were recorded:- OST (Occlusion Start Time) is the lag time for the flow pressure to reach 10 kPa due to partial occlusion of the capillary; OT (Occlusion Time) is the lag time for the flow pressure to reach 60 kPa with full occlusion of the capillary; The AUC (Area Under the Curve) is the area under the flow pressure versus the time curve (overall thrombus formation) i.e. lower values reflect slower thrombus formation (Figure 2.1).

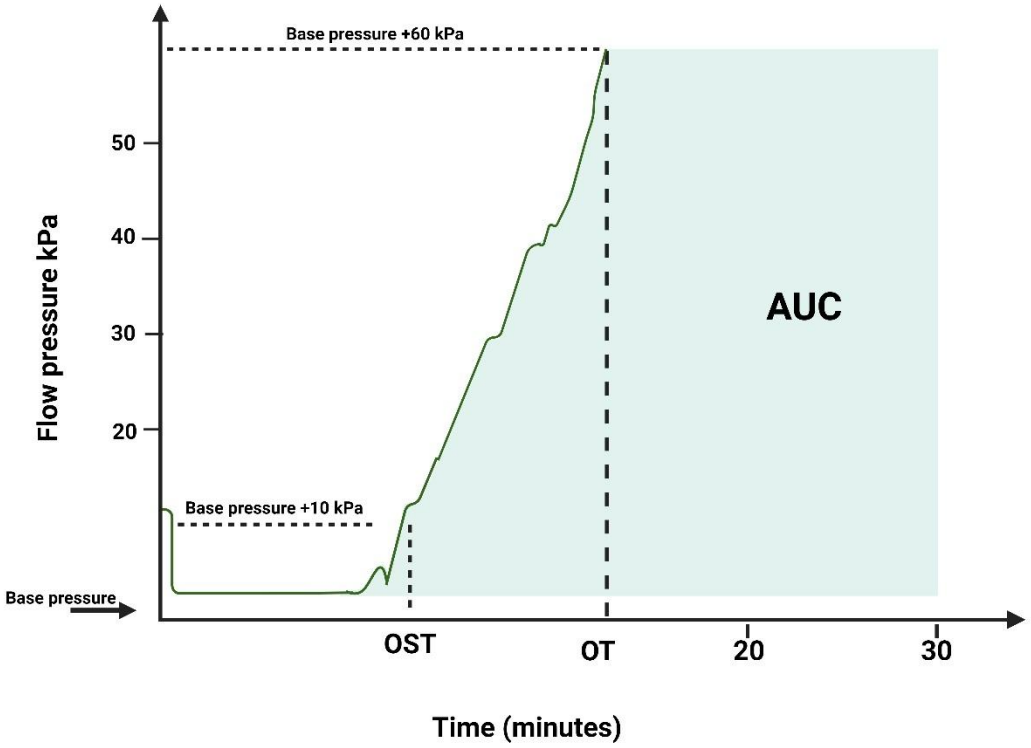

Figure 2.1: T-TAS parameters measured during thrombus formation. T-TAS assesses thrombus formation by monitoring changes in flow pressure over time. The Onset Time (OST) marks is the time when the pressure reaches 10 kPa, indicating partial capillary occlusion. The Occlusion Time (OT) is recorded when the pressure reaches 60 kPa, signifying full capillary occlusion. The Area Under the Curve (AUC) represents the overall thrombus formation; lower AUC values indicate slower rates of thrombus formation. This comprehensive measurement system enables the quantification of clot formation dynamics in response to platelet function and coagulation. This figure has been modified from ZACROS Corporation-T-TAS product information using BioRender software [408].

2.8 Neutrophil isolation from healthy donors *ex vivo*

Blood samples were collected from healthy volunteers into EDTA vacutainer tubes through venepuncture of the antecubital vein. An FBC test was performed for each sample using the XN-1000. Blood was then transferred into a sterile 50 ml Falcon tube (ThermoFisher, Cheshire, UK), and 1 ml of 2% Dextran (Sigma-Aldrich, Poole, UK) was added for each 6 ml of blood and kept at room temperature for 30-40 minutes. This procedure allows the sedimentation of RBCs and platelets with subsequent layers comprising white blood cells (WBC). After 30-40 minutes, the WBC-rich layer was transferred carefully onto the top of a discontinuous density gradient of Percoll (Sigma-Aldrich, Poole, UK) to isolate neutrophils from the WBC-rich buffy coat. The Percoll gradient consists of 2.5 ml of 80% Percoll diluted with 1x saline in distilled water at the bottom and 5 ml of 56% Percoll above the 80% Percoll layer in 15 ml Falcon tubes (ThermoFisher, Cheshire, UK). After transferring the WBC-rich layer, tubes subsequently were centrifuged for 20 minutes at 220 x g without brake at room temperature. After centrifugation, the supernatant of plasma and peripheral blood mononuclear cells (PBMCs) were discarded, and the neutrophil layer at the 56-80% Percoll interface was extracted and transferred into a sterile 15 ml Falcon tube. Extracted neutrophils were suspended in RPMI 1640 medium (Sigma-Aldrich, Poole, UK) containing 10% heat-inactivated foetal bovine serum (FBS), 2 mM glutamine, 100 U/ml penicillin, and 100 µg/ml streptomycin (Sigma-Aldrich, Poole, UK) and subsequently centrifuged at 461 x g for 10 minutes at room temperature. After centrifugation, the supernatant was discarded, and neutrophils were resuspended in RPMI-1640 medium and diluted to the desired final concentration. The cell count was measured by the XN-1000, and the final concentration was modified according to the individual experiment (Figure 2.2).

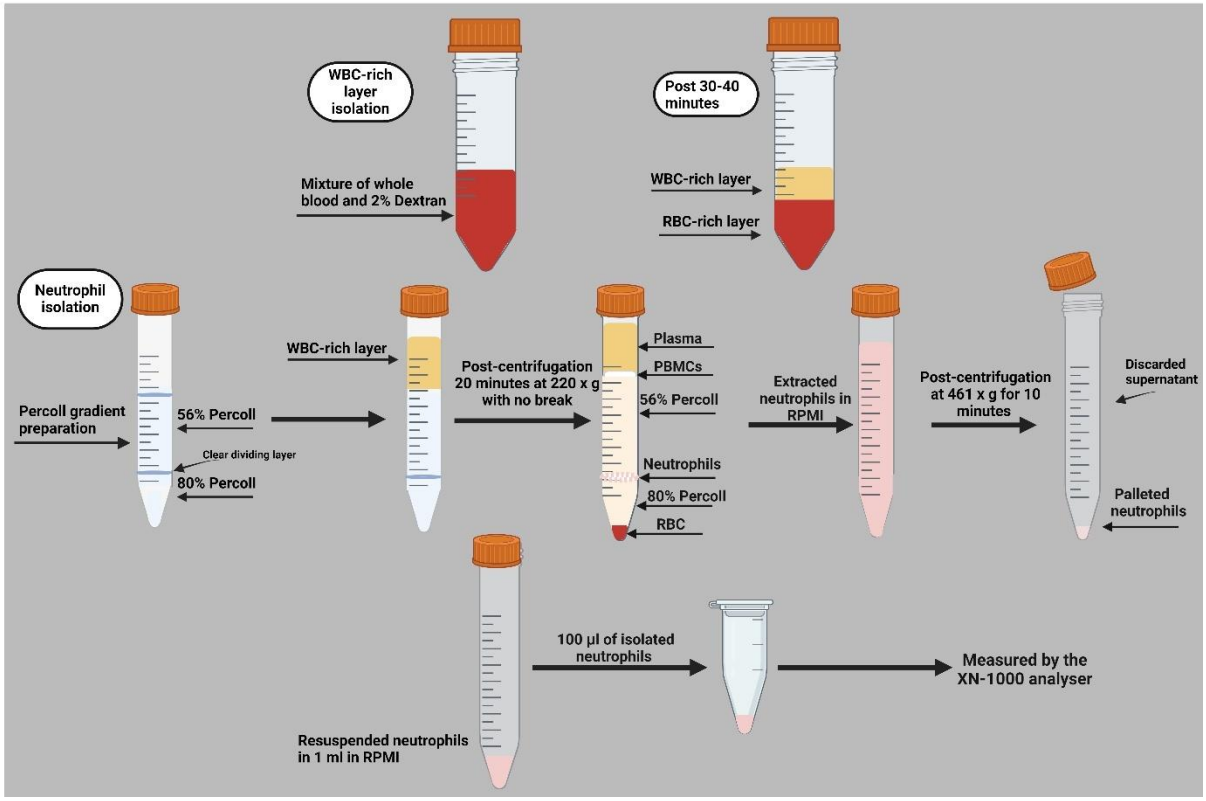

Figure 2.2: Neutrophil isolation *ex vivo*. The diagram illustrates the stepwise process of isolating neutrophils from whole blood using a Percoll gradient. First, whole blood is mixed with 2% dextran and allowed to settle for 30-40 minutes, separating a WBC-rich layer. This layer is collected and transferred to the top of a prepared Percoll gradient, consisting of 80% and 56% Percoll. Following centrifugation at 220 x g for 20 minutes without a bake, neutrophils are isolated in the dividing layer between 80% and 56% Percoll. The plasma and peripheral blood mononuclear cells (PBMCs) at the top of the Percoll gradient are separated. The neutrophil layer is carefully extracted at 56-80% Percoll interface, transferred into a fresh 15 ml Falcon tube, and centrifuged at 461 x g for 10 minutes. After washing, the supernatant is discarded, leaving pelleted neutrophils. Finally, the isolated neutrophils are resuspended in RPMI medium. A 100 µl of suspended neutrophils is prepared for analysis using the XN-1000 analyser to quantify neutrophil counts. The figure was created using BioRender Software.

2.9 NET generation *ex vivo*

2.9.1 NET generation from isolated neutrophils

Isolated neutrophils ($2x10^5$-$4x10^6$) resuspended in RPMI media supplemented with 10% FBS, 2 mM glutamine, 100 U/ml penicillin, and 100 µg/ml streptomycin were dispensed into 12 well cell culture plates (Corning, Flintshire, UK), glass chamber slides (BD Biosciences, Berkshire, UK) for 4 hours at 37ºC and 5% CO_2 with the following stimuli:

- 25 or 50 nM PMA.
- Burn patient serum samples categorised as containing low (<150 pg/mL), medium (150–500 pg/mL) or high (>500 pg/mL) levels of IL-8.
- 100 pg/ml recombinant human IL-8 (Fine-Test Biotech, Boulder, US).
- 4 µM ionomycin

Post-incubation, cells seeded in glass chamber slides were fixed with 4% paraformaldehyde (Sigma-Aldrich, Poole, UK) for 30 min. After fixation, supernatants were collected into 0.5 mL Eppendorf tubes and centrifuged at 2200 × g for 2 minutes at 4ºC to remove any remaining cells and debris, aliquoted and stored at -80ºC for the measurement of release cfDNA of treated samples. HC and burn serum samples were also incubated in separated wells without cells as background for generated cfDNA levels *in vitro*. In some samples, 1 µg/mL of human IL-8 monoclonal antibody (R&D Systems, MAB208-100, Abingdon, UK) or a mouse IgG1 isotype control (R&D systems, Abingdon, UK) was incubated for 15 min in isolated neutrophils at 37 °C and 5% CO_2 before treating cells with serum or recombinant IL-8 to inhibit the production of NETs by IL-8. To inhibit the potential degradation of generated NETs by DNase I,

some serum samples were also treated with 2.5 µM Actin (Sigma-Aldrich, Poole, UK) for 30 min prior to incubation to inhibit serum DNase I activity to prevent NET degradation.

2.9.2 NET generation from whole blood

500 µl of tri-sodium citrate vacutainers of whole blood from healthy volunteers were aliquoted into 1.5 ml Eppendorf tubes, stimulated with 25 nM PMA, 4 µM ionomycin or vehicle control, and incubated for 4 hours at 37ºC and 5% CO_2.

2.10 Fluorescence microscopy analysis and quantification of generated NETs

Treated isolated neutrophils, in glass chamber slides with either with 25 nM PMA, HC or burns serum samples, recombinant IL-8 *in vitro* as described in section 2.9.1 were washed with sterile PBS and stained for 5 min with 5 µM SYTOX green. After washing with PBS, cells were incubated with in PBS containing 1% BSA for 1 hour. Post-blocking, cells were washed and incubated with 1 µg/mL anti-citH3 Ab or isotype control (Abcam, Cambridge, UK) overnight at 4°C. Cells were washed with PBS containing 1% BSA and stained with 0.1 µg/mL Donkey anti-Rabbit IgG secondary antibody conjugated to Alexa Fluor™ 568 for one hour in the dark. Finally, cells were washed with PBS containing 1% BSA and analysed by fluorescent microscopy using and Olympus IX71 epifluorescence microscope at x 20 magnification and analysed using ImageJ software (version 1.54f). Quantification of generated NETs was performed by ImageJ software by adjusting the image area using a calibrated scale slide to ensure accurate size measurement. Empty areas within images were measured to calculate the value through the Summarised Analysis function. The mean

value of each imported image was then subtracted to eliminate background interference. NETs were identified by adjusting the threshold to detect generated NETs, and noise was eliminated to ensure accurate quantification. The number of generated NETs in selected fields was automatically counted using the Analyse Particles function. Finally, generated NETs number/mm^2 was calculated by the following formula:

$$\boldsymbol{NETs/mm^2 = \frac{Number\ of\ analysed\ particles}{Length\ x\ width\ of\ measured\ image\ area}}$$

2.11 Microfluidic capture of NET derived chromatin

Capturing circulated neutrophil extracellular traps (NETs) from burns whole blood was performed by employing the microfluidic assay developed by Sakuma et al. (2022) to capture circulating neutrophil extracellular traps (NETs) from whole blood [314]. NETs were captured from untreated and PMA-treated whole blood samples and isolated neutrophils as described in sections 2.9.1 and 2.9.2. Circulating NETs in the whole blood of burns samples were measured at 4 timepoints; days 1, 4, 8, and day 14 post-injury. The microfluidic chips were obtained in collaboration with Dr Daniel Irimia from Harvard University. Briefly, microfluidic chips were prepared by removing gases from them in a desiccator under vacuum for 10 minutes and then loaded with 100 µL of phosphate buffer solution (PBS) (Sigma-Aldrich, Poole, UK) by inserting it through the outlet using a 200 µL pipette until the entire device was completely filled with the fluid and left for 5 minutes to ensure the chip contained no air bubbles. A buffer well was then attached to a 10 mL syringe (Fisher Scientific, Leicestershire, UK) connected to Tygon tubing measuring 12 cm in length and with an inner diameter of 0.02 inches

and an outer diameter of 0.06 inches (VWR International Ltd, Leicestershire, UK) that tubing was then attached to a 22-gauge blunt needle measuring half an inch length (Needlez, Hoyland, UK) to connect the tubing to the syringe. The syringe was subsequently attached to a syringe pump (PhD 2000 Programmable, Harvard Apparatus, Holliston, MA) and configured to operate in 'Refill' mode at a flow rate of 10 µL/min. The desired volume was set to 50 µL. After the observation of PBS moving through the pipe, the pump was stopped, and the PBS was replaced in the buffer reservoir with a total volume of 100 µL of sample that was diluted 1:10 with 5 µM SYTOX green (ThermoFisher, Cheshire, UK) in PBS, and samples were processed to be withdrawn by the adaptor (Figure 2.3). Next, samples were washed and blocked with 100 µl of 1% bovine serum albumin (BSA) (Sigma-Aldrich, Poole, UK) in PBS by adding to the reservoir, and the device was set at a rate of 10µL/min for 2 minutes and incubated for 1 hour at room temperature. Post-blocking, 1 µg/ml anti-citrullinated histone antibody (anti-citH3 Ab) (Abcam, Cambridge, UK) (anti-citH3 Ab) was drawn into the chip at a rate of 10 µL/min for 2 minutes twice. After the flow was stopped, chips were wrapped within aluminium foil and incubated in the dark overnight at 4°C. Post-incubation, chips were washed with 50 µL PBS containing 1% BSA [.0.1 µg/ml Donkey anti-Rabbit IgG secondary antibody conjugated to Alexa Fluor™ 488 (ThermoFisher, Cheshire, UK) was then drawn through the device at 10 µL/min for 2 minutes and incubated for 1 hour and wrapped in aluminium foil. After incubation, chips were washed with 50 µL PBS containing 1% BSA. Captured NETs were visualised by fluorescent microscopy using an Olympus IX71 epifluorescence microscope at ×4 magnification. To quantify captured NETs, Images were manually arranged and stitched together using the Mosaic J plugin in ImageJ software (version 1.54f). Images were imported into Mosaic J, and overlapping regions were manually

aligned to create a seamless composite image. The resulting image provided a comprehensive view of the sample, allowing for consistent analysis across the entire area of interest. Images were cropped at fixed dimensions to select the area of the post-stitching. Appropriate thresholds were applied for cropped images, and NET-derived chromatin fibres were quantified by image analysis by setting the area at 100 μm^2 with a value of 0–0.5 shape circularity. The total area of NET derived chromatin (μm^2) was measured for each tested sample.

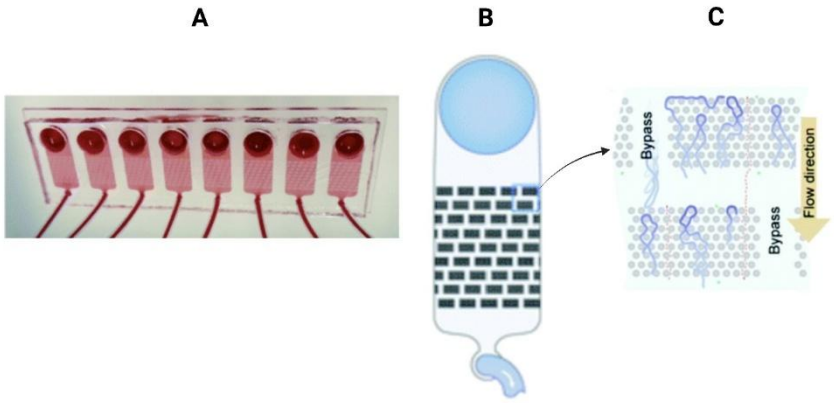

Figure 2.3: Microfluidic chip capture of NET derived chromatin. (A) A microfluidic device including 8 channels was designed for capturing NETs from whole blood. (B) A single microfluidic device flow diagram showing the blood loading reservoir, post-array designed for NET capture, and an outflow channel. The post-array composed of micropillars (post-patches) that effectively trap chromatin fibres as blood flows through the channel. (C) Detailed schematic of the post-patch array, illustrating the flow direction of blood. NET fibres (blue) are captured in the post-patches, while bypass channels allow for cell and oligonucleotide flow. This figure has been modified using BioRender software from Figure 1 of “Microfluidic capture of chromatin fibres measures neutrophil extracellular traps (NETs) released in a drop of human blood” by Sakuma et al. (2022) [314].

2.12 Fluorometric assay for cfDNA measurement

2.12.1 CfDNA levels in HC, burns, trauma PFP samples and extracted cfDNA *in vitro*.

A Fluorescence-based assay was performed to measure cfDNA concentrations in plasma samples obtained from HC, trauma and burns patients as well as extracted cfDNA *in vitro* from HC, trauma, and burns plasma, and extracted cfDNA from degraded generated NETs with MNase and DNase I *in vitro* (Sections 2.12 and 2.15). Frozen samples were thawed for 5 minutes at 37 °C. Samples were vortexed for 5 seconds. cfDNA levels was measured using the method developed by Goldshteub et al. (2009) [409]. 10 µL of plasma or extracted cfDNA *in vitro* was transferred into wells of a 96-well flat-bottomed black plate (Corning, Flintshire, UK). The plates were then stained with 0.1 mM SYTOX green with a total volume of 150 µL at room temperature for 10 minutes. A standard curve was generated by incorporating Lambda DNA (ThermoFisher, Cheshire, UK) from 1000 ng/mL to 0 ng/ml. Fluorescence was measured using a BioTek Synergy 2 fluorometric plate reader (NorthStar Scientific Ltd., Sandy, UK) with excitation and emission wavelengths set at 485 and 528 nm, respectively.

2.12.2 Levels of generated cfDNA in the supernatant of treated isolated neutrophils *ex vivo*

The levels of generated cfDNA in the supernatants of treated neutrophils *ex vivo*, as described in section 2.9.1, were measured by first thawing frozen samples for 5 minutes at 37 °C, followed by vortexing for 5 seconds. The measurements were conducted as outlined in section 2.12.1, with the only difference being the

concentrations of the samples and SYTOX Green. A total of 50 µL of the cell-free supernatants of untreated and treated neutrophils with PMA, HC or burns serum IL-8, or the supernatants of incubated serum or actin alone without cells was transferred to a 96-well flat-bottom black plate and stained for 10 minutes at room temperature with 0.5 mM SYTOX Green, bringing the total volume to 100 µL.

2.13 DNA extraction from plasma samples

Stored PFP samples of burns, trauma, and HC were thawed for 5 minutes at 37°C. Samples were vortexed for 5 seconds, and DNA was extracted using the DNeasy Blood and Tissue kit and protocol (Qiagen, Manchester, UK). 200 µL of plasma was transferred into Eppendorf tubes (1.5 ml). 20 µL of proteinase K and 200 µL of AL Buffer were added to the samples, and the mixture was thoroughly vortexed before incubation at 56°C for 10 minutes. After incubation, 200 µL of ethanol (96-100%) was added to precipitate DNA, followed by vortexing to ensure uniform mixing. Samples were then transferred into DNeasy Mini spin columns, placed in 2 ml collection tubes and centrifuged at ≥6000 x g for 1 minute. The flow-through was discarded, and the spin columns were transferred into 2 ml collection tubes and washed with 500 µL of AW1 Buffer and centrifuged at ≥6000 x g for 1 minute. The flow-through was discarded, and samples were transferred into 2 ml collection tubes and washed with 500 µL of AW2 Buffer, followed by centrifugation at 20,000 x g for 3 minutes. The spin columns were then transferred into a 1.5 microcentrifuge tube, and the DNA in the spin columns was eluted by adding 200 µL of AE Buffer and incubated at room temperature for 1 minute. Finally, tubes were centrifuged at ≥6000 x g for 1 minute and stored at -80^{o}C.

2.14 Qualitative Analysis of cfDNA sizes by agarose electrophoresis.

CfDNA size of extracted cfDNA (base pairs (bp)) was measured using the Agilent 2100 Bioanalyzer (Agilent, Cheshire, UK) following the manufacturer's Agilent high sensitivity DNA kit and protocol. Firstly, the gel-dye mix was prepared by equilibrating the High Sensitivity DNA dye concentrate and the gel matrix at room temperature for 30 minutes and followed by vortex for 10 seconds to ensure complete mixing. 15 µL of the dye was then transferred into the gel matrix vial, and vortexed for 10 seconds. The gel-dye mix was then transferred into the top receptacle of a spin filter and centrifuged at 2240 g for 10 minutes at room temperature. The gel-dye mixture was then stored at 4^{o}C.

To measure cfDNA sizes, the gel-dye mix was placed in room temperature for 30 minutes in dark. A high sensitivity DNA chip was placed on the chip priming station. 9 µL of the gel-dye mix was pipetted into the designated well on the chip, and the plunger on the chip priming station was set to 1 ml and pressed down until it locks into place. After 60 seconds, the plunger was released and allowed to return to the 0.3 ml mark. The chip was then primed by pulling the plunger back to the 1 ml position, and 9 µL of the gel-dye mix was pipetted into each of the designated wells. Next, 5 µL of high-sensitivity DNA concentrate markers (35/10380 bp) were loaded into the well marked with a ladder symbol and into each of the 11 sample wells. Then, 1 µL of the DNA ladder was pipetted into the designated ladder well, and 1 µL of each extracted DNA sample was added to the sample wells. After loading samples, the chip was carefully placed into the adapter of the IKA vortex mixer and vortexed at 2400 rpm for 60 seconds to ensure proper mixing of the gel-dye mixture and DNA. Finally, the chip was inserted into the Agilent 2100 bioanalyser and the high sensitivity DNA software

was selected to perform electrophoresis to measure the DNA size of each loaded sample.

2.15 Measurement of circulating nucleosomes by ELISA

Nucleosome levels in burns and HC were measured in PFP samples using the Nu.Q® Discover H3.1 ELISA Assay, reference number 1001-01-03 (Volition Diagnostics Ltd, London, UK). Initially, the kit reagents, including assay standards, buffer, and kit controls, were allowed to reach room temperature for 30 minutes. Stored plasma samples at -80ºC were thawed at 37ºC for 5 minutes and vortexed for 5 seconds. Finally, samples were diluted 1:20 (10 µL sample and 190 µL of the reagent diluent). The ELISA plate was washed 3 times with 200 µL of diluted wash buffer and blotted dry. Subsequently, 80 µL of assay buffer was added to each well, followed by 20 µL of the standards, controls, or diluted plasma samples. The plate was sealed and incubated at room temperature on a microplate incubator with orbital shaking at 700 rpm for 150 minutes.

After incubation, the wells were washed 3 times with wash buffer, blotted dry and 100 µL of the HRP-labelled detection antibody to each well, and sealed and incubated on the shaker for 90 minutes at 700 rpm. Wells were then washed x 3 before adding 100 µL of substrate solution -3,3',5,5'-Tetramethylbenzidine (TMB) (Cell Signaling Technology, Leiden, The Netherlands) to each well. Plates were sealed and incubated for 20 minutes on the shaker in the dark at 700 rpm. Finally, the reaction was then stopped by adding 100 µL of stop solution to all wells and mixed for 1 minute on the shaker. The optical density of each well was immediately measured using a BioTek Synergy fluorometric plate reader (NorthStar Scientific Ltd., Sandy, UK) set at 450 nm.

2.16 Degradation of NETs in vitro

1.5 x10^6/ml of isolated neutrophils from healthy donors (as described in Section 2.8) were seeded into 12 well cell culture plates (Corning, Flintshire, UK) and treated with 50 nM PMA with a total volume of 1000 µl RPMI supplemented with 2 mM glutamine, 100 U/ml penicillin, and 100 µg/ml and incubated for 4 hours at 37 °C and 5% CO_2. Post incubation. NETS were washed 3 times with PBS. Then NETs were degraded with 10 U/ml DNase (Roche, Mannheim, Germany) supplemented with 2 mM magnesium chloride ($MgCL_2$) or with 10 U/ml micrococcal nuclease (MNase) (New England Biolabs, Herts, UK) supplemented with 50 mM Tris (hydroxymethyl) aminomethane-hydrogen chloride (Tris-HCl) and 5 mM calcium chloride ($CaCl_2$) and pH 7.9 in a total volume 500 µl with Hanks' Balanced Salt Solution (HBSS) with no $MgCL_2$ or $CaCl_2$ (ThermoFisher, Cheshire, UK) for 20 minutes at 37°C and 5% CO_2. Immediately, post-incubation supernatants of degraded NETs were aliquoted and centrifuged at 4ºC for 2 minutes at 2200 x g. The supernatants were aliquoted and stored at -80ºC. Degraded NETs were extracted (section 2.13) and DNA size and levels were measured as described in Section 2.14. and 2.12.1, respectively.

2.17 Quantification of circulated IL-8 in burns serum

IL-8 levels post-burn were measured in serum samples using a Bio-Plex Pro Human Cytokine Assay kit (Bio-Rad Laboratories Ltd, Hertfordshire, UK), following manufacturer's guidelines. The assay is a magnetic bead-based system, where beads conjugated with IL-8 antibodies are mixed with serum samples. Prior to analysis, all reagents were equilibrated to room temperature. The assay standard stock was reconstituted with 500 µL of Bio-Plex® sample diluent HB. The assay beads were

vortexed for 20 seconds, and 50 µL of the bead mixture was added to each well of a 96-well assay plate.

Serum samples were thawed in a water bath at 37°C for 5 minutes, followed by vortexing for 5 seconds. The samples were then diluted at a ratio of 1:4 with the provided reagent diluent (20 µL of serum and 60 µL of reagent diluent). Then, 50 µL of the diluted serum samples, standards, and blanks were added to their respective wells. After adding the samples, the plate was covered with aluminium foil and incubated at room temperature on a platform shaker for 30 minutes at 300 rpm. After incubation, the plate was washed twice with 100 µL of 1x wash buffer per well. Next, 25 µL of detection antibody was added to each well, and the plate was incubated for an additional 30 minutes on the shaker at 300 rpm. Following this incubation, the plate was washed twice with 100 µL of 1X wash buffer per well. Then, 50 µL of 1x Streptavidin-PE (SA-PE) was added to each well, and the plate was incubated for 10 minutes on the shaker. Followed by washing twice more with 100 µL of 1x wash buffer per well. 125 µL of assay buffer was added to each well, and the plate was placed on the shaker for 30 seconds before being analysed using the Luminex BioPlex 200 System (Bio-Rad Laboratories Ltd). Data were analysed using Bio-Plex Manager software (Bio-Rad Laboratories Ltd), and the fluorescent intensity for each well recorded. The concentration of IL-8 was calculated using a 5-parameter logistic (5PL) regression standard curve, which was generated from the fluorescent intensity of the standard curve wells.

2.18 Enzyme linked immunosorbent assay (ELISA)

All ELISA were performed as per manufacturer's instructions. Briefly, 96-well plates were pre-coated with a specific capture antibody and incubated overnight. The plates

were then washed, diluted standards and samples were added to the wells. After incubation, wells were washed, followed by the addition of specific detection antibodies. After the washing step to remove unbound components, substrate solution was added to develop the colormetric reaction. A stop solution was then added to stop the reaction, and absorbance was measured at the specified wavelength using a microplate reader.

2.18.1 Quantification of VWF by ELISA

VWF was measured in PFP samples using a human VWF ELISA kit, catalogue number DY2764 (R&D Systems, Abingdon, UK). First, a 96-well microplate was coated with 100 µL per well of diluted Human VWF Capture Antibody then sealed and incubated overnight at room temperature. Next day, stored PFP samples were thawed at 37^{o}C for 5 minutes and vortexed for 5 seconds. The plates were aspirated and washed with wash buffer three times, ensuring the complete removal of liquid. The wells were then blocked with 300 µL of reagent diluent to avoid non-specific binding and incubated for at least 1 hour at room temperature, followed by aspiration and washing 3 times with wash buffer. Standards ranging from 3000 to 0 pg/ml were prepared according to the manufacturer's instructions. Samples also were prepared with a dilution factor of 1:100; 2 µL of each sample diluted with 198 µL of reagent diluent. 100 µL of standards or samples were added to the wells and incubated for 2 hours at room temperature. After aspiration and washing, 100 µL of detection antibody solution was added to each well, followed by another 2 hours of incubation. The wells were rewashed, and 100 µL of diluted Streptavidin-HRP (Horseradish Peroxidase) at 1:40 dilution and incubated for 20 minutes in the dark to ensure proper binding. Following a final wash, 100 µL of substrate solution was added to each well and

incubated for 20 minutes at room temperature in the dark. To stop the reaction, 50 µL of stop solution was added, and the optical density (OD) of each well was immediately measured at 450 nm using the BioTek Synergy fluorometric plate reader with wavelength correction at 570 nm.

2.18.2 Quantification of ADAMTS13 by ELISA

ADAMTS13 was measured in burns PFP using a human ADAMTS13 ELISA kit, catalogue number DY4245 (R&D Systems, Abingdon, UK). First, a 96-well microplate was coated with 100 µL per well of diluted Human ADAMTS13 Capture Antibody then sealed and incubated overnight at room temperature. The next day, stored PFP samples were thawed at 37^{o}C for 5 minutes, and vortexed for 5 seconds. Plates were washed with wash buffer three times, ensuring the complete removal of liquid. The wells were then blocked with 300 µL of reagent diluent to avoid non-specific binding and incubated for at least 1 hour at room temperature, followed by aspiration and washing 3 times with wash buffer. Standards ranged from 50 to 0 ng/ml were prepared according to the manufacture instructions. Samples also were prepared with a dilution factor of 1:100; 2 µL of each sample diluted with 198 µL of reagent diluent. 100 µL of standards or samples were added to the wells and incubated for 2 hours at room temperature. After aspiration and washing, 100 µL of prepared detection antibody was added to each well, followed by another 2 hours incubation. The wells were washed again, and 100 µL of diluted Streptavidin-HRP 1:40 was added and incubated for 20 minutes in the dark to ensure proper binding. Following a final wash, 100 µL of substrate solution was added to each well and incubated for 20 minutes at room temperature in the dark. To stop the reaction, 50 µL of stop solution was added, and

the OD of each well was immediately measured at 450 nm using the BioTek Synergy fluorometric plate reader with wavelength correction at 570 nm.

2.19 Statistics

Appropriate statistical approaches were utilised to analyse in vitro and clinical patient data. The data type (parametric or non-parametric) and whether it comprised repeated measures or independent comparisons determined the statistical test. Each part of the analysis was tested using several forms of experimental data, patient biomarker comparisons, and prediction models.

2.19.1 Statistical analysis of *in vitro* experiments

The results of the *in vitro* tests were analysed using GraphPad Prism (version 10.0). We assessed the normality of the data distribution with the Kolmogorov-Smirnov test. For parametric data, we compared experimental groups using One-Way ANOVA. Tukey's multiple comparisons test for group-to-group comparisons. For parametric data, Dunnett's multiple comparisons test to compare each experimental group with the control. We used the Kruskal-Wallis test for non-parametric data and the Friedman test for non-parametric and repeated measures. Additionally, paired t-tests were conducted for comparing treated versus untreated samples.

2.19.2 Analysis of generated data from burns and trauma patients

For data collected from burn and trauma patients, statistical comparisons among different patient groups (such as septic, non-septic, and healthy controls) were performed using One-Way ANOVA for parametric data and the Kruskal-Wallis test for non-parametric data. To examine the interaction between time and patient status, Two-Way ANOVA was utilized. Mann-Whitney U tests were conducted at specific time points to compare differences between groups. Linear regression models were developed to describe relationships between variables. Additionally, Pearson or Spearman correlations were employed to assess associations between continuous variables where appropriate.

2.19.3 Logistic regression analyses

Logistic regression models were developed to assess the relationship between various haematological parameters and the risk of sepsis. Odds ratios (ORs) and 95% confidence intervals (CIs) were calculated to quantify these associations. The model's discriminatory power was evaluated using the area under the receiver operating characteristic curve (AUROC), while predictive accuracy was measured using the Brier score. Both univariable and multivariable models, including models that incorporated the Revised Baux score, were compared to determine improvements in predictive performance, including models that incorporated the Revised Baux score.

- Odds Ratio (OR): Indicates the probability of an outcome, for example; risk of sepsis incedence. OR >1 indicates an increased possibility, whereas an OR <1 indicates a decreased possibility.

- Area under the receiver operating characteristic curve (AUROC): Evaluate the capacity of the model to differentiate between outcomes, for example; sepsis vs non-sepsis. An elevated AUROC signifies superior discriminatory capability. The AUROC scores can be interpreted as the following:

  0.5-0.6: Poor discrimination.

  0.6-0.7: Acceptable, minimal predictive power.

  0.7-0.8: Moderate discrimination.

  0.8-0.9: Good, excellent discrimination.

  >0.9: Outstanding, high discriminatory power.

- The 95% Confidence Interval (CI): defines the range in which actual OR is expected to fall within 95% of the time, signifying accuracy.

- The Revised Baux score (rBaux): A vital predictive tool for assessing mortality risk in severe burn patients by combining the patient age and TBSA, and can be adjusted for inhalation injuries.

- Brier Score: evaluate predictive accuracy by measuring the difference between predicted chances and actual outcomes; a lower score indicates better accuracy. A score ≤0 indicates perfect accuracy, >0 to 0.25 is generally acceptable predictive accuracy, and >0.25 Indicates less predictive accuracy.

2.19.4 Longitudinal data analysis

Longitudinal data were analysed using linear mixed-effects models, which accounted for variability within subjects over multiple time points. This approach enabled the assessment of trends in the measured parameters over time. Additionally, comparisons among septic, non-septic, and healthy groups were made at each individual time point. Mean values and 95% CIs were reported for these group comparisons, and *p* values were used to determine statistical significance.

2.19.5 Regression models

Multiple logistic regression models were used to evaluate the relationship between biomarkers and clinical outcomes, including sepsis. The AUROC was calculated to determine the predictive value of these biomarkers over time. A 95% CIs was applied, and the model's performance was assessed using both univariable and multivariable approaches.

Chapter 3: Qualitative and Quantitative Analysis of Circulating NET-Derived Nucleic Acid after Severe Thermal Injury

3 Qualitative and quantitative analysis of circulating NET-derived nucleic acid after severe thermal injuries

3.1 Introduction

Neutrophil-derived chromatin and cell-free DNA (cfDNA) are critical components of generated neutrophil extracellular traps (NETs) during the immunological response to injuries and infections [410]. During NET generation (NETosis), neutrophil-derived chromatin and cfDNA are released extracellularly to capture and neutralise pathogens and microorganisms [250]. Released NETs into the extracellular environment are fibres consisting of nuclear chromatin, histones, granular antimicrobial proteins such as myeloperoxidase (MPO), neutrophil elastase (NE) and cathepsin-G [249, 411]. Upon injury and infections, neutrophil activation is triggered by DAMPS, bacterial PAMPs, viruses, pro-inflammatory cytokines such as tumour necrosis factor- α (TNF-α), IL-β1 and IL-8 to undergo NETosis [411-414]. Upon neutrophil stimulation for NET formation, the chromatin undergoes decondensation, including enzymatic citrullination of histone H3 by peptidylarginine deiminase 4 (PAD4), leading to a depletion of positive charge in arginine residues, diminishing the connection between histones and DNA, hence facilitating the unravelling of chromatin [415-417]. The citrullination of histone H3 (CitH3) is a key feature of NETosis, allowing for the expulsion of chromatin into the extracellular environment as cfDNA [418, 419].

However, while neutrophils are vital for preventing infection, excessive activation can contribute to secondary tissue damage and exacerbate inflammation, delaying healing and potentially leading to further systemic complications [420]. Korkmaz et al. (2017) highlighted a substantial correlation between the pro-coagulant status of the microvascular endothelium in the burn site and the presence of NETs, suggesting excessively generated NETs are involved in coagulation-related thrombotic

complications in burn patients [421]. Narasaraju et al. (2011) have shown evidence that more tissue and endothelial damage occurs due to excessive NETosis, which promotes microvascular thrombosis and contributes to the immunopathology of respiratory failure [422]. Additionally, excessive NETosis leads to an increased coagulation state by activating the vascular endothelium and by interacting with platelets and the coagulation system, causing platelet aggregation and clotting in the microvessels, leading to DIC and MOF [311, 423].

Deoxyribonucleases (DNases) play a critical role in regulating and degrading generated NETs by cleaving the DNA backbone. This enzymatic activity is essential for preventing the excessive inflammation, clotting and tissue injury that are caused by the accumulation of generated NETs [309]. However, degradation of generated NETs with DNase I releases high levels of cfDNA [335, 424]. The process of degrading NET derived large fragments of chromatin by DNase I subsequently releases smaller fragments of cfDNA into the circulation [285, 425]. Several studies have reported significant elevation in cfDNA levels following trauma and severe burn injuries [73, 74, 306, 426, 427]. Additionally, circulating cfDNA has been increasingly recognised as a critical biomarker in the aftermath of injury and inflammation, as it indicates immune response activation and tissue damage. Dwivedi et al. (2012) and Altrichter et al. (2010) have reported that elevated levels of cfDNA following severe thermal and trauma injuries were strongly associated with sepsis incidence, increased mortality and poor clinical outcomes, suggesting that cfDNA could be a reliable biomarker for predicting the prognosis of septic patients [73, 428]. Furthermore, Hampson et al. (2017) have demonstrated that cfDNA biomarker is a strong early predictor of sepsis following severe thermal injuries [74]. These results emphasise the potential of cfDNA

as a biomarker for the surveillance of inflammation and injury, which can provide valuable insights into patient management and therapeutic strategies.

Circulating cfDNA fragments post injuries have been reported with sizes varying between 140-170 base pairs (bp) [429-432]. Measuring cfDNA post-severe thermal injuries or trauma is essential for evaluating inflammation severity and predicting patient outcomes. Several studies have measured cfDNA using different sources of samples for the measurement, including serum, heparin plasma, and citrate plasma. Measuring cfDNA post-severe thermal injuries or trauma is associated with several challenges. CfDNA levels in serum samples were reported with higher levels than in plasma samples, suggesting the presence of non-specific binding proteins or more released DNA during the clotting [433-435]. Also, cfDNA analysis in EDTA and citrated plasma were reported to be more accurate than in heparinised plasma due to the leucocyte activation and interference with PCR-based cfDNA assays due to heparin's inhibitory effects on polymerase activity [436, 437]. However, the possibility of contamination with leukocyte DNA in either serum or EDTA tubes, tri-sodium citrate anticoagulation is now mostly preferred [436, 438, 439].

Importantly, the preparation processes for measurement of plasma cfDNA typically involve centrifugation, which potentially results in the loss of large, undigested chromatin fragments due to their size and density. Consequently, the larger chromatin fragments of generated NETs are therefore excluded from analysis in plasma. This is supported by Sakuma et al. (2022), who demonstrated the presence of circulating large chromatin fragments within *in vitro* PMA-stimulated whole blood using a microfluidic assay designed to capture circulating NETs. [314]. This provides a more comprehensive approach for detecting the true nature of circulating DNA, including these larger chromatin structures in clinical samples and settings.

Therefore, this study aims to provide a comprehensive analysis of the post-injury dynamic changes in circulating NET-derived chromatin and cfDNA in patients with burns and trauma, focusing on both quantitative and qualitative analysis of nucleic acids within whole blood, plasma and from experiments with *in vitro* NET release.

3.2 Results

3.2.1 Circulating plasma levels of cfDNA following severe burns and trauma

NET-derived cfDNA levels in post-injury platelet-free plasma (PFP) of burns and trauma patients (detailed patient cohort and demographics in sections 2.1.2, Table 2.1 and 2.2) were measured and compared to cfDNA levels of healthy controls (HC). Figure 3.1 shows that plasma cfDNA levels were significantly elevated in both burns and trauma patients compared to HC. Figure 3.1A illustrates that cfDNA levels in burns were significantly increased on days D1 to D3 (p <0.05), D4 (p <0.01), and D5 to14 (p < 0.0001). cfDNA levels in trauma patients were also significantly increased at all measured timepoints (T0, T4-12h, and T-48-72h) (p <0.0001) compared to HC cfDNA levels (Figure 3.1B).

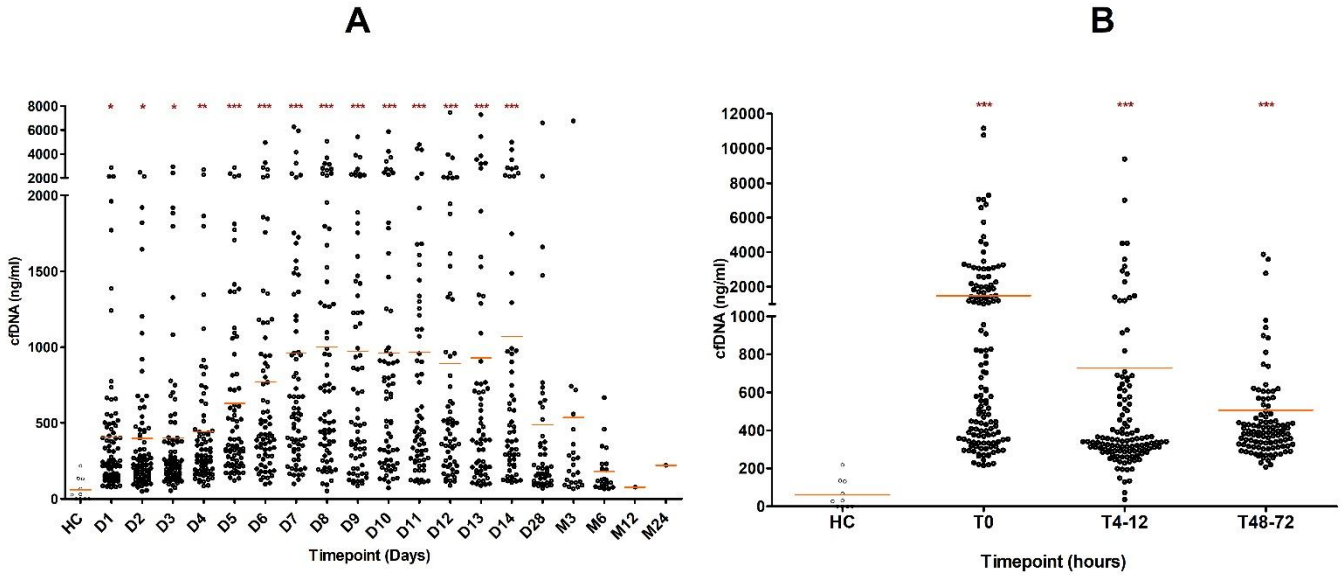

Figure 3.1: Quantification of cfDNA in burns and trauma plasma. Plasma cfDNA levels across time following burn injury (n=96) (A) and trauma (n=135) (B). Data at each timepoint was compared to healthy control (HC) (n=10) values using One way ANOVA (Kruskal-Wallis test). *p* values; * <0.05 for SIFTI2 patients, * <0.001 for GH patients. Orange bands show the median levels of cfDNA.

3.2.2 CfDNA as a biomarker of sepsis following severe thermal injury.

CfDNA levels were significantly increased in septic burns compared to non-septic burns on days 7-14, with a peak of increased levels on day 8 (*p* <0.001) (Figure 3.2 A). The longitudinal analyses in Figure 3.2 B shows cfDNA levels are rapidly increased in the early days post burns in both septic and non-septic burns with high elevation observed between days 7 and 14 compared to HC. The levels were significantly elevated in septic burns compared to non-septic burns between days 7 and 14. The prognostic modelling in Table 3.1 evaluated the cfDNA association with sepsis post severe thermal injuries. The odds ratio (OR) for cfDNA and sepsis on day 1 was 1.133 (95% CI: 0.944 to 1.359), with an area under the receiver operating curve (AUROC) of 0.599 (95% CI: 0.472 to 0.727), The association of cfDNA levels and sepsis were

then significantly increased on days 7, 14 and 28, peaked at day 14 with an excellent discrimination between septic and non-septic burns with an OR of 1.154 (95%: 1.022 to 1.303) and an AUROC of 0.823 (95% CI: 0.711 to 0.934), .

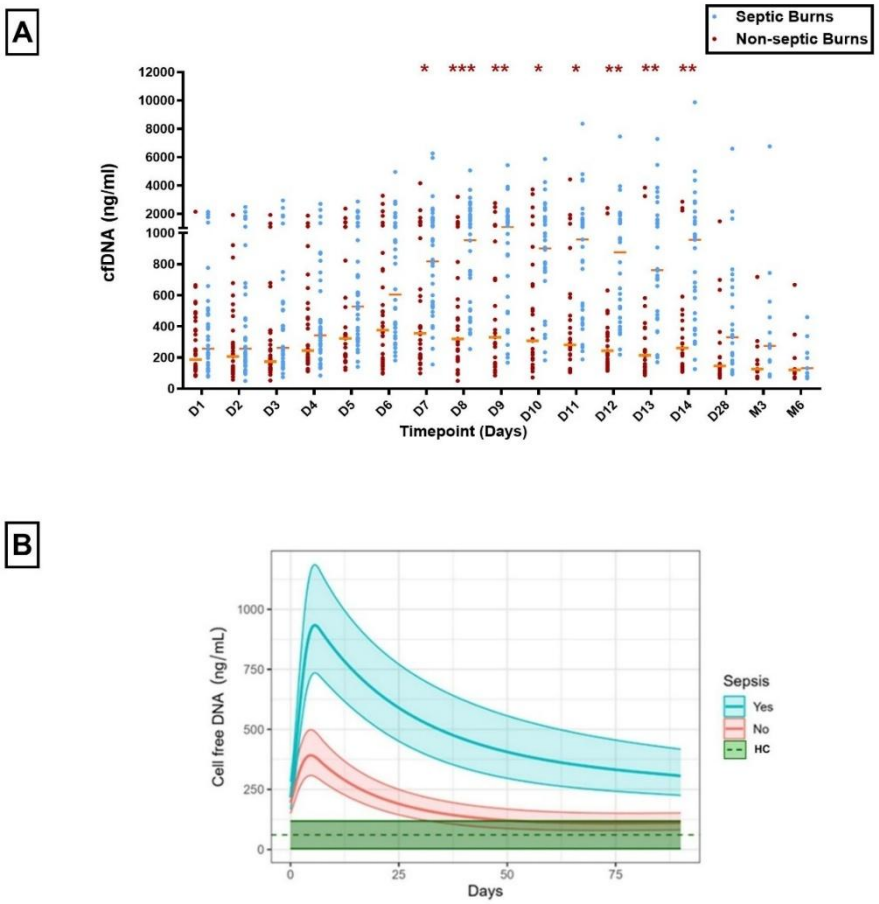

Figure 3.2: CfDNA levels in septic and non-septic burns. (A) Comparison between cfDNA levels in septic (blue) and non-septic burns (red). CfDNA levels were significantly increased in septic burns on days 7-14 compared to non-septic burns. (B) Longitudinal model analysis was performed using linear mixed-effects models to examine the changes in cfDNA dynamics in septic burns (blue), non-septic burns (red), and healthy controls (HC; green). The lines represent the means for each group, while the shaded regions indicate the 95% confidence intervals. CfDNA levels were rapidly increased from day 1 to day 28 in both septic and non-septic burns with peak elevations on days 7-14 compared to HC levels. The levels of septic burns were significantly increased compared to non-septic burns on days 7-14. Data in (A) were analysed using two-way ANOVA test (Tukey's multiple comparisons test), *p* *** < 0.001, ** < 0.01, * < 0.05.

Table 3.1: Prognostic modelling of cfDNA for sepsis prediction in septic and non-septic burns							
Day	**Sepsis**		**Odds Ratio**		**AUROC**		**Brier Score**
	Yes	**No**	**OR**	**95% CI**	**AUROC**	**95% CI**	
1	39	39	1.133	(0.944 to 1.359)	0.599	(0.472 to 0.727)	0.243
2	35	31	1.115	(0.941 to 1.321)	0.595	(0.456 to 0.735)	0.243
3	36	36	1.096	(0.949 to 1.266)	0.633	(0.502 to 0.764)	0.244
4	35	31	1.076	(0.922 to 1.255)	0.595	(0.453 to 0.738)	0.246
5	37	32	1.110	(0.971 to 1.269)	0.669	(0.536 to 0.803)	0.239
6	32	29	1.068	(0.968 to 1.177)	0.658	(0.517 to 0.800)	0.241
7	35	31	1.105	(0.997 to 1.224)	0.738	(0.610 to 0.865)	0.227
14	31	29	1.154	(1.022 to 1.303)	0.823	(0.711 to 0.934)	0.207
28	23	19	1.199	(0.897 to 1.603)	0.756	(0.595 to 0.917)	0.236

3.2.3 Characterisation of the qualitative nature of plasma cfDNA in burn and trauma patients

To determine the qualitative nature of circulating NET-derived cfDNA in burns and trauma, cfDNA was extracted from platelet-free plasma and measured by a high-sensitivity DNA electrophoresis analyser. Figure 3.3 shows the time course of post injury burns samples (D1-D28) from a single patient with severe thermal injury (65% TBSA). Figure 3.3 A illustrates the size of the cfDNA in base pairs (bp) with a prominent nucleosome band apparent between 140 to 170 bp (red arrow) [440] in

lanes 3-11 (days 2 - 28). In contrast, no bands were detected in HC (green arrow, lane 2, Figure 3.3A). Furthermore, there was no detectable DNA less than 7000 bp in lane 2 (day 1). In Lanes 3 and 4 (days 2 and 3), bands just less than 7000 bp became visible and coincided with the appearance of a faint 150 bp band, and the density of the 150 bp band increased on subsequent days and correlated with measured cfDNA concentrations in plasma (Figure 3.3B). Figure 3.3C shows the gel densitometry of the DNA peaks measured in the samples. Blue and black arrows show the lower and higher calibration peaks at 35bp and 10,380bp, respectively. The red arrows illustrate DNA bands at ~150bp in the majority of burns samples compared with the negative healthy donor sample (HC). The density of the ~150 bp nucleosome bands (Figure 3.3A) also correlated with measured cfDNA concentrations (Figure 3.3B). Figure 3.4 shows other representative examples for measured cfDNA size in a further 4 burns patients. Figure 3.4A shows the electrophoresis gels of measured extracted DNA size on days 1-28 for each burn patient (Lanes 2-11) compared to HC in Lane 1 (green arrow), corresponding to measured plasma cfDNA concentrations for each one in Figure 3.4B. The densities of measured nucleosome band bands (at the red arrows) in Figure 3.4A correlated with measured cfDNA concentrations in those burns plasma in Figure 3.4B. Interestingly, there was some heterogeneity observed between patients with a prominent nucleosome band in the day 1 sample from the 4th burns patient.

Golden Hour trauma plasma samples are shown in Figure 3.5. Although the predominant nucleosome band of ~ 150 bp is observed further nucleosome oligomers (i.e. ~ 300 and 450 bp) were also present within all 3 trauma patient samples at T0 (< 1 hour post-injury). Fainter nucleosome bands but no oligomers were detected at ~150 bp at 4-12h and 48-72h post-injury (Figure 3.5A, Lanes 3-11) A HC (Lane 1) and a D8

burn sample (Lane 2) were also run as negative and positive controls. The densities of the nucleosome bands also correlated with measured cfDNA levels in trauma patients (Figure 3-5B) and with the densitometry peaks in Figure 3-5C.

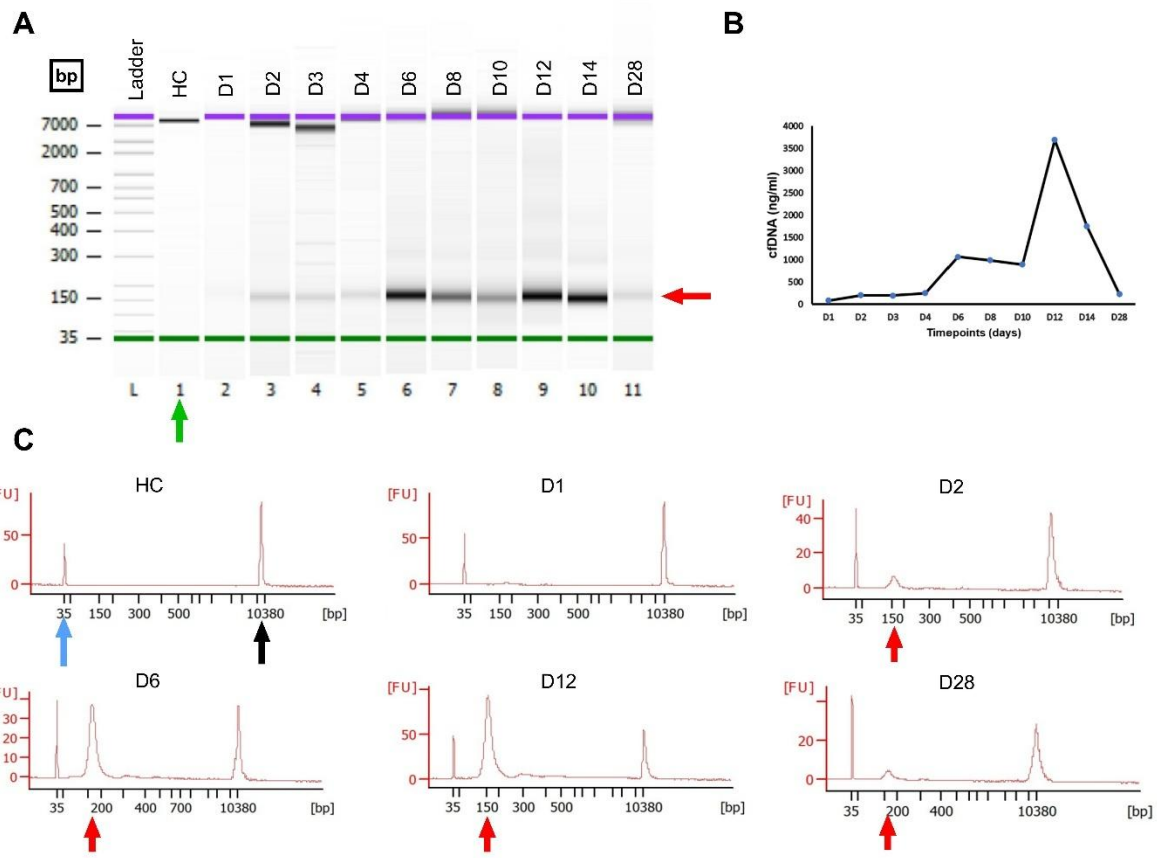

Figure 3.3: Measurement of chromatin and cfDNA size in burns. DNA size within plasma samples from a SIFTI-2 burns patient. (A) The red arrow shows the DNA bands at ~140-170 bp representing nucleosomes. Lane L is the calibration ladder. The green arrow (Lane 1) shows a healthy sample (HC). Lanes 2-11 are days 1 - 28 post-injury. (B) Time course of the changes in cfDNA concentration over 28 days post-injury in SIFTI-2 A-028. (C) Gel densitometry shows examples of the DNA peaks measured in the samples. The blue and black arrows show the lower and higher calibration peaks at 35bp and 10,380bp, respectively. The red arrows show DNA at ~140-170 bp in burns samples compared with the healthy donor sample (HC). DNA peaks correlated with nucleosome density(A) and measured plasma-cfDNA concentrations (B).

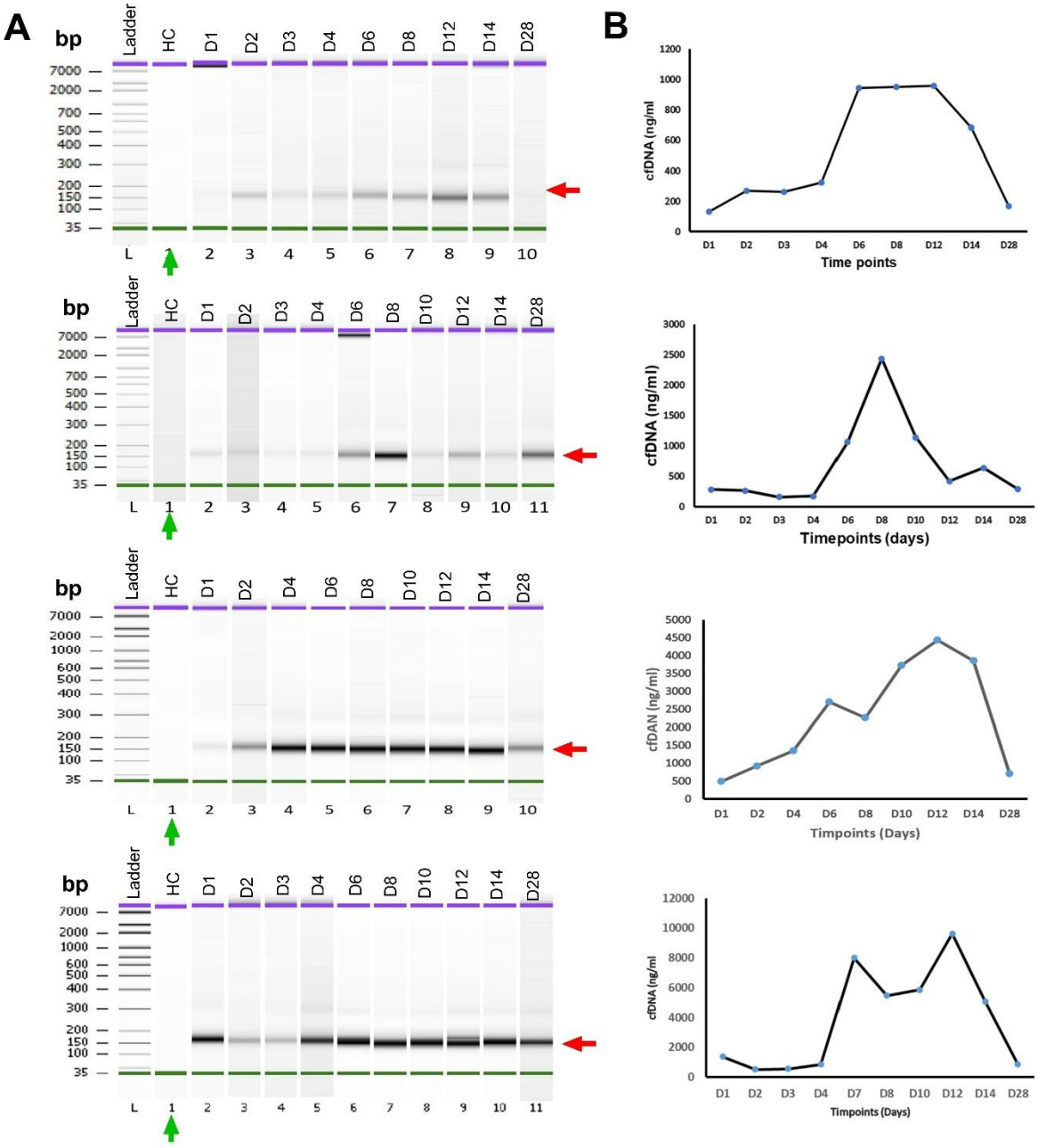

Figure 3.4: Measurement of chromatin and cfDNA size in burns. The figure illustrates the DNA size within plasma samples from a further four SIFTI-2 burns patients. (A) illustrates 4 electrophoresis gels for each burn of measured extracted DNA sizes on days 1-28. The green arrow in Lane 1 represents the HC. Lanes 2-11 are days 1–28 post-injury. The red arrows indicate nucleosome DNA fragments (~140-170 bp). (B) shows the corresponding plasma cfDNA levels.

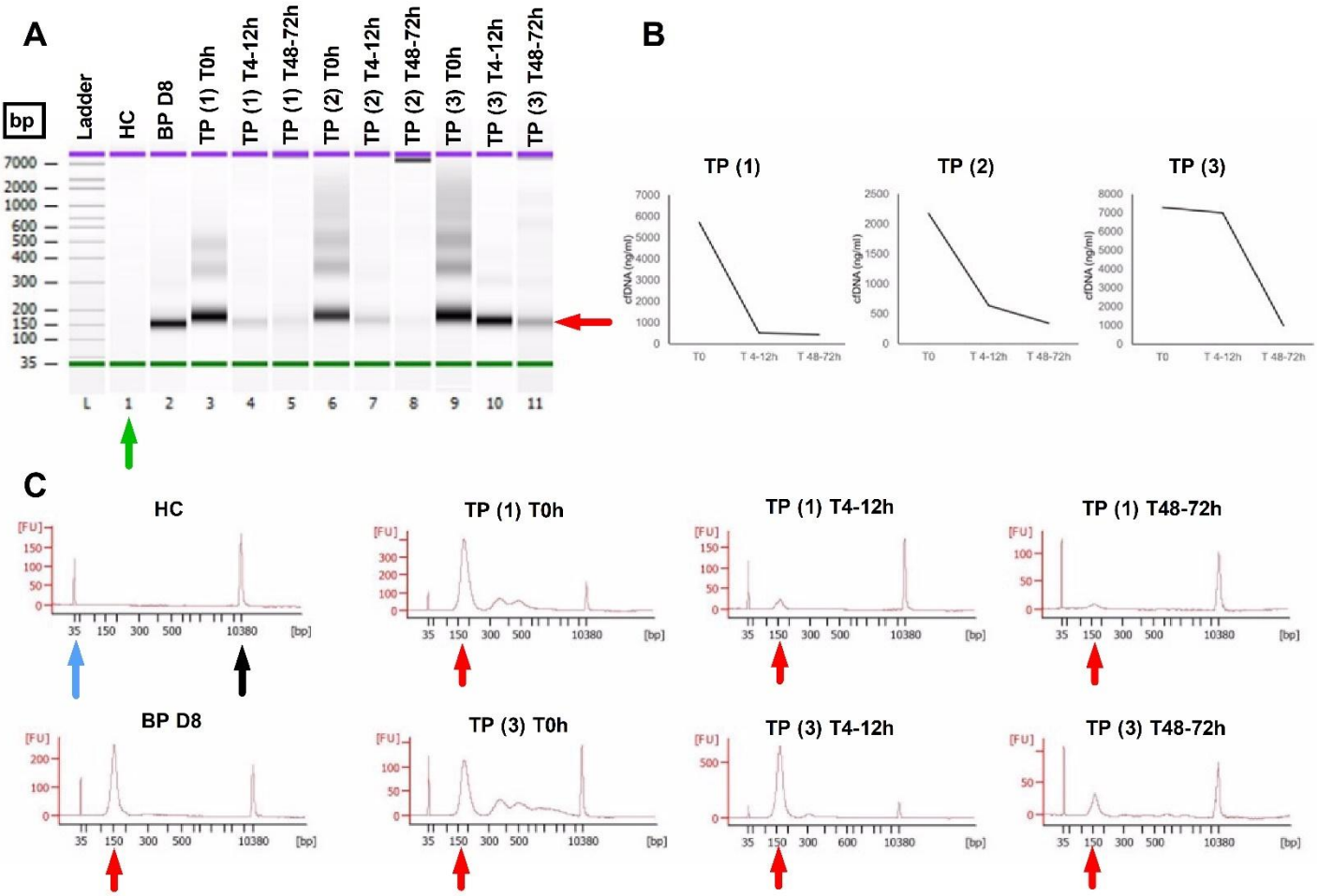

Figure 3.5: Chromatin and cfDNA size measurement in trauma (GH patients). (A) DNA size within GH Trauma patients (TP) plasma samples compared to HC and a D8 sample from a burns patient (BP). The red arrow shows the nucleosome bands at 140-170bp. The green arrow shows the DNA of a healthy donor. T0 for all trauma patients' samples shows that larger nucleosome oligomer sizes were detected. (B) Time course of the changes in cfDNA concentrations measured for trauma samples. High cfDNA concentrations were significantly associated with the density of the nucleosome bands. (C) Densitometry shows the DNA band peaks.

3.2.4 Generation of nucleosomes from digestion of NETs in vitro

To validate that NET degradation by digestion leads to the generation of nucleosomes of ~150 bp, we stimulated purified neutrophils with PMA to generate NETs *in vitro.* NETs were degraded with either 20U/ml MNase or 10U/ml DNase I or left undigested. Figure 3.6 shows that NET degradation with either MNase (Lane 4) or DNase I (Lane 5) resulted in the generation of nucleosome bands of ~150 bp compared to controls of a commercial nucleosome preparation (Lane 1), normal HC plasma (Lane 2), and undegraded NETs (Lane 3) (Figure 3.6A). Densitometry analysis in Figure 3.6B confirms the DNA peaks with nucleosome bands of ~ 150 bp.

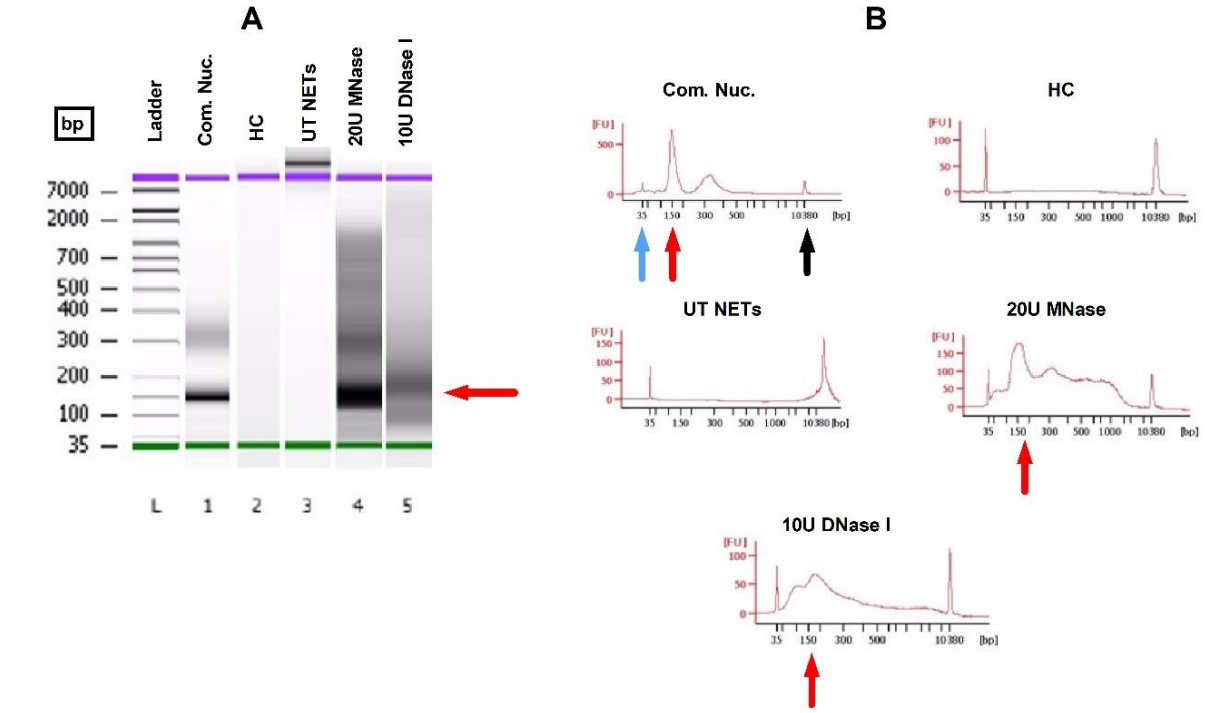

Figure 3.6: Measurement of chromatin and cfDNA size generated by digestion of isolated NETs. (A) Lanes 1 and 2 show the commercial nucleosome (Com. Nuc.) and healthy control (HC). Lane 3 is untreated (UT) NETs. Lanes 5-6 show the DNA size for treated NETs with 20U MNase or 10U DNase I for 20 minutes, respectively. Treated NETs with MNase and DNase I have generated nucleosomes in Lanes 4 and 5. (B) Densitometry showing the DNA band peaks measured for commercial nucleosome, HC, UT NETs, and treated NETs with MNase and DNase I samples. Blue and black arrows illustrate the lower and higher calibration peaks at 35bp and 10,380bp, respectively. The red arrows show nucleosome peaks. DNA peaks correlated with nucleosome densities of the purified nucleosome, generated nucleosomes by MNase and DNase I.

3.2.5 Circulating nucleosome H3.1 in burns

3.2.5.1 Levels of circulating nucleosome H3.1 post thermal injury

Measured circulated nucleosomes H3.1 (NuQ. H3.1) by ELISA in burns were significantly elevated on days 1, 7, 10, and 14 compared to the levels in HC (Figure 3.7).

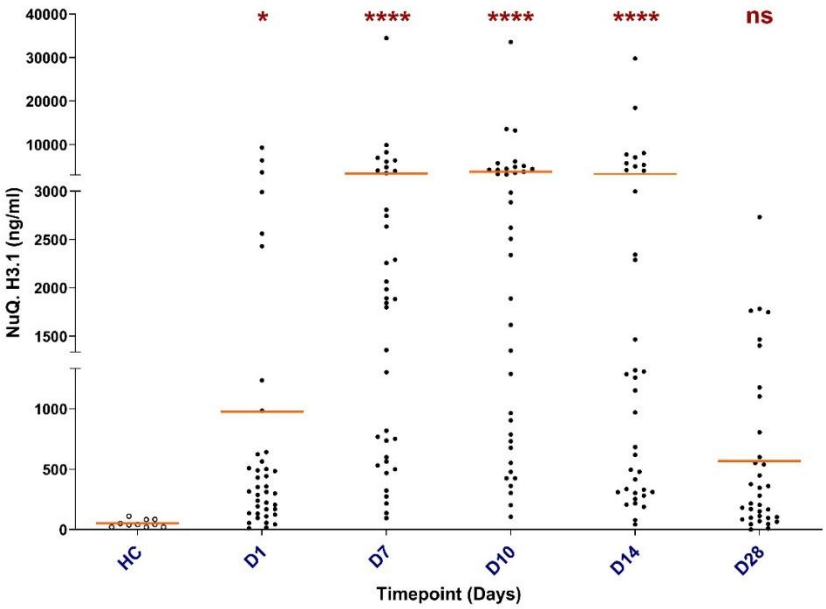

Figure 3.7: Quantification of circulating NuQ. H3.1 post thermal injuries. Plasma NuQ. H3.1 levels on days, 1, 7,10,14, and 28 following burn injury (n=36) were measured by ELISA and compared to HC (n=10). Levels were significantly elevated on days 1, 7, 10, and 14 compared to the levels measured in HC. Data at each timepoint was compared to healthy control values using One way ANOVA (Kruskal-Wallis test); *p<0.05, ****p<0.0001. Orange bands show the median levels of NuQ. H3.1.

3.2.5.2 NuQ H3.1 levels are significantly correlated with cfDNA levels in severe thermal injuries

We investigated the correlation between circulating NuQ. H3.1 and cfDNA levels within the identical samples and cohort of burns patients (n=39) (days 1, 7, 10, 14, and 28) to assess the relationship between these two biomarkers. As shown in Table 3.1, a significant positive correlation was observed between NuQ. H3.1 and cfDNA levels from day 1 through day 28 post-injury. On day 1, there was a moderate but significant correlation (p =0.0033) with an R value of 0.4583. The strength of the correlation increased over time, peaking on day 10 (R = 0.8001, p < 0.0001) and day 14 (R =

0.8156, $p < 0.0001$). By day 28, the correlation remained significant ($p = 0.0006$) with an R value of 0.5587. Overall, across all measured time points, the correlation between NuQ. H3.1 and cfDNA was highly significant ($p < 0.0001$) with a strong R value of 0.7282 (Figure 3.8).

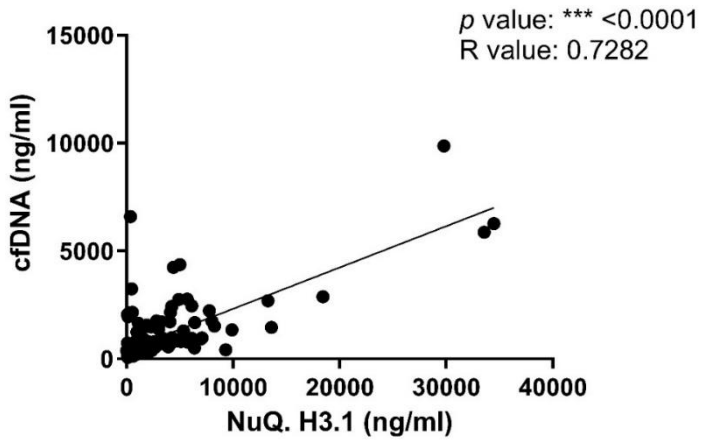

Figure 3.8: NuQ. H3.1 correlation with cfDNA levels post severe burn injury. There was a significant overall correlation between plasma NuQ. H3.1 and cfDNA levels overall post-injury time points measured in thermal injuries (n = 39). [Spearman *p* value]: *** < 0.0001, R value =0.7282.

Table 3.2: The correlation between plasma levels of NuQ. H3.1 and cfDNA over time post severe thermal injury (N = 39)				
Days	Number of Burn Patients	Correlation (Y/N)	*p* Value	R Value
DAY 1	39	Y **	0.0033	0.4583
DAY 7	37	Y ***	0.0005	0.5446
DAY 10	37	Y ***	<0.0001	0.8001
DAY 14	37	Y ***	<0.0001	0.8156
DAY 28	34	Y ***	0.0006	0.5587
Overall	177	Y ***	<0.0001	0.7282

Spearman *p* value: ***p*<0.01, ****p*<0.001

3.2.5.3 Dynamics of circulating NuQ. H3.1 and cfDNA levels in septic and non-septic burns

Levels of circulating NuQ. H3.1 and cfDNA in burn (n=39) were further analysed using longitudinal analysis to understand the dynamics and differences between both biomarkers in septic and non-septic burns and compared to HC levels in measured timepoints. Figure 3.9A illustrates the combined trends for NuQ. H3.1 and cfDNA with both biomarkers peaking around day 12 post-burn. NuQ. H3.1 levels were also consistently higher than cfDNA. Figure 3.9B and 3.9C further illustrate the divergence between burns who developed sepsis or not. In both Figure 3.9B and 3.9C, septic

burns exhibited significantly higher levels of NuQ. H3.1 (Figure 3-9B) and cfDNA (Figure 3-9C) compared to non-sepsis patients and healthy controls.

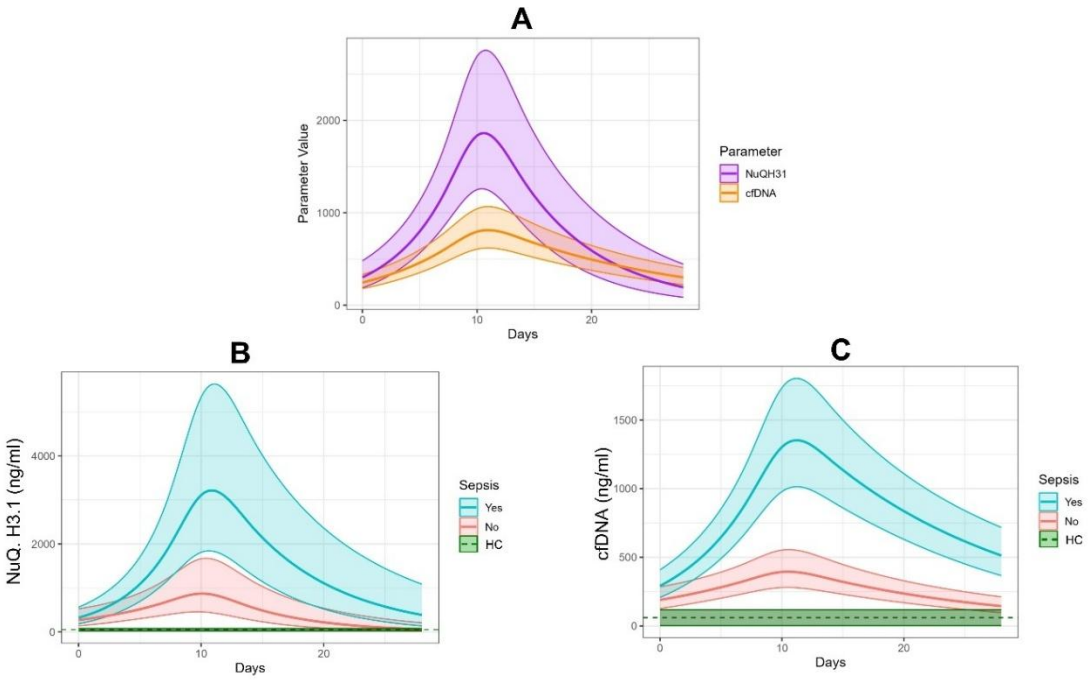

Figure 3.9: Dynamics of NuQ. H3.1 and cfDNA levels in burn injury. The levels of NuQ. H3.1 and cfDNA post burns (n=39) were compared by performing a longitudinal modelling assay, using linear mixed-effects models to investigate the relationship between time and either cfDNA or NuQ. H3 levels, illustrating the mean values and 95% CI for each measured timepoint. (A) Illustrates the longitudinal modelling for the combined trends of NuQ. H3.1 (purple) and cfDNA (orange) levels in burn patients were associated with a similar trend, with values peaking around 12 days post-thermal injury, reaching higher levels of NuQ. H3.1 compared to cfDNA. (B) specifically compares NuQ. H3.1 levels between burn patients who developed sepsis (blue), those who did not develop sepsis (red), and HC (green). NuQ. H3.1 levels were significantly elevated in septic burns patients, particularly around day 12, compared to non-septic burns and controls. (C) shows the cfDNA levels across the same groups, with septic burns exhibiting higher levels compared to non-septic burns and HC.

3.2.5.4 A comparative analysis of circulating NuQ. H3.1 and cfDNA Levels post thermal injuries in sepsis progression

To further investigate elevated NuQ. H3.1 and cfDNA levels in septic burns, we performed a prognostic analysis for sepsis prediction on measured timepoints. In this study, 51.2% of recruited burn patients developed sepsis between days 2 and 28, with the majority of cases occurring on days 5–7. Table 3.2 shows the association of measured levels with sepsis were higher in cfDNA than in NuQ. H3.1. The potential of sepsis prediction on day 1 is higher in cfDNA with an odds ratio (OR) of 1.989 (95% CI: 0.833 to 4.750) and an AUROC of 0.69 (95% CI: 0.520 to 0.861) compared to NuQ. H3.1 with an OR of 1.115 (95% CI: 0.881 to 1.412) and an AUROC of 0.587 (95% CI: 0.399 to 0.775). By day 14, cfDNA outperforms NuQ. H3.1 in sepsis prediction, with a higher OR (2.002, 95% CI: 1.072 to 3.741) and AUROC (0.923, 95% CI: 10.822 to 1.000) levels. We investigated sepsis progression by performing prognostic modelling combined cfDNA and NuQ. H3.1 levels to see if this improves the performance comparing to the univariable models. Table 3-3 shows the combined modelling of cfDNA and NuQ. H3.1 did not significantly improve the performance of sepsis prediction on day 1, but the performance resulted in a stronger association with sepsis on days 7, 10, 14, and day 28. For example, on day 7, the association of the combined model with sepsis was with an AUROC of 0.815 (95% CI: 0.660 to 0.971). Adding the revised Baux Score to the combination of cfDNA and NuQ. H3.1 further improved the performance, particularly on day 1, and was stronger with an AUROC 0.88 (95% CI: 0.779 to 0.993) compared to the combination of cfDNA and NuQ H3.1 that was with an AUROC 0.693 (95% CI: 0.522 to 0.863).

Table 3.3: A Comparative Analysis of NuQ. H3.1 and cfDNA Levels post thermal injuries (burns=39).								
Day	**Type**	**Sepsis Yes**	**Sepsis No**	**Odds Ratio**	**95% CI**	**AUROC**	**AUROC 95% CI**	**Brier Score**
1	**NuQ. H3.1**	23	16	1.115	(0.881 to 1.412)	0.587	(0.399 to 0.775)	0.237
	cfDNA	23	16	1.989	(0.833 to 4.750)	0.69	(0.520 to 0.861)	0.217
7	**NuQ. H3.1**	22	15	1.134	(0.954 to 1.347)	0.676	(0.493 to 0.859)	0.22
	cfDNA	22	16	1.532	(1.037 to 2.264)	0.773	(0.609 to 0.936)	0.198
10	**NuQ. H3.1**	22	15	1.352	(1.059 to 1.726)	0.815	(0.667 to 0.964)	0.175
	cfDNA	22	16	1.818	(1.087 to 3.040)	0.881	(0.758 to 1.000)	0.154
14	**NuQ. H3.1**	21	16	1.235	(1.000 to 1.525)	0.792	(0.641 to 0.942)	0.194
	cfDNA	22	16	2.002	(1.072 to 3.741)	0.923	(0.822 to 1.000)	0.139
28	**NuQ. H3.1**	20	14	6.168	(1.115 to 34.13)	0.779	(0.621 to 0.936)	0.176
	cfDNA	20	16	5.704	(1.472 to 22.10)	0.884	(0.774 to 0.995)	0.157

Table 3.4: Sepsis prediction models using cfDNA, NuQ. H3.1, and Revised Baux Score (burns=39).						
Day	**Sepsis Yes**	**Sepsis No**	**Model Combination**	**AUROC**	**95% CI**	**Brier Score**
1	23	16	cfDNA + NuQ. H3.1	0.693	(0.522 to 0.863)	0.216
			cfDNA + NuQ. H3.1 + Revised Baux	0.886	(0.779 to 0.993)	0.145
7	22	15	cfDNA + NuQ. H3.1	0.815	(0.660 to 0.971)	0.184
			cfDNA + NuQ. H3.1 + Revised Baux	0.894	(0.79 to 0.998)	0.137
10	22	15	cfDNA + NuQ. H3.1	0.879	(0.755 to 1.000)	0.152
			cfDNA + NuQ. H3.1 + Revised Baux	0.876	(0.748 to 1.000)	0.131
14	21	16	cfDNA + NuQ. H3.1	0.920	(0.818 to 1.000)	0.141
			cfDNA + NuQ. H3.1 + Revised Baux	0.890	(0.774 to 1.000)	0.142
28	20	14	cfDNA + NuQ. H3.1	0.939	(0.867 to 1.000)	0.110
			cfDNA + NuQ. H3.1 + Revised Baux	0.943	(0.859 to 1.000)	0.082

3.2.6 Circulating NET derived chromatin in whole blood following severe thermal injury

Circulating NET derived chromatin in whole blood samples was measured using the chip based capture method developed by Sakuma et al. (2022) [314]. To validate the method, chromatin was initially captured from normal whole blood (WB) (Figure 3.10A), and isolated neutrophils (NEUTs) with both stimulated with and without PMA. Captured chromatin specifically derived from NETs was labelled with SYTOX green and Citrullinated Histone H3. The area was measured by ImageJ software. The area of captured chromatin from both PMA-treated WB or NEUTs was significantly

increased ($p < 0.05$ and $p < 0.01$ respectively) compared to untreated controls (Figure 3.10B).

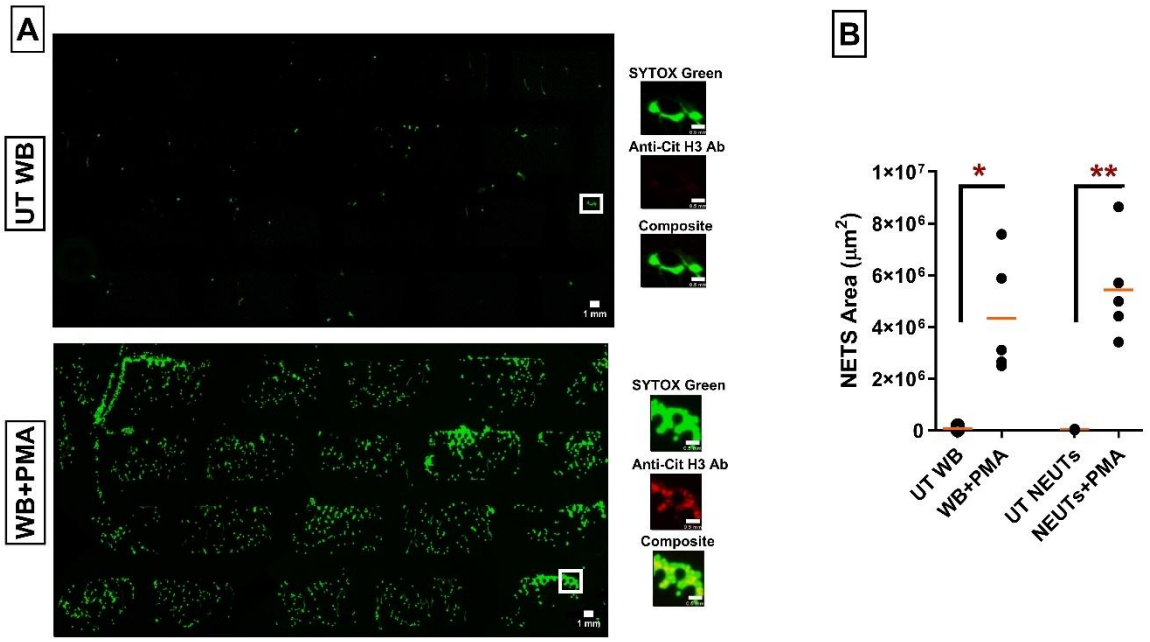

Figure 3.10: Captured circulating NETs from stimulated neutrophils and whole blood. (A) Fluorescent images of SYTOX green stained captured NETs across the microfluidic chip from untreated whole blood (WB) and treated WB with PMA (WB+PMA). The scale bar represents 1mm. Magnification of white squared area as confirmation of neutrophil-derived chromatin fibres, the chromatin fibres were double-stained with SYTOX green and anti-citH3 Ab (labelled with Donkey anti-Rabbit IgG secondary Ab) to verify the overlap between citrullinated histone-positive regions and DNA. The scale bar represents 0.5 mm. (B) A comparison between the area of captured NETs (μm^2) from untreated (UT) and treated WB and neutrophils with PMA. The area of captured NETs was significantly higher from treated WB and NEUTs with PMA compared to UT WB and NEUTs, respectively. Data was analysed using Paired t test. *p* value *< 0.05, **<0.01.

Circulated NET-derived chromatin was then measured within whole blood at Days 1, 4, 8 and 14 following burn injury. Figure 3.11 is a representative example of captured circulated NETs from whole blood from a burns patient with 29.2% TBSA. Day 1 sample (~ 23 hours post-burn) shows increased area of captured NETs stained with SYTOX green compared to days 4, 8 and 14. A magnified image was double-labelled with SYTOX green and Anti-CitH3 Ab, confirming the captured chromatin was generated from NETs. The composite shows the co-localisation. Figure 3.12A shows a representative image of captured chromatin from another burns patient with 28.5% TBSA, labelled with SYTOX green with a significantly increased area on day 1 sample (~ 19 hours post-burn) compared to days 4, 8 and 14 post-injury. Magnified images were also double-labelled with SYTOX green and citrullinated histone H3 to confirm the origin from NETs. The area of captured NETs from PMA-treated WB samples and D1 post-burn were significantly increased ($p < 0.001$ and $p < 0.01$ respectively) compared to UT WB (Figure 3-12B).

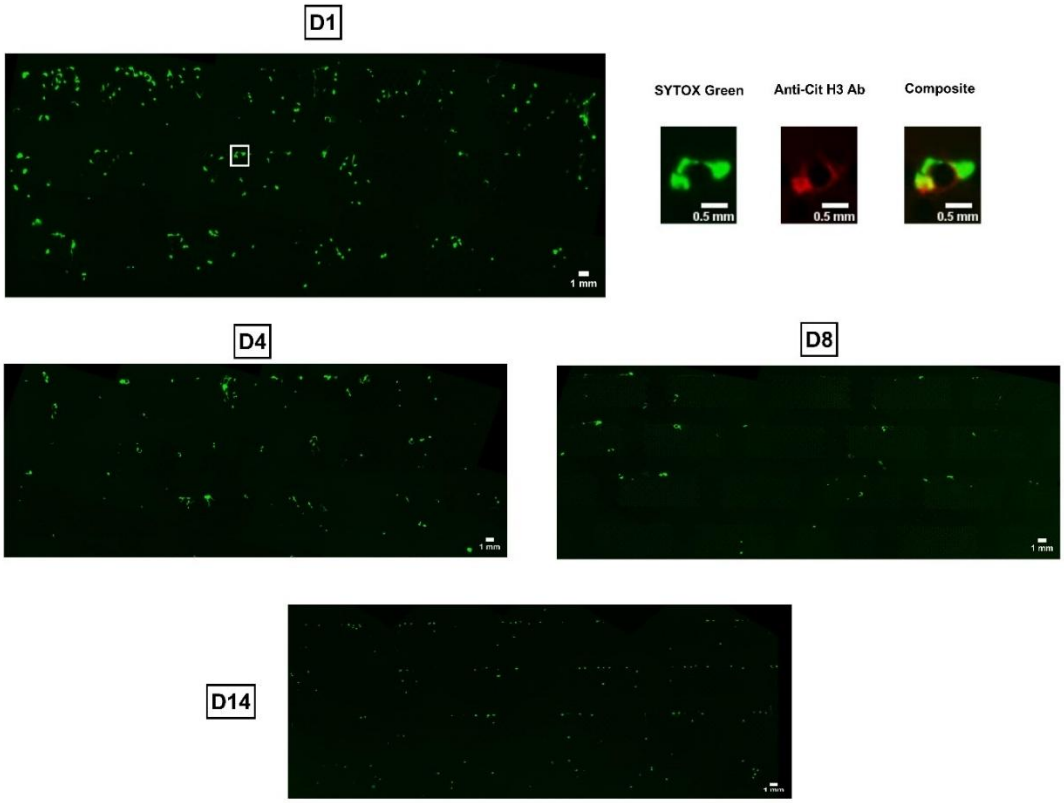

Figure 3.11: Captured circulating NETs in whole blood following severe burn injury. Captured circulated NETs in whole blood samples from a burns patient within microfluidic chips were increased on day 1 compared to days 4, 8 and 14. The scale bar represents 1mm. A magnification of the white squared area on the day one sample as confirmation of NET derived chromatin fibres double-stained with SYTOX green and anti-citH3 Ab (labelled with Donkey anti-Rabbit IgG secondary Ab).

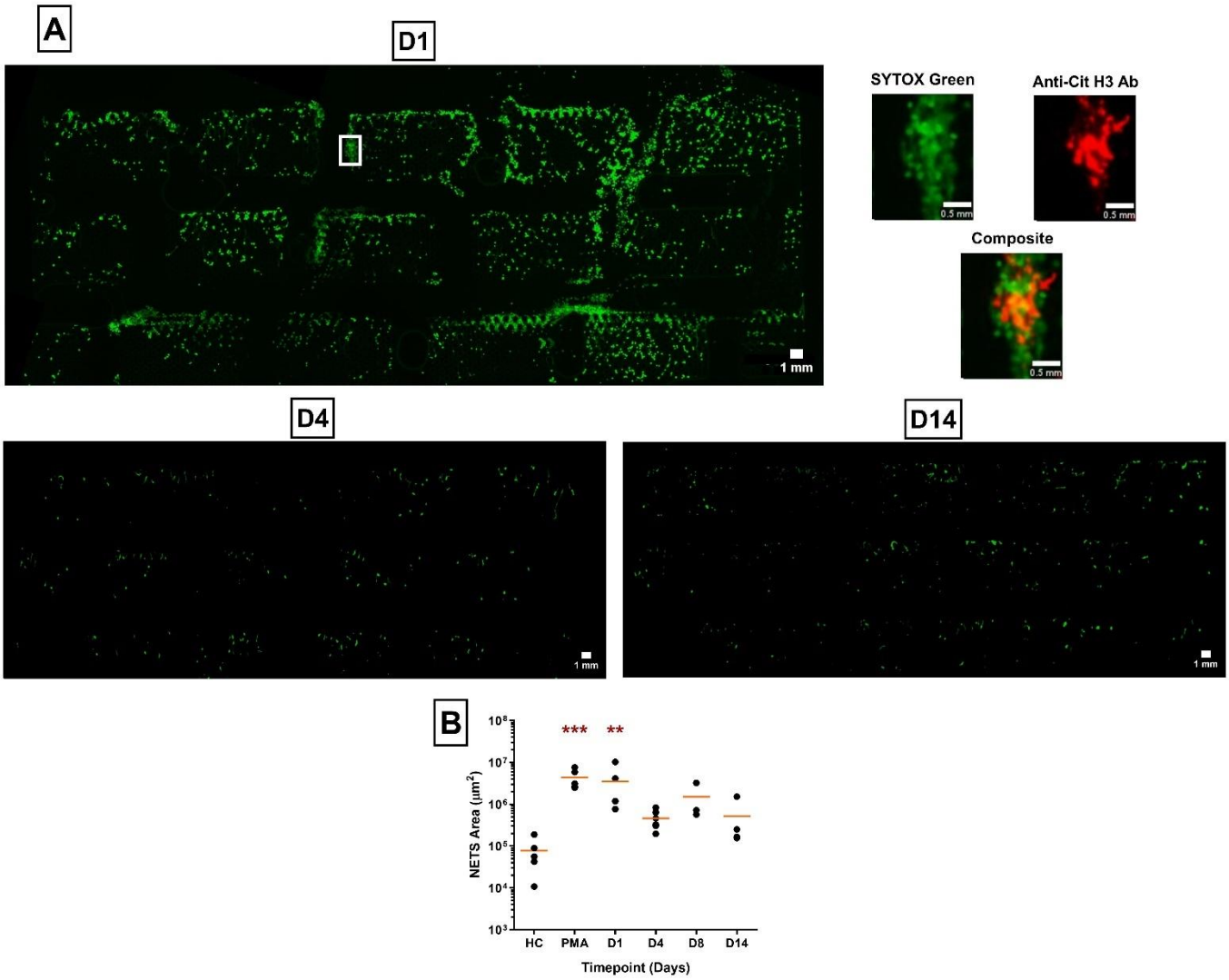

Figure 3.12: Captured circulating NETs in whole blood following severe burn injury. (A) Captured circulated NETs by the microfluidic chips were increased on day 1 than days 4-14. The scale bar represents 1mm. A magnification of the white squared area on the day one sample as confirmation of NET-derived chromatin double-stained with SYTOX green and anti-citH3 Ab. (B) A comparison between the area of captured NET from HC whole blood, treated WB with PMA and captured NETs from burns WB on days 1, 4, 8, and 14. The area of captured NETs were significantly higher in PMA-treated WB and in day 1 of burns WB compared to HC. Captured NETs area on days 4, 8, and 14 were not significantly higher compared to HC. Data was analysed using One way ANOVA (Kruskal-Wallis test). *p* value ***<0.001, **< 0.01.

3.3 Discussion

Monitoring circulating NETs and NET-derived cfDNA is essential for comprehending the inflammatory and neutrophil responses and pathophysiology of severe burns and trauma. The potential of cfDNA as a biomarker for patient prognosis and a therapeutic target has been underscored by the association between elevated levels and adverse clinical outcomes, such as an increased risk of thrombosis and organ dysfunction [74, 441]. Our data confirm the presence of significantly high cfDNA levels following burn and trauma injuries and its association with sepsis. In burn patients, cfDNA levels were sustained and elevated across the majority of measured timepoints from admission till day 28 post-injury. The cfDNA peak was between day 5 and day 28, indicating substantial NET generation release and prolonged inflammatory response due to the severity of inflammation and immune activation. The significant increase in cfDNA levels in septic burns in our study confirms their enormous potential as an early biomarker for sepsis. High levels of cfDNA do seem to reflect ongoing NETosis, eliminating bacterial and pathogens invasion, as several studies demonstrated the correlations between cfDNA levels and NET production during severe inflammation and sepsis [442]. Severe sepsis is characterised by the extensive infiltration of neutrophils into the affected tissue and distant organs, NET formation occurs, resulting in the release of decondensed chromatin and, consequently, the generation of high levels of cfDNA [443]. Our data indicates that cfDNA is associated with poor discrimination of sepsis on day 1 with an AUROC of 0.599 (95% CI: 0.472 to 0.727). The association, however, increased between days 7 and 28, peaked at day14, with an improved AUROC of 0.823 (95% CI: 0.711 to 0.934). Our findings on cfDNA levels confirm our previous studies that also show significantly increased cfDNA levels in septic burns, suggesting a potentially useful marker for sepsis detection burn severity

and mortality [73, 74, 444]. In addition, trauma patients show a rapid and sustained increase in cfDNA levels (T0, T4-12h, T48-72h), indicating an immediate pre-hospital response to the impact of trauma and sterile injury on neutrophils. Our findings confirm previous studies demonstrating increased cfDNA levels following severe thermal and trauma injuries [73, 74, 306, 426, 427]. Importantly, measurements have also confirmed that the cfDNA is not only derived from human nuclei but is associated with the presence of citrullinated histone H3 as a specific marker of NETosis [74, 407]. The DNA is therefore not derived from infections or other cells in the body injured or activated either during or subsequent to injury.

Analysis of the qualitative nature of the cfDNA and the use of a nucleosome specific ELISA suggests that our in-house assay of fluorescent DNA predominantly measures a nucleosome fragment composed of ~150 base pairs. This is the basic building block of DNA and contains an octamer of histones surrounded by a small strand of DNA [445, 446]. Densitometry analysis of detected nucleosome bands in the electrophoresis gels correlated with the measured cfDNA concentrations in plasma. Interestingly, the results also appeared to be different between burns and trauma cohorts, but this is probably a reflection of the differences in sample timing between the 2 cohorts. In trauma, the sterile injury induced a very rapid acute and pre-hospital (< 60 minutes from injury) appearance of nucleosome bands including higher molecular weight oligomers of 300 and 450 bp. This also emphasizes the importance and uniqueness of the golden hour study in the trauma field as we have also identified this and many other early prehospital changes that are unique [407] within 24 and 72 hours the oligomers disappear with a single predominant 150 bp band remaining and starting to fade as the cfDNA levels start to fall. As this study was designed to focus on the ultra-early responses to injury we did not measure the longer term and

dynamics of biomarkers over the first 14 days and a month post-injury as we did in the burns cohort. In contrast, day 1 samples from burns were obtained at an average of ~ 8 hours post injury. Despite this there is only a faint nucleosome 150 bp band present in the majority of the first few samples along with some higher MW DNA species present. One burns patient did show a prominent nucleosome band at day 1 samples (~16 hours post-burn) with 65% TBSA. This was confirmed by measuring the highest levels of whole blood NET-derived chromatin at day 1 post injury using the microfluidic chips. It is likely that nucleosomes are subsequently released by the action of DNase on the large chromatin fragments released from the NETs in the first few days following burn injury (Figures 3.11, and 3.12). This hypothesis is further supported by the previous findings of Dinsdale et al. (2020), who reported a significant reduction in DNase I activity on day 1 post-burn [353].

Measuring extracted DNA size within trauma plasma samples shows the presence of nucleosome oligomers within the < 1 h T0 samples, suggesting that DNA degradation by DNase I was not fully completed and digestion was continuing and T4-12h and T48-72 trauma samples show single nucleosome bands without the oligomers. To validate that degraded generated NETs by DNase I results in nucleosome generation post-burn and trauma, we degraded generated NETs *in vitro* by 20U MNase and 10U DNase I or left untreated. Data (Figure 3.6) shows that extracted DNA for digested NETs with MNase and DNase I produced nucleosome bands at 140-170 pb, which correlates with the positive control of commercial nucleosome and compared to undetected DNA bands in HC and untreated NETs. Our data suggested that cfDNA in burns and traumatic patients predominantly consists of nucleosomes generated from degraded NETs by DNase I, which may be significant for understanding its potential role in MODS and sepsis. DNase I is required for chromatin fragmentation to release

nucleosomes into the extracellular environment [447]. The presence of nucleosome oligomers in T0 of trauma samples suggests that DNase activity rapidly mediated chromatin fragmentation to release large nucleosomes extracellularly. Subtle changes in the molecular size of the terminal nucleosome digestion product suggest that DNase I can also digest the histones' linkers, resulting in a change in the size of the final nucleosome product in the later samples.

Furthermore, digested chromatin by MNase also results in nucleosome-nucleosome interactions forming oligomer structures [448]. Previously, it has been demonstrated that DNase I has a role in the cleavage of free DNA, while DNase 1L3 can cleave DNA-protein complexes such as histones [338, 449]. Our data demonstrate that 10U DNase was capable of generating nucleosomes within 20 minutes of incubation. Undetected DNA bands in measured extracted DNA in untreated NETs with either MNase or DNase I suggest that generated NETs were larger than 7000 pb, which is the maximum measurement of the highly sensitive gel detection chip by the Agilent 2100 bioanalyser.

In our study we measured circulating nucleosomes post severe thermal injuries in 39 burns (at days 1, 7, 10, 14, and 28) post burns using specific ELISA kits for detecting nucleosome H3.1 and compared the levels to healthy controls. Our data shows significant elevated circulated nucleosomes on days 1, 7, 10, and 14 post burns compared to healthy controls. The increase was associated with significant and strong correlation with cfDNA levels in burn. Our data confirms the previous results by Cato et al. (2021) who demonstrated high circulated levels of nucleosomes in burns with significant positive correlations with cfDNA levels [450]. In addition, Goswami et al. (2022) demonstrated significant high nucleosome levels that were associated with generated NET in trauma patients [451].

Also, we conducted more analysis for NuQ H3.1 and cfDNA levels in burns. Our data illustrate similar pattern for both through the longitudinal modelling. The dynamics of circulating NuQ. H3.1 and cfDNA levels post-burn injury provided valuable insights into the inflammatory response and sepsis prognosis. The observed peaks of both biomarkers were around day 12 post-burn highlights the critical window in which immune activation and sepsis prognosis are at their highest, corresponding to the elevated release of nucleosomes and cfDNA into the bloodstream. These findings suggest that circulating nucleosome H3.1 levels closely reflect cfDNA dynamics in response to severe thermal injuries, further supporting the role of both biomarkers in tracking inflammation and cellular damage in burn patients.

The comparison between septic and non-septic burn patients underscores the significant prognostic value of these biomarkers. Elevated NuQ. H3.1 and cfDNA levels in septic burns suggest their reliable indicators of sepsis. cfDNA shows a stronger association with sepsis risk on day 1, with higher odds ratios and AUROC values compared to NuQ. H3.1. The longitudinal assessment of sepsis prediction revealed that the combined model of cfDNA and NuQ. H3.1 did not significantly improve predictive performance on day 1, but it showed enhanced accuracy on subsequent days (e.g., day 7 and day 10). This suggests that while cfDNA alone may be more effective in early sepsis detection, combining cfDNA and NuQ. H3.1 enhances predictive accuracy as the inflammatory process evolves. Interestingly, the addition of the Revised Baux Score to the combination model on day 1 substantially improved the AUROC to 0.886, emphasizing the importance of integrating clinical scoring systems with molecular biomarkers to improve sepsis prognosis in burn patients.

Monitoring circulating NETs post-severe injury is crucial, as elevated levels are associated with increased risks of thrombosis, MOF, and poor clinical outcomes. Sakuma et al. (2022) developed a novel microfluidic technique for measuring circulating NETs in whole blood by capturing chromatin fibres [314]. This method provided valuable insights into inflammatory and immune responses by offering a precise and efficient method of quantifying NETs. We processed untreated and PMA-treated whole blood and isolated neutrophils through the microfluidic devices to validate the method. Our data illustrate that the area of captured NETs in PMA-treated whole blood and isolated neutrophils were significantly higher than untreated controls. We then applied this assay to capture circulating NETs following burn injuries on days 1, 4, 8, and day 14. Our data demonstrate a significant presence of whole blood circulating NETs that were captured through the microfluidic devices following burn injury. Captured circulated NETs were significantly high on the admission day (day 1) and significantly decreased on days 4 and 14, with no significant decrease observed on day 8. The temporal dynamics of NETs suggest a rapid and robust inflammatory response immediately following the burn injury. Comparing captured NETs in HC and PMA-treated whole blood with captured NETs in burns in our data shows that significant NETs were generated on day 1 post-burn compared to healthy controls.

The existence of circulating NETs post-burn is a significant concern of their association with heightened inflammation and risk of mortality. NETs contribute to SIRS, exacerbating tissue damage and promoting a pro-coagulant state, subsequently leading to DIC and MOF [442, 452]. Ng et al. (2020) found that increased levels of circulating NET markers, such as neutrophil elastase (NE), citrullinated histone H3, and cell-free DNA (cfDNA), exhibit a significant correlation with markers of inflammation and damage to the endothelial cells [453]. Meanwhile, Dinsdale et al.

(2020) demonstrated a significant reduction of DNase I activities on day 1 post-severe burn, which explains the cause of high levels of captured NETs on day 1 in our data [353]. Fedorov et al. (2023) recently demonstrated excited circulated NETs in whole blood of bacterial-infected patients using peripheral blood smear [454]. Therefore, monitoring and targeting NET formation is crucial to mitigate these severe outcomes and improve patient prognosis.

The formation of NETs results in the release of chromatin, including DNA complexed with histones, into the circulation [249] that subsequently undergoes degradation by DNase I [303]. Elevated levels of biomarkers such as cfDNA, histones, and interleukins reflect the extent of tissue damage and systemic inflammation, providing an overview of insights into the patient's prognosis [285, 441], which helps identify severe cases early and to potentially guide therapeutic strategies to improve future patient management [74, 455].

Circulating released cfDNA has been implicated in exacerbating cytotoxicity and the inflammatory response. cfDNA is released into the bloodstream and can activate immune cells via Toll-like receptor 9 (TLR9), producing proinflammatory cytokines [456]. This inflammatory cascade can cause tissue damage and organ dysfunction, particularly in severe conditions such as sepsis and tumours [457]. Paunel-Gorgulu et al. (2017) determined that cfDNA serves as an early indicator for inflammation caused by Cardiopulmonary bypass and may contribute to endothelial damage following cardiac surgery due to the elevation of endothelial cell injury markers ICAM-1 and sCD141 (soluble thrombomodulin). CfDNA has the ability to enhance inflammation by amplifying NETosis through a separate mechanism involving endosomal TLR9 and ROS [458]. Yang et al. (2016) investigated how extracellular histones stimulate TF expression in endothelial cells. Demonstrating that histones interact with Toll-like

receptors (TLR2 and TLR4), activating the nuclear translocation of NF-κB (c-Rel/p65) and AP-1 expression pathways. This activation increases TF expression, contributing to thrombosis and coagulation [429]. Furthermore, circulating histones post-trauma have been shown to induce endothelial injury, inflammation, and coagulation, serving as principal mediators of trauma-induced lung injury and MOF in patients with sepsis, trauma, and pancreatitis. Histone cytotoxicity was significantly reduced by heparin [459, 460]. Recently, Medeiros et al. (2023) reported that histones on its own are cytotoxic to endothelial cells and contribute to coagulation and inflammation stimulation in septic mice. While DNA and nucleosomes were not associated with significant impact, the application of DNase I to nucleosomes resulted in an increase in cytotoxicity compared to nucleosomes, which was reduced by adding heparin [461].Our previous data demonstrated that nucleosomes could also neutralise the anticoagulant effect of heparin in burns patients [388].

In conclusion, monitoring circulating NETs and NET-derived cfDNA is critical for understanding the inflammatory response following severe burns and trauma. Our study demonstrates that cfDNA levels are significantly elevated in burn patients throughout most of the measured timepoints, with peaks observed between days 5 and 28, suggesting a prolonged inflammatory response and substantial NET generation. In trauma patients, cfDNA levels showed a rapid increase, indicating an immediate response to cellular damage within 1 hour from injury Moreover, we observed that high levels of circulating NETs on day 1 post-burn using the microfluidic assay for capturing NETs, suggesting an immediate and rapid inflammatory response to the injury. Our findings also demonstrated that the circulating cfDNA fragments post-injury predominantly consist of nucleosome-sized fragments (~140-170 base pairs), which appear in most patients from day 2 to day 28 post-burn. The absence of these

nucleosome bands on day 1 in the majority of patients, coupled with the significant presence of NETs, suggests that initial injury responses are dominated by NET formation, with subsequent nucleosome release by DNase I. The significant generation of NETs and the presence of nucleosome oligomers, particularly in trauma patients within the first hour post-injury, underscores the critical role of DNase I in chromatin fragmentation and the release of nucleosomes. High levels of measured circulated nucleosomes and its strong positive correlation with cfDNA levels revealed the viability of those biomarkers on monitoring inflammation severity and sepsis prognosis, providing potential strong biomarkers for early sepsis prediction diagnosis, especially when combined with the Revised Baux Score. Our study underscores the importance of monitoring circulating nucleosomes and NETs as biomarkers to understand the dynamics of inflammation and coagulation post-severe injury. These findings have significant implications for patient prognosis and could guide therapeutic strategies aimed at mitigating the risk of DIC, MODS, and sepsis following severe burns and trauma.

Chapter 4: IL-8 Induces Neutrophil Extracellular Trap Formation in Severe Thermal Injury

4 IL-8 Induces Neutrophil Extracellular Trap Formation in Severe Thermal Injury

4.1 Introduction

Neutrophils are front-line innate cells that can eliminate pathogens through three distinct mechanisms: phagocytosis and the production of reactive oxygen species (ROS), degranulation, and the formation of neutrophil extracellular traps (NETs). Phagocytosis involves the engulfment and subsequent killing of bacteria. Degranulation refers to the release of such antimicrobial proteins as neutrophil elastase and myeloperoxidase, which aid in destroying pathogens. The process of neutrophils forming NETs was initially described by Brinkmann et al. in 2004 [249]. NETs are web-like structures comprised of chromatin, histones and antimicrobial proteins released by neutrophils to capture and neutralise pathogens [250].

The mechanisms behind NET formation are still not fully understood and they occur not only through diverse stimulations and multiple signalling pathways, but with unknown interdependence. Although the major pathways described include suicidal and vital NETosis or mitochondrial DNA (mtDNA) release [285, 462], it remains controversial how both the suicidal and more rapid vital NETosis pathways co-exist and which are more relevant *in vivo*. In the originally described suicidal pathway induced by phorbol 12-myristate 13-acetate (PMA) or bacteria, neutrophils release extracellular chromatin via the NADPH oxidase 2 (NOX-2) dependent pathway, resulting in cell death [463, 464]. NOX-2 is an enzyme complex responsible for generating ROS within the neutrophil and promotes chromatin de-condensation and breakdown of nuclear and granular membranes [250, 463]. The vital NETosis (NADPH oxidase independent) pathway can be induced through stimuli such as lipopolysaccharide (LPS) from Gram-negative bacteria and lipoteichoic acid (LTA)

from Gram-positive bacteria, interleukin-8 (IL-8) and tumour necrosis factor-alpha (TNF-α). These induce cytoskeletal rearrangements within the neutrophil, leading to the formation of vesicles containing chromatin and antimicrobial proteins [263, 264]. The mtDNA release pathway is initiated by neutrophils in response to infection or stress within the mitochondria. MtDNA, along with nuclear chromatin and other components of the NET, is subsequently transported into the cytoplasm and released extracellularly [283]. Despite the advances in this field, more research is required to fully understand the regulation and mechanisms of NETosis.

Although NETs are widely recognised as an initial line of defence against infection, excessive NETs are double-edged swords as they have also been observed in immunothrombosis [465]. This promotes disseminated intravascular coagulation (DIC) [466, 467], impairing microcirculation flow and contributing to multiple organ failure (MOF) [468]. Deoxyribonuclease I (DNase I) is important for the homeostatic regulation of NETs [303]. Dinsdale et al. (2020) and Hazeldine et al (2021) demonstrated that DNase activity in serum is not only capable of eliminating NETs *in vitro,* but it also can be inhibited by tissue-derived actin in burns and trauma resulting in excessive unregulated NET formation [353, 469].

Excessive NETosis can therefore occur during acute inflammation and sepsis. Laggner et al. (2022) and Otawara et al. (2018) have illustrated that severe thermal injuries are associated with excessive NET production in humans and rodents, respectively [313, 470]. However, NET formation is not just initiated directly by microbes and PAMPs, but can also be triggered by a range of pro-inflammatory mediators, including TNF-α, IL-8, activated platelets and activated endothelial cells [471]. Furthermore, platelet–neutrophil interactions have been shown to substantially contribute to initiating thrombosis via the rapid generation of NETs during vital NETosis

[318]. Although we and others have demonstrated that NETs are generated in patients with severe thermal injury, the pathophysiological mechanism(s) of NET generation in trauma and burns remains unclear.

IL-8 is a key chemokine and inflammatory mediator, which induces adhesion molecule expression on the vessel wall, stimulating neutrophil rolling, adhesion and migration to the tissues [197, 472]. The biological effects of IL-8 are mediated by its binding to CXCR1 and CXCR2, which are cognate G-protein-coupled CXC chemokine receptors. This binding initiates a phosphorylation cascade by the activation of intracellular signaling cascades, including PI3K/AKT, mitogen-activated protein kinase (MAPK)/ERK, and Janus kinase (JAK)/STAT pathways, promoting cytoskeletal reorganisation, chemotaxis and neutrophil activation as components of the inflammatory response [473-476]. Moreover, IL-8 signalling includes calcium mobilisation and the activation of small GTPases, including Rac and Rho, which further modulate the dynamics of neutrophil motility and adhesion [477].

However, dysregulated signalling along the IL-8/CXCR1/2 axis has been recognised as a potential contributor to immunopathology, which results in prothrombotic activation, neutrophil degranulation and NET generation [478, 479]. Teijeira et al. (2021) have illustrated that the concentrations of IL-8 needed to trigger NETosis in human neutrophils are at least double those necessary for chemoattraction. IL-8-induced NETosis relies upon the activation of different pathways compared to chemotaxis, with NET formation less reliant on G-proteins and more dependent upon ROS generation [480]. Abrams et al (2019) demonstrated that high IL-8 levels in plasma or serum obtained from intensive care unit (ICU) patients significantly contribute to NET formation. This study emphasised the therapeutic potential of reparixin, an IL-8 inhibitor that blocks CXCR1/2 receptors, consequently decreasing

NET production and reducing inflammation[272]. Moreover, Alsabani et al. (2022) expanded upon these findings by employing mouse sepsis models, demonstrating that inhibiting CXCR1/2 with reparixin significantly decreased NET production, MOF, and death [144]. In addition, Nie et al (2019) have demonstrated that IL-8 contributes to excessive NETosis in diffuse large B-cell lymphoma patients [481]. According to Kilic et al. (2023), COVID-19 patients showed increased IL-8 levels, and serum from these patients induced NETosis *in vitro*, which was reduced by co-culture with the IL-8 inhibitor, reparixin. [482]. Reparixin blocks IL-8 receptor CXCR receptors on neutrophils, reducing recruiting neutrophils and NET mediation by IL-8 that has been shown to be associated with survival improvement in critically ill patients, including diabetic, COVID-19 and transplant patients [483, 484]. Other IL-8 inhibitors have been clinically investigated, including Ladarixin, which blocks CXCR1/2, and CXCR2-selective inhibitors such as SX-682 and AZD8309, which inhibit IL-8-induced neutrophil chemotaxis [484]. Here, based on these observations, we aimed to determine the potential role of IL-8 in NET generation in patients with severe thermal injury.

4.2 Results

4.2.1 Circulating IL-8 levels in thermal injury

Serum IL-8 levels were measured in healthy controls (HC, N=10) and in burns patients, with patient demographics detailed in Chapter 2 (Section 2.1.2, Table 2.1). Measurements were conducted from the day of hospital admission to month 24 post-burn. Figure 4.1A illustrates longitudinal IL-8 levels in burns patients compared to HC, with IL-8 levels significantly higher at days 3 and 5 post-burn ($p < 0.05$). Figure 4.1B shows the comparison of IL-8 levels between burns patients who did or did not develop sepsis. IL-8 concentrations were significantly higher at day 5 post-burn in patients with

sepsis (p< 0.001). A comparison of IL-8 levels between patients with and without sepsis and HC found IL-8 was significantly increased in patients who developed sepsis compared to HC at days 3, 5, 7 (p < 0.001), 10 (p < 0.05) 12 and 14 (p< 0.01) (Figure 1.C–D).

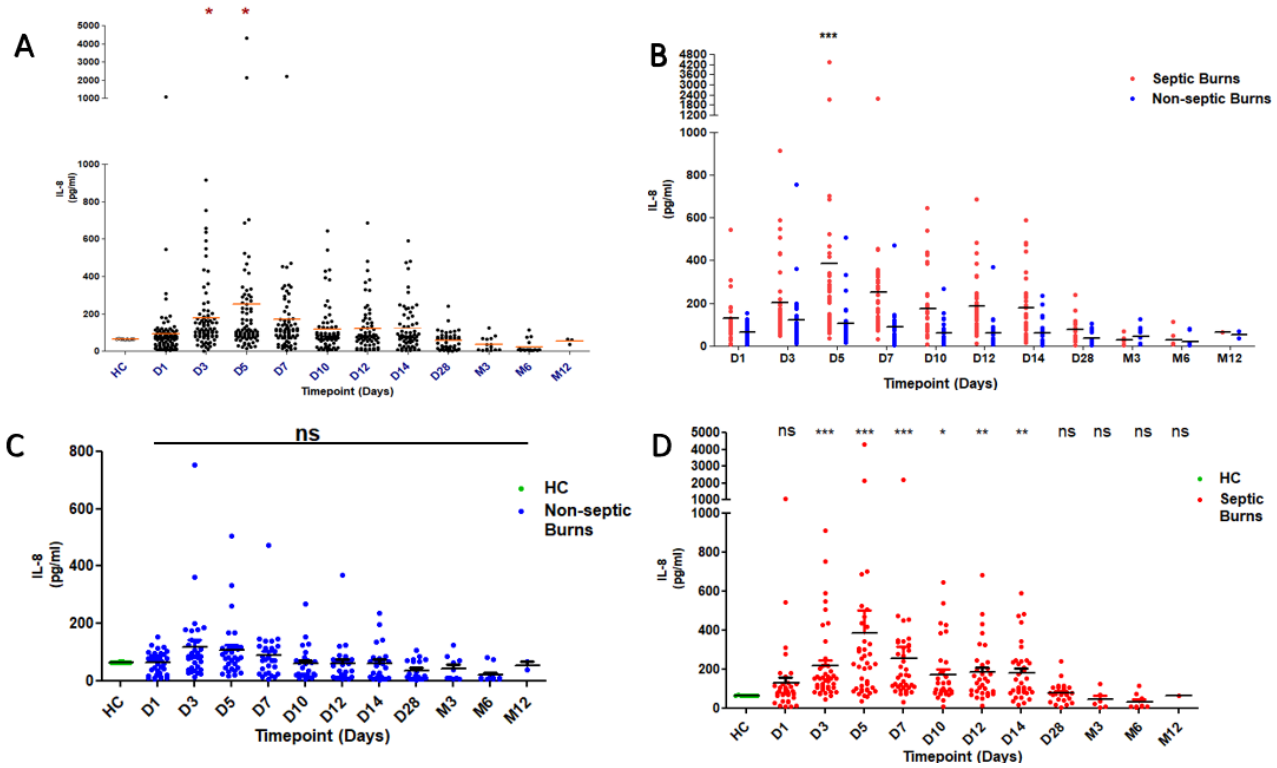

Figure 4.1: IL-8 levels in thermal injury. (A) IL-8 levels in Healthy Control (HC) and burns serum samples from admission to D14, D28, M3, M6, and M12. IL-8 levels were significantly increased on days 3 and 5 compared to HC. (B) A comparison between IL-8 levels in burns patients who developed sepsis or not. IL-8 levels were significantly higher in septic than non-septic burns on D5. (C, D) IL-8 levels for non-septic and septic burns, respectively, compared to HC. Non-septic burns were not significantly different from HC. In burns patients who developed sepsis, IL-8 levels were significantly increased on days 5–14 compared to HC. Burns data were compared to HC using One-way ANOVA (Kruskal Wallis test). Septic and non-septic data were compared using Two-way ANOVA. p value *** < 0.001, ** < 0.01, * < 0.05. (ns) not significant.

4.2.2 NET formation can be induced by IL-8 in serum from severe burns patients

Fluorescence microscopy was used to assess the capacity of burns serum containing IL-8 to induce *ex vivo* NET generation by neutrophils isolated from HC. Figure 4.2 shows a comparison of NET formation by untreated and PMA-treated neutrophils, which served as negative and positive controls, respectively. Untreated neutrophils retained their normal nuclear morphology and size. PMA stimulation induced NETs consisting of extracellular chromatin labelled with SYTOX Green and an anti-CitH3 Antibody. Neutrophils treated with serum containing high levels of IL-8 also generated NETs. In contrast, neutrophils stimulated by serum from HC did not generate NETs (Figure 4.2). Treatment with 100 pg/ml of recombinant IL-8 in either RPMI medium or HC serum also induced NETs (Figure 4.2).

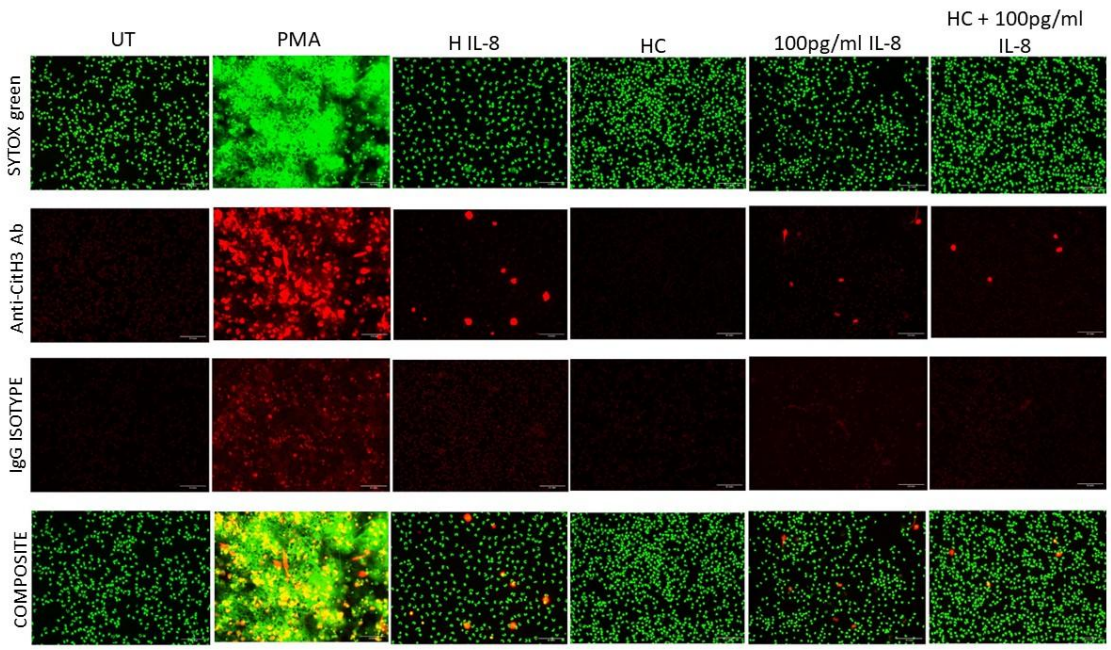

Figure 4.2: IL-8 induces *ex vivo* NETosis. Isolated neutrophils were untreated as a negative control (UT) or stimulated with PMA (positive control), burn patient serum containing a high IL-8 (H IL-8) level (725.49 pg/mL), HC serum, 100 pg/mL recombinant IL-8 or HC serum supplemented with 100 pg/mL IL-8 for 4 h. Induced NETs were labelled with SYTOX Green and anti-citH3 Ab (labelled with Donkey anti-Rabbit IgG secondary Ab). Composite between cells double labelled with SYTOX and anti-citH3 Ab shows co-localisation. The scale bar represents 0.1 mm. Images are representative of five independent experiments.

We next determined whether there was a dose–response effect of serum IL-8 levels on NET generation. Serum samples were classified into three groups: high IL-8 serum (H IL-8) contained very high levels (>500 pg/ml); medium IL-8 serum (M IL-8) contained between 150 and 500 pg/ml and low IL-8 (L IL-8) contained <150 pg/ml. Figure 4.3A illustrates a clear dose–response effect of serum IL-8 with H IL-8 serum increasing NET formation > M IL-8 and L IL-8 serum. Quantification of generated NETs using ImageJ software (Figure 4.3B) confirmed that H IL-8 serum and the PMA positive control significantly increased NETosis compared to untreated control (p <

0.05). Measurement of supernatant cell-free DNA (cfDNA) levels (Figure 4.3C) also confirmed a dose–response effect of serum IL-8 levels on NET generation. Given that DNase activity is present within serum, the data would suggest that cfDNA is being released from NETs in the presence of serum, as demonstrated previously by Dinsdale et al. (2020) [353].

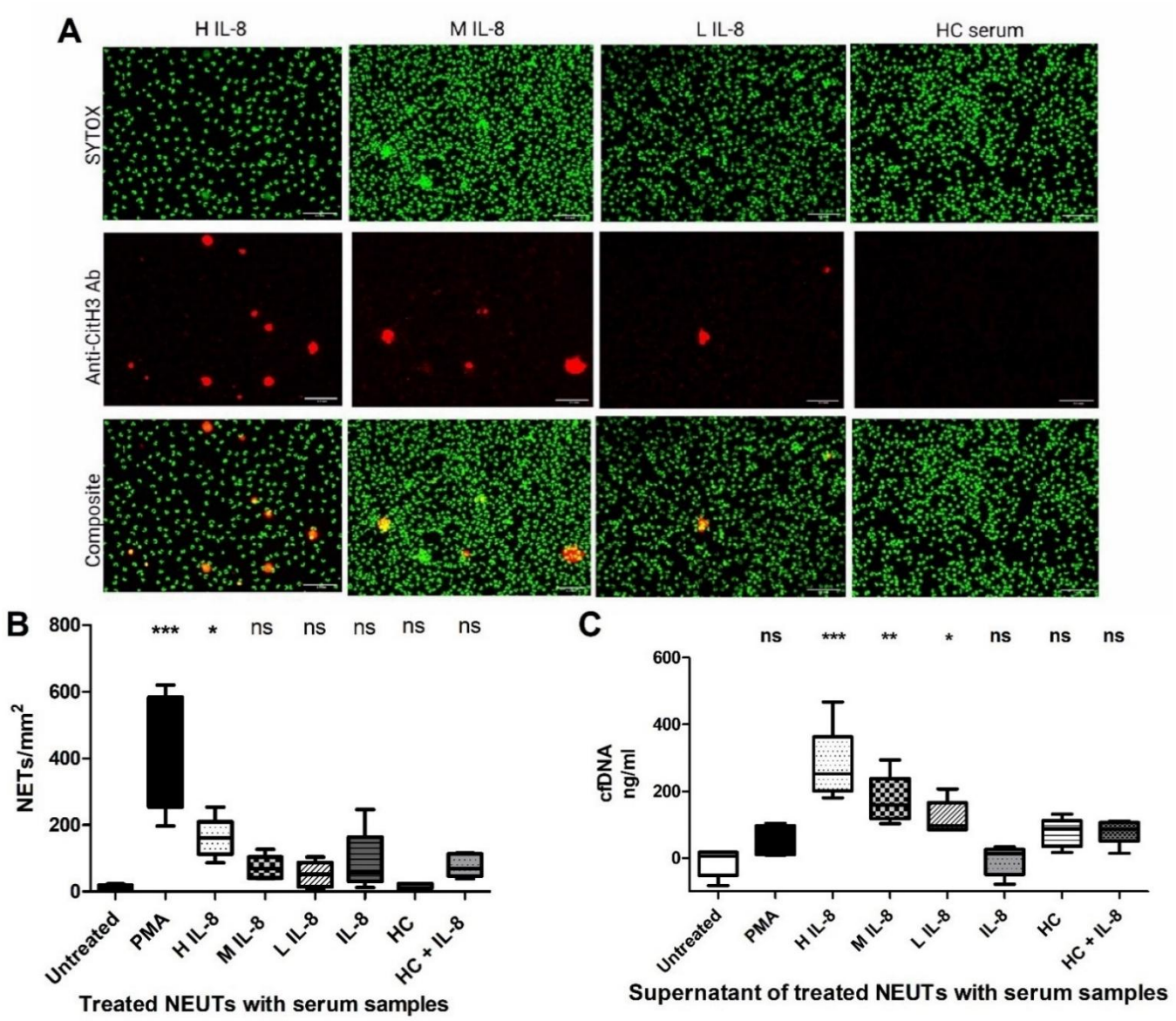

Figure 4.3: NET formation correlates with IL-8 levels in burns serum. (A) Fluorescent microscopy of NETs induced by burns serum containing either high (H), medium (M) or low (L) levels of IL-8, compared to HC serum. Generated NETs were labelled with SYTOX green and an anti-CitH3 Ab (labelled with Donkey anti-Rabbit IgG secondary Ab). (B) Quantification of NETs in all treatment conditions. (**C**) CfDNA levels in the supernatants of treated neutrophils. Data were analysed using one-way ANOVA (Dunnett's multiple comparisons test) to compare each experimental group with the control. *p* value] *** < 0.001, ** < 0.01, * < 0.05. (ns) not significant. Data are representative of n = 5.

4.2.3 Inhibition of DNase increases NET generation by IL-8 serum

To test whether serum samples were potentially degrading NETs, identical experiments were performed in the presence and absence of the specific DNase inhibitor, actin. Figure 4.4 illustrates that by inhibiting DNase I with actin, more extensive NET generation occurred (Figures 4.4A–C), with less liberation of cfDNA into the supernatants (Figures 4.4D).

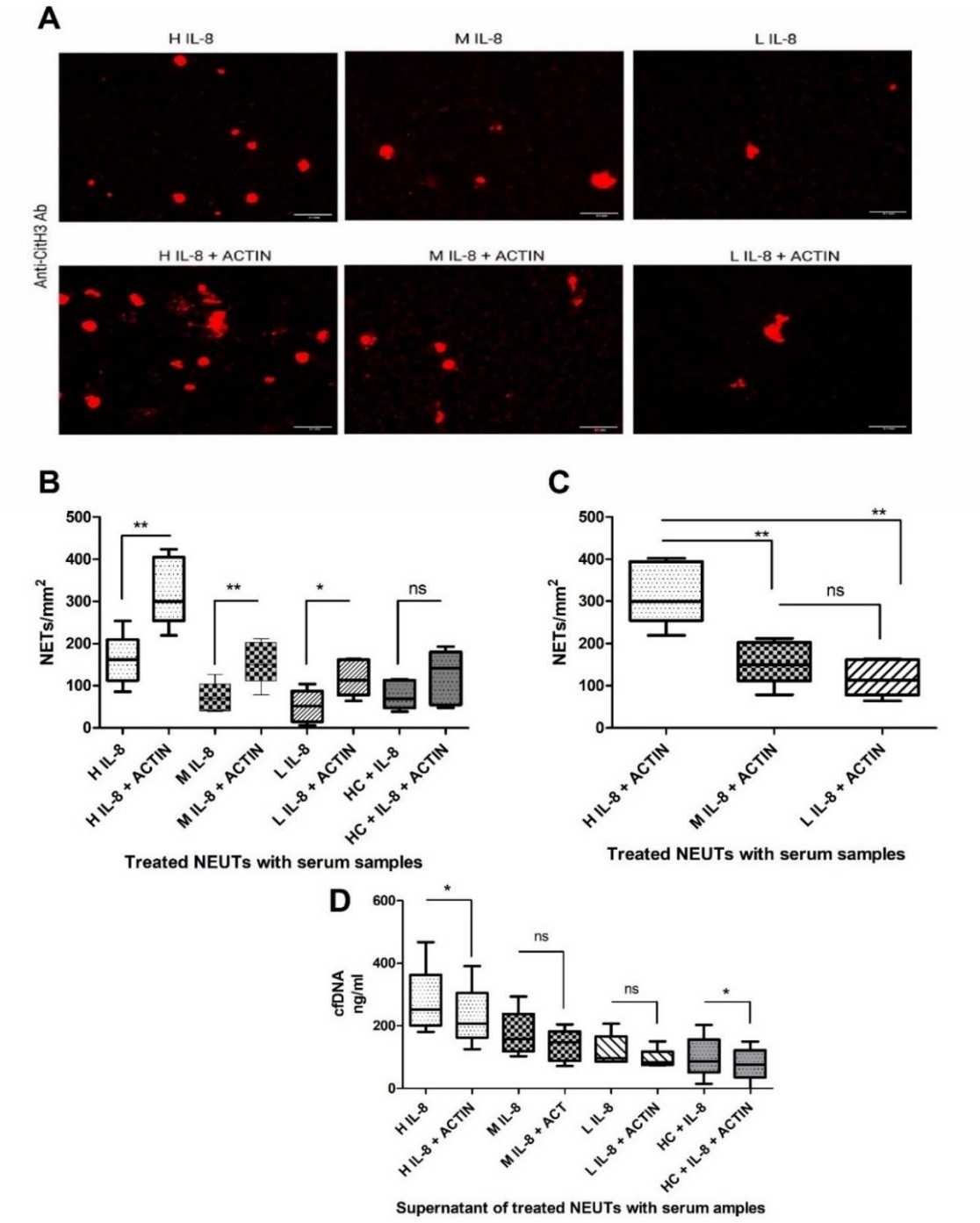

Figure 4.4: DNase I inhibition induces more extensive NET formation by serum IL-8. (A) Fluorescent microscopy of neutrophils stimulated with high (H), medium (M) or low (L) IL-8 levels in the absence or presence of 2.5 µM actin. Released chromatin was labelled with an anti-CitH3 Ab *(labelled with* Donkey anti-Rabbit IgG secondary *Ab)*. (B) Comparison of NET formation by neutrophils stimulated with H, M, L IL-8, or HC supplemented with 100 pg/mL IL-8 with or without actin. (C) NET formation of H, M and L IL-8 serum. (D) cfDNA levels in burns IL-8 groups with or without actin. [Paired t-test *p* value]: * < 0.05, ** < 0.01. Data are representative of n = 5.

4.2.4 IL-8 is a major contributor to burns serum NET-inducing capacity

To determine whether IL-8 is the predominant mediator of NETosis in burns serum, experiments were undertaken in the presence of an anti-IL-8 monoclonal antibody (mAb). Figure 4.5 illustrates that the addition of an anti-IL-8 mAb significantly reduced NET generation compared to an isotype control within H and M IL-8 serum samples ($p < 0.05$) and inhibited the action of recombinant IL-8 added to normal serum ($p < 0.05$).

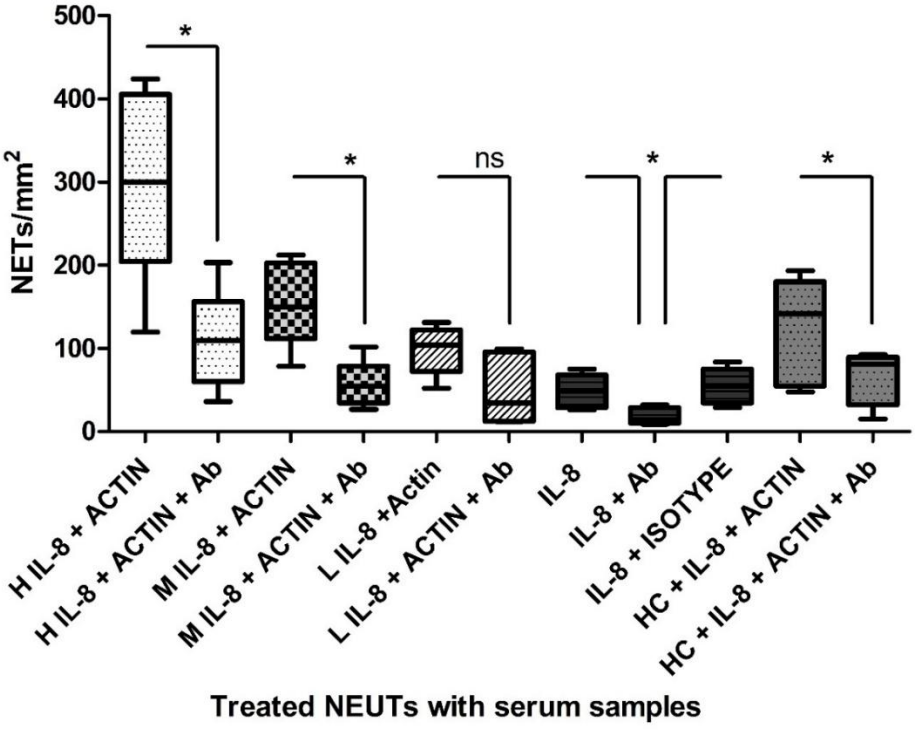

Figure 4.5: The effect of anti-IL-8 antibodies on NET formation. NET quantification induced by burns serum from high (H), medium (M) or low (L) IL-8 samples, recombinant IL-8, anti-IL-8 Ab isotype, or supplemented HC serum in the presence of 2.5 µM actin and with or without anti-IL-8 Ab. [Paired t-test *p* value]: * < 0.05. Data are representative of n = 5.

4.2.5 IL-8 levels are significantly correlated with cfDNA levels in severe thermal injury

We next determined if there was a correlation between circulating IL-8 and cfDNA levels in burns. Table 4.1 shows a significant correlation between IL-8 and cfDNA levels in burns from admission day to month 3. The *p* value was < 0.05 on days 1 and 3, and < 0.001 on days 5, 7, 10, 12, 14, and 28 with the *R* value ranging from 0.46 to 0.79. The overall correlation is also significant with a *p* value < 0.001, and an *R* value of 0.53 (Figure 4.6).

Table 4.1: Correlation between IL-8 and cfDNA levels in thermal injuries (n = 96)

Days	Number of burn patients	correlation (Y/N)	P value	R value
DAY 1	78	Y *	0.0259	0.2523
DAY 3	69	Y *	0.0425	0.2449
DAY 5	69	Y ***	< 0.0001	0.4578
DAY 7	66	Y ***	< 0.0001	0.5096
DAY 10	60	Y ***	< 0.0001	0.6917
DAY 12	59	Y ***	< 0.0001	0.7687
DAY 14	57	Y ***	< 0.0001	0.6744
DAY 28	38	Y ***	< 0.0001	0.7902
Month 3	10	Y **	0.0036	0.8207
Overall	506	Y ***	< 0.0001	0.53

p value *** < 0.001, ** < 0.01, * < 0.05.

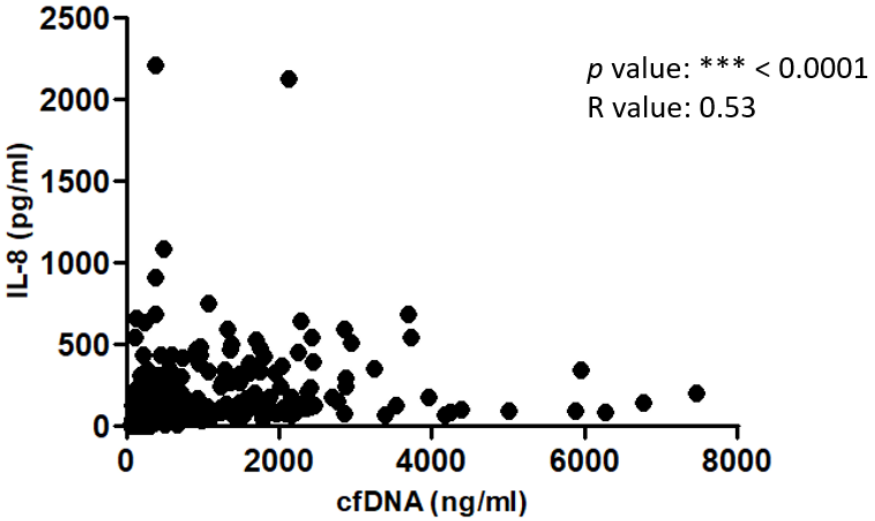

Figure 4.6: The overall IL-8 correlation with cfDNA levels in thermal injuries. Significant overall correlation between IL-8 and cfDNA levels in thermal injuries (n = 96). [Spearman correlation *p* value]: *** < 0.0001.

4.3 Discussion

NET formation was first described by Brinkmann et al. (2004) [249]. Neutrophils augment their antimicrobial capabilities via the release of NETs, which consist of extracellular chromatin adorned with histones and other granular proteins [485]. These NETs have been recognised as components of the innate immune response, potentially exerting a combination of therapeutic or pathogenic effects [249, 255, 485]. NETs are important as mediators of DIC and MOF in burns patients with sepsis, they not only offer potential new prognostic biomarkers but point to a range of potential new therapies to either inhibit their formation or degradation [13]. Therefore, understanding

the pathophysiological mechanisms by which NETs are generated and degraded is key for identifying and optimising new therapeutic targets.

In 2019, Abrams et al demonstrated that high IL-8 levels in the serum from ICU patients were a major contributor to NET formation [272]. In this study, we show that IL-8 levels are significantly increased in patients with severe thermal injury on days 3 and 5 following injury compared to healthy controls. Comparison of levels between patients with and without sepsis also demonstrated increased levels at day 5 in patients who developed sepsis. Furthermore, IL-8 levels in patients who developed sepsis were significantly higher than healthy controls at the majority of time points from day 3 to day 14 following injury. Our findings confirm previous studies showing increased IL-8 levels following thermal injuries and its significant correlation with sepsis burns [412, 486-489]. Additionally, the observed increase in IL-8 levels in septic burns is consistent with previous studies that demonstrated significantly elevated IL-8 in critically ill septic patients [272, 490-492].

We next investigated the biological activity of serum containing low to high IL-8 levels on the capacity to induce *ex vivo* NET generation. Our initial results confirmed that incubating neutrophils with serum containing high concentrations of IL-8 induced NET formation in contrast to the negative control of healthy control serum. Supplementing healthy control serum with 100 pg/ml recombinant IL-8 as a positive control also confirmed the ability of IL-8 to induce *ex vivo* NET production. We then categorised the burns serum into three groups based on their IL-8 levels (low, medium and high) and investigated their capacity to induce NET generation. As expected, there was a dose–response effect correlating with the levels of serum IL-8, an observation that confirms the study by Abrams et al. in ICU patients [272].

Various studies have demonstrated the involvement of other pro-inflammatory mediators in the generation of NETs. For example, cytokines such as IL-1β and TNF-α have been shown to be involved in NET production in SIRS subjects [260, 308, 412]. Moreover, Itagaki et al (2015) demonstrated significant NET generation by treating purified neutrophils with mitochondrial DNA [282]. In addition, Zhang et al. (2020) reported that IL-17 promotes NET production by recruiting neutrophils and triggering NETosis in pancreatic cancer patients [493]. Extracellular histones from trauma patients were also reported to induce NET formation *ex vivo* [459]. Van Avondt et al (2023) have shown that released iron from red blood cells (RBC) also contributes to NETosis [494]. Additionally, Heme has been identified as a significant mediator that triggers neutrophil adhesion, which is dependent on nuclear factor-κappa B (NFκB) and ROS pathways [495]. Recently, Teng et al. (2024) emphasised the ability of interferon-gamma (IFNγ) to generate NETs and proposed its potential use in enhancing the activity of eliminating tumours in microsatellite stable colorectal cancer [496].

In the experiments we conducted on serum IL-8 dose-response effects on *ex vivo* NETosis, we also measured cfDNA in cell supernatants. Interestingly, these results confirmed a dose-response effect, with increased cfDNA correlating with high, medium and low levels of IL-8. However, given that DNase activity is also present within normal serum, the data would also suggest that cfDNA is being released from degraded NETs in the presence of serum, particularly as the PMA-positive control in the absence of serum induced the most NETs observed by microscopy but with a reduced amount of released cfDNA in the supernatant compared to serum samples. DNase activity is therefore a likely significant potential confounding variable when using serum samples in these experiments.

We therefore tested this hypothesis by performing identical experiments in the presence and absence of a specific DNase inhibitor actin. These experiments confirmed that the inhibition of DNase caused a significant increase in NET formation as observed by microscopy. However, this also reduced the release of cfDNA in the supernatants and demonstrates that *ex vivo* experiments on NETs using serum as an inducer ideally need to take this into account and may underestimate the true magnitude of NET formation being measured.

Major tissue damage following severe burns results in the excessive release of circulating actin from tissues, which directly inhibits DNase I [469, 497, 498]. Dinsdale et al. (2020) previously demonstrated that actin reduces DNase I activity and that the actin scavenging system normally protects DNase I activity, which is important for NET homeostasis. [353]. In line with these observations, we found that *in vitro* inhibition of DNase I activity by actin resulted in increased NET formation with less degradation into cfDNA in the supernatants. A limitation of this study is that we were unable to study any potential relationship between IL-8 and actin levels in burns samples as the presence of actin was only qualitatively analysed by Western blotting in our previous study (Dinsdale et al, 2020) [353].

To determine whether IL-8 is the predominant mediator of NETosis in burns serum, experiments were undertaken in the presence of an anti-IL-8 monoclonal antibody. The addition of an anti-IL-8 mAb not only significantly reduced NET generation by high and medium IL-8 serum samples ($p< 0.05$) but also inhibited the action of recombinant IL-8 added to normal serum ($p< 0.05$). Given the magnitude of the inhibition observed, it seems likely that IL-8 is a major contributor to NET formation in thermal injury both *in vivo* and within *ex vivo* assays but also suggests that other mediators are likely to be involved. We have also confirmed that Heme levels not only significantly increased

post-injury but released from RBC in this cohort and associated with immune suppression and poor outcomes [499]. It would be also interesting to determine the exact contributions of Heme and IL-8 to *ex vivo* NETosis given that Heme is also a well known mediator of NETosis [494, 495].

Our results suggest that increased IL-8 levels may contribute to excessive NETosis that subsequently results in cfDNA elevation levels in thermal patients due to NET degradation by DNase. Previously, we have demonstrated that cfDNA levels are also elevated post-thermal injury [74]. Therefore, we evaluated the relationship between IL-8 and cfDNA levels in burns. Our data demonstrate a significant correlation between IL-8 and cfDNA levels in burns from admission day to month 3 (Figure 4.5). The overall correlation was also significant, suggesting that high IL-8 levels significantly contribute to increased NET-derived circulating cfDNA levels, which are a pro-inflammatory damage-associated molecular pattern (DAMP) biomarker for DIC and MOF [314, 466, 468].

In conclusion, this study demonstrates the importance of serum IL-8 in inducing NET formation following thermal injury. Levels of circulating IL-8 were shown not only to be increased in patients with burn injury, but also to be increased in patients that developed sepsis. Furthermore, an *ex vivo* dose-response effect was confirmed that could be inhibited by anti-IL-8 antibodies. Inhibition of DNase activity in serum by actin not only confirms the importance of this enzyme in the regulation of NETs but also demonstrates its potential as a confounding variable in serum-based neutrophil stimulation assays.

Chapter 5: Novel Haematological and Neutrophil Parameters in Severe Thermal Injury

5 Novel Haematological and Neutrophil Parameters in Severe Thermal Injury

5.1 Introduction

Neutrophils play a crucial role in the innate immune system by swiftly responding to infection and tissue damage. Upon activation, neutrophils migrate towards the infection or injury site, performing various host defence functions, including phagocytosis, degranulation, and generation of neutrophil extracellular traps (NETs) to eradicate pathogens [189, 263]. NETs are web-like structures composed of DNA and antimicrobial proteins that trap and neutralise pathogens, preventing their spread by immobilisation and induction of death [250]. However, the dysregulation of NET formation can result in pathological complications. Excessive or inappropriate NET release has been implicated in various inflammatory and autoimmune diseases, such as systemic lupus erythematosus (SLE) and rheumatoid arthritis, where NETs contribute to tissue damage and exacerbate the inflammatory response [443]. Moreover, NET-derived chromatin is degraded by DNase I to cell-free DNA (cfDNA), which further promotes inflammation and is linked to poor prognosis, sepsis incidence, disseminated intravascular coagulation (DIC) and multiple organ failure (MOF) [74].

Previously, Hampson et al. (2017) demonstrated that a combination of neutrophil function (i.e. phagocytosis), Immature Granulocytes (IG count), and cfDNA levels are early biomarkers for predicting sepsis in burns at day 1 post-injury, especially in combination with the Revised Baux Score. [74]. Dinsdale et al. (2017) further illustrated a significant increase in WBC, and neutrophil parameters as strong predictors of sepsis along with platelet parameters [13]. Severe thermal injuries also significantly impact upon haematological parameters. Substantial haematological changes are induced due to the acute inflammatory response, including increased white blood cell (WBC) counts, as part of SIRS, reflecting the immune system's

mobilisation to the injury site [500]. Moreover, modern haematological analysers (e.g. Sysmex XN and XR series) incorporating automated flow cytometry measurements provide detailed insights into the morphology, functionality, and maturity of different leukocyte populations. Neutrophil and monocyte extended parameters can rapidly measure cell function and maturity, offering valuable information about the immune response to injury, infection and inflammation. Neutrophil and monocyte parameters (X, Y and Z) derived from fluorescent and light scatter plots correspond to the overall x, y and z coordinates of the individual cell populations and reflect nucleic acid content, cytoplasmic structure, and complexity [501-503]. Neutrophil and monocyte Z parameters provide a comprehensive evaluation of cells by integrating X and Y parameters, expressing the width of dispersion in cell size (Figure 5.1) [504]. The activation status of neutrophils can be also described by neutrophil granularity intensity (NEUT-GI) and neutrophil reactive intensity (NEUT-RI) [505]. Lymphocyte parameters RE (reactivity) and AS (antibody-synthesising lymphocytes) provide data on lymphocyte size and the degree of cellular activation. Larger lymphocytes with increased reactivity represent activated T cells that can be defined by an increased RE parameter. Lymphocyte AS specifically measures B lymphocytes, which are identified by their high fluorescence signal in the WDF scattergram [506].

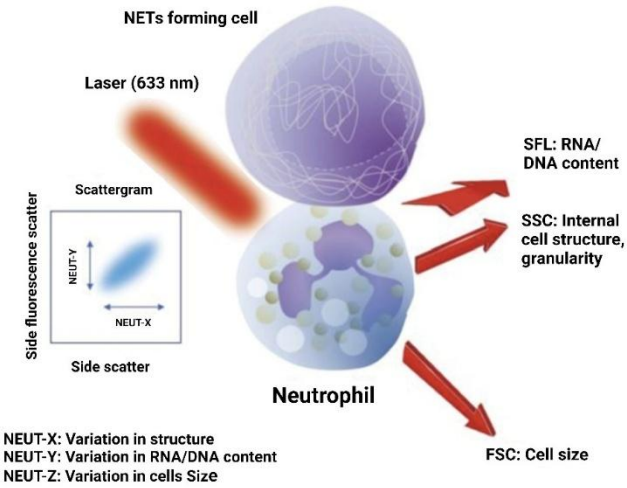

Figure 5.1: Neutrophil population analysis by Sysmex haematology analysers. The analyser detects labelled neutrophil fluorescence by laser-based flow cytometry (633 nm). The scattergram fluorescence signals (SFL) represents RNA/DNA content, side scatter (SSC) indicates internal structure/granularity, FSC (forward scatter) provides additional data on cell size. Neutrophil extended parameters (NEUT-X, Y, and Z), provide variations in cell structure (NEUT-X), RNA/DNA content (NEUT-Y), and cell size (NEUT-Z). This figure has been modified using BioRender software from Figure 2 of “The Detection of Neutrophil Activation by Automated Blood Cell Counter in Sepsis” by Helms et al. (2024) [507].

Neutrophils, a key component of the innate immune response, exhibit significant activation and morphological changes with previously described alterations in neutrophil extended parameters such as neutrophil RI (NEUT-RI) and neutrophil Y (NEUT-Y). Dinsdale et al. (2017) demonstrated a significant increase in levels of NEUT-RI and Y post thermal injury, which correlated with the severity of the inflammatory response and incidence of sepsis [13]. Furthermore, release of high levels of Immature Granulocytes (IGs) into the bloodstream indicates a stress response with increased bone marrow activity and has been shown to be an early biomarker of sepsis in burn patients [500].

In this study, we aimed to fully re-investigate the dynamics all these biomarkers along with some extended parameters within a prospective study focusing in much more

detail including all the first 14 days post-injury. Additionally, we sought to explore the association between these parameters and poor clinical outcomes and sepsis in severe burns patients.

Unfortunately, during recruitment during the middle of this new study, the commercial neutrophil phagocytosis assay (PHAGO-TEST) became unavailable so were unable to re-test this in combination with other markers as we previously reported in 2017 [74].

5.2 Results

5.2.1 Changes in circulating leucocytes following severe thermal injury

Leukocyte dynamic changes following severe thermal injuries were investigated in 96 burn patients, with demographics described in Section 2.1.2 (Table 2.1). Figure 5.2 shows the dynamics of leukocytes and IG's over time in septic and non-septic burns compared to healthy controls and highlights the impact of thermal injury on the immune system. The median neutrophil counts and percentages in septic burns and non-septic burns were significantly higher ($p < 0.001$) than HC on days 1 and 2 (Figure 5.2A, 5.2B and Appendix Tables 1 and 2). Despite declining in counts between days 3 and 5, a second wave of elevated counts was observed between days 6 and 28 ($p < 0.001$), with higher values in septic burns. By day 28, the neutrophil counts and % declined again but were still significantly higher than in HC ($p < 0.001$). Prognostic modelling of neutrophil counts for sepsis prediction on day 1 revealed an odds ratio (OR) of 1.026 (95% CI: 0.881 to 1.196) with an AUROC of 0.533 (95% CI: 0.406 to 0.660). A stronger association between neutrophil counts and sepsis was observed on day 28 with an

OR of 2.452 (95% CI: 1.342 to 4.481) and an AUROC of 0.776 (95% CI: 0.640 to 0.912) (Appendix Table 3).

Figure 5.2C, and 5.2D show that lymphocytes exhibited a different pattern, with significant reductions observed in the early days post-injury. Lymphocyte levels were significantly reduced ($p < 0.001$) on day 3 in both septic and non-septic burns compared to HC and remained significantly reduced ($p < 0.001$) to day 7 compared to HC (Appendix Table 4). % Lymphocytes were significantly reduced ($p < 0.001$) in all measured timepoints from the admission day to day 28 compared to HC (Appendix Table 5). There was no significant difference in lymphocyte counts between septic and non-septic burns (data not shown). Monocytes show an initial rapid response on day 1, with significant elevations ($p < 0.001$) (Appendix Table 6). A second wave was also observed between days 6 and 28, with a sustained increased of monocyte count in septic burns (Figure 5.2E, 5.2F). The monocyte count OR for sepsis on day 28 was 1.991 (95% CI: 1.144 to 3.465), with an AUROC of 0.696 (95% CI: 0.548 to 0.845) (Appendix Table 7). The monocyte % was significantly increased ($p = 0.001$) in septic burns on days 4-6 and significantly decreased on days 14 ($p =0.001$) and 28 ($p <0.05$) compared to HC. In non-septic burns, monocyte % were significantly elevated on days 2-6 with the largest difference at day 2 ($p <0.001$) (Appendix Table 8). Eosinophils (Figure 5.2G, and 5.2H) were significantly reduced ($p <0.001$) in both count and % levels in the early phase across both septic and non-septic burns, with minimal recovery over time (Appendix Table 9, and Table 10).

IG counts and % were significantly increased ($p < 0.001$) in both septic and non-septic burns on day 1 (Figure 5.2I, 5.2J) compared to HC ($p < 0.001$). A second peak was observed between days 5-28, compared to HC (Appendix Table 11, and Table 12). The difference in IG counts between septic and non-septic burns gave an OR of 1.079 (95% CI: 0.996 to 1.168) with an AUROC of 0.712 (95% CI: 0.582 to 0.843) at day 14. The difference in IG % gave an OR of 1.193 (95% CI: 1.026 to 1.387) with an AUROC of 0.699 (95% CI: 0.564 to 0.835) at day 7 (Appendix Table 13 and Table 14).

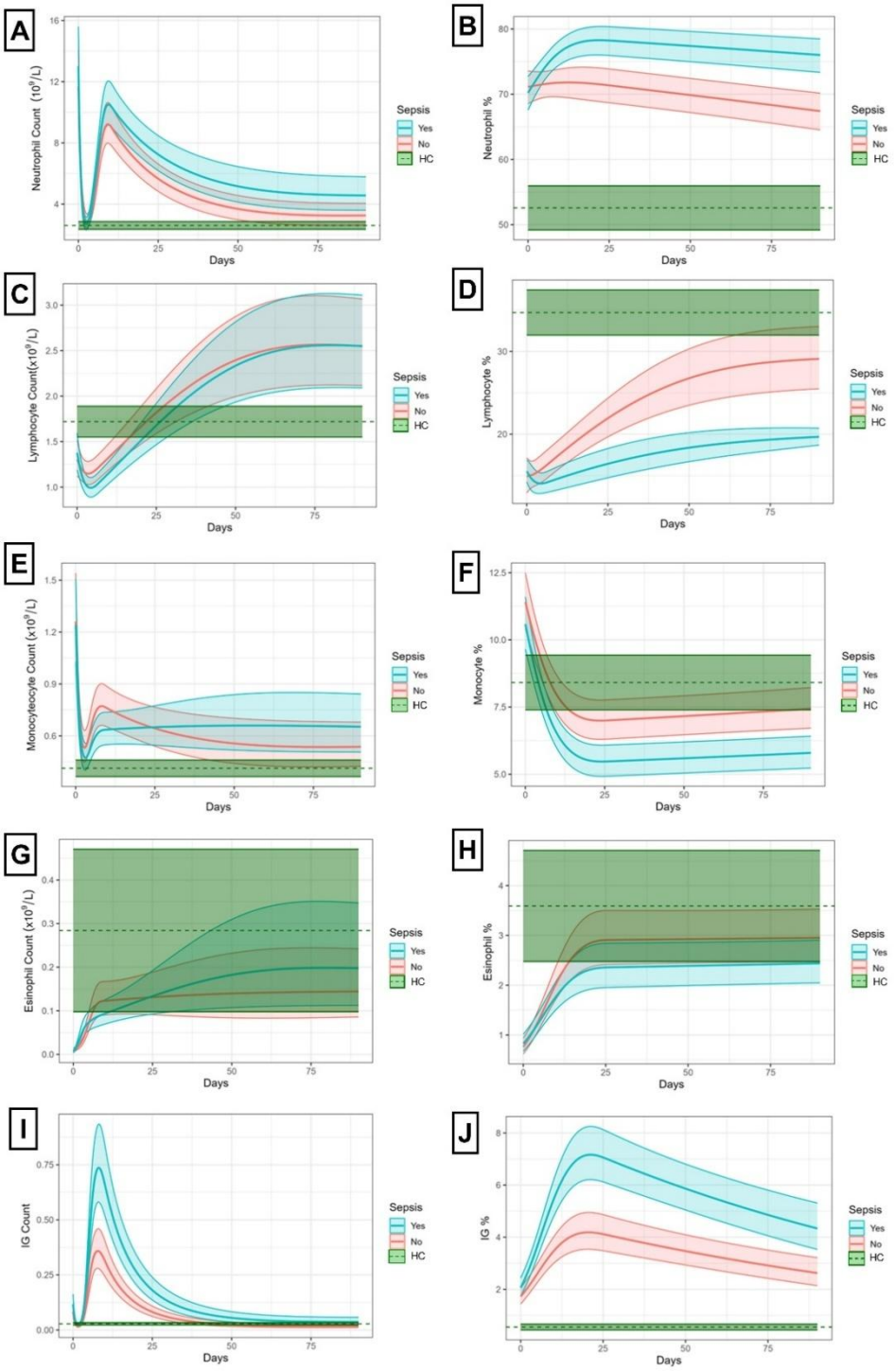

Figure 5.2: WBC parameters post severe thermal injuries. Longitudinal analyses were performed using linear mixed-effects models to examine the changes in the count and percentage of the neutrophils (A, B), lymphocytes (C, D), monocytes (E, F), eosinophils (G, H), and IGs (I, J) post-burn (N = 96) and to differentiate between septic (blue) and non-septic burns (red) compared to healthy controls (HC) (green). The lines represent the indicated mean, while the shaded region indicates the 95% confidence intervals.

5.2.2 Characteristics of circulating leukocytes following thermal injury

5.2.2.1 Analysis of Neutrophils activated *in vitro*

As a positive control. the effects of Neutrophil activation on neutrophil X, Y and Z (NEUT-X, Y and Z) parameters was studied *in vitro* by comparing untreated (UT) whole blood (WB) and purified neutrophils (NEUTs) obtained from healthy donors with and without activation with 4 µM ionomycin (Iono) for 4 hours. Neutrophil X, Y, and Z levels were significantly increased (p <0.01) within activated whole blood or purified neutrophils compared to untreated controls (Figure 5.3).

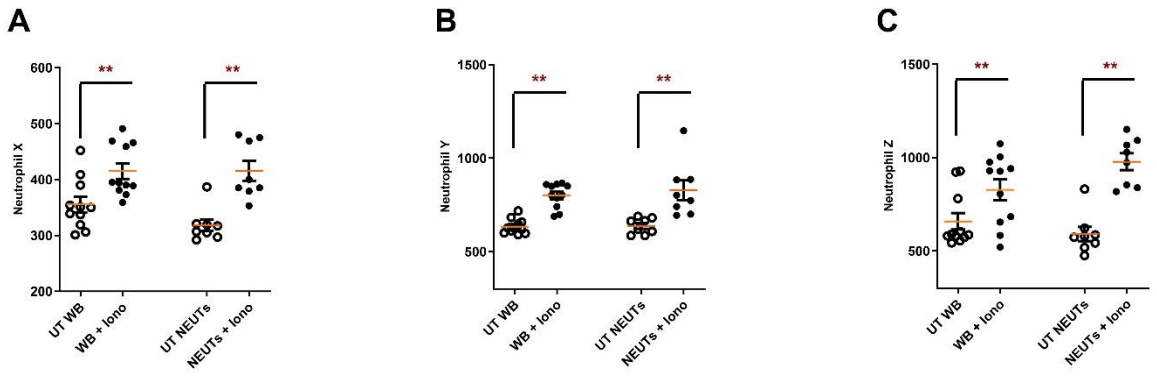

Figure 5.3: Effect of *in vitro* activation on Neutrophil parameters. Neutrophil parameters (X, Y, Z) were measured for untreated (UT) or treated whole blood (WB) or isolated neutrophils (NEUTs) with ionomycin (Iono) *in vitro*. (A), (B) and (C) illustrate that neutrophils X, Y, and Z of treated WB and NEUTs were significantly elevated compared to UT WB and UT NEUTs. p value **<0.01. Paired t-test. Data are representative of independent experiments conducted with WB (N=10) and NEUTs (N=8).

5.2.2.2 Neutrophils

Neutrophil parameters demonstrated distinct patterns post-injury, particularly in patients who developed sepsis (Figure 5.4). On day 1, NEUT-X (Figure 5.4A) was significantly increased in septic ($p < 0.001$) and non-septic burns ($p < 0.05$) compared to HC. The NEUT-X OR for predicting sepsis on day 1 was 2.010 (95% CI: 1.076 to 3.754) with an AUROC of 0.657 (95% CI: 0.539 to 0.775). A further peak in NEUT-X ($p < 0.001$) also occurred at day14, compared to HC ($p < 0.001$) (Appendix Table 15) with a stronger observed association with sepsis (OR 1.574 (95% CI: 1.076 to 2.303), AUROC 0.700 (95% CI: 0.566 to 0.835) (Appendix Table 16).

NEUT-Y was significantly increased ($p < 0.001$) in both septic and non-septic burns across all measured time points, with lower but still significant elevation in non-septic burns at day 28 ($p <0.05$) (Figure 5.4B). The OR for NEUT-Y and sepsis on day 1 was 1.011 (95% CI: 0.737 to 1.385), and AUROC of 0.538 (95% CI: 0.410 to 0.666). Increased NEUT-Y values persisted with a stronger association at day 14 with sepsis (OR 1.318 (95%: 1.028 to 1.689), AUROC 0.748 (95% CI: 0.621 to 0.876) (Appendix Table 17 and Table 18). Figure 5.4C shows significant increases in NEUT-Z levels between days 6 and 14 in septic ($p < 0.001$) and non-septic ($p < 0.01$) burns, compared to HC. The OR for NEUT-Z and sepsis on day 14 was 1.334 (95% CI: 1.012 to 1.758), with an AUROC of 0.652 (95% CI: 0.513 to 0.790) (Appendix Table 19 and Table 20).

NEUT-RI values were significantly increased ($p < 0.001$) across all measured time points in both septic and non-septic burns compared to HC, but was non-significant at day 28 in non-septic burns. (Figure 5.4D). On day 1, NEUT-RI was significantly increased ($p <0.001$) in septic burns, compared to HC. The OR for sepsis was 0.913

(95% CI: 0.658 to 1.267) with an AUROC of 0.500 (95%CI: 0.361 to 0.640). Levels peaked at day 7 (OR of 1.999 (95% CI: 1.272 to 3.141), AUROC of 0.771 (95% CI: 0.639 to 0.903) (Appendix Table 21 and Table 22). NEUT-GI levels were significantly increased in both septic and non-septic-burns compared HC at day 1 with p <0.01 and <0.001, respectively, and at days 2-4 with p <0.001 for both septic and non-septic burns (Figure 5.4E) (Appendix Table 23).

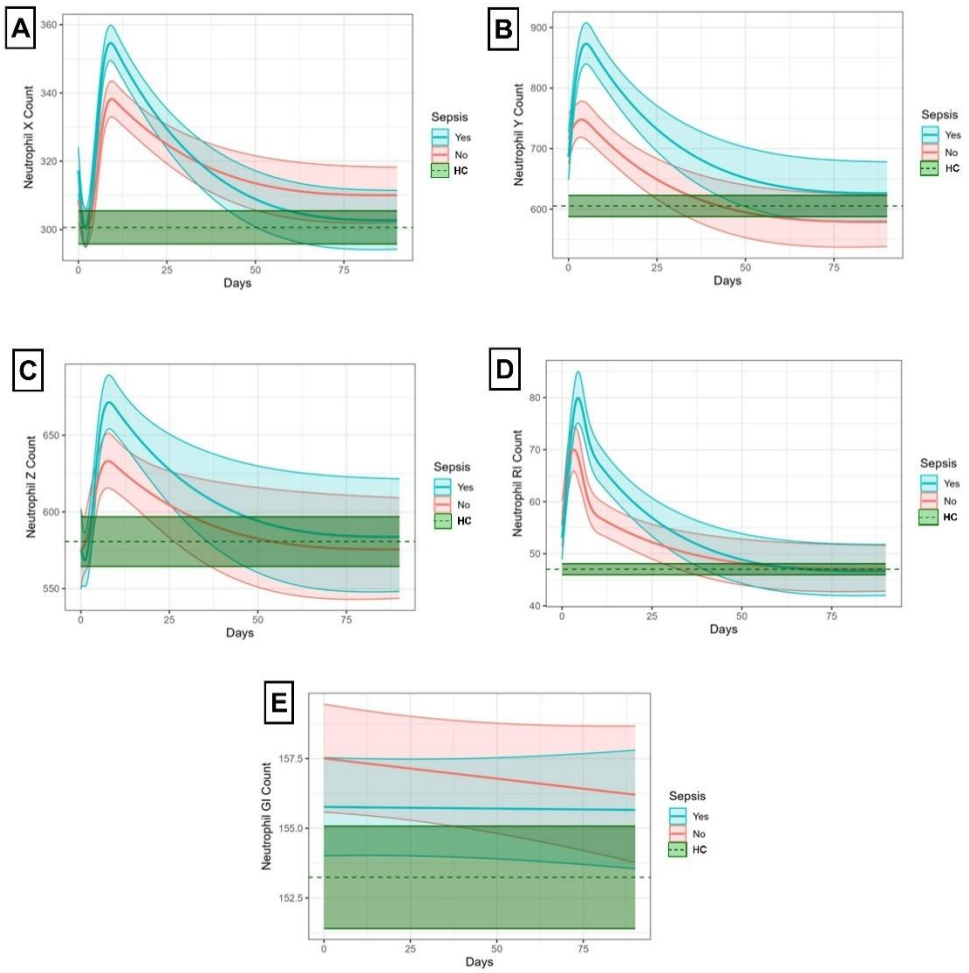

Figure 5.4: Extended neutrophil parameters post severe thermal injury. Longitudinal analyses illustrate changes in extended neutrophil parameters (A: NEUT-X, B: NEUT-Y, C: NEUT-Z, D: NEUT-RI, and E: NEUT-GI) over time in burn patients (N = 96), comparing septic (blue) and non-septic burns (red) to HC (green). The lines represent means while the shaded region indicates the 95% confidence intervals. Significant elevations were observed in all extended neutrophil parameters in the early post-burn phase for both septic and non-septic groups relative to HC, with septic patients displaying higher levels overall.

5.2.2.3 Lymphocytes

Lymphocyte AS levels were not significantly increased in burns compared to healthy controls in all measured time points. However, a more pronounced response was observed in the lymphocyte RE count (Figure 5.5A, 5B) with significant increases at day 7 ($p < 0.05$) and days 14-28 ($p < 0.001$) in burns compared to HC (Appendix Table 24). The OR for sepsis was 1.149 (95% CI: 0.856 to 1.541), with an AUROC of 0.599 (95% CI: 0.436 to 0.763) at day 14 (Appendix Table 25). Lymphocyte RE% was significantly reduced in both septic and non-septic burns compared to HC on days 1-3 with a p <0.001 on day 1, followed by a significant increase on days 14 (p <0.001) and 28 (p <0.01) (Appendix Table 26).

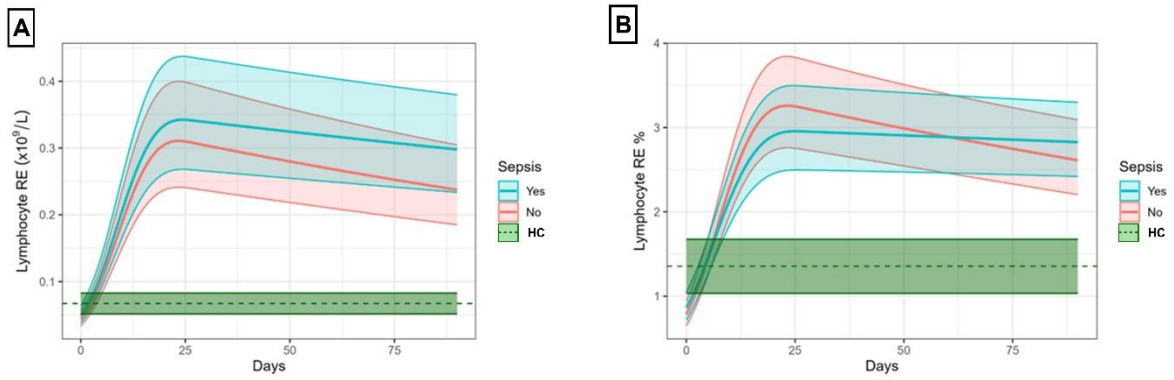

Figure 5.5: Lymphocyte RE parameter post severe thermal injuries. Longitudinal analyses show a significant increase in lymphocyte RE count (A) days 7-28 post burn (N = 96) for both septic (blue) and non-septic burns (red) compared to HC (green). Lymphocyte RE % (B) significantly increased on days 14-28. Lines represent the means while the shaded region indicates the 95% confidence intervals.

5.2.2.4 Monocytes

Figure 5.6A shows that monocyte X counts were significantly increased on day 1 ($p < 0.01$) and on days 2-28 ($p < 0.001$) in septic burns and on day 1 ($p < 0.05$), days 2-14 ($p < 0.001$), and day 28 ($p < 0.01$) in non-septic burns compared to HC (Appendix Table 27). At day 5, the OR for sepsis was 1.62 (95% CI: 0.925 to 2.080), with an AUROC of 0.674 (95% CI: 0.519 to 0.794) (Appendix Table 28). Monocyte Y (Figure 5.6B) levels were significantly decreased in septic burns ($p < 0.001$) and in no-septic burns ($p < 0.05$) on day 1 with a significant increase from days 2 to 7 in septic burns and days 2-5 in non-septic burns compared to HC. Monocyte Y levels peaked ($p < 0.001$) on day 4 in both septic and non-septic burns (Appendix Table 29). Monocyte Z levels exhibited a significant increase ($p < 0.01$) in septic burns on day 1, followed by a significant decrease ($p <0.05$) on day 14 in both septic ($p < 0.01$) and non-septic burns ($p < 0.05$) (Figure 5.6C) compared to HC (Appendix Table 30).

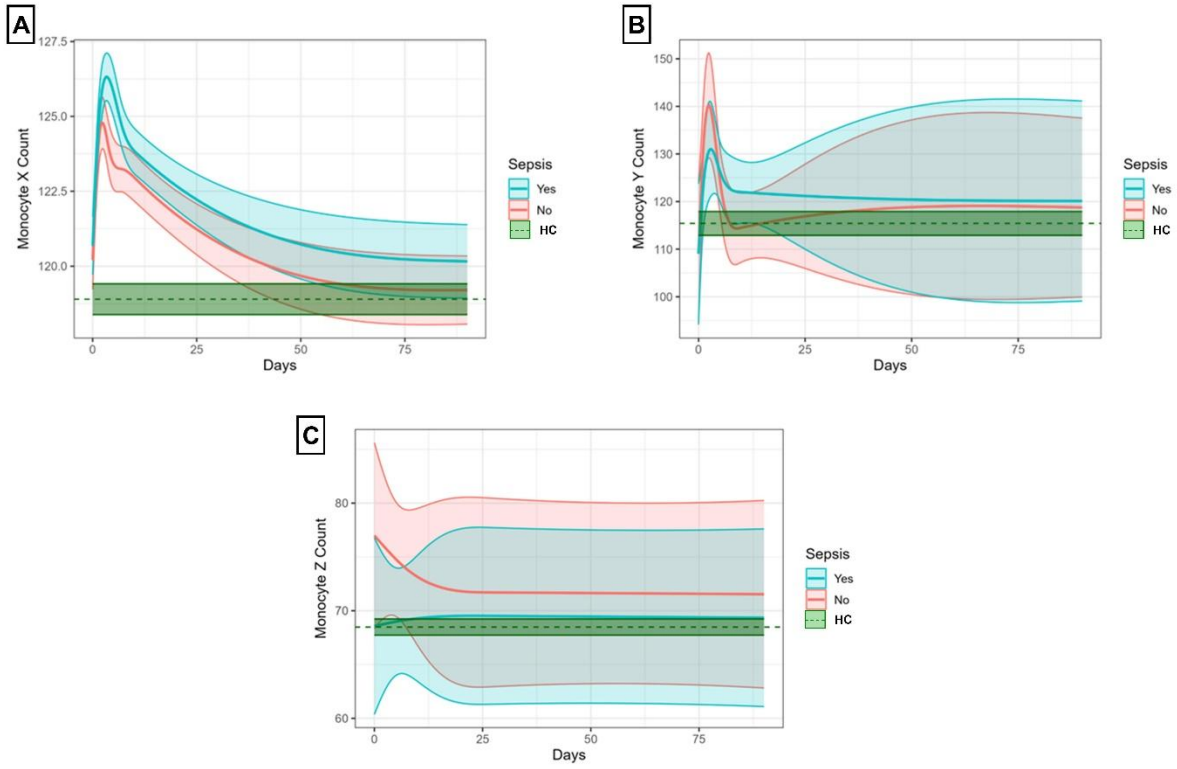

Figure 5.6: Monocyte parameters post severe thermal injuries. Longitudinal analyses shows that monocyte X levels (A) were significantly high at days 1-28 post burn (N = 96) in both septic (blue) and non-septic burns (red) compared to HC (green). Monocyte Y (B) were significantly increased on the early days (days 1-7) post burn for both septic and non-septic burns compared to HC. There was no significant elevation observed in the levels of monocyte Z (C) compared to HC. Lines represent the means, while the shaded region indicates the 95% confidence intervals.

5.2.3 CfDNA levels are significantly correlated with neutrophil Y in severe thermal injury

We previously demonstrated that cfDNA levels were increased in post severe thermal injuries with significant levels increased in septic burns on days 7-28 compared to non-septic burns (Section 3.2.2, Figure 3.2 in Chapter 3). Figure 5.7A shows the longitudinal analysis of NEUT-Y and cfDNA levels post burn injury with both parameters appearing to peak at the time (days 6-14). Closer examination illustrates that the NEUT-Y levels peak slightly earlier (at day 6) than the cfDNA levels (at day 8). Figure 5.7B confirms that there is a significant correlation ($p < 0.0001$, $R = 0.51$) across all time points. Analysis of individual time points (Table 5.1) confirmed significant correlations on all days except days 4 and 28.

There was a significant correlation between NEUT-Y and cfDNA levels in burns from day 1 to day 3 and days 5-14. The correlation peaks on days 8-14($p < 0.0001$). The overall correlation is significant ($p < 0.0001$ and $R = 0.508$) (Figure 5.7). Table 5.1 shows the individual daily correlations between cfDNA and NEUT-Y levels from days 1-14.

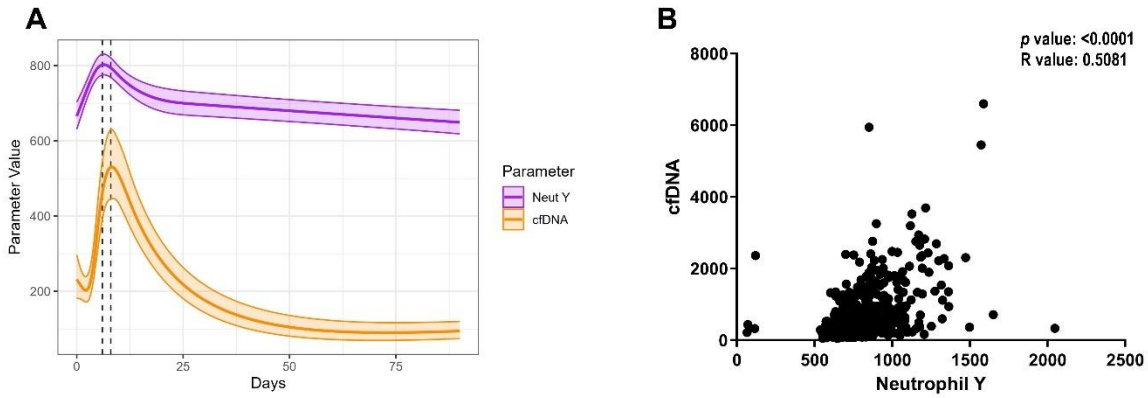

Figure 5.7: Correlation between cfDNA and NEUT-Y levels post severe thermal injury. (A) shows a longitudinal modelling for evaluating levels trends of NEUT-Y (purple) and cfDNA (orange) post burns (N = 96). Lines represent the indicated mean fixed effects, while the shaded region indicates the 95% confidence intervals. NEUT-Y levels were peaked at day 6, and cfDNA levels peaked at day 8. (A) illustrates both levels elevation and correlation are observed between days 6 and 14 with an earlier peaks observed in NEUT-Y levels (at day 6) in contrast to the peaks of cfDNA levels (at day 8). Lines represent the means while the shaded region indicates the 95% confidence intervals. (B) shows the overall correlation between cfDNA and NEUT-Y which were significant. Spearman correlation test; p<0.0001, R= 0.5081.

Table 5.1: Daily correlations between neutrophil Y and cfDNA			
	No.	**P value**	**R value**
DAY 1	72	0.0115	0.2962
DAY 2	60	0.0284	0.283
DAY 3	65	0.0004	0.4261
DAY 4	56	Ns	0.09816
DAY 5	61	0.0014	0.4001
DAY 6	54	0.0073	0.3614
DAY 7	61	0.0016	0.3951
DAY 8	52	< 0.0001	0.5389
DAY 9	52	< 0.0001	0.6172
DAY 10	53	< 0.0001	0.6607
DAY 11	47	< 0.0001	0.6032
DAY 12	53	< 0.0001	0.702
DAY 13	46	< 0.0001	0.7089
DAY 14	53	< 0.0001	0.7099
DAY 28	35	Ns	0.3153
Overall	767	< 0.0001	0.5081

5.2.4 A potential use of IG, cfDNA, and NEUT-Y as biomarkers of sepsis in thermal injuries

Combined models incorporating IG counts and cfDNA reveal an improvement in prognostic accuracy over time for predicting sepsis in burns. Initially, on day 1, the combined model only exhibited a modest AUROC of 0.593 (95% CI: 0.465 to 0.721) with a Brier score of 0.243. However, at day 14, the AUROC of was 0.796 (95% CI: 0.679 to 0.914) and a Brier score of 0.204 by day 14, giving a moderate discriminatory power (Table 5-2). The addition of NEUT-Y further increased prognostic accuracy moderately, particularly on day 3, where the AUROC increased to 0.718 (95% CI: 0.601 to 0.836), with no significant improvement for the discrimination power on days 1, 7 and 14 (Table 5-2).

The Revised Baux (R-Baux) score is a clinical index (using TBSA, inhalation injury and age) used to predict mortality in burns patients. The R-Baux alone performed well across all time points, with AUROC values consistently above 0.700, peaking at 0.754 (95% CI: 0.649 to 0.860) on day 1 and maintaining an accepted predictive accuracy through day 28 (AUROC: 0.756; 95% CI: 0.616 to 0.896) (Table 5.2). A model combining IG, cfDNA, NEUT-Y, and the Revised Baux score yielded the highest prognostic accuracy, particularly on day 1, with an AUROC of 0.793 (95% CI: 0.693 to 0.893) and a Brier score of 0.184. The performance remained accepted across all subsequent days, with AUROC values consistently above 0.700, highlighting the synergistic effect of combining these biomarkers with the R-Baux score for more accurate sepsis prediction in post-burn patients (Table 5.2).

Table 5.2: Combination of Biomarkers and R-Baux score for sepsis prediction						
Day	**Sepsis (Yes)**	**Sepsis (No)**	**Model**	**AUROC**	**95% CI**	**Brier Score**
1	39	39	cfDNA +IG	0.593	(0.465 to 0.721)	0.243
			cfDNA + IG+ NEUT-Y	0.581	(0.452 to 0.711)	0.243
			R-Baux Score	0.754	(0.649 to 0.860)	0.200
			cfDNA + IG + NEUT-Y + R-Baux	0.793	(0.693 to 0.893)	0.184
3	36	36	cfDNA + IG	0.630	(0.499 to 0.762)	0.244
			cfDNA + IG + NEUT-Y	0.718	(0.601 to 0.836)	0.215
			R-Baux Score	0.746	(0.636 to 0.856)	0.201
			cfDNA + IG + NEUT-Y + R-Baux	0.791	(0.689 to 0.893)	0.189
7	35	31	cfDNA + IG	0.725	(0.600 to 0.851)	0.224
			cfDNA + IG + NEUT-Y	0.720	(0.594 to 0.846)	0.216
			R-Baux Score	0.749	(0.632 to 0.865)	0.202
			cfDNA + IG+ NEUT-Y + R-Baux	0.769	(0.655 to 0.883)	0.193
14	31	29	cfDNA + IG	0.796	(0.679 to 0.914)	0.204
			cfDNA + IG + NEUT-Y	0.784	(0.666 to 0.903)	0.205
			R-Baux Score	0.736	(0.612 to 0.861)	0.206
			cfDNA + I + NEUT-Y + R-Baux	0.768	(0.646 to 0.889)	0.188
28	23	19	cfDNA + IG	0.753	(0.592 to 0.914)	0.232
			cfDNA + IG + NEUT-Y	0.705	(0.542 to 0.868)	0.222
			R-Baux Score	0.756	(0.616 to 0.896)	0.203
			cfDNA + I + NEUT-Y + R-Baux	0.728	(0.565 to 0.890)	0.205

5.3 Discussion

Our previous study in 2017 identified a combination of novel early (day 1) biomarkers (cfDNA, IG and neutrophil function in combination with the R-Baux score) for predicting sepsis in patients with severe burns injury within the SIFTI-1 cohort [74]. The SIFTI-2 study was designed to study in more detail the dynamic changes in these biomarkers across daily samples taken in the first 2 weeks post-injury [406]. In addition, we also identified some promising extended parameters such as NEUT-Y, NEUT-RI, and platelet impedance count (PLT-I) from a state of the art haematological analyser using automated flow cytometry measurements of cell [13].

Modern Haematological Analysers (e.g. Sysmex XN and XR series) have evolved into sophisticated automated flow cytometers that can offer the rapid measurement of extended parameters for all blood cell populations by measuring scattered light and fluorescence in addition to cell counts and size distributions to provide detailed information on the immaturity and activation status of cells. Such extended data provides both quantitative and qualitative analysis on key morphological and functional features of all leukocytes, including neutrophils, lymphocytes, and monocytes, which can potentially provide important prognostic and diagnostic information during inflammation induced by severe thermal and traumatic injuries [508-511].

In this study we have also explored the dynamics of the changes in extended leukocyte parameters following severe thermal injury to not only provide significant insights into the immune and inflammatory responses but with the aim of identifying unique biomarkers that may have potential clinical utility. Both Neutrophils and monocytes demonstrate the classical significant increases in peak counts post-injury on day 1 post thermal injury in both septic and non-septic burns compared to healthy controls,

highlighting the rapid and acute inflammatory response to injury [13, 470, 512, 513]. Despite normalising between days 2 and 3, a second wave of peaks occurred between days 6 and 28. In addition, IG counts were increased between days 1-28. In contrast, Lymphocyte counts were significantly reduced in the early days post-burn injury between days 3 and 7. Also, eosinophil counts were significantly reduced across all measured time points, with minimal recovery by day 28. Our measurement of WBC subtypes confirms the well-established increases in leucocytes early post severe thermal injuries as part of the inflammatory response to severe injury [13, 514, 515].

The dynamics in WBC numbers and their subtypes can provide insight into the body's response to injury and infection. The initial increases in neutrophils and monocytes are primarily caused by the acute inflammatory response, which is intended to defend against infection and promote tissue healing [516]. Neutrophils, being the first responders to infection, quickly migrate to the injury site, leading to bone marrow stimulation with a substantial rise in counts during the early phases of severe injury [517]. Additionally, increased IGs in the bloodstream indicate an acute activation of the bone marrow in response to severe inflammation and infection [74, 407, 518, 519]. Monocytes play several important functions in the immune system. Upon injury, monocytes are activated and produce chemokines and cytokines that attract other immune cells to the site of injury and enhance their response to the inflammation [184]. In addition, monocytes undergo differentiation into macrophages and dendritic cells, resulting in an increase in their counts and playing a critical role in phagocytosis and antigen presentation, which is essential for the adaptive immune response during prolonged inflammation [520]. In contrast, lymphocyte counts often decrease, especially in severe inflammation, due to the movement of lymphocytes to the

inflammation site and cell death caused by excessive stress and infection [521, 522]. The acute stress and the release of corticosteroids post injury usually lead to a decrease in eosinophil counts as they suppress the production and mobilization of eosinophils [514].

We initially investigated the changes in neutrophil extended parameters (X, Y, Z) *ex vivo* by stimulating whole blood or isolated neutrophils with 4µM ionomycin for 4 hours and comparing the results to untreated controls. Our findings revealed a significant increase in these parameters for treated samples, thus validating that these parameters reflect cellular activation *in vivo*. These results also confirm the results of Stiel et al. (2019), who demonstrated increased NEUT-Y in treated neutrophils with ionomycin that resulted in generated NETs [467]. Although Kremer et al. measured neutrophil activation by ionomycin by flow cytometry, neutrophil side scatter (SSC) was increased compared to untreated neutrophils. Although SSC and NEUT-X are not identical parameters, they share similarities in measuring certain aspects of cell complexity and granularity [523].

Next, we measured the extended parameters of WBC subtypes to understand the changes and dynamics of into cell morphology, maturity, and functionality post-injury. Our data demonstrates that neutrophil extended parameters (X, Y, Z, RI and GI) were significantly increased in the early phase post-burns, particularly in patients who subsequently developed sepsis. Significant increases in NEUT-X and Y occurred at day 1 post-injury and were associated with increased risk of sepsis. The persistence of NEUT-Y and the pronounced elevation of NEUT- Z on day 14, were also associated with risk of sepsis. NEUT- RI was consistently elevated across all time points, peaking at day 7, reflecting its potential use as a marker of sepsis. However, NEUT-GI levels

were significantly elevated in the early days post burns but were not associated with sepsis.

Our findings thus support our previous data [13]. Several other studies have also demonstrated changes in neutrophil extended parameters in response to inflammation, injury, and sepsis. Luo et al. (2013) demonstrated significant increases in NEUT-X, Y, and Z in cancer patients with sepsis, highlighting a positive correlation between the levels of neutrophil parameters and the levels of the classical inflammatory markers C-reactive protein (CRP) and procalcitonin (PCT) [524]. Additionally, Kwiecien et al. (2023) demonstrated a significant increase of NEUT-X, Y, and Z levels in myelodysplastic syndrome (MDS) patients [508]. NEUT-Y levels were also significantly increased in patients with DIC [525]. Moreover, Cornet et al. (2015) and Park et al. (2015) demonstrated that increased NEUT-RI and Y reflect increased neutrophil activation and an immature phenotype, aiding in early prediction of sepsis [509, 526]. Our data also shows a constant elevation of NEUT-Y and RI in burns patients with sepsis supporting the potential utility of these parameters as biomarkers. These observations further support the utility of detailed neutrophil analysis in predicting sepsis and monitoring immune responses post-severe thermal injuries.

The levels of lymphocytes and monocytes in our study show different patterns in post-thermal injuries, reflecting the dynamic immune response in septic burns. While the levels of lymphocyte AS remained relatively stable in the early phase, there were significant increases in lymphocyte RE counts and their percentage from day 5 post-burn, particularly in septic burns. It has been suggested that the early lymphocyte AS elevation is acute response to the viral infections [527]. Delayed lymphocyte RE response emphasises the important role of lymphocyte activation in severe inflammation [506, 527, 528]. The moderate odds ratio and AUROC scores for

lymphocyte RE suggest limited diagnostic value to distinguish sepsis in burns. Lymphocyte RE and other extended parameters, such as NEUT-RI and lymphocyte AS, have shown significant early association with sepsis and inflammation severity in ICU patients [529]. However, our data show low scores of OR and AUROC in lymphocyte AS and RE, suggesting limited potential for predicting sepsis. Monocyte parameters also show significant changes, with monocyte X consistently elevated at all time points compared to healthy controls. The association of monocytes with sepsis peaked at day 14, with a moderate increase (OR 1.387, AUROC 0.606), suggesting a limited use for sepsis prediction and diagnosis. Although a significant decrease was observed on the admission day in monocyte Y levels, particularly in septic burns, levels were significantly increased on days 2-7, specifically in septic burns, suggesting a complex role for monocytes, potentially related to their dual roles in inflammation and immune suppression. Increased monocyte X and Y levels has been reported to be significantly associated with sepsis [530]. Contrary to our findings, monocyte X has been proposed as a valuable biomarker for sepsis prognosis, along with neutrophil X and Y, due to an early increase in monocyte X levels.[503].

The significant increase in cfDNA levels in septic burns in our study (Figure 3.2, Section 3.2.2 in Chapter 3) confirms their enormous potential as an early biomarker for sepsis. High levels of cfDNA do seem to reflect ongoing NETosis, eliminating bacterial and pathogens invasion, as several studies demonstrated the correlations between cfDNA levels and NET production during severe inflammation and sepsis [442]. Severe sepsis is characterised by the extensive infiltration of neutrophils into the affected tissue and distant organs, NET formation occurs, resulting in the release of decondensed chromatin and, consequently, the generation of high levels of cfDNA [443]. Our data indicates that cfDNA is a moderate predictor of sepsis on day 1 with

an AUROC of 0.599 (CI). The association, however, peaked at day 7, with an improved AUROC of 0.738 (CI). Our findings on cfDNA levels confirm our previous studies that also show significantly increased cfDNA levels in burns, suggesting a potentially useful marker for sepsis detection burn severity and mortality [73, 74, 444]. In this chapter we also evaluated the relationship between cfDNA and NEUT-Y levels. Our data demonstrate a near coincident peak of both parameters with an overall significant correlation across all time points as well as the majority of individual days post-injury (Figure 5.7).

NEUT-Y measures the fluorescent intensity of neutrophils and is a reflection of the amount of internal nucleic acids and granules within the cells. However, other researchers have suggested that NEUT-Y could also be a biomarker of NETosis and correlates with increased NET formation [454, 467, 526]. It is therefore possible that the nucleic acid dye used in the Sysmex is also measuring released extracellular DNA associated with surface of the cells. Although extracellular NETs are thought to be ephemeral, degradable and potentially fragile and therefore potentially lost during cytometry measurements, researchers have also successfully measured NETs by flow cytometry therefore suggesting that NEUT Y is also capable of measuring surface bound chromatin released by activated neutrophils [454, 467, 507, 531]. Furthermore, using a positive control as proof of principle, we also activated neutrophils either purified and within whole blood and verified that ionomycin stimulation a known *in vitro* inducer of suicidal NETosis also increases the NEUT-Y signal *in vitro*. It is interesting that the peaks of NEUT-Y and cfDNA are not quite coincidental which could suggest that NEUT-Y is an earlier measure of cell associated NETS which are then digested by DNase to release cfDNA which peaks slightly later. Fortier et al. (2022) illustrated

high levels of NEUT-Y were strongly associated with mortality in COVID-19 patients, suggesting an indicator marker for NETosis [532]. Previously, Dinsdale et al. (2017) also demonstrated NEUT-Y as an excellent biomarker for sepsis on day 3 and when combined with platelet impedance count (PLT-I), gave an AUROC score of 0.915 [13]. Therefore, NEUT-Y and cfDNA are both potentially excellent useful biomarkers for monitoring excessive NETosis following severe thermal injuries. Their strong correlation indicates high neutrophil activity, which is associated with the generation of NETs and cfDNA. Furthermore, NEUT-Y and cfDNA serve as effective biomarkers for monitoring sepsis, demonstrating moderate to excellent discriminatory capabilities between days 7 and 14.

The combination of IGs, cfDNA, and NEUT-Y in prognostic models for sepsis showed a steady improvement in predictive accuracy over time. On day 1, the combined model IGs and cfDNA had a modest AUROC of 0.593, which increased to 0.796 by day 14. Comparing our findings to our previous study from 2017 [74], the SIFTI-2 data show significantly lower AUROC value at early time point days 1 (AUROC = 0.593) compared to Hampson et al. findings of the combination of cfDNA, IG (AUROC = 0.829) (Appendix Table 31).

The addition of NEUT-Y in our study improved prognostic accuracy, especially on day 3, where the AUROC increased to 0.718 reflecting ongoing neutrophil activation and its association with the progression of systemic inflammation in septic burns. Our previous study demonstrated that the combination of IGs, cfDNA and neutrophil dysfunction measured by phagocytosis shows a strong early prediction of sepsis on day 1 with AUROC of 0.935 which is significantly higher than the combination of IGs, cfDNA, and NEUT-Y with an AUROC of 0.581 in our study [74]. Neutrophil function measurement was unavailable in our study as the manufacturer no longer could

provide the test kit anymore to complete the study. Moreover, Dinsdale et al. (2017) show significant sepsis prediction on day 3 post-burns by the combination of platelet impedance count (PLT-I) and NEUT-Y with an AUROC of 0.915 [13], which is also higher than our discriminatory power at day 3 by the combination of cfDNA, IG, and NEUT-Y (AUROC = 0.718).

In our study, the Revised Baux score, a well-established predictor of mortality in burn patients, consistently performed well across all time points, with AUROC values consistently above 0.700. The model that combined IGs, cfDNA, neutrophil count, and the Revised Baux score demonstrated the highest prognostic accuracy with an AUROC of 0.793 on day 1, highlighting the combined effect of these biomarkers in predicting sepsis in post-burn patients. Comparing our finding to SIFTI-1, the combination of cfDNA, IG, and rBAUX gave a strong discrimination on day 1 with and AUROC of 0.949 compared to our discrimination power on day 1 (AUROC = 0.793) [74]. These findings emphasise the importance of using multiple biomarkers to enhance sepsis prediction in critically ill patients.

In conclusion, this study emphasises the importance of extended haematological parameters in evaluating immune responses following thermal injuries, particularly in predicting sepsis. Early increases in neutrophil and monocyte parameters (X, Y) were observed, indicating their role in the acute inflammatory response. NEUT-Y, NEUT-RI, and IGs consistently elevated at all time points, particularly in septic burns, suggesting their potential as sepsis biomarkers. The strong correlation between cfDNA and neutrophil Y suggests excessively generated and subsequently degraded NETs, providing potential valuable biomarkers for monitoring excessive NETosis, Sepsis, DIC, and MOF. The combination of IGs, cfDNA, and neutrophil Y showed progressive

improvements in predicting sepsis, especially when combined with the Revised Baux score, indicating that a multi-biomarker approach enhances diagnostic accuracy in septic burns. These findings support previous studies advocating for the use of advanced rapid haematological profiling to better understand the immune dysregulation and inflammation following burns and sepsis. Future research into the functional and morphological changes in leukocyte subtypes is crucial for improving sepsis management and early intervention strategies. This study provides valuable insights into the clinical usefulness of integrating traditional and novel haematological markers for monitoring immune responses and sepsis in critically ill patients.

Chapter 6 Measurement of Platelet Thrombus formation in patients following Severe Thermal Injury

6 Measurement of Platelet Thrombus formation in patients following Severe Thermal Injury

6.1 Introduction

Platelets are crucial for normal haemostasis but are now increasingly recognised for their additional important roles in immunity, inflammation and host defence [533]. [534]. Burns are characterised by tissue necrosis leading to inflammation, immune dysfunction and disruption to circulating cells and vessel wall integrity that results in tissue oedema [535]. Platelets are therefore crucial during the acute response to burn injury to promote normal haemostasis, host defence and wound healing. However, thermal injury causes either direct or indirect effects on platelets that may compromise their important role(s) in normal physiology thereby further contributing to inflammation, immune dysregulation, infection and poor wound healing in burns patients [374]. For example, burns directly thermally injure circulating platelets in the blood vessels when temporarily exposed to high temperatures. Both *in vitro* and *ex vivo* measurements have confirmed the destructive effects of direct heat on platelets resulting in altered structure and impaired function [374, 536, 537]. Many studies have confirmed that platelet consumption is also a classical feature of burns resulting in thrombocytopenia with a nadir from days ~2-5 post-injury followed by a rebound thrombocytosis with high counts (>450 x 10^9/L) peaking at days ~11-21 [374, 388, 538-540]. Interestingly, the level of thrombocytopenia is related to severity of injury as patients with milder injuries of <10% TBSA do not experience thrombocytopenia [374]. The degree of thrombocytopenia and lack of the thrombocytosis response are also associated with sepsis and death in severe burns [388, 539, 540]. Lower platelet counts also significantly impact upon platelet function as many commonly used platelet tests (e.g. light transmission aggregometry) are sensitive to platelet count [541].

Therefore, in thrombocytopenia, it can be difficult to determine whether there is an underlying acquired platelet defect independent of the count.

Thermal injury results in impairment to platelet aggregation responses to a range of agonists, including arachidonic acid, ristocetin and thrombin receptor activating peptide [374]. In contrast, high shear platelet function measured by global haemostasis tests including PFA-100 and TEG/ROTEM are unaffected [374]. Furthermore, there is some evidence for burn-injury induced platelet activation including increased platelet micro-aggregates, monocyte and neutrophil platelet aggregates, platelet procoagulant activity, TxA_2 metabolites, soluble sCD40L and soluble GPVI [374, 542-544]. There is also evidence for either increased sensitivity or desensitisation to *ex vivo* stimulation of platelets. This may be due to the timing of samples and whether thrombopoietin (TPO) production that partly drives the rebound thrombocytosis will also prime platelets to be more reactive at later time points [374, 545]. It is now clear that platelets are a key component of the innate immune system and act as sentinel cells to injury and/or infections and can interact with immune cells to elicit an appropriate response but also trigger immunothrombosis. Platelets can be activated when exposed to either DAMPS and infectious organisms (including PAMPS) and begin expressing ligands (e.g. PSGL-1) which promote platelet neutrophil interactions and trigger rapid NET formation via the vital NETosis pathway [315]. As severe thermal injury also triggers a massive SIRS response, the levels of circulating key bridging proteins (e.g. VWF and Fibrinogen) can also massively increase in the circulation as part of the acute phase response to further promote platelet neutrophil interactions and NETosis [120, 401]. VWF in particular has been shown to bind activated αIIbβ3 integrin and bridge to SLC44A2 on neutrophils [331]. As VWF function and size is regulated by ADAMTS13 we hypothesize that the

VWF/ADAMTS13 ratio will be increased post injury to promote high shear dependent platelet function and also vital NETosis via these interactions.

The Total Thrombus-formation analyser System (T-TAS) is a whole blood system that measures *in vitro* thrombus formation under physiological shear stress conditions [546, 547]. The system therefore provides a more comprehensive and physiological relevant measurement of thrombus formation compared to traditional laboratory tests which typically measure either platelet function, coagulation or fibrinolysis independently. Furthermore, the T-TAS is a disposable chip-based system with two types of chips (AR and HD) that measure haemostasis within flow chambers coated with collagen and tissue factor at physiological shear rates of 600 and 1200 s^{-1} respectively [547]. Importantly, the HD chip is independent of platelet count in contrast to the AR chip [548]. The purpose of this study was to confirm the classical changes in the dynamics of platelet count that occur following severe burn injury and to measure platelet physiological thrombus formation *in vitro* using the T-TAS with both AR and HD chips. We also measured VWF and ADAMST13 levels in plasma samples and related these to platelet function and NET biomarkers.

6.2 Results

6.2.1 Patient Demographics

A total of 10 burn patients were included in the study. The median age of patients with thermal injuries was 41 years (range 20-61 years), and the median burn size was 44.5% TBSA (range 18–85%). The incidence of sepsis and mortality in this cohort was 50% and 30%, respectively. Detailed patient demographics are displayed in Table 6-1.

Table 6.1: Patient demographics for measurement of platelet thrombus formation.	
Characteristic	**Burns patients (n=10)**
Age, years (range)	41 (20-61)
Gender, (M:F)	9:1
% TBSA (range)	44.45 (18-85)
% FT TBSA (range)	16 (0-55)
Inhalation injury (Y: N)	5:5
Mechanism of injury Flash, n (%) Flame, n (%) Flame and flash, n (%) Electrical, n (%) Scald, n (%)	 1 (10) 8 (80) 1 (10) 0 (0) 0 (0)
ABSI (range)	7 (2-14)
Baux (range)	85.9 (40-132)
rBaux (range)	94.4 (40-149)
SOFA	9 (2-15)
Sepsis Y:N (%)	5:5 (50)
Mortality Y: N, (%)	3:7 (30)

6.2.2 Platelet Counts following thermal injury

Severe burn injury caused a significant fall in platelet counts, with a classical nadir in impedance platelet counts at days 2, 3, 4 ($p < 0.0001$) and 5 ($p< 0.01$) post-injury compared to HC (Figure 6.1). This was followed by a rebound thrombocytosis from days 10-14 (Figure 6.1). Similar results were obtained with optical and fluorescent platelet counts (data not shown).

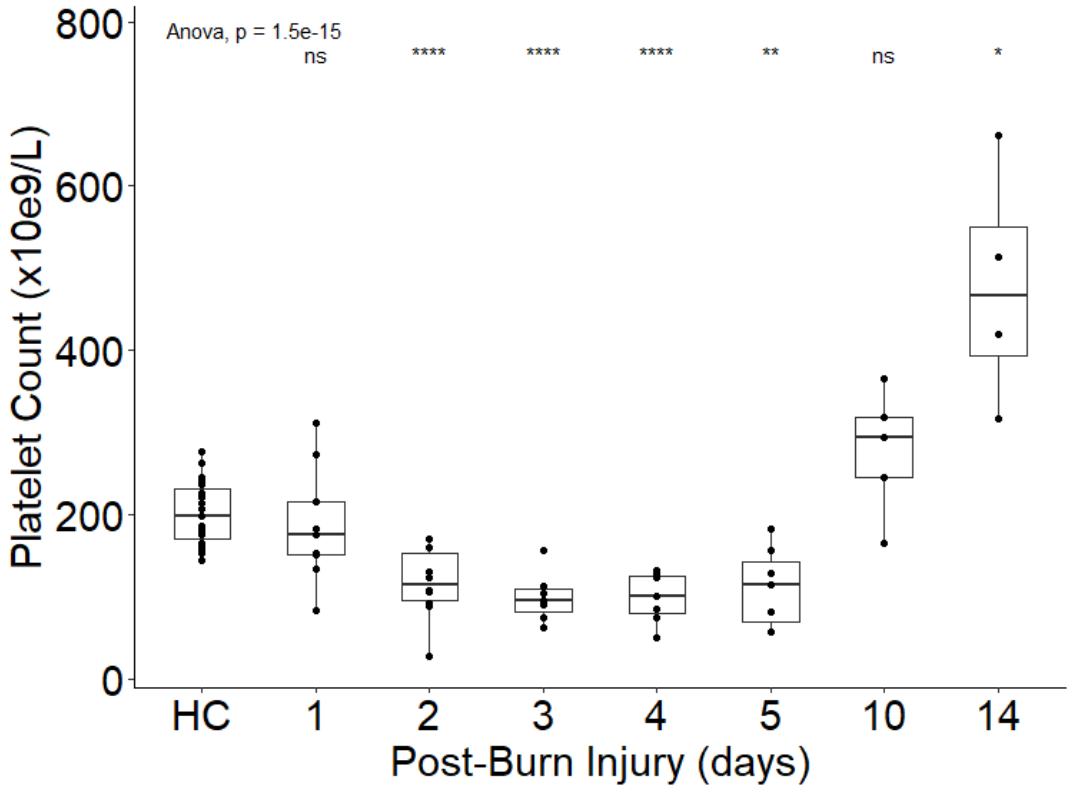

Figure 6.1: Influence of Severe Thermal Injury on Platelet Counts. Impedance platelet counts in (x 10^9/L) are plotted against time (day post-injury). There is a significant fall in platelet counts at days 2-5 compared to healthy controls (HC, N = 19) followed by a rebound thrombocytosis at day 14. **** p<0.0001, ** p< 0.01. ANOVA p< 1.5 e-15.

6.2.3 Post-burn platelet function within the T-TAS AR chip

The effect of severe burn injury on AUC, OT and OST in the T-TAS AR chip are shown in Figures 6.2A, 6.2B and 6.2C, respectively. There was a loss of haemostatic function as reflected at day 3 with a significant fall in the AUC ($p < 0.01$) associated with significant increases in both occlusion time parameters OT ($p < 0.05$) and OST ($p < 0.01$). At later time points, haemostatic function returned to normal. As the trends were remarkably similar to the above platelet count time course (Figure 6.1), we investigated the associations between platelet count and T-TAS parameters (Figure 6.3). We found significant negative correlations between platelet counts and AUC (R=0.47, $p<0.05$), OT (R = -0.49, $p< 0.01$) and OST (R = -0.47, $p<0.05$) in normal controls and AUC (R=0.63, $p<0.001$).OST (R=-0.48, $p<0.05$) and OT (R=-0.43, $p>0.05$) post-burn injury. This confirmed that the T-TAS AR chip results are dependent on platelet numbers.

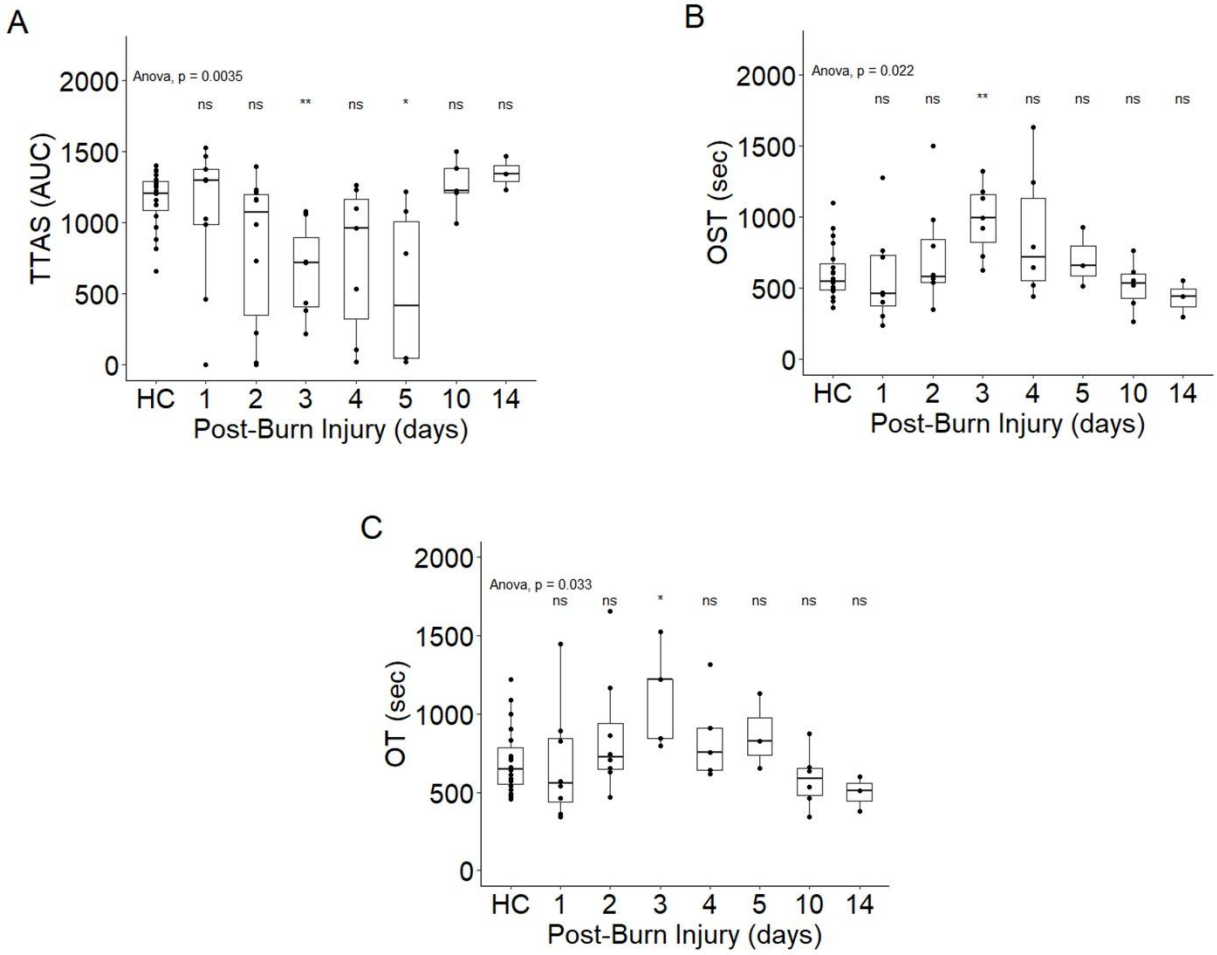

Figure 6.2: Influence of Severe Thermal Injury on thrombus formation within the T-TAS AR chip. The T-TAS AR chip parameters AUC, OST and OT are shown in figures 6.2A, 2B and 2C. There is a significant decrease in thrombus formation at day 3 (decrease in AUC and increase in OST and OT) (T-test, $p < 0.01$ and $p < 0.05$). The AR chip AUC was also significantly decreased at day 5 ($p < 0.05$).

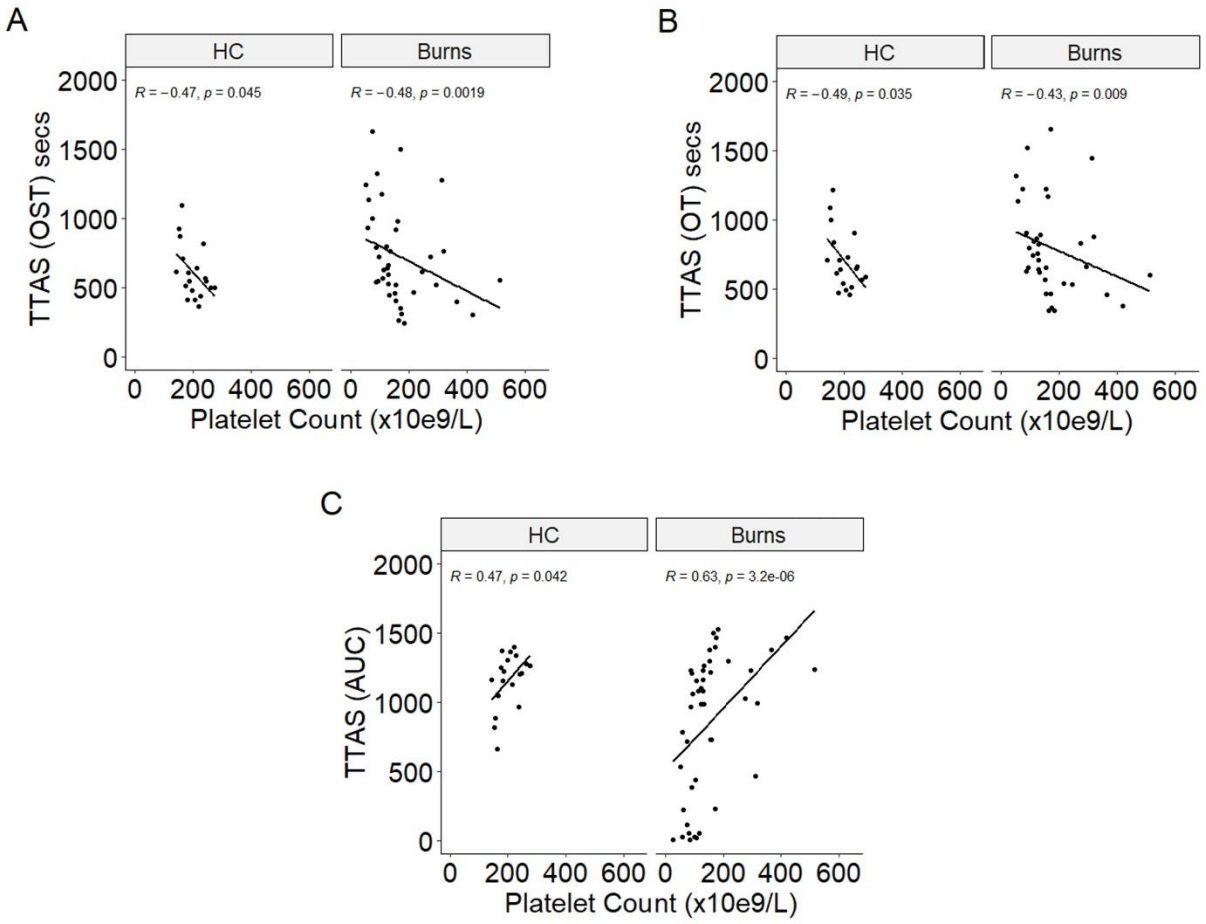

Figure 6.3: The relationship between T-TAS AR chip thrombus formation and platelet count. Significant correlations of T-TAS AR chip parameters AUC, OST and OT with platelet counts are shown in figures A, B and C in healthy controls (HC) (Pearson correlation) and burns patients (Spearman correlation).

6.2.4 Post-burn platelet function within the T-TAS HD chip

The effect of severe burn injury on AUC, OT and OST in the T-TAS HR chip are shown in Figure 6.4. Although there were no overall significant changes in all parameters across all time points, a small number of patients consistently exhibited clear haemostatic dysfunction over the first 5 days post-injury. However, in contrast to the AR chip, there were no significant correlations between platelet counts and AUC (Figure 6.5) (R=0.12, *p*=0.58, OT (R=0.0092, *p*=0.97 and OST (R=0.069, *p*=0.75) in

normal controls or, OT (R= -0.22, *p*=0.22) and OST (R= -0.25, *p*=0.75) post-burn injury. The correlation with AUC (R=0.39, p=0.02) was significant post burn injury. Overall this data confirms that the T-TAS HD chip is less dependent on platelet number and thus potentially provides a more accurate measurement of platelet function in burn injury despite the thrombocytopenia. Platelet counts are an important potential confounder in platelet function testing as indicated within the T-TAS AR chip.

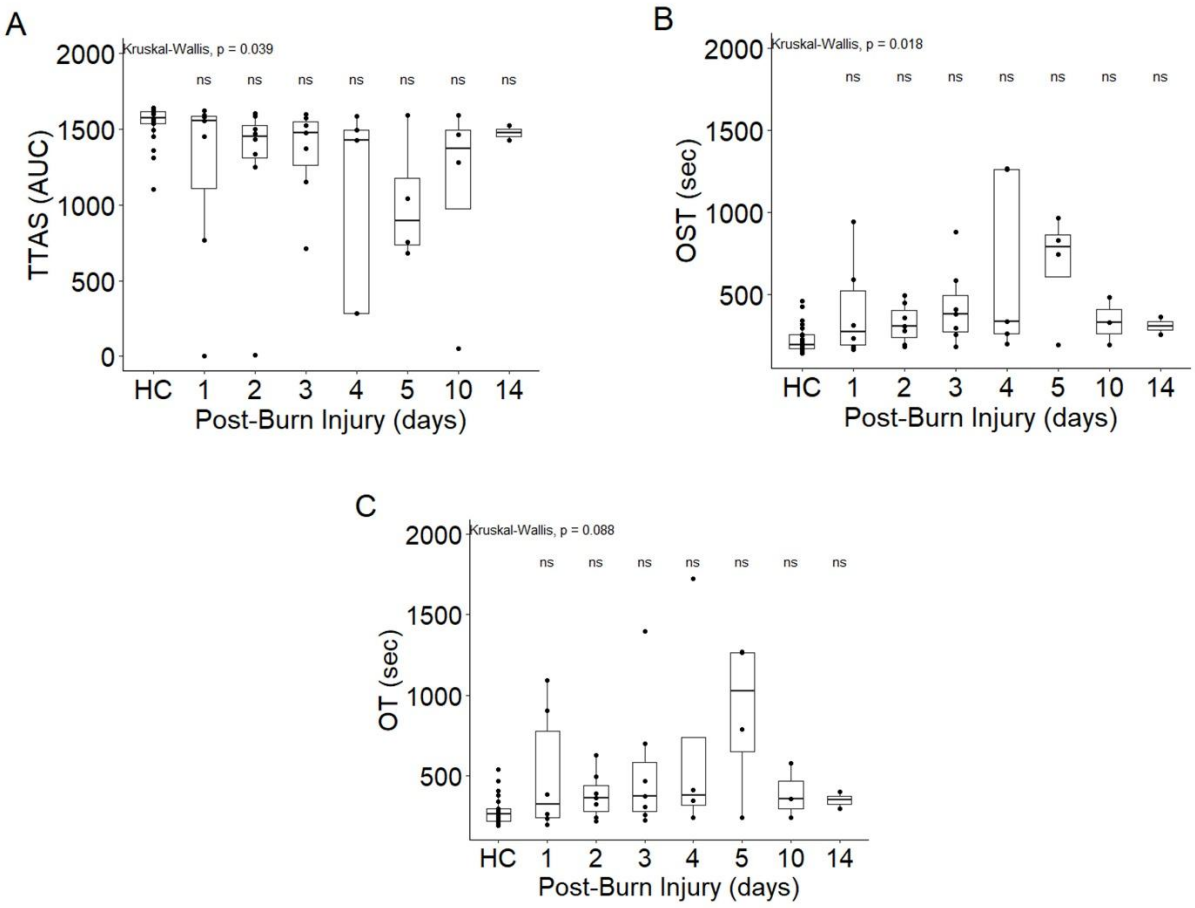

Figure 6.4: Influence of Severe Thermal Injury on thrombus formation within the T-TAS HD chip. The T-TAS AR chip parameters AUC, OST and OT are shown in figures 6.4A, 4B and 4C. There was no overall significant effect on thrombus formation at all time points ($p > 0.05$, Wilcoxon signed rank test).

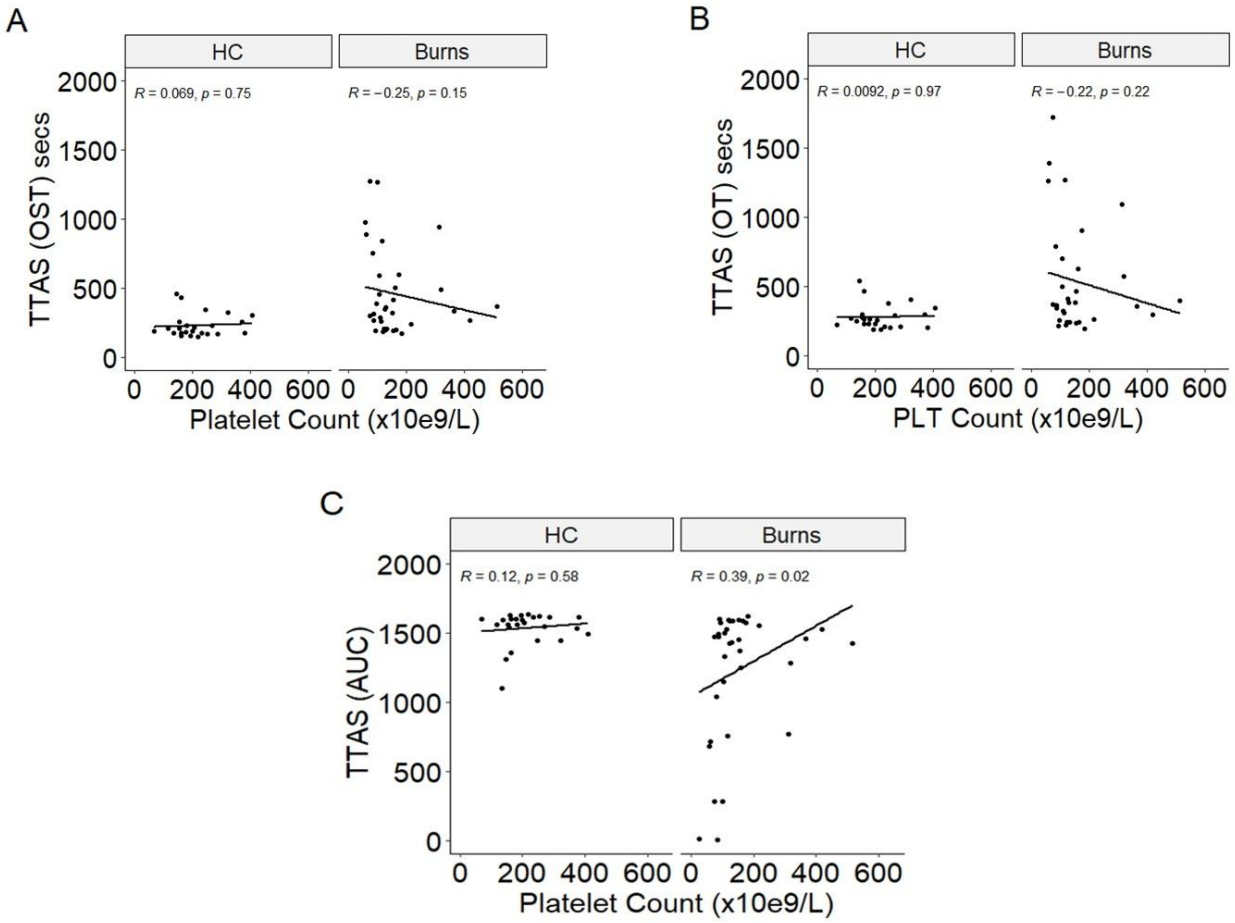

Figure 6.5: The relationship between T-TAS HD chip thrombus formation and platelet count. Lack of correlations between T-TAS AR chip parameters OST and OT with platelet counts are shown in figures 6.5A and 5B and C in healthy controls (HC) (Pearson correlation) and burns patients (Spearman correlation) The AUC significantly correlated ($p < 0.05$) with platelet counts in burns but not HC ($p = 0.58$).

6.2.5 Platelet Function, severity of injury and survival

Figure 6.6A and 6.6B shows that there were significant negative correlations between AUC and severity of injury (%TBSA) on both the T-TAS AR (R=-0.54, p<0.0001) and HD chips (R=- 0.53, *p<0*.001) respectively. Furthermore, the AUC on the AR chip at day 1 post-injury was significantly lower in non-survivors (p<0.05) (Figure 6.6C). Severity of injury (% TBSA) was also significantly higher in non-survivors (p<0.05) (Figure 6.6D). Figure 6.6E shows that the platelet count at day 1 post-injury is not significantly associated with survival. Figure 6.-6F shows the survival curve post-injury.

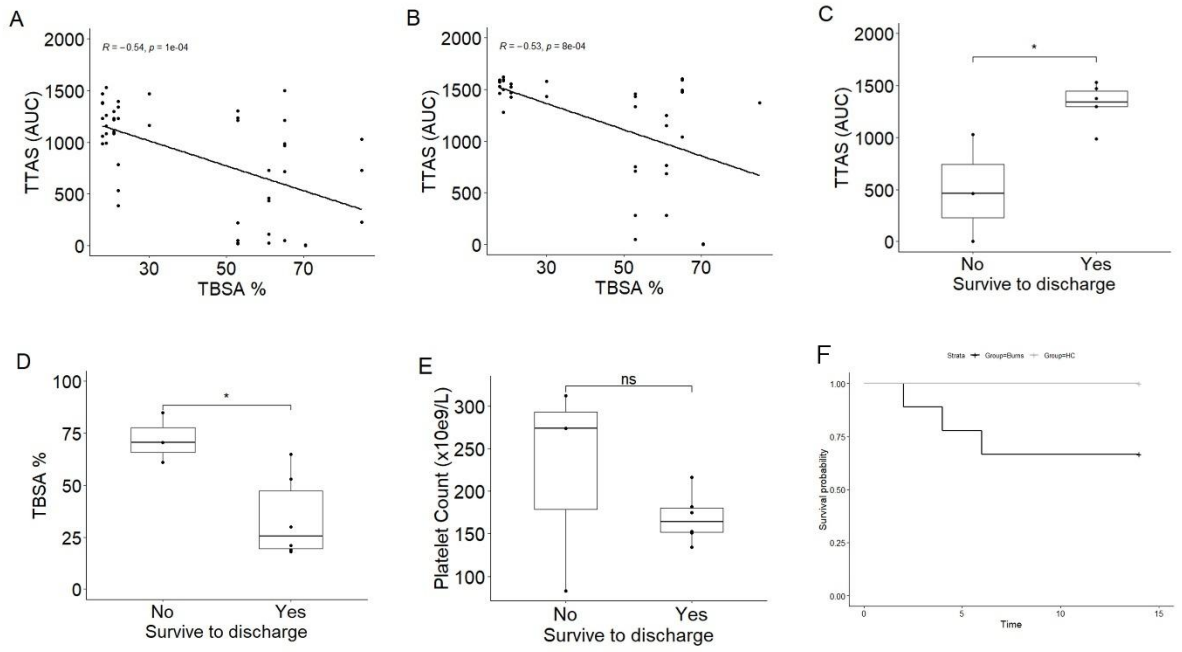

Figure 6.6: Relationship between thrombus formation and patient survival and severity of injury. Spearman correlations between severity of injury (%TBSA) with T-TAS thrombus formation AUC in AR chips (Figure 6.6A) and HD chips (Figure 6.6B). T-TAS AR chip thrombus formation (AUC) and survival at day 1 post-injury (p < 0.05, Wilcoxon signed rank test) (Figure 6.6C) and severity of injury (%TBSA) (p < 0.05, Wilcoxon signed ranked test) (Figure 6.6D). There was a non-significant (Wilcoxon signed ranked test) relationship between day 1 post-injury platelet counts and survival (Figure 6.6E). The survival curve for the burns cohort (Kaplan-Meier) is shown in Figure 6.6F.

6.2.6 The effect of severe burn injury on platelet, VWF and ADAMTS13 levels

Post injury fluorescent platelet counts (PLT-F) and the levels of VWF and ADAMTS13 in PFP were compared to healthy controls (HC) (Figure 6.7). The levels were measured in 96 burns, with demographics described in Section 2.1.2 (Table 2.1). Platelet levels were significantly decreased on days 2-6, with a significant reduced levels on day 3 ($p < 0.0001$) compared to the levels in HCs (Figure 6.7A). VWF levels were significantly elevated ($p < 0.0001$) in burns plasma samples from the admission day post burns to day 14 compared to HC VWF (Figure 6.7B). In contrast, ADAMTS13 levels were significantly decreased post injury from admission day to day 28 ($p < 0.05$ on day 1 and $p < 0.0001$ at days 4-28) (Figure 6.7C).

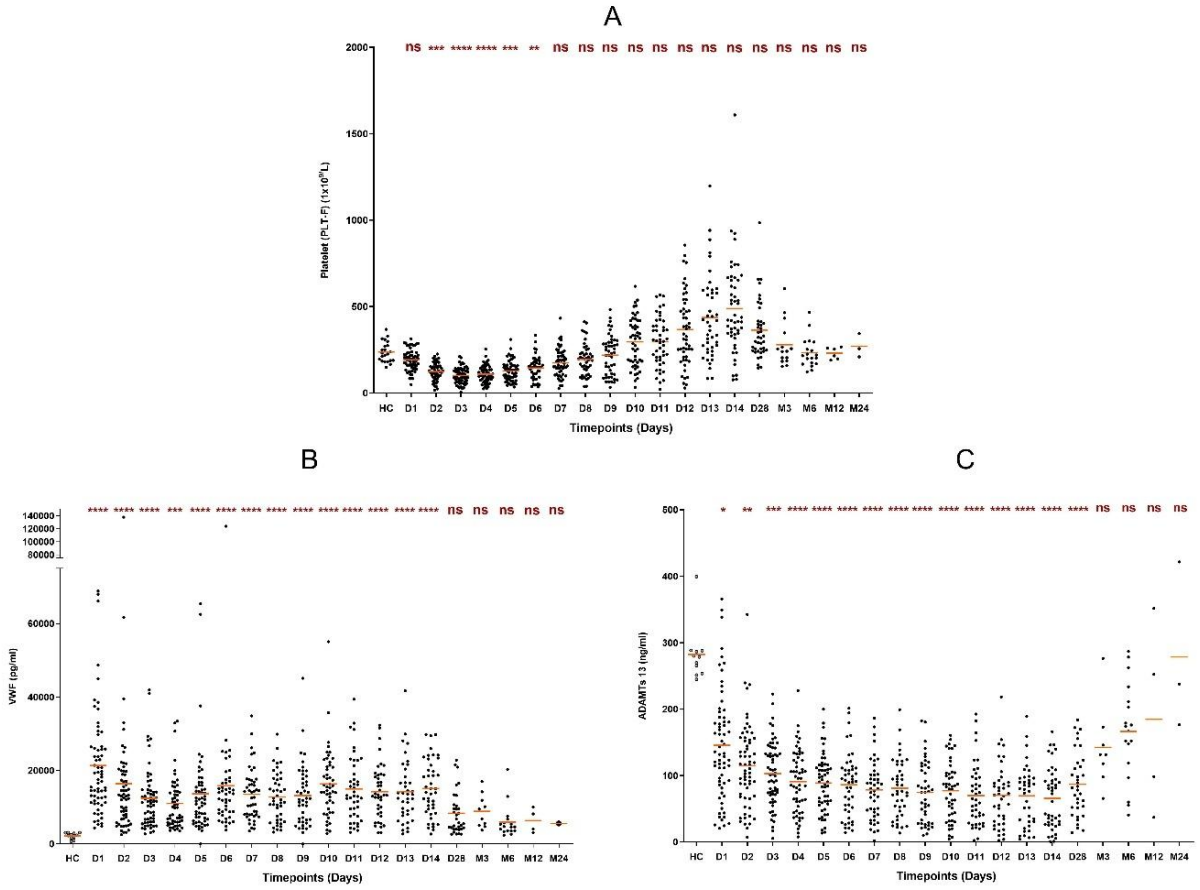

Figure 6.7: Platelet, VWF and ADAMTS13 levels in thermal injury. (A) Platelet levels in Healthy Control (HC) and burns blood samples from admission to D14, D28, M3, M6, M12 and M24. platelet levels were significantly decreased at days 2-6 compared to HC. (B) VWF levels in plasma samples were significantly increased from the admission day (D1) to day 14 post thermal injury compared to HC. (C) ADAMTS13 levels were significantly decreased from day to day 28 post burn injury compared to HC. One way ANOVA (Dunn's multiple comparisons test); *p* value ****<0.0001, *** < 0.001, ** < 0.01, * < 0.05. (ns) not significant.

6.2.7 Correlation of VWF and ADAMTS13 with platelet function.

We investigated the correlations between VWF and ADAMTS13 with T-TAS platelet function using both AR and HD chips (N=10), as shown in Figure 6.8. The T-TAS AR measurements of platelet function displayed non-significant correlations with VWF (R = 0.15, *p* = 0.34) and ADAMTS13 (R = 0.23, *p* = 0.13), illustrated in Figures 6.8A and 6.8B. The thrombus formation measured by T-TAS HD, depicted in Figure 6.8C also demonstrated a non-significant correlation with VWF (R = 0.28, *p* = 0.14). However, the T-TAS HD measurements showed a significant positive correlation with ADAMTS13 (R = 0.63, *p* = 0.00013), as illustrated in Figure 6.8D.

The relationships between VWF, ADAMTS13 levels, and the thrombus formation parameter OST, measured by T-TAS AR and HD chips, are shown in Figure 6.9. There were no significant correlations with either VWF in Figure 6.9A (R = -0.27, *p* = 0.099) or ADAMTS13 in Figure 6.9B (R = -0.12, *p* = 0.45). Nonetheless, the HD chip showed a significant negative correlation with ADAMTS13 for OST in Figure 6.9D (R = -0.43, *p* = 0.018) and a non-significant negative correlation with VWF in Figure 6.9C (R = -0.25, *p* = 0.20).

Furthermore, the correlations between VWF, ADAMTS13 levels, and the thrombus formation parameter OT, as measured by T-TAS AR and HD chips, are presented in Figure 6.10. There were no significant correlations with either VWF in Figure 6.10A (R = -0.18, *p* = 0.31) or ADAMTS13 in Figure 6.10B (R = -0.033, *p* = 0.85) in AR chips. However, in the HD chip, ADAMTS13 demonstrated a significant negative correlation with OT in Figure 6.10D (R = -0.42, *p* = 0.027) and a non-significant correlation with VWF in Figure 6.10C (R = -0.26, *p* = 0.20).

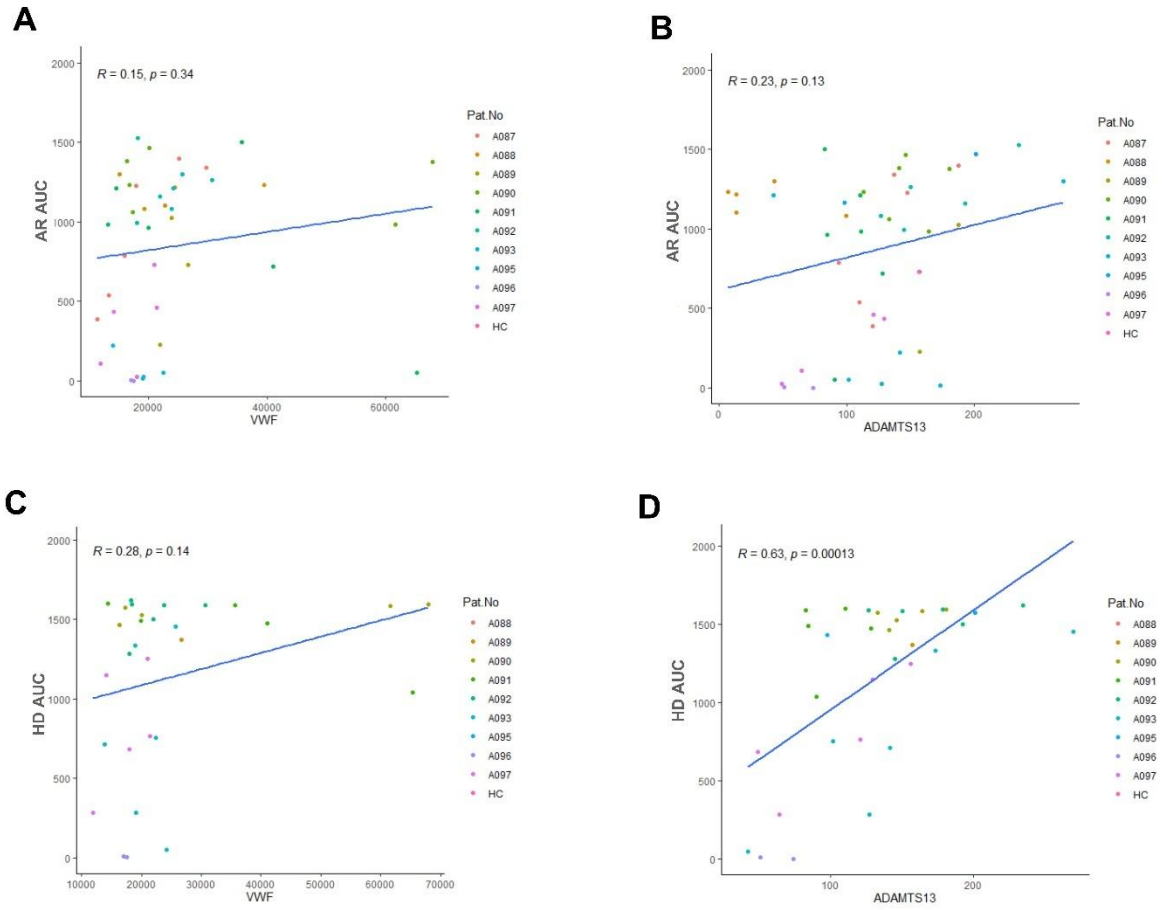

Figure 6.8: T-TAS Platelet Function correlations with VWF and ADAMTS13. Spearman correlations were analysed between the measured thrombus formation (AUC) in AR chips (A, B) and HD chips (C, D), and the levels of VWF and ADAMTS13 in burns. The AR chips showed no correlations with VWF in A (R = 0.15, *p* = 0.34) and with ADAMTS13 in B (R = 0.23, *p* = 0.13). In contrast, the HD chips demonstrated no correlation with VWF in C (R = 0.28, *p* = 0.14) but a significant correlation with ADAMTS13 in D (R = 0.63, *p* = 0.00013). The plots are colour-coded by patient number.

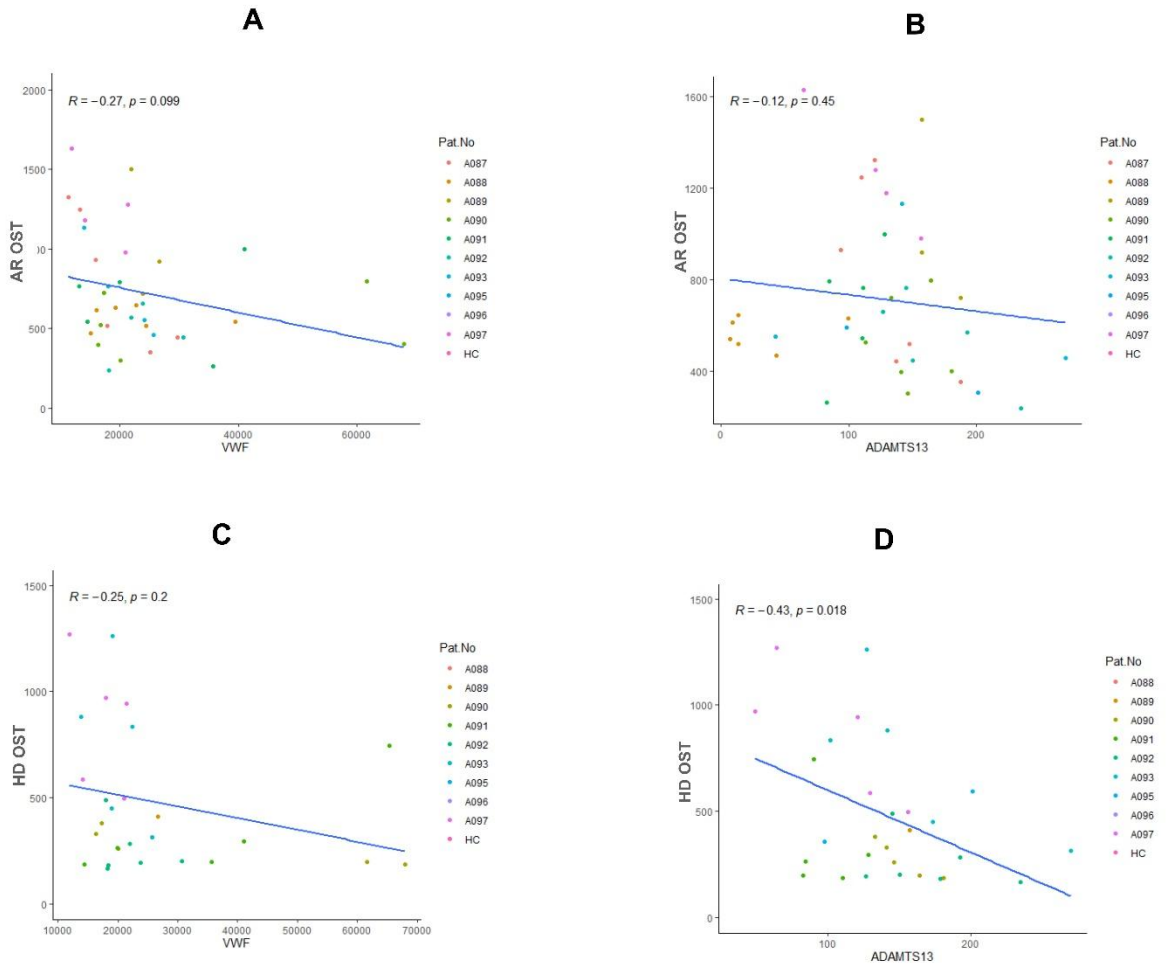

Figure 6.9: Correlations of Platelet Function Parameters within T-TAS HD and AR Chips with ADAMTS13 Levels. Spearman correlations were analysed between VWF and ADAMTS13 levels with the measured thrombus times (OST) in T-TAS AR chips (A, B) and HD chips (C, D). The AR chips show no significant correlation with either VWF in A (R = -0.27, *p* = 0.099) or ADAMTS13 in B (R = -0.12, *p* = 0.45). In contrast, the HD chips demonstrated a significant negative correlation with ADAMTS13 for OST in D (R = -0.43, *p* = 0.018) but a non-significant negative correlation with VWF in C (R = -0.25, *p* = 0.2). The plots are colour-coded by patient number.

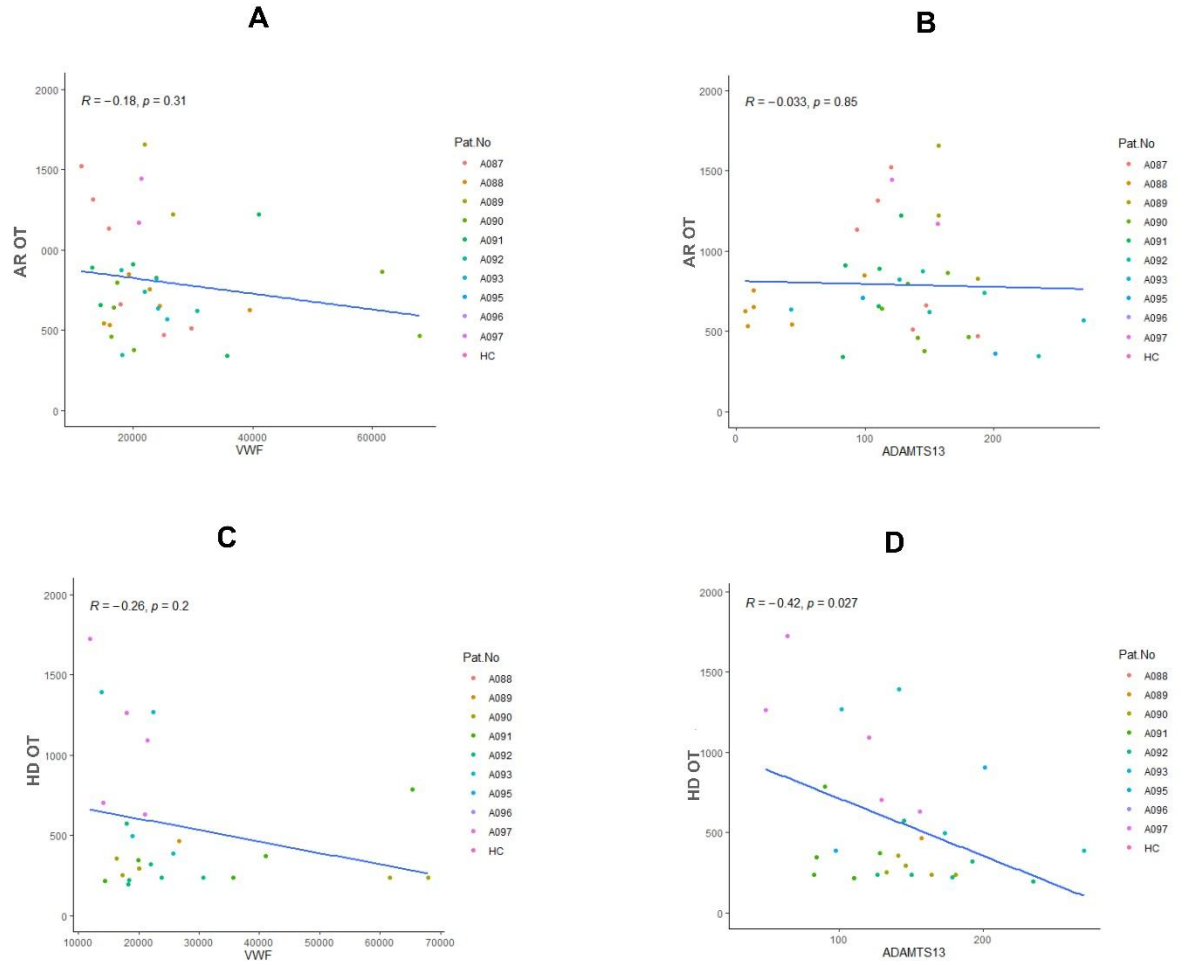

Figure 6.10: Correlations of Platelet Function (OT) within T-TAS HD and AR Chips with VWF and ADAMTS13 Levels. Spearman correlations were analysed between VWF, ADAMTS13 levels and the measured thrombus time (OT) in T-TAS AR chips (A, B) and HD chips (C, D). The AR chip showed no significant correlation with either VWF in A (R = -0.18, *p* = 0.31) or ADAMTS13 in B (R = -0.033, *p* = 0.85). The HD chip demonstrated a significant negative correlation with ADAMTS13 for OT in D (R = -0.42, *p* = 0.027) but a non-significant negative correlation with VWF in C (R = -0.26, *p* = 0.2). The plots are colour-coded by patient number.

6.2.8 Relationship between VWF, ADAMST13 and the NET biomarkers cfDNA and NEUT-Y

As VWF is implicated in inducing vital NETosis via platelet bridging to neutrophils, we investigated the potential relationships between VWF and ADAMST13 levels and the NET biomarkers cfDNA in Chapter 3 (Section 3.2.1) and NEUT-Y in Chapter 5 (Section 5.2.2.2). Our measurements show that VWF significantly correlated (r = 0.2666, p< 0.0001) with cfDNA and NEUT-Y (r = 0.2146, p< 0.0001) across all post-injury time points (Figures 6.9A and C). In contrast, ADAMTS13 levels significantly negatively correlated with cfDNA levels (r-0.1891, p < 0.0001) and NEUT-Y (r = -0.1817, p < 0.0001) across all time points (Figure 6.11) (Appendix Table 35).

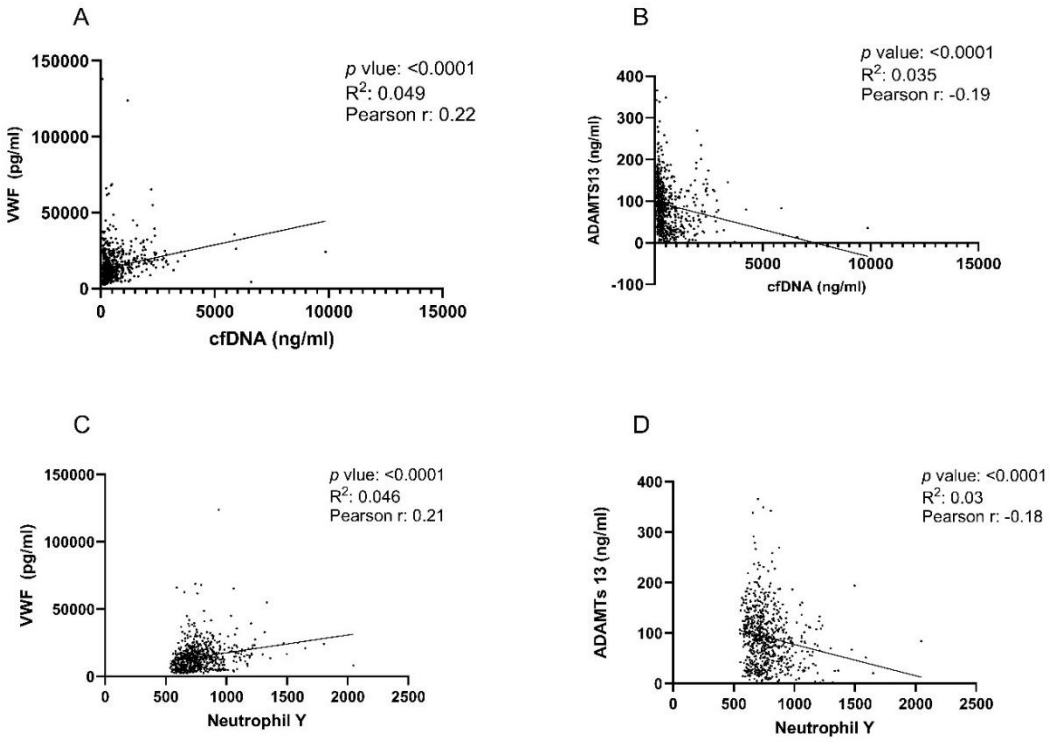

Figure 6.11: Correlations between VWF and ADAMTS13 with NET biomarkers in patients with severe burns. (A) Correlation between VWF levels and cfDNA (Pearson r = 0.22, $p < 0.0001$). (B) Correlation between ADAMTS13 levels and cfDNA (Pearson r = -0.19, $p < 0.0001$). (C) Correlation between VWF and NEUTY (Pearson r = 0.21, $p < 0.0001$). (D) Correlation between ADAMTS13 and NEUT-YY (Pearson r = -0.18, $p < 0.0001$).

6.2.9 VWF, ADAMTS13, cfDNA and NEUT-Y as biomarkers of sepsis.

We performed a combined model for multiple logistic regression analysis of sepsis using VWF and ADAMTS13 in combination with NETs. Predictive performance was analysed across all timepoints:- On day 1 the AUROC was 0.6624 (95% CI: 0.4753 to 0.8774). On day 3, the AUROC increased to 0.7456 (95% CI: 0.6123 to 0.8779), p <0.01. However, at day 13 the AUROC increased to 0.9571 (95% CI: 0.8848 to 1.000) p <0.0001 (Table 6.2).

Figure 6.10 shows a summary of the ROC curve plot and the discrimination of sepsis (Figure 6.10 A). The area under the ROC curve (AUC) is approximately 0.76 (Table 6-2), indicating a moderate predictive performance. Figure 6.10B shows a violin plot of the predicted vs. observed plot which compares the predicted probability distributions for septic (Observed 1) and non-septic (Observed 0) burns. The shape of each violin plot presents the density and distribution of predicted probabilities. The wider parts of the plot indicate where more data points are concentrated. Non-septic burns (Observed 0), the plot is wider at the bottom, that correspond with the outcome. In contrast, the septic burns violin plot (Observed 1) shows a wider distribution in the middle and upper sections, indicating that the model gives a higher probability for predicting sepsis.

Table 6.2: A combined model of VWF, ADAMTS13, cfDNA and NEUT-Y for multiple logistic regression analysis of sepsis.								
Day	Non-Septic Patients	Septic Patients	AUROC		P-Value	% Correctly Classified	Negative Predictive Power (%)	Positive Predictive Power (%)
			AUROC Value	95% CI				
Day 1	28	26	0.6624	0.4753 to 0.8774	0.1112	59.26	57.69	60.71
Day 2	19	27	0.6989	0.5487 to 0.8490	*<0.05	58.7	57.89	66.67
Day 3	16	29	0.7456	0.6123 to 0.8779	**<0.01	67.31	69.57	65.52
Day 4	15	30	0.7421	0.5931 to 0.8910	**<0.01	75.56	75	76
Day 5	12	31	0.6876	0.5241 to 0.8351	*<0.05	64	63.16	64.52
Day 6	13	21	0.7857	0.6433 to 0.9281	**<0.01	74.36	72.22	76.19
Day 7	14	26	0.78	0.6484 to 0.9116	***<0.001	68.09	66.67	69.23
Day 8	12	23	0.865	0.7416 to 0.9703	****<0.0001	76.92	70.59	81.82
Day 9	14	24	0.863	0.7534 to 0.9727	****<0.0001	79.07	78.95	79.17
Day 10	20	23	0.86	0.7036 to 0.9654	****<0.0001	76.74	75	78.26
Day 11	17	22	0.861	0.7476 to 0.9743	****<0.0001	74.36	70.59	77.27
Day 12	18	22	0.8831	0.7802 to 0.9860	****<0.0001	81.4	78.26	85
Day 13	13	19	0.9571	0.8848 to 1.0000	****<0.0001	94.12	92.86	95
Day 14	14	16	0.9222	0.8391 to 1.000	****<0.0001	80	77.78	80.95
Day 28	12	14	0.8791	0.7388 to 0.9528	***<0.001	77.78	75	81.82
Overall Model	300	339	0.7631	0.7265 to 0.7997	****<0.0001	70.27	59.77	72.37

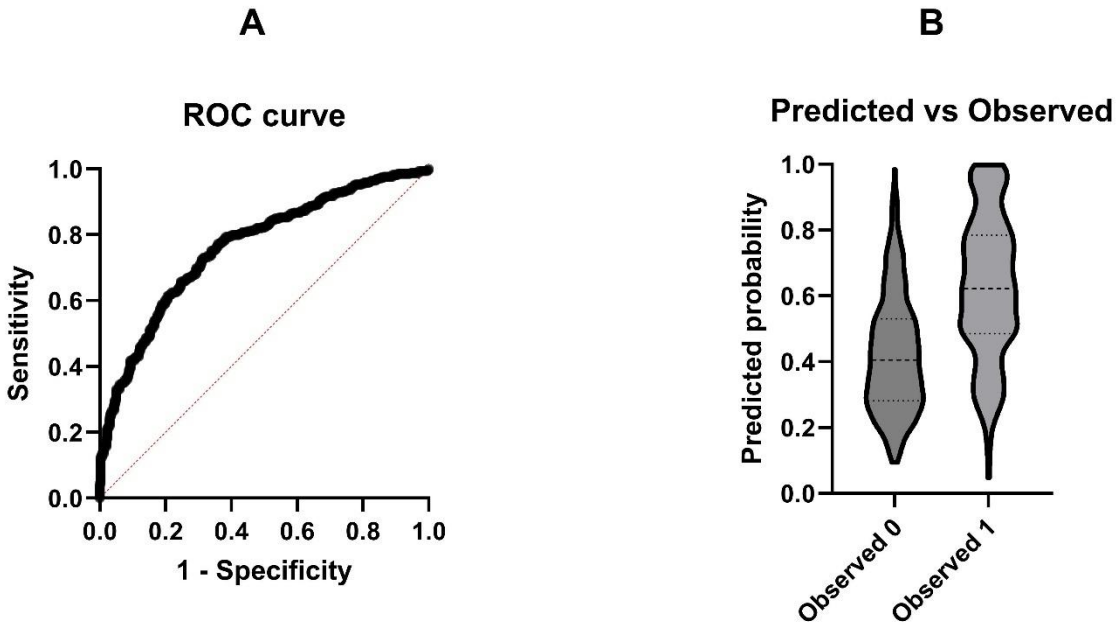

Figure 6.12: Receiver Operating Characteristic (ROC) analysis for the combined model of VWF, ADAMTS13, cfDNA and NEUT-Y for multiple logistic regression analysis of sepsis. The ROC curve plots sensitivity against specificity, representing the model's ability to distinguish between septic and non-septic patients. The area under the curve (AUROC) provides a measure of the model's predictive accuracy. (B) displays a violin plot comparing predicted probabilities with observed outcomes. It shows the distribution of predicted probabilities for non-septic (Observed 0) and septic (Observed 1) groups.

6.3 Discussion

Severe burn injury is known to significantly impact the blood circulation by directly and indirectly affecting the homeostasis, turnover and function of circulating blood cells [13]. It is well known that high temperatures not only directly thermally injure the two most numerous circulating cells (erythrocytes and platelets) in the vicinity of the burn injury but also cause their direct sequestration into the microcirculation in the central

necrotic zone of coagulation within the wound [374, 549]. This coupled with removal of any circulating damaged cells by the spleen then contributes to anaemia and thrombocytopenia, which will significantly impair oxygen supply and haemostasis, therefore impacting upon wound healing. Because of the classic systemic inflammatory response post-injury, the efficiency of the bone marrow to restore normal circulating cell numbers is often compromised by the profound post-injury leukocytosis and neutrophilia [74]. This is well known to impact upon or delay new erythrocyte (i.e. the anaemia of disease) and platelet production. For example, it usually takes about 10 days to start restoring platelet counts through TPO production which then results in an excessive thrombocytosis as a further consequence of inflammation boosting platelet production [374, 388, 545]. In this study, we set out to measure *ex vivo* physiological thrombus formation using T-TAS from day 1-14 days post severe burn injury (>20% TBSA). We confirmed that platelet counts demonstrated the classically observed nadir (at day 3-4 post-injury) and rebound thrombocytosis (from day 10-14 post injury) [388, 538]. This essentially validates the cohort in terms of the well-known classical impact of severe thermal injury on circulating platelets. The T-TAS results show that the AR chip parameters AUC, OT and OST demonstrated a reduction in thrombus formation over time with significant ($p< 0.05$) defective thrombus formation at day 3 post-injury with normalisation during the later thrombocytosis phase. Although platelet function normalised at day 4, the AUC parameter but not OT and OST was significant ($p< 0.05$) at day 5. Although platelet counts were still decreased it was surprising to see that platelet function was not abnormal at day 4. This may have been caused by increased platelet production of immature platelets in response to post-injury platelet consumption. However, measurement of the immature platelet fraction (IPF) demonstrated that the IPF was not increased at these time points (data not

shown). However, as the AUC, OT and OST parameters all significantly negatively correlated with platelet counts in both HC and burns samples, this shows how important this is as a potential confounder not only in measuring platelet function in thermal injury but in platelet function testing practice in general. Many platelet function tests including platelet aggregometry, PFA-100 and TEG/ROTEM are all affected by platelet counts [541]. In contrast, the HD chip parameters AUC, OT and OST were shown to be independent of platelet counts in HC. OT and OST but not AUC were also independent of platelet counts in burns samples. Although the overall T-TAS HD chip results were not significantly different from controls at any of our post-injury time points, there were a small number of individual patients that still exhibited platelet dysfunction from days 2-5 post-injury. The AUC parameter within both AR and HD chips also significantly correlated with the severity of injury (% TBSA) in agreement with previous observations on platelet function in burns [374]. As 30% of this small cohort did not survive their injuries, we demonstrated that the injury severity (%TBSA) was also significantly associated with mortality. Interestingly, low AUC within the T-TAS AR chip at day 1 post-injury was also significantly associated with non-survival. However, interestingly the platelet count at day 1 was not associated with non-survival. This suggests that the T-TAS test may have potential clinical utility in measuring the initial impact of burn injury on clinical outcomes. The HD chip will also facilitate the study of platelet function and be more independent of the platelet count, which is important and most likely previously ignored in the context of the burn-induced thrombocytopenia. Post injury platelet count trajectories with lower counts throughout the nadir and thrombocytosis phases have previously been shown to be associated with poor outcomes including survival [388, 539, 540]. The limitations of this study are the small number of patients (N=10) tested across 14 days post-injury. Ideally, we

would also have performed a comparison of T-TAS with other platelet function tests in this study but were significantly limited by the volume of blood available for testing. Despite this, a previous study has shown that T-TAS platelet function matches well with lumi-aggregometry for measuring platelet dysfunction in patients with bleeding disorders [546]. Also, we did not study the potential impact of blood or platelet transfusions or surgery on the test. Larger studies are therefore warranted to understand the role of *ex vivo* physiological measurement of platelet thrombus formation in severe burns.

We then conducted a study to measure the levels of VWF and ADAMTS13 in the burns cohort and compared them to the levels in healthy individuals. Our data show a rapid and significant increase in VWF levels following injury, which remained significantly elevated up to day 14 post-injury. This increase is probably caused by the post-injury SIRS response, leading to the acute release of VWF into the circulation which is important to promote primary haemostasis and aid in vessel wall repair [550]. VWF is a well-known acute phase marker [551, 552]. Our data also indicates sustained elevated VWF levels from the day of admission to day 14 post-injury. This sustained elevation may contribute to coagulopathy by promoting excessive platelet adhesion and aggregation, leading to microvascular blood clot formation [553].

ADAMTS13 is a metalloprotease that regulates VWF activity by breaking down ultra-large and large multimers, maintaining normal blood clotting and preventing spontaneous platelet aggregation as observed in TTP [554]. Our data also shows a significant decrease in ADAMTS13 levels from day 2 to day 28 post-burns compared to healthy controls. This decrease is caused by the consumption of ADAMTS13 resulting from the excessive release of VWF. Decreased ADAMTS13 synthesis may

also contribute to lower levels via endothelial damage and release of inflammatory cytokines such as TNF-α and lL-4, which directly decrease ADAMTS13 production and function [555, 556]. Matsumoto et al. (2021) illustrated that decreased ADAMTS13 activity is associated with the development of coagulopathy and disseminated intravascular coagulation (DIC). This reduction in ADAMTS13 activity leads to an accumulation of large VWF multimers, which can promote platelet aggregation, resulting in microvascular thrombosis [557]. Therefore, we investigated the roles of VWF and ADAMTS13 in platelet activity as measured by T-TAS thrombus formation assay. Our data showed no significant correlation between VWF and thrombus formation in both AR and HD chips across all platelet function T-TAS parameters: AUC, OST, and OT. Additionally, we found no significant correlations between ADAMTS13 and platelet function metrics in AR chips. However, in HD chips, ADAMTS13 levels were significantly positively correlated with AUC and significantly negatively correlated with the OST and OT parameters (Figures 6.8D, 6.9D, and 6.10D).

Increased platelet function in the T-TAS is theoretically indicated by a higher AUC and lower OST and OT parameters [558]. Elevated VWF levels and low ADAMST13 would potentially lead to the accumulation of large VWF multimers, thus promoting platelet aggregation under high-shear conditions. However, there were no observed correlations of VWF with any T-TAS parameters on both chips, and although there were correlations with ADAMTS13 with HD chip parameters, these were opposite to the expected results if ultra-large VWF is impacting upon this test and platelet function in burns [559]. However, the limited number of burn patients recruited for these measurements may have influenced our results, highlighting a larger cohort is

probably required to accurately clarify the interactions between VWF, ADAMTS13, and platelet function in the context of thermal injury. Also, it is well known that VWF size is much more important at higher shear rates (~5000 s^{-1}) [560, 561] and the shear rates are only 600 or 1200 s-1 within the T-TAS AR and HD chips respectively which might explain the correlations obtained.

Furthermore, VWF is also known to play a significant role in promoting vital NETosis. VWF facilitates the adhesion of neutrophils to the endothelium and contributes to the formation of platelet-neutrophil aggregates, which are key in promoting NET release [465]. Upon injury, neutrophils begin rolling over released ultra-large VWF by injured/activated endothelial cells. Neutrophils will also bind to P-selectin on VWF-bound activated platelets, promoting neutrophil adhesion and interaction with platelets through activated αIIbβ3 on the platelet surface by bridging to the neutrophil SLC44A2 receptor. This results in further activation of neutrophils and NET generation [562]. Our results demonstrate significant positive correlations between VWF and the NET biomarkers cfDNA or NEUT-Y. Furthermore, there was a significant negative correlation between ADAMTS13 and cfDNA and NEUT-Y (Figure 6.11). Multiple logistic regression analysis of VWF and ADAMTS13 and the NET biomarkers cfDNA and NEUT-Y demonstrates significant associations with the incidence of sepsis. AUROC values ranged from 0.7456 at day 3 to 0.957 at day 13, Moreover, Yang et al. (2020) illustrated the role of NETs in generating ROS production during NETosis, which results in oxidisation of ADAMTS13, impairing its effectiveness in cleaving large VWF. Uncleaved VWF will further promote neutrophil platelet adhesion leading to increased NET production. Moreover, neutrophil elastase and plasmin can degrade ADAMTS13, further resulting in low circulating levels. In addition, neutrophil-derived

DNA-histone complexes can also directly decrease ADAMTS13 function, resulted in further uncleaved large VWF to promote NETs and thrombosis[465].

In conclusion, our study demonstrates a classical pattern of platelet count decline observed followed by thrombocytosis, with significant impairment in platelet function during the early days post-burns, as measured by T-TAS. This impairment, particularly evident at day 3, associated with reduced thrombus formation, though platelet function normalized later despite ongoing thrombocytopenia. The correlation of T-TAS parameters with injury severity and survival underscores the importance of platelet function as a clinical indicator. Furthermore, our findings show sustained post-injury significant increase and decreases in VWF and ADAMTS13 levels respectively. The significant positive and negative correlations of VWF and ADAMTS13, respectively, with markers of generated NETs, cfDNA, and NEUT-Y reveal their strong association with excessive NET generation. Combining VWF and ADAMTS13 with NETs markers, cfDNA, and NEUT-Y suggests their potential role in predicting sepsis. These insights provide a foundation for future research into therapeutic interventions targeting the impact of VWF and ADAMTS13 on NETosis.

Chapter 7: General Discussion

7 General Discussion

NETs are complex structures composed of released chromatin fibres composed of DNA, histones, and embedded antimicrobial proteins released by activated neutrophils as part of the innate immune response to infection and injury for the purpose of killing and eliminating pathogens [249, 250]. In trauma and severe thermal injuries, NET formation is significantly upregulated, rolling as a double-edged sword as serving as both a defensive mechanism and a driver and contributor of pathological inflammation and immunothrobosis [465]. Although NETs are important for capturing and eliminating pathogens, excessive NETs produced promote complications, delaying the healing of damaged tissue, promoting microvascular occlusion and endothelial dysfunction, leading to ARDS, MOF and DIC [311, 420-423]. Moreover, released NETs are subsequently degraded with DNase enzymes, resulting in high circulating levels of generated cfDNA [335, 424].

This thesis investigated the quality, quantity and dynamics of cfDNA post-trauma in severe burns. cfDNA levels in burns and trauma were shown to significantly increase shortly after injury compared to healthy controls with a sustained elevation in burns, peaking between days 5-28 post-injury. The ultra-early samples (<1 hour) in trauma measured a higher level of released cfDNA than 24-72 hours post-injury. Measuring the quality of released cfDNA demonstrated that they predominantly consisted of nucleosome fragments measured at ~140-170 bp that appear in most patients between days 2-28 post-injury. These findings were also further verified by measuring high levels of nucleosome H3 that significantly correlated with measured cfDNA peaking at the same time points. The absence of these nucleosome bands on day 1 in most patients corresponded with the significant presence of large circulating NETs

post burns observed within whole blood. This suggests that initial injury responses are dominated by NET formation, with subsequent nucleosome release via the action of DNase I activity. Additionally, the ultra-early (< 1 hour) released cfDNA post injuries in trauma were found to be composed of the presence of nucleosome oligomers, underscoring the role of DNase I in NET degradation in chromatin fragmentation and the subsequent release of nucleosomes. The findings of this study have important implications for managing burn and trauma patients, particularly in reducing complications such as DIC, MODS, and sepsis. The research offers insights into monitoring NETs and circulating nucleosomes/cfDNA as biomarkers, which could help manage patients and mitigate risks associated with excessive NET-derived fragments post severe thermal and trauma injuries.IL-8 is an important inflammatory mediator and cytokine, playing a crucial role in neutrophil rolling, adhesion, and migration to injured tissues by inducing the production of adhesion molecules on the vessel wall [197, 472]. Previous studies have shown increased IL-8 levels following thermal injuries and correlated with sepsis [412, 486-489]. Interestingly, Abrams et al. (2019) demonstrated that released IL-8 in ICU patients is a major contributor to NET formation [272]. Our findings demonstrated that high IL-8 levels were released post-burn injury and were significantly higher on days 3-14 in patients who developed sepsis. The *ex vivo* study in burns serum demonstrated that IL-8 is a major NET mediator in burns with a significant correlation of generated NETs with serum IL-8 levels. We also further demonstrated the important regulation of NETs by serum DNase I, resulting in NET degradation and more generation of cfDNA. Inhibition of DNAse in serum-based NET generation assays, therefore is an important confounder for accurately measuring *ex vivo* NET production and cfDNA release,

Moreover, leukocyte dynamic changes post severe thermal injuries are crucial for understanding immune inflammatory responses and monitoring sepsis prognosis in severe thermal injury cases. The Sysmex analysers enable detailed and rapid quantification of extended haematological parameters, providing new insights into cell morphology, activation, and immune status [508-511]. Our previous studies in the SIFTI-1 highlighted the strong predictive values of early increased biomarkers such as cfDNA, IGs, NEUT-Y, NEUT- RI, PLT-I and neutrophil function combined with the Revised Baux score, emphasising their potential for identifying sepsis in critical burn patients [13, 74]. In this study, we further examined various leukocyte parameters during the first two weeks following thermal injury, revealing a biphasic inflammatory response. We observed an early elevation of neutrophils and monocytes on day 1 in both septic and non-septic burns, followed by a second peak at days 6-28, which indicated prolonged inflammation probably caused by secondary hits by infection and/or surgery. Our investigation into the extended parameters of leukocyte subtypes revealed a strong correlation between NEUT-Y levels and cfDNA. A significant peak in NEUT-Y levels at day 6 indicated hyperactivation of neutrophils and potential increased formation of NETs. This was followed by a notable increase in cfDNA levels at day 8, enhancing our understanding of the role of NETosis, which is regulated by DNase I and leads to subsequent elevated cfDNA levels. Furthermore, consistently high levels of NEUT-Y and IGs in septic burns highlighted their potential as biomarkers for sepsis, especially when used in combination with cfDNA levels and the Revised Baux score. These findings suggest that these markers are important for monitoring NETosis and immune dysregulation in trauma and burns patients and for predicting sepsis, DIC, and MOF.

We also investigated platelet function and dynamic changes post severe thermal injuries. In response to the injury, platelets rapidly adhere to vascular damage, form clots, and release cytokines and growth factors that stimulate tissue healing and control inflammation [369]. Platelet adherence is facilitated by released VWF and collagen by injured tissue [369]. Severe burns are associated with platelet consumption, followed by thrombocytopenia from days 2-5 post-injury, and a rebound thrombocytosis with high counts (>450 x 10^9/L) peaking at days 11-21 [374, 388, 538-540]. Platelet assays, such as light transmission aggregometry, are sensitive to platelet count, impacting the measurement of platelet function in burn patients with thrombocytopenia [541]. In this thesis, we investigated platelet dynamics, thrombus formation using whole blood using the T-TAS assay, and the potential role of VWF and ADAMTS13 post severe burns. Our findings validate the classic post-burn trajectory of platelet counts, with an initial nadir around day 3-4 post-injury and a rebound thrombocytosis by days 10-14. Thrombus formation, assessed by T-TAS, showed significant functional impairment, particularly on day 3, indicating early disruptions in haemostatic capacity. Additionally, our measurements illustrated significantly increased and decreased VWF and ADAMTS13 levels, respectively, post-burn compared to the levels in healthy controls. Sustained elevation of VWF and decreased levels of ADAMTS13 after a burn may together contribute to coagulopathies, as low ADAMTS13 fails to regulate VWF, resulting in enhanced high shear platelet function and potential thrombotic complications [557]. Interestingly, the correlations between VWF, ADAMTS13 and T-TAS platelet function did not indicate any meaningful relationships. The small study size (n = 10) or the relatively low shear values of 600 and 1200 s^{-1} may not have contributed to this. Furthermore, our findings demonstrated strong positive correlations between VWF and NETs markers (cfDNA

and NEUT-Y), with ADAMTS13 showing inverse correlations, suggesting a complex interplay in promoting NET generation. This is consistent with studies indicating that NET-induced reactive ROS impair ADAMTS13 functionality, thus exacerbating thrombotic risk by leaving large VWF multimers uncleaved [465]. The logistic regression modelling incorporating VWF, ADAMTS13, cfDNA, and NEUT-Y showed predictive potential for sepsis with between moderate and strong discrimination on days 12-28, suggesting a potential role for these biomarkers in early sepsis detection in burns. This study underscores the dual roles of platelets and VWF/ADAMTS13 dynamics in burn-induced NETosis, coagulopathy and inflammation, offering insights for therapeutic approaches to improve burn outcomes by targeting VWF, ADAMTS13, and NET interactions. Larger-scale studies will be critical to validate these associations and expand on potential clinical applications of T-TAS and related biomarkers in burn care.

In summary, these studies highlight the crucial role of released NETs and cfDNA in the inflammatory and thrombotic responses post severe burns and trauma. Elevated levels of cfDNA result from the degradation of excessive NETs by DNase enzymes and are primarily comprised of nucleosome fragments, as confirmed by electrophoresis and specific nucleosome H3 ELISA assays. indicating the dynamics of NET derived chromatin generation and breakdown after injury. A key finding is the significant role of released IL-8 in promoting NET generation in burns. Monitoring cfDNA and IL-8 levels could also help in understanding and potentially moderating this inflammatory cascade. The observed dynamic changes in leukocytes, IGs, and cfDNA highlight critical shifts in immune responses. Sustained elevation in these markers may serve as potential indicators for sepsis risk. Parameters such as cfDNA/nucleosomes, NEUT-Y, and IGs, particularly when combined with the rBaux score, have proven

effective in distinguishing and predicting sepsis in burn patients. Additionally, levels of VWF and ADAMTS13 have shown a strong association with NET generation biomarkers, NEUT-Y and cfDNA. Progression modelling that combines VWF, ADAMTS13, and NET markers, cfDNA and NEUT-Y suggests their potential role in predicting sepsis. Furthermore, the observed platelet dysfunction shortly after a burn underscores a significant haemostatic imbalance, which further increases patient risk. These findings emphasize the importance of monitoring these biomarkers and developing targeted therapeutic strategies to manage NETs, inflammation, coagulopathy, and immune dysregulation in critically ill burn and trauma patients.

7.1 Limitations

As a result of the COVID-19 crisis, the planned research in the first two years (2020 and 2021) was significantly impacted, because of the limited access, my delayed training and effects on patient recruitments. The investigation of the mechanism and involvement of the interaction between platelets and neutrophils through the αIIbβ3 receptor on the platelet surface and the neutrophil SLC44A2 receptor was initially planned. Unfortunately, we were unable to get the required ethical approval to study the impact of SLC44A2 genotype on *in vivo* and *ex vivo* NETosis and its potential impact upon clinical outcomes in patients. Additionally, researching the potential cytotoxic effects of nucleosomes and histones on endothelial cells was also planned but unfortunately was not fully completed. We encountered ongoing bacterial contamination of our microvascular endothelial cells (HMEC-1) and human dermal blood endothelial cells (HDBEC) which delayed our ability to generate sufficient data for reliable interpretation. It has been demonstrated in the past that histones have a significant cytotoxic effects on HMEC-1 [563].

7.2 Future research

As a consequence of the major findings in this thesis we are now planning future research including:-

1) Investigation into the biological activities of nucleosomes and histones on cellular cytotoxicity *ex vivo* and *in vivo* and the heparin neutralisation and resistance. The heparin study will also be extended to study the use of anti-Xa monitoring on thrombosis and heparin dosaging in burns patients. The aim is to fund a prospective multi-centre study on heparin resistance in burns
2) As IL-8 was confirmed as a major pathway for inducing NETs in burns patients, we will perform studies to determine the exact contributions of IL-8, Heme and other mediators in inducing NETosis in burns and trauma samples *in vivo* and *ex vivo*.
3) We aim to re-apply for the ethics to study the SLC44A2 genotype on receptor copy-density on neutrophils and *ex vivo* and *in vivo* platelet-induced vital NETosis formation, biomarkers and patient outcomes.
4) Increasing the number of burns patients samples tested by the T-TAS platelet function test to increase the statistical power.
5) In collaboration with Dr. Andrew Retter from Kings and Volition, we will set up and validate a rapid automated version of the NuQ 3.1 ELISA kit to measure nucleosome levels within the full SIFTI-2 and GH trauma cohorts to determine hether this is a suitable test for predicting sepsis. We will also compare the data with our cfDNA assay and extend the study into ITU patients at the Queen Elizabeth University Hospital Birmingham. The aim is to also eventually develop and validate a point of care test.

References

1. Peek-Asa C., Zwerling C. and Stallones L., *Acute traumatic injuries in rural populations.* Am J Public Health, 2004. **94**(10): p. 1689-93.
2. Toussaint J. and Singer A. J., *The evaluation and management of thermal injuries: 2014 update.* Clin Exp Emerg Med, 2014. **1**(1): p. 8-18.
3. Dumovich J. and Singh P., *Physiology, Trauma*, in *StatPearls*. 2020: Treasure Island (FL).
4. World Health Orgnisation. *WHO urges more effective prevention of injuries and violence causing 1 in 12 deaths worldwide*. 2022 29 November 2022]; Available from: https://www.who.int/news/item/29-11-2022-who-urges-more-effective-prevention-of-injuries-and-violence--causing-1-in-12-deaths-worldwide/.
5. Evans J., Murch H., Begley R., Roland D., Lyttle M. D., Bouamra O. and Mullen S., *Mortality in adolescent trauma: a comparison of children's, mixed and adult major trauma centres.* Emerg Med J, 2021. **38**(7): p. 488-494.
6. Beck B., Smith K., Mercier E., Bernard S., Jones C., Meadley B., Clair T. S., Jennings P. A., Nehme Z., Burke M., Bassed R., Fitzgerald M., Judson R., Teague W., Mitra B., Mathew J., Buck A., Varma D., Gabbe B., Bray J., Mclellan S., Ford J., Siedenburg J. and Cameron P., *Potentially preventable trauma deaths: A retrospective review.* Injury, 2019. **50**(5): p. 1009-1016.
7. Kauvar D. S., Lefering R. and Wade C. E., *Impact of hemorrhage on trauma outcome: an overview of epidemiology, clinical presentations, and therapeutic considerations.* J Trauma, 2006. **60**(6 Suppl): p. S3-11.
8. Joseph B., Aziz H., Pandit V., Kulvatunyou N., O'keeffe T., Wynne J., Tang A., Friese R. S. and Rhee P., *Improving survival rates after civilian gunshot wounds to the brain.* J Am Coll Surg, 2014. **218**(1): p. 58-65.
9. Tiwari V. K., *Burn wound: How it differs from other wounds?* Indian J Plast Surg, 2012. **45**(2): p. 364-73.
10. Brusselaers N., Monstrey S., Vogelaers D., Hoste E. and Blot S., *Severe burn injury in Europe: a systematic review of the incidence, etiology, morbidity, and mortality.* Crit Care, 2010. **14**(5): p. R188.
11. Church D., Elsayed S., Reid O., Winston B. and Lindsay R., *Burn wound infections.* Clin Microbiol Rev, 2006. **19**(2): p. 403-34.
12. Calum H., Moser C., Jensen P. O., Christophersen L., Maling D. S., Van Gennip M., Bjarnsholt T., Hougen H. P., Givskov M., Jacobsen G. K. and Hoiby N., *Thermal injury induces impaired function in polymorphonuclear neutrophil granulocytes and reduced control of burn wound infection.* Clin Exp Immunol, 2009. **156**(1): p. 102-10.
13. Dinsdale R. J., Devi A., Hampson P., Wearn C. M., Bamford A. L., Hazeldine J., Bishop J., Ahmed S., Watson C., Lord J. M., Moiemen N. and Harrison P., *Changes in novel haematological parameters following thermal injury: A prospective observational cohort study.* Sci Rep, 2017. **7**(1): p. 3211.
14. Foex B. A., *Systemic responses to trauma.* Br Med Bull, 1999. **55**(4): p. 726-43.
15. Jeschke M. G., Patsouris D., Stanojcic M., Abdullahi A., Rehou S., Pinto R., Chen P., Burnett M. and Amini-Nik S., *Pathophysiologic Response to Burns in the Elderly.* EBioMedicine, 2015. **2**(10): p. 1536-48.
16. Jackson P. C., Hardwicke J., Bamford A., Nightingale P., Wilson Y., Papini R. and Moiemen N., *Revised estimates of mortality from the Birmingham Burn Centre, 2001-2010: a continuing analysis over 65 years.* Ann Surg, 2014. **259**(5): p. 979-84.
17. Mann E. A., Baun M. M., Meininger J. C. and Wade C. E., *Comparison of mortality associated with sepsis in the burn, trauma, and general intensive care unit patient: a systematic review of the literature.* Shock, 2012. **37**(1): p. 4-16.

18. Greenhalgh D. G., *Sepsis in the burn patient: a different problem than sepsis in the general population.* Burns Trauma, 2017. **5**: p. 23.
19. Venet F. and Monneret G., *Advances in the understanding and treatment of sepsis-induced immunosuppression.* Nat Rev Nephrol, 2018. **14**(2): p. 121-137.
20. Binkowska A. M., Michalak G. and Slotwinski R., *Current views on the mechanisms of immune responses to trauma and infection.* Cent Eur J Immunol, 2015. **40**(2): p. 206-16.
21. Hayakawa M., *Pathophysiology of trauma-induced coagulopathy: disseminated intravascular coagulation with the fibrinolytic phenotype.* J Intensive Care, 2017. **5**: p. 14.
22. Savioli G., Ceresa I. F., Caneva L., Gerosa S. and Ricevuti G., *Trauma-Induced Coagulopathy: Overview of an Emerging Medical Problem from Pathophysiology to Outcomes.* Medicines (Basel), 2021. **8**(4).
23. Maegele M., *Update on the pathophysiology and management of acute trauma hemorrhage and trauma-induced coagulopathy based upon viscoelastic testing.* Clin Exp Emerg Med, 2024. **11**(3): p. 259-267.
24. Lord J. M., Midwinter M. J., Chen Y. F., Belli A., Brohi K., Kovacs E. J., Koenderman L., Kubes P. and Lilford R. J., *The systemic immune response to trauma: an overview of pathophysiology and treatment.* Lancet, 2014. **384**(9952): p. 1455-65.
25. Chadda K. R. and Puthucheary Z., *Persistent inflammation, immunosuppression, and catabolism syndrome (PICS): a review of definitions, potential therapies, and research priorities.* Br J Anaesth, 2024. **132**(3): p. 507-518.
26. Brochner A. C. and Toft P., *Pathophysiology of the systemic inflammatory response after major accidental trauma.* Scand J Trauma Resusc Emerg Med, 2009. **17**: p. 43.
27. Jackson D. M., *[The diagnosis of the depth of burning].* Br J Surg, 1953. **40**(164): p. 588-96.
28. Hettiaratchy S. and Dziewulski P., *ABC of burns: pathophysiology and types of burns.* BMJ, 2004. **328**(7453): p. 1427-9.
29. Edwards S., *Shock: types, classifications and explorations of their physiological effects.* Emerg Nurse, 2001. **9**(2): p. 29-38.
30. Gurney J. M., Kozar R. A. and Cancio L. C., *Plasma for burn shock resuscitation: is it time to go back to the future?* Transfusion, 2019. **59**(S2): p. 1578-1586.
31. Worthley L. I., *Shock: a review of pathophysiology and management. Part I.* Crit Care Resusc, 2000. **2**(1): p. 55-65.
32. Yao Y. M., Redl H., Bahrami S. and Schlag G., *The inflammatory basis of trauma/shock-associated multiple organ failure.* Inflamm Res, 1998. **47**(5): p. 201-10.
33. Latenser B. A., *Critical care of the burn patient: the first 48 hours.* Crit Care Med, 2009. **37**(10): p. 2819-26.
34. Wang J., Liang T., Louis L., Nicolaou S. and Mclaughlin P. D., *Hypovolemic shock complex in the trauma setting: a pictorial review.* Can Assoc Radiol J, 2013. **64**(2): p. 156-63.
35. Bougle A., Harrois A. and Duranteau J., *Resuscitative strategies in traumatic hemorrhagic shock.* Ann Intensive Care, 2013. **3**(1): p. 1.
36. Hotchkiss R. S., Moldawer L. L., Opal S. M., Reinhart K., Turnbull I. R. and Vincent J. L., *Sepsis and septic shock.* Nat Rev Dis Primers, 2016. **2**: p. 16045.
37. Morrell M. R., Micek S. T. and Kollef M. H., *The management of severe sepsis and septic shock.* Infect Dis Clin North Am, 2009. **23**(3): p. 485-501.
38. Al-Mousawi A. M., Mecott-Rivera G. A., Jeschke M. G. and Herndon D. N., *Burn teams and burn centers: the importance of a comprehensive team approach to burn care.* Clin Plast Surg, 2009. **36**(4): p. 547-54.
39. Stylianou N., Buchan I. and Dunn K. W., *A review of the international Burn Injury Database (iBID) for England and Wales: descriptive analysis of burn injuries 2003-2011.* BMJ Open, 2015. **5**(2): p. e006184.

40. Mitra B., Fitzgerald M., Cameron P. and Cleland H., *Fluid resuscitation in major burns.* ANZ J Surg, 2006. **76**(1-2): p. 35-8.
41. Barrow R. E., Jeschke M. G. and Herndon D. N., *Early fluid resuscitation improves outcomes in severely burned children.* Resuscitation, 2000. **45**(2): p. 91-6.
42. Snell J. A., Loh N. H., Mahambrey T. and Shokrollahi K., *Clinical review: the critical care management of the burn patient.* Crit Care, 2013. **17**(5): p. 241.
43. Endorf F. W. and Gamelli R. L., *Inhalation injury, pulmonary perturbations, and fluid resuscitation.* J Burn Care Res, 2007. **28**(1): p. 80-3.
44. Mlcak R. P., Suman O. E. and Herndon D. N., *Respiratory management of inhalation injury.* Burns, 2007. **33**(1): p. 2-13.
45. Walker P. F., Buehner M. F., Wood L. A., Boyer N. L., Driscoll I. R., Lundy J. B., Cancio L. C. and Chung K. K., *Diagnosis and management of inhalation injury: an updated review.* Crit Care, 2015. **19**: p. 351.
46. Reid A. and Ha J. F., *Inhalational injury and the larynx: A review.* Burns, 2019. **45**(6): p. 1266-1274.
47. Nieman G. F., Clark W. R., Jr., Wax S. D. and Webb S. R., *The effect of smoke inhalation on pulmonary surfactant.* Ann Surg, 1980. **191**(2): p. 171-81.
48. Lange M., Hamahata A., Traber D. L., Esechie A., Jonkam C., Bansal K., Nakano Y., Traber L. D. and Enkhbaatar P., *A murine model of sepsis following smoke inhalation injury.* Biochem Biophys Res Commun, 2010. **391**(3): p. 1555-60.
49. Rehberg S., Maybauer M. O., Enkhbaatar P., Maybauer D. M., Yamamoto Y. and Traber D. L., *Pathophysiology, management and treatment of smoke inhalation injury.* Expert Rev Respir Med, 2009. **3**(3): p. 283-297.
50. Singh V., Devgan L., Bhat S. and Milner S. M., *The pathogenesis of burn wound conversion.* Ann Plast Surg, 2007. **59**(1): p. 109-15.
51. Rowan M. P., Cancio L. C., Elster E. A., Burmeister D. M., Rose L. F., Natesan S., Chan R. K., Christy R. J. and Chung K. K., *Burn wound healing and treatment: review and advancements.* Crit Care, 2015. **19**: p. 243.
52. Xiao-Wu W., Herndon D. N., Spies M., Sanford A. P. and Wolf S. E., *Effects of delayed wound excision and grafting in severely burned children.* Arch Surg, 2002. **137**(9): p. 1049-54.
53. Muangman P., Sullivan S. R., Honari S., Engrav L. H., Heimbach D. M. and Gibran N. S., *The optimal time for early excision in major burn injury.* J Med Assoc Thai, 2006. **89**(1): p. 29-36.
54. Guggenheim M., Zbinden R., Handschin A. E., Gohritz A., Altintas M. A. and Giovanoli P., *Changes in bacterial isolates from burn wounds and their antibiograms: a 20-year study (1986-2005).* Burns, 2009. **35**(4): p. 553-60.
55. Lenz A., Franklin G. A. and Cheadle W. G., *Systemic inflammation after trauma.* Injury, 2007. **38**(12): p. 1336-45.
56. Sener G., Sehirli A. O., Satiroglu H., Keyer-Uysal M. and Yegen B. C., *Melatonin improves oxidative organ damage in a rat model of thermal injury.* Burns, 2002. **28**(5): p. 419-25.
57. Bone R. C., Balk R. A., Cerra F. B., Dellinger R. P., Fein A. M., Knaus W. A., Schein R. M. and Sibbald W. J., *Definitions for sepsis and organ failure and guidelines for the use of innovative therapies in sepsis. The ACCP/SCCM Consensus Conference Committee. American College of Chest Physicians/Society of Critical Care Medicine.* Chest, 1992. **101**(6): p. 1644-55.
58. Gentile L. F., Cuenca A. G., Efron P. A., Ang D., Bihorac A., Mckinley B. A., Moldawer L. L. and Moore F. A., *Persistent inflammation and immunosuppression: a common syndrome and new horizon for surgical intensive care.* J Trauma Acute Care Surg, 2012. **72**(6): p. 1491-501.
59. Lu J., Goh S. J., Tng P. Y., Deng Y. Y., Ling E. A. and Moochhala S., *Systemic inflammatory response following acute traumatic brain injury.* Front Biosci (Landmark Ed), 2009. **14**: p. 3795-813.

60. Pugin J., *How tissue injury alarms the immune system and causes a systemic inflammatory response syndrome.* Ann Intensive Care, 2012. **2**(1): p. 27.
61. Su L., Han B., Liu C., Liang L., Jiang Z., Deng J., Yan P., Jia Y., Feng D. and Xie L., *Value of soluble TREM-1, procalcitonin, and C-reactive protein serum levels as biomarkers for detecting bacteremia among sepsis patients with new fever in intensive care units: a prospective cohort study.* BMC Infect Dis, 2012. **12**: p. 157.
62. Malham G. M. and Souter M. J., *Systemic inflammatory response syndrome and acute neurological disease.* Br J Neurosurg, 2001. **15**(5): p. 381-7.
63. Xiao W., Mindrinos M. N., Seok J., Cuschieri J., Cuenca A. G., Gao H., Hayden D. L., Hennessy L., Moore E. E., Minei J. P., Bankey P. E., Johnson J. L., Sperry J., Nathens A. B., Billiar T. R., West M. A., Brownstein B. H., Mason P. H., Baker H. V., Finnerty C. C., Jeschke M. G., Lopez M. C., Klein M. B., Gamelli R. L., Gibran N. S., Arnoldo B., Xu W., Zhang Y., Calvano S. E., Mcdonald-Smith G. P., Schoenfeld D. A., Storey J. D., Cobb J. P., Warren H. S., Moldawer L. L., Herndon D. N., Lowry S. F., Maier R. V., Davis R. W., Tompkins R. G., Inflammation and Host Response to Injury Large-Scale Collaborative Research Program, *A genomic storm in critically injured humans.* J Exp Med, 2011. **208**(13): p. 2581-90.
64. Leijte G. P., Custers H., Gerretsen J., Heijne A., Roth J., Vogl T., Scheffer G. J., Pickkers P. and Kox M., *Increased Plasma Levels of Danger-Associated Molecular Patterns Are Associated With Immune Suppression and Postoperative Infections in Patients Undergoing Cytoreductive Surgery and Hyperthermic Intraperitoneal Chemotherapy.* Front Immunol, 2018. **9**: p. 663.
65. Krysko D. V., Agostinis P., Krysko O., Garg A. D., Bachert C., Lambrecht B. N. and Vandenabeele P., *Emerging role of damage-associated molecular patterns derived from mitochondria in inflammation.* Trends Immunol, 2011. **32**(4): p. 157-64.
66. Magna M. and Pisetsky D. S., *The Alarmin Properties of DNA and DNA-associated Nuclear Proteins.* Clin Ther, 2016. **38**(5): p. 1029-41.
67. Horner E., Lord J. M. and Hazeldine J., *The immune suppressive properties of damage associated molecular patterns in the setting of sterile traumatic injury.* Front Immunol, 2023. **14**: p. 1239683.
68. Zindel J. and Kubes P., *DAMPs, PAMPs, and LAMPs in Immunity and Sterile Inflammation.* Annu Rev Pathol, 2020. **15**: p. 493-518.
69. Singh P. and Ali S. A., *Multifunctional Role of S100 Protein Family in the Immune System: An Update.* Cells, 2022. **11**(15).
70. Menges P., Kessler W., Kloecker C., Feuerherd M., Gaubert S., Diedrich S., Van Der Linde J., Hegenbart A., Busemann A., Traeger T., Cziupka K., Heidecke C. D. and Maier S., *Surgical trauma and postoperative immune dysfunction.* Eur Surg Res, 2012. **48**(4): p. 180-6.
71. Rani M., Nicholson S. E., Zhang Q. and Schwacha M. G., *Damage-associated molecular patterns (DAMPs) released after burn are associated with inflammation and monocyte activation.* Burns, 2017. **43**(2): p. 297-303.
72. Simmons J. D., Lee Y. L., Mulekar S., Kuck J. L., Brevard S. B., Gonzalez R. P., Gillespie M. N. and Richards W. O., *Elevated levels of plasma mitochondrial DNA DAMPs are linked to clinical outcome in severely injured human subjects.* Ann Surg, 2013. **258**(4): p. 591-6; discussion 596-8.
73. Altrichter J., Zedler S., Kraft R., Faist E., Mitzner S. R., Sauer M., Windolf J., Scholz M. and Logters T., *Neutrophil-derived circulating free DNA (cf-DNA/NETs), a potential prognostic marker for mortality in patients with severe burn injury.* Eur J Trauma Emerg Surg, 2010. **36**(6): p. 551-7.
74. Hampson P., Dinsdale R. J., Wearn C. M., Bamford A. L., Bishop J. R. B., Hazeldine J., Moiemen N. S., Harrison P. and Lord J. M., *Neutrophil Dysfunction, Immature Granulocytes, and Cell-free DNA are Early Biomarkers of Sepsis in Burn-injured Patients: A Prospective Observational Cohort Study.* Ann Surg, 2017. **265**(6): p. 1241-1249.

75. Pantalone D., Bergamini C., Martellucci J., Alemanno G., Bruscino A., Maltinti G., Sheiterle M., Viligiardi R., Panconesi R., Guagni T. and Prosperi P., *The Role of DAMPS in Burns and Hemorrhagic Shock Immune Response: Pathophysiology and Clinical Issues. Review.* Int J Mol Sci, 2021. **22**(13).
76. Fitzwater J., Purdue G. F., Hunt J. L. and O'keefe G. E., *The risk factors and time course of sepsis and organ dysfunction after burn trauma.* J Trauma, 2003. **54**(5): p. 959-66.
77. Caraballo C. and Jaimes F., *Organ Dysfunction in Sepsis: An Ominous Trajectory From Infection To Death.* Yale J Biol Med, 2019. **92**(4): p. 629-640.
78. Greenhalgh D. G., Saffle J. R., Holmes J. H. Th, Gamelli R. L., Palmieri T. L., Horton J. W., Tompkins R. G., Traber D. L., Mozingo D. W., Deitch E. A., Goodwin C. W., Herndon D. N., Gallagher J. J., Sanford A. P., Jeng J. C., Ahrenholz D. H., Neely A. N., O'mara M. S., Wolf S. E., Purdue G. F., Garner W. L., Yowler C. J., Latenser B. A., American Burn Association Consensus Conference on Burn Sepsis and Infection Group, *American Burn Association consensus conference to define sepsis and infection in burns.* J Burn Care Res, 2007. **28**(6): p. 776-90.
79. Singer M., Deutschman C. S., Seymour C. W., Shankar-Hari M., Annane D., Bauer M., Bellomo R., Bernard G. R., Chiche J. D., Coopersmith C. M., Hotchkiss R. S., Levy M. M., Marshall J. C., Martin G. S., Opal S. M., Rubenfeld G. D., Van Der Poll T., Vincent J. L. and Angus D. C., *The Third International Consensus Definitions for Sepsis and Septic Shock (Sepsis-3).* JAMA, 2016. **315**(8): p. 801-10.
80. Angus D. C., Linde-Zwirble W. T., Lidicker J., Clermont G., Carcillo J. and Pinsky M. R., *Epidemiology of severe sepsis in the United States: analysis of incidence, outcome, and associated costs of care.* Crit Care Med, 2001. **29**(7): p. 1303-10.
81. Mayr F. B., Yende S., Linde-Zwirble W. T., Peck-Palmer O. M., Barnato A. E., Weissfeld L. A. and Angus D. C., *Infection rate and acute organ dysfunction risk as explanations for racial differences in severe sepsis.* JAMA, 2010. **303**(24): p. 2495-503.
82. Weiss S. L., Fitzgerald J. C., Pappachan J., Wheeler D., Jaramillo-Bustamante J. C., Salloo A., Singhi S. C., Erickson S., Roy J. A., Bush J. L., Nadkarni V. M., Thomas N. J., Sepsis Prevalence Outcomes, Therapies Study Investigators, Pediatric Acute Lung Injury and Sepsis Investigators Network, *Global epidemiology of pediatric severe sepsis: the sepsis prevalence, outcomes, and therapies study.* Am J Respir Crit Care Med, 2015. **191**(10): p. 1147-57.
83. Shen X. F., Cao K., Jiang J. P., Guan W. X. and Du J. F., *Neutrophil dysregulation during sepsis: an overview and update.* J Cell Mol Med, 2017. **21**(9): p. 1687-1697.
84. Belba M. K., Petrela E. Y. and Belba A. G., *Epidemiology and outcome analysis of sepsis and organ dysfunction/failure after burns.* Burns, 2017. **43**(6): p. 1335-1347.
85. Chung S., Choi D., Cho J., Huh Y., Moon J., Kwon J., Jung K., Lee J. J. and Kang B. H., *Timing and Associated Factors for Sepsis-3 in Severe Trauma Patients: A 3-Year Single Trauma Center Experience.* Acute Crit Care, 2018. **33**(3): p. 130-134.
86. Osborn T. M., Tracy J. K., Dunne J. R., Pasquale M. and Napolitano L. M., *Epidemiology of sepsis in patients with traumatic injury.* Crit Care Med, 2004. **32**(11): p. 2234-40.
87. Linde-Zwirble W. T. and Angus D. C., *Severe sepsis epidemiology: sampling, selection, and society.* Crit Care, 2004. **8**(4): p. 222-6.
88. Remick D. G., *Pathophysiology of sepsis.* Am J Pathol, 2007. **170**(5): p. 1435-44.
89. Waage A., Halstensen A. and Espevik T., *Association between tumour necrosis factor in serum and fatal outcome in patients with meningococcal disease.* Lancet, 1987. **1**(8529): p. 355-7.
90. Duan X., Yarmush D., Leeder A., Yarmush M. L. and Mitchell R. N., *Burn-induced immunosuppression: attenuated T cell signaling independent of IFN-gamma- and nitric oxide-mediated pathways.* J Leukoc Biol, 2008. **83**(2): p. 305-13.
91. Patenaude J., D'elia M., Hamelin C., Garrel D. and Bernier J., *Burn injury induces a change in T cell homeostasis affecting preferentially CD4+ T cells.* J Leukoc Biol, 2005. **77**(2): p. 141-50.

92. Boomer J. S., Green J. M. and Hotchkiss R. S., *The changing immune system in sepsis: is individualized immuno-modulatory therapy the answer?* Virulence, 2014. **5**(1): p. 45-56.
93. Madoiwa S., *Recent advances in disseminated intravascular coagulation: endothelial cells and fibrinolysis in sepsis-induced DIC.* J Intensive Care, 2015. **3**: p. 8.
94. Chang J. C., *Sepsis and septic shock: endothelial molecular pathogenesis associated with vascular microthrombotic disease.* Thromb J, 2019. **17**: p. 10.
95. Levi M., De Jonge E., Van Der Poll T. and Ten Cate H., *Disseminated intravascular coagulation.* Thromb Haemost, 1999. **82**(2): p. 695-705.
96. Williams B., Zou L., Pittet J. F. and Chao W., *Sepsis-Induced Coagulopathy: A Comprehensive Narrative Review of Pathophysiology, Clinical Presentation, Diagnosis, and Management Strategies.* Anesth Analg, 2024. **138**(4): p. 696-711.
97. Iba T., Levy J. H., Raj A. and Warkentin T. E., *Advance in the Management of Sepsis-Induced Coagulopathy and Disseminated Intravascular Coagulation.* J Clin Med, 2019. **8**(5).
98. Levi M., *Disseminated intravascular coagulation.* Crit Care Med, 2007. **35**(9): p. 2191-5.
99. Wilhelm G., Mertowska P., Mertowski S., Przysucha A., Struzyna J., Grywalska E. and Torres K., *The Crossroads of the Coagulation System and the Immune System: Interactions and Connections.* Int J Mol Sci, 2023. **24**(16).
100. Ball R. L., Keyloun J. W., Brummel-Ziedins K., Orfeo T., Palmieri T. L., Johnson L. S., Moffatt L. T., Pusateri A. E. and Shupp J. W., *Burn-Induced Coagulopathies: a Comprehensive Review.* Shock, 2020. **54**(2): p. 154-167.
101. Song J. C., Yang L. K., Zhao W., Zhu F., Wang G., Chen Y. P., Li W. Q., Chinese People's Liberation Army Professional Committee of Critical Care Medicine, Chinese Society of Thrombosis Hemostasis and Critical Care Chinese Medicine Education Association, *Chinese expert consensus on diagnosis and treatment of trauma-induced hypercoagulopathy.* Mil Med Res, 2021. **8**(1): p. 25.
102. Lavrentieva A., Kontakiotis T., Bitzani M., Papaioannou-Gaki G., Parlapani A., Thomareis O., Tsotsolis N. and Giala M. A., *Early coagulation disorders after severe burn injury: impact on mortality.* Intensive Care Med, 2008. **34**(4): p. 700-6.
103. Levi M., Van Der Poll T., Ten Cate H. and Van Deventer S. J., *The cytokine-mediated imbalance between coagulant and anticoagulant mechanisms in sepsis and endotoxaemia.* Eur J Clin Invest, 1997. **27**(1): p. 3-9.
104. Wada H., Matsumoto T. and Yamashita Y., *Diagnosis and treatment of disseminated intravascular coagulation (DIC) according to four DIC guidelines.* J Intensive Care, 2014. **2**(1): p. 15.
105. Lehman C. M., Wilson L. W. and Rodgers G. M., *Analytic validation and clinical evaluation of the STA LIATEST immunoturbidimetric D-dimer assay for the diagnosis of disseminated intravascular coagulation.* Am J Clin Pathol, 2004. **122**(2): p. 178-84.
106. White N. J., Ward K. R., Pati S., Strandenes G. and Cap A. P., *Hemorrhagic blood failure: Oxygen debt, coagulopathy, and endothelial damage.* J Trauma Acute Care Surg, 2017. **82**(6S Suppl 1): p. S41-S49.
107. Olgasi C., Assanelli S., Cucci A. and Follenzi A., *Hemostasis and endothelial functionality: the double face of coagulation factors.* Haematologica, 2024. **109**(7): p. 2041-2048.
108. Palta S., Saroa R. and Palta A., *Overview of the coagulation system.* Indian J Anaesth, 2014. **58**(5): p. 515-23.
109. Al-Koussa H., Alzaim I. and El-Sabban M. E., *Pathophysiology of Coagulation and Emerging Roles for Extracellular Vesicles in Coagulation Cascades and Disorders.* J Clin Med, 2022. **11**(16).
110. Beura S. K., Panigrahi A. R., Yadav P., Agrawal S. and Singh S. K., *Role of Neurons and Glia Cells in Wound Healing as a Novel Perspective Considering Platelet as a Conventional Player.* Mol Neurobiol, 2022. **59**(1): p. 137-160.

111. Liu Y., Zhang Y., Yao W., Chen P., Cao Y., Shan M., Yu S., Zhang L., Bao B. and Cheng F. F., *Recent Advances in Topical Hemostatic Materials.* ACS Appl Bio Mater, 2024. **7**(3): p. 1362-1380.
112. Summer M., Ali S., Fiaz U., Hussain T., Khan R. R. M. and Fiaz H., *Revealing the molecular mechanisms in wound healing and the effects of different physiological factors including diabetes, age, and stress.* J Mol Histol, 2024. **55**(5): p. 637-654.
113. Maegele M., *The coagulopathy of trauma.* Eur J Trauma Emerg Surg, 2014. **40**(2): p. 113-26.
114. Brohi K., Cohen M. J., Ganter M. T., Schultz M. J., Levi M., Mackersie R. C. and Pittet J. F., *Acute coagulopathy of trauma: hypoperfusion induces systemic anticoagulation and hyperfibrinolysis.* J Trauma, 2008. **64**(5): p. 1211-7; discussion 1217.
115. Bhattarai A., Shah S., Bagherieh S., Mirmosayyeb O., Thapa S., Paudel S., Gyawali P. and Khanal P., *Endothelium, Platelets, and Coagulation Factors as the Three Vital Components for Diagnosing Bleeding Disorders: A Simplified Perspective with Clinical Relevance.* Int J Clin Pract, 2022. **2022**: p. 5369001.
116. Chapin J. C. and Hajjar K. A., *Fibrinolysis and the control of blood coagulation.* Blood Rev, 2015. **29**(1): p. 17-24.
117. Colling M. E., Tourdot B. E. and Kanthi Y., *Inflammation, Infection and Venous Thromboembolism.* Circ Res, 2021. **128**(12): p. 2017-2036.
118. Khalaf F., Touma D., Pappas A., Hatim L., Wojtowicz-Piotrowski S. and Jeschke M. G., *Decoding burn trauma: biomarkers for early diagnosis of burn-induced pathologies.* Biomark Res, 2024. **12**(1): p. 160.
119. Zanza C., Romenskaya T., Racca F., Rocca E., Piccolella F., Piccioni A., Saviano A., Formenti-Ujlaki G., Savioli G., Franceschi F. and Longhitano Y., *Severe Trauma-Induced Coagulopathy: Molecular Mechanisms Underlying Critical Illness.* Int J Mol Sci, 2023. **24**(8).
120. Pusateri A. E., Le T. D., Keyloun J. W., Moffatt L. T., Orfeo T., Brummel-Ziedins K. E., Mclawhorn M. M., Callcut R. A., Shupp J. W. and Group Syscot Study, *Early abnormal fibrinolysis and mortality in patients with thermal injury: a prospective cohort study.* BJS Open, 2021. **5**(2).
121. Duque P., Calvo A., Lockie C. and Schochl H., *Pathophysiology of Trauma-Induced Coagulopathy.* Transfus Med Rev, 2021. **35**(4): p. 80-86.
122. Chang R., Cardenas J. C., Wade C. E. and Holcomb J. B., *Advances in the understanding of trauma-induced coagulopathy.* Blood, 2016. **128**(8): p. 1043-9.
123. Dutton R. P., Stansbury L. G., Leone S., Kramer E., Hess J. R. and Scalea T. M., *Trauma mortality in mature trauma systems: are we doing better? An analysis of trauma mortality patterns, 1997-2008.* J Trauma, 2010. **69**(3): p. 620-6.
124. Kallinen O., Maisniemi K., Bohling T., Tukiainen E. and Koljonen V., *Multiple organ failure as a cause of death in patients with severe burns.* J Burn Care Res, 2012. **33**(2): p. 206-11.
125. Sheridan R. L., Ryan C. M., Yin L. M., Hurley J. and Tompkins R. G., *Death in the burn unit: sterile multiple organ failure.* Burns, 1998. **24**(4): p. 307-11.
126. Ogura A., Tsurumi A., Que Y. A., Almpani M., Zheng H., Tompkins R. G., Ryan C. M. and Rahme L. G., *Associations between clinical characteristics and the development of multiple organ failure after severe burns in adult patients.* Burns, 2019. **45**(8): p. 1775-1782.
127. Cumming J., Purdue G. F., Hunt J. L. and O'keefe G. E., *Objective estimates of the incidence and consequences of multiple organ dysfunction and sepsis after burn trauma.* J Trauma, 2001. **50**(3): p. 510-5.
128. Semeraro N., Ammollo C. T., Semeraro F. and Colucci M., *Sepsis, thrombosis and organ dysfunction.* Thromb Res, 2012. **129**(3): p. 290-5.
129. Semeraro N., Ammollo C. T., Semeraro F. and Colucci M., *Sepsis-associated disseminated intravascular coagulation and thromboembolic disease.* Mediterr J Hematol Infect Dis, 2010. **2**(3): p. e2010024.

130. Cho S. Y. and Choi J. H., *Biomarkers of sepsis.* Infect Chemother, 2014. **46**(1): p. 1-12.
131. Fan S. L., Miller N. S., Lee J. and Remick D. G., *Diagnosing sepsis - The role of laboratory medicine.* Clin Chim Acta, 2016. **460**: p. 203-10.
132. Kumar A., Roberts D., Wood K. E., Light B., Parrillo J. E., Sharma S., Suppes R., Feinstein D., Zanotti S., Taiberg L., Gurka D., Kumar A. and Cheang M., *Duration of hypotension before initiation of effective antimicrobial therapy is the critical determinant of survival in human septic shock.* Crit Care Med, 2006. **34**(6): p. 1589-96.
133. Bloos F. and Reinhart K., *Rapid diagnosis of sepsis.* Virulence, 2014. **5**(1): p. 154-60.
134. Pradipta I. S., Sodik D. C., Lestari K., Parwati I., Halimah E., Diantini A. and Abdulah R., *Antibiotic resistance in sepsis patients: evaluation and recommendation of antibiotic use.* N Am J Med Sci, 2013. **5**(6): p. 344-52.
135. Kumar A., Ellis P., Arabi Y., Roberts D., Light B., Parrillo J. E., Dodek P., Wood G., Kumar A., Simon D., Peters C., Ahsan M., Chateau D. and Cooperative Antimicrobial Therapy of Septic Shock Database Research Group, *Initiation of inappropriate antimicrobial therapy results in a fivefold reduction of survival in human septic shock.* Chest, 2009. **136**(5): p. 1237-1248.
136. Orsini J., Mainardi C., Muzylo E., Karki N., Cohen N. and Sakoulas G., *Microbiological profile of organisms causing bloodstream infection in critically ill patients.* J Clin Med Res, 2012. **4**(6): p. 371-7.
137. Turnidge J., *Impact of antibiotic resistance on the treatment of sepsis.* Scand J Infect Dis, 2003. **35**(9): p. 677-82.
138. Sinha M., Jupe J., Mack H., Coleman T. P., Lawrence S. M. and Fraley S. I., *Emerging Technologies for Molecular Diagnosis of Sepsis.* Clin Microbiol Rev, 2018. **31**(2).
139. Chaudhry H., Zhou J., Zhong Y., Ali M. M., Mcguire F., Nagarkatti P. S. and Nagarkatti M., *Role of cytokines as a double-edged sword in sepsis.* In Vivo, 2013. **27**(6): p. 669-84.
140. Tamayo E., Fernandez A., Almansa R., Carrasco E., Heredia M., Lajo C., Goncalves L., Gomez-Herreras J. I., De Lejarazu R. O. and Bermejo-Martin J. F., *Pro- and anti-inflammatory responses are regulated simultaneously from the first moments of septic shock.* Eur Cytokine Netw, 2011. **22**(2): p. 82-7.
141. Kabir K., Keller H., Grass G., Minor T., Stueber F., Schroeder S., Putensen C., Paul C., Burger C., Rangger C., Neville L. F. and Mathiak G., *Cytokines and chemokines in serum and urine as early predictors to identify septic patients on intensive care unit.* Int J Mol Med, 2003. **12**(4): p. 565-70.
142. Castellheim A., Brekke O. L., Espevik T., Harboe M. and Mollnes T. E., *Innate immune responses to danger signals in systemic inflammatory response syndrome and sepsis.* Scand J Immunol, 2009. **69**(6): p. 479-91.
143. Prashant A., Vishwanath P., Kulkarni P., Sathya Narayana P., Gowdara V., Nataraj S. M. and Nagaraj R., *Comparative assessment of cytokines and other inflammatory markers for the early diagnosis of neonatal sepsis-a case control study.* PLoS One, 2013. **8**(7): p. e68426.
144. Alsabani M., Abrams S. T., Cheng Z., Morton B., Lane S., Alosaimi S., Yu W., Wang G. and Toh C. H., *Reduction of NETosis by targeting CXCR1/2 reduces thrombosis, lung injury, and mortality in experimental human and murine sepsis.* Br J Anaesth, 2022. **128**(2): p. 283-293.
145. Wang X. and Quinn P. J., *Lipopolysaccharide: Biosynthetic pathway and structure modification.* Prog Lipid Res, 2010. **49**(2): p. 97-107.
146. Gaini S., Koldkjaer O. G., Pedersen C. and Pedersen S. S., *Procalcitonin, lipopolysaccharide-binding protein, interleukin-6 and C-reactive protein in community-acquired infections and sepsis: a prospective study.* Crit Care, 2006. **10**(2): p. R53.
147. Sakr Y., Burgett U., Nacul F. E., Reinhart K. and Brunkhorst F., *Lipopolysaccharide binding protein in a surgical intensive care unit: a marker of sepsis?* Crit Care Med, 2008. **36**(7): p. 2014-22.

148. Povoa P., Almeida E., Moreira P., Fernandes A., Mealha R., Aragao A. and Sabino H., *C-reactive protein as an indicator of sepsis.* Intensive Care Med, 1998. **24**(10): p. 1052-6.
149. Wang H. E., Shapiro N. I., Safford M. M., Griffin R., Judd S., Rodgers J. B., Warnock D. G., Cushman M. and Howard G., *High-sensitivity C-reactive protein and risk of sepsis.* PLoS One, 2013. **8**(7): p. e69232.
150. Coelho L., Povoa P., Almeida E., Fernandes A., Mealha R., Moreira P. and Sabino H., *Usefulness of C-reactive protein in monitoring the severe community-acquired pneumonia clinical course.* Crit Care, 2007. **11**(4): p. R92.
151. Povoa P., Coelho L., Almeida E., Fernandes A., Mealha R., Moreira P. and Sabino H., *C-reactive protein as a marker of ventilator-associated pneumonia resolution: a pilot study.* Eur Respir J, 2005. **25**(5): p. 804-12.
152. Povoa P., Teixeira-Pinto A. M., Carneiro A. H. and Portuguese Community-Acquired Sepsis Study Group Saciuci, *C-reactive protein, an early marker of community-acquired sepsis resolution: a multi-center prospective observational study.* Crit Care, 2011. **15**(4): p. R169.
153. Tschaikowsky K., Hedwig-Geissing M., Braun G. G. and Radespiel-Troeger M., *Predictive value of procalcitonin, interleukin-6, and C-reactive protein for survival in postoperative patients with severe sepsis.* J Crit Care, 2011. **26**(1): p. 54-64.
154. Tschaikowsky K., Hedwig-Geissing M., Schiele A., Bremer F., Schywalsky M. and Schuttler J., *Coincidence of pro- and anti-inflammatory responses in the early phase of severe sepsis: Longitudinal study of mononuclear histocompatibility leukocyte antigen-DR expression, procalcitonin, C-reactive protein, and changes in T-cell subsets in septic and postoperative patients.* Crit Care Med, 2002. **30**(5): p. 1015-23.
155. Li A. T., Moussa A., Gus E., Paul E., Yii E., Romero L., Lin Z. C., Padiglione A., Lo C. H., Cleland H. and Cheng A. C., *Biomarkers for the Early Diagnosis of Sepsis in Burns: Systematic Review and Meta-analysis.* Ann Surg, 2022. **275**(4): p. 654-662.
156. Schuetz P., Birkhahn R., Sherwin R., Jones A. E., Singer A., Kline J. A., Runyon M. S., Self W. H., Courtney D. M., Nowak R. M., Gaieski D. F., Ebmeyer S., Johannes S., Wiemer J. C., Schwabe A. and Shapiro N. I., *Serial Procalcitonin Predicts Mortality in Severe Sepsis Patients: Results From the Multicenter Procalcitonin MOnitoring SEpsis (MOSES) Study.* Crit Care Med, 2017. **45**(5): p. 781-789.
157. Wacker C., Prkno A., Brunkhorst F. M. and Schlattmann P., *Procalcitonin as a diagnostic marker for sepsis: a systematic review and meta-analysis.* Lancet Infect Dis, 2013. **13**(5): p. 426-35.
158. Luzzani A., Polati E., Dorizzi R., Rungatscher A., Pavan R. and Merlini A., *Comparison of procalcitonin and C-reactive protein as markers of sepsis.* Crit Care Med, 2003. **31**(6): p. 1737-41.
159. Schuetz P., Muller B., Christ-Crain M., Stolz D., Tamm M., Bouadma L., Luyt C. E., Wolff M., Chastre J., Tubach F., Kristoffersen K. B., Burkhardt O., Welte T., Schroeder S., Nobre V., Wei L., Bhatnagar N., Bucher H. C. and Briel M., *Procalcitonin to initiate or discontinue antibiotics in acute respiratory tract infections.* Cochrane Database Syst Rev, 2012. **2012**(9): p. CD007498.
160. Nguyen H. B., Rivers E. P., Knoblich B. P., Jacobsen G., Muzzin A., Ressler J. A. and Tomlanovich M. C., *Early lactate clearance is associated with improved outcome in severe sepsis and septic shock.* Crit Care Med, 2004. **32**(8): p. 1637-42.
161. Mikkelsen M. E., Miltiades A. N., Gaieski D. F., Goyal M., Fuchs B. D., Shah C. V., Bellamy S. L. and Christie J. D., *Serum lactate is associated with mortality in severe sepsis independent of organ failure and shock.* Crit Care Med, 2009. **37**(5): p. 1670-7.
162. Garcia-Alvarez M., Marik P. and Bellomo R., *Sepsis-associated hyperlactatemia.* Crit Care, 2014. **18**(5): p. 503.

163. Christ-Crain M. and Muller B., *Biomarkers in respiratory tract infections: diagnostic guides to antibiotic prescription, prognostic markers and mediators.* Eur Respir J, 2007. **30**(3): p. 556-73.
164. Christ-Crain M., Morgenthaler N. G., Struck J., Harbarth S., Bergmann A. and Muller B., *Mid-regional pro-adrenomedullin as a prognostic marker in sepsis: an observational study.* Crit Care, 2005. **9**(6): p. R816-24.
165. Struck J., Tao C., Morgenthaler N. G. and Bergmann A., *Identification of an Adrenomedullin precursor fragment in plasma of sepsis patients.* Peptides, 2004. **25**(8): p. 1369-72.
166. Leinonen E., Wathen K. A., Alfthan H., Ylikorkala O., Andersson S., Stenman U. H. and Vuorela P., *Maternal serum angiopoietin-1 and -2 and tie-2 in early pregnancy ending in preeclampsia or intrauterine growth retardation.* J Clin Endocrinol Metab, 2010. **95**(1): p. 126-33.
167. Ricciuto D. R., Dos Santos C. C., Hawkes M., Toltl L. J., Conroy A. L., Rajwans N., Lafferty E. I., Cook D. J., Fox-Robichaud A., Kahnamoui K., Kain K. C., Liaw P. C. and Liles W. C., *Angiopoietin-1 and angiopoietin-2 as clinically informative prognostic biomarkers of morbidity and mortality in severe sepsis.* Crit Care Med, 2011. **39**(4): p. 702-10.
168. Yang H., Wang H., Chavan S. S. and Andersson U., *High Mobility Group Box Protein 1 (HMGB1): The Prototypical Endogenous Danger Molecule.* Mol Med, 2015. **21 Suppl 1**: p. S6-S12.
169. Andersson U. and Tracey K. J., *HMGB1 in sepsis.* Scand J Infect Dis, 2003. **35**(9): p. 577-84.
170. Wang H., Bloom O., Zhang M., Vishnubhakat J. M., Ombrellino M., Che J., Frazier A., Yang H., Ivanova S., Borovikova L., Manogue K. R., Faist E., Abraham E., Andersson J., Andersson U., Molina P. E., Abumrad N. N., Sama A. and Tracey K. J., *HMG-1 as a late mediator of endotoxin lethality in mice.* Science, 1999. **285**(5425): p. 248-51.
171. Huang W., Tang Y. and Li L., *HMGB1, a potent proinflammatory cytokine in sepsis.* Cytokine, 2010. **51**(2): p. 119-26.
172. Sunden-Cullberg J., Norrby-Teglund A., Rouhiainen A., Rauvala H., Herman G., Tracey K. J., Lee M. L., Andersson J., Tokics L. and Treutiger C. J., *Persistent elevation of high mobility group box-1 protein (HMGB1) in patients with severe sepsis and septic shock.* Crit Care Med, 2005. **33**(3): p. 564-73.
173. Karlsson S., Pettila V., Tenhunen J., Laru-Sompa R., Hynninen M. and Ruokonen E., *HMGB1 as a predictor of organ dysfunction and outcome in patients with severe sepsis.* Intensive Care Med, 2008. **34**(6): p. 1046-53.
174. Mitchell R. A., Liao H., Chesney J., Fingerle-Rowson G., Baugh J., David J. and Bucala R., *Macrophage migration inhibitory factor (MIF) sustains macrophage proinflammatory function by inhibiting p53: regulatory role in the innate immune response.* Proc Natl Acad Sci U S A, 2002. **99**(1): p. 345-50.
175. Bozza F. A., Gomes R. N., Japiassu A. M., Soares M., Castro-Faria-Neto H. C., Bozza P. T. and Bozza M. T., *Macrophage migration inhibitory factor levels correlate with fatal outcome in sepsis.* Shock, 2004. **22**(4): p. 309-13.
176. Zipfel P. F., *Complement and immune defense: from innate immunity to human diseases.* Immunol Lett, 2009. **126**(1-2): p. 1-7.
177. Markiewski M. M., Deangelis R. A. and Lambris J. D., *Complexity of complement activation in sepsis.* J Cell Mol Med, 2008. **12**(6A): p. 2245-54.
178. Singer M. and Jones A. M., *Bench-to-bedside review: the role of C1-esterase inhibitor in sepsis and other critical illnesses.* Crit Care, 2011. **15**(1): p. 203.
179. Ward P. A., *Role of the complement in experimental sepsis.* J Leukoc Biol, 2008. **83**(3): p. 467-70.
180. Faix J. D., *Biomarkers of sepsis.* Crit Rev Clin Lab Sci, 2013. **50**(1): p. 23-36.

181. Flierl M. A., Rittirsch D., Nadeau B. A., Day D. E., Zetoune F. S., Sarma J. V., Huber-Lang M. S. and Ward P. A., *Functions of the complement components C3 and C5 during sepsis.* FASEB J, 2008. **22**(10): p. 3483-90.
182. Oh H., Park H. E., Song M. S., Kim H. and Baek J. H., *The Therapeutic Potential of Anticoagulation in Organ Fibrosis.* Front Med (Lausanne), 2022. **9**: p. 866746.
183. Kovtun A., Messerer D. A. C., Scharffetter-Kochanek K., Huber-Lang M. and Ignatius A., *Neutrophils in Tissue Trauma of the Skin, Bone, and Lung: Two Sides of the Same Coin.* J Immunol Res, 2018. **2018**: p. 8173983.
184. Sierawska O., Malkowska P., Taskin C., Hrynkiewicz R., Mertowska P., Grywalska E., Korzeniowski T., Torres K., Surowiecka A., Niedzwiedzka-Rystwej P. and Struzyna J., *Innate Immune System Response to Burn Damage-Focus on Cytokine Alteration.* Int J Mol Sci, 2022. **23**(2).
185. Zhu C. L., Wang Y., Liu Q., Li H. R., Yu C. M., Li P., Deng X. M. and Wang J. F., *Dysregulation of neutrophil death in sepsis.* Front Immunol, 2022. **13**: p. 963955.
186. Galli S. J., Borregaard N. and Wynn T. A., *Phenotypic and functional plasticity of cells of innate immunity: macrophages, mast cells and neutrophils.* Nat Immunol, 2011. **12**(11): p. 1035-44.
187. Grieshaber-Bouyer R. and Nigrovic P. A., *Neutrophil Heterogeneity as Therapeutic Opportunity in Immune-Mediated Disease.* Front Immunol, 2019. **10**: p. 346.
188. Sonego F., Castanheira F. V., Ferreira R. G., Kanashiro A., Leite C. A., Nascimento D. C., Colon D. F., Borges Vde F., Alves-Filho J. C. and Cunha F. Q., *Paradoxical Roles of the Neutrophil in Sepsis: Protective and Deleterious.* Front Immunol, 2016. **7**: p. 155.
189. Kolaczkowska E. and Kubes P., *Neutrophil recruitment and function in health and inflammation.* Nat Rev Immunol, 2013. **13**(3): p. 159-75.
190. Lee W. L., Harrison R. E. and Grinstein S., *Phagocytosis by neutrophils.* Microbes Infect, 2003. **5**(14): p. 1299-306.
191. Lacy P., *Mechanisms of degranulation in neutrophils.* Allergy Asthma Clin Immunol, 2006. **2**(3): p. 98-108.
192. Camicia G., Pozner R. and De Larranaga G., *Neutrophil extracellular traps in sepsis.* Shock, 2014. **42**(4): p. 286-94.
193. Li Jeon N., Baskaran H., Dertinger S. K., Whitesides G. M., Van De Water L. and Toner M., *Neutrophil chemotaxis in linear and complex gradients of interleukin-8 formed in a microfabricated device.* Nat Biotechnol, 2002. **20**(8): p. 826-30.
194. Lerman Y. V. and Kim M., *Neutrophil migration under normal and sepsis conditions.* Cardiovasc Hematol Disord Drug Targets, 2015. **15**(1): p. 19-28.
195. Asimakopoulos G. and Taylor K. M., *Effects of cardiopulmonary bypass on leukocyte and endothelial adhesion molecules.* Ann Thorac Surg, 1998. **66**(6): p. 2135-44.
196. Alves-Filho J. C., De Freitas A., Spiller F., Souto F. O. and Cunha F. Q., *The role of neutrophils in severe sepsis.* Shock, 2008. **30 Suppl 1**: p. 3-9.
197. Kovach M. A. and Standiford T. J., *The function of neutrophils in sepsis.* Curr Opin Infect Dis, 2012. **25**(3): p. 321-7.
198. Johnston B. and Butcher E. C., *Chemokines in rapid leukocyte adhesion triggering and migration.* Semin Immunol, 2002. **14**(2): p. 83-92.
199. Amulic B., Cazalet C., Hayes G. L., Metzler K. D. and Zychlinsky A., *Neutrophil function: from mechanisms to disease.* Annu Rev Immunol, 2012. **30**: p. 459-89.
200. Sun H., Hu L. and Fan Z., *beta2 integrin activation and signal transduction in leukocyte recruitment.* Am J Physiol Cell Physiol, 2021. **321**(2): p. C308-C316.
201. Hazeldine J., Hampson P. and Lord J. M., *The impact of trauma on neutrophil function.* Injury, 2014. **45**(12): p. 1824-33.

202. Reutershan J., Morris M. A., Burcin T. L., Smith D. F., Chang D., Saprito M. S. and Ley K., *Critical role of endothelial CXCR2 in LPS-induced neutrophil migration into the lung.* J Clin Invest, 2006. **116**(3): p. 695-702.
203. Zhang F., Liu A. L., Gao S., Ma S. and Guo S. B., *Neutrophil Dysfunction in Sepsis.* Chin Med J (Engl), 2016. **129**(22): p. 2741-2744.
204. Leliefeld P. H., Wessels C. M., Leenen L. P., Koenderman L. and Pillay J., *The role of neutrophils in immune dysfunction during severe inflammation.* Crit Care, 2016. **20**: p. 73.
205. Caster D. J., Powell D. W., Miralda I., Ward R. A. and Mcleish K. R., *Re-Examining Neutrophil Participation in GN.* J Am Soc Nephrol, 2017. **28**(8): p. 2275-2289.
206. Verdrengh M. and Tarkowski A., *Role of neutrophils in experimental septicemia and septic arthritis induced by Staphylococcus aureus.* Infect Immun, 1997. **65**(7): p. 2517-21.
207. Segal A. W., Dorling J. and Coade S., *Kinetics of fusion of the cytoplasmic granules with phagocytic vacuoles in human polymorphonuclear leukocytes. Biochemical and morphological studies.* J Cell Biol, 1980. **85**(1): p. 42-59.
208. Marshall J. C., *Neutrophils in the pathogenesis of sepsis.* Crit Care Med, 2005. **33**(12 Suppl): p. S502-5.
209. Harter L., Mica L., Stocker R., Trentz O. and Keel M., *Increased expression of toll-like receptor-2 and -4 on leukocytes from patients with sepsis.* Shock, 2004. **22**(5): p. 403-9.
210. Lim J. J., Grinstein S. and Roth Z., *Diversity and Versatility of Phagocytosis: Roles in Innate Immunity, Tissue Remodeling, and Homeostasis.* Front Cell Infect Microbiol, 2017. **7**: p. 191.
211. Foote J. R., Levine A. P., Behe P., Duchen M. R. and Segal A. W., *Imaging the Neutrophil Phagosome and Cytoplasm Using a Ratiometric pH Indicator.* J Vis Exp, 2017(122).
212. Levine A. P., Duchen M. R., De Villiers S., Rich P. R. and Segal A. W., *Alkalinity of neutrophil phagocytic vacuoles is modulated by HVCN1 and has consequences for myeloperoxidase activity.* PLoS One, 2015. **10**(4): p. e0125906.
213. Nusse O. and Lindau M., *The dynamics of exocytosis in human neutrophils.* J Cell Biol, 1988. **107**(6 Pt 1): p. 2117-23.
214. Lacy P. and Eitzen G., *Control of granule exocytosis in neutrophils.* Front Biosci, 2008. **13**: p. 5559-70.
215. Akgul C., Moulding D. A. and Edwards S. W., *Molecular control of neutrophil apoptosis.* FEBS Lett, 2001. **487**(3): p. 318-22.
216. Elbim C., Katsikis P. D. and Estaquier J., *Neutrophil apoptosis during viral infections.* Open Virol J, 2009. **3**: p. 52-9.
217. Weinmann P., Scharffetter-Kochanek K., Forlow S. B., Peters T. and Walzog B., *A role for apoptosis in the control of neutrophil homeostasis in the circulation: insights from CD18-deficient mice.* Blood, 2003. **101**(2): p. 739-46.
218. Kennedy A. D. and Deleo F. R., *Neutrophil apoptosis and the resolution of infection.* Immunol Res, 2009. **43**(1-3): p. 25-61.
219. Maianski N. A., Geissler J., Srinivasula S. M., Alnemri E. S., Roos D. and Kuijpers T. W., *Functional characterization of mitochondria in neutrophils: a role restricted to apoptosis.* Cell Death Differ, 2004. **11**(2): p. 143-53.
220. Fox S., Leitch A. E., Duffin R., Haslett C. and Rossi A. G., *Neutrophil apoptosis: relevance to the innate immune response and inflammatory disease.* J Innate Immun, 2010. **2**(3): p. 216-27.
221. Catarzi S., Marcucci T., Papucci L., Favilli F., Donnini M., Tonelli F., Vincenzini M. T. and Iantomasi T., *Apoptosis and Bax, Bcl-2, Mcl-1 expression in neutrophils of Crohn's disease patients.* Inflamm Bowel Dis, 2008. **14**(6): p. 819-25.
222. Milot E. and Filep J. G., *Regulation of neutrophil survival/apoptosis by Mcl-1.* ScientificWorldJournal, 2011. **11**: p. 1948-62.

223. Edwards S. W., Derouet M., Howse M. and Moots R. J., *Regulation of neutrophil apoptosis by Mcl-1.* Biochem Soc Trans, 2004. **32**(Pt3): p. 489-92.
224. Beyrau M., Bodkin J. V. and Nourshargh S., *Neutrophil heterogeneity in health and disease: a revitalized avenue in inflammation and immunity.* Open Biol, 2012. **2**(11): p. 120134.
225. Denk S., Taylor R. P., Wiegner R., Cook E. M., Lindorfer M. A., Pfeiffer K., Paschke S., Eiseler T., Weiss M., Barth E., Lambris J. D., Kalbitz M., Martin T., Barth H., Messerer D. A. C., Gebhard F. and Huber-Lang M. S., *Complement C5a-Induced Changes in Neutrophil Morphology During Inflammation.* Scand J Immunol, 2017. **86**(3): p. 143-155.
226. Scapini P., Marini O., Tecchio C. and Cassatella M. A., *Human neutrophils in the saga of cellular heterogeneity: insights and open questions.* Immunol Rev, 2016. **273**(1): p. 48-60.
227. Bryk J. A., Popovic P. J., Zenati M. S., Munera V., Pribis J. P. and Ochoa J. B., *Nature of myeloid cells expressing arginase 1 in peripheral blood after trauma.* J Trauma, 2010. **68**(4): p. 843-52.
228. Shen X., Cao K., Zhao Y. and Du J., *Targeting Neutrophils in Sepsis: From Mechanism to Translation.* Front Pharmacol, 2021. **12**: p. 644270.
229. Zhang X., Zhang Y., Yuan S. and Zhang J., *The potential immunological mechanisms of sepsis.* Front Immunol, 2024. **15**: p. 1434688.
230. Mortaz E., Alipoor S. D., Adcock I. M., Mumby S. and Koenderman L., *Update on Neutrophil Function in Severe Inflammation.* Front Immunol, 2018. **9**: p. 2171.
231. Zhou Y. Y. and Sun B. W., *Recent advances in neutrophil chemotaxis abnormalities during sepsis.* Chin J Traumatol, 2022. **25**(6): p. 317-324.
232. Zhang P., Zou B., Liou Y. C. and Huang C., *The pathogenesis and diagnosis of sepsis post burn injury.* Burns Trauma, 2021. **9**: p. tkaa047.
233. Wang H., Kim S. J., Lei Y., Wang S., Wang H., Huang H., Zhang H. and Tsung A., *Neutrophil extracellular traps in homeostasis and disease.* Signal Transduct Target Ther, 2024. **9**(1): p. 235.
234. Mcdonald B., *Neutrophils in critical illness.* Cell Tissue Res, 2018. **371**(3): p. 607-615.
235. Heit B., Tavener S., Raharjo E. and Kubes P., *An intracellular signaling hierarchy determines direction of migration in opposing chemotactic gradients.* J Cell Biol, 2002. **159**(1): p. 91-102.
236. Phillipson M. and Kubes P., *The neutrophil in vascular inflammation.* Nat Med, 2011. **17**(11): p. 1381-90.
237. Chishti A. D., Shenton B. K., Kirby J. A. and Baudouin S. V., *Neutrophil chemotaxis and receptor expression in clinical septic shock.* Intensive Care Med, 2004. **30**(4): p. 605-11.
238. Tarlowe M. H., Duffy A., Kannan K. B., Itagaki K., Lavery R. F., Livingston D. H., Bankey P. and Hauser C. J., *Prospective study of neutrophil chemokine responses in trauma patients at risk for pneumonia.* Am J Respir Crit Care Med, 2005. **171**(7): p. 753-9.
239. Brown K. A., Brain S. D., Pearson J. D., Edgeworth J. D., Lewis S. M. and Treacher D. F., *Neutrophils in development of multiple organ failure in sepsis.* Lancet, 2006. **368**(9530): p. 157-69.
240. Patel J. M., Sapey E., Parekh D., Scott A., Dosanjh D., Gao F. and Thickett D. R., *Sepsis Induces a Dysregulated Neutrophil Phenotype That Is Associated with Increased Mortality.* Mediators Inflamm, 2018. **2018**: p. 4065362.
241. Lyn-Kew K. and Standiford T. J., *Immunosuppression in sepsis.* Curr Pharm Des, 2008. **14**(19): p. 1870-81.
242. Puri K. D., Doggett T. A., Douangpanya J., Hou Y., Tino W. T., Wilson T., Graf T., Clayton E., Turner M., Hayflick J. S. and Diacovo T. G., *Mechanisms and implications of phosphoinositide 3-kinase delta in promoting neutrophil trafficking into inflamed tissue.* Blood, 2004. **103**(9): p. 3448-56.

243. Guha M. and Mackman N., *The phosphatidylinositol 3-kinase-Akt pathway limits lipopolysaccharide activation of signaling pathways and expression of inflammatory mediators in human monocytic cells.* J Biol Chem, 2002. **277**(35): p. 32124-32.
244. Mittal M., Siddiqui M. R., Tran K., Reddy S. P. and Malik A. B., *Reactive oxygen species in inflammation and tissue injury.* Antioxid Redox Signal, 2014. **20**(7): p. 1126-67.
245. Simms H. H. and D'amico R., *Increased PMN CD11b/CD18 expression following post-traumatic ARDS.* J Surg Res, 1991. **50**(4): p. 362-7.
246. Chen G., Deng H., Song X., Lu M., Zhao L., Xia S., You G., Zhao J., Zhang Y., Dong A. and Zhou H., *Reactive oxygen species-responsive polymeric nanoparticles for alleviating sepsis-induced acute liver injury in mice.* Biomaterials, 2017. **144**: p. 30-41.
247. Ogawa K., Suzuki K., Okutsu M., Yamazaki K. and Shinkai S., *The association of elevated reactive oxygen species levels from neutrophils with low-grade inflammation in the elderly.* Immun Ageing, 2008. **5**: p. 13.
248. Ma A. C. and Kubes P., *Platelets, neutrophils, and neutrophil extracellular traps (NETs) in sepsis.* J Thromb Haemost, 2008. **6**(3): p. 415-20.
249. Brinkmann V., Reichard U., Goosmann C., Fauler B., Uhlemann Y., Weiss D. S., Weinrauch Y. and Zychlinsky A., *Neutrophil extracellular traps kill bacteria.* Science, 2004. **303**(5663): p. 1532-5.
250. Brinkmann V. and Zychlinsky A., *Neutrophil extracellular traps: is immunity the second function of chromatin?* J Cell Biol, 2012. **198**(5): p. 773-83.
251. Cooper P. R., Palmer L. J. and Chapple I. L., *Neutrophil extracellular traps as a new paradigm in innate immunity: friend or foe?* Periodontol 2000, 2013. **63**(1): p. 165-97.
252. Neeli I., Khan S. N. and Radic M., *Histone deimination as a response to inflammatory stimuli in neutrophils.* J Immunol, 2008. **180**(3): p. 1895-902.
253. Fuchs T. A., Abed U., Goosmann C., Hurwitz R., Schulze I., Wahn V., Weinrauch Y., Brinkmann V. and Zychlinsky A., *Novel cell death program leads to neutrophil extracellular traps.* J Cell Biol, 2007. **176**(2): p. 231-41.
254. Steinberg B. E. and Grinstein S., *Unconventional roles of the NADPH oxidase: signaling, ion homeostasis, and cell death.* Sci STKE, 2007. **2007**(379): p. pe11.
255. Papayannopoulos V., Metzler K. D., Hakkim A. and Zychlinsky A., *Neutrophil elastase and myeloperoxidase regulate the formation of neutrophil extracellular traps.* J Cell Biol, 2010. **191**(3): p. 677-91.
256. Yousefi S. and Simon H. U., *NETosis - Does It Really Represent Nature's "Suicide Bomber"?* Front Immunol, 2016. **7**: p. 328.
257. De Buhr N. and Von Kockritz-Blickwede M., *How Neutrophil Extracellular Traps Become Visible.* J Immunol Res, 2016. **2016**: p. 4604713.
258. Clark S. R., Ma A. C., Tavener S. A., Mcdonald B., Goodarzi Z., Kelly M. M., Patel K. D., Chakrabarti S., Mcavoy E., Sinclair G. D., Keys E. M., Allen-Vercoe E., Devinney R., Doig C. J., Green F. H. and Kubes P., *Platelet TLR4 activates neutrophil extracellular traps to ensnare bacteria in septic blood.* Nat Med, 2007. **13**(4): p. 463-9.
259. Masuda S., Nakazawa D., Shida H., Miyoshi A., Kusunoki Y., Tomaru U. and Ishizu A., *NETosis markers: Quest for specific, objective, and quantitative markers.* Clin Chim Acta, 2016. **459**: p. 89-93.
260. Keshari R. S., Jyoti A., Dubey M., Kothari N., Kohli M., Bogra J., Barthwal M. K. and Dikshit M., *Cytokines induced neutrophil extracellular traps formation: implication for the inflammatory disease condition.* PLoS One, 2012. **7**(10): p. e48111.
261. Yousefi S., Mihalache C., Kozlowski E., Schmid I. and Simon H. U., *Viable neutrophils release mitochondrial DNA to form neutrophil extracellular traps.* Cell Death Differ, 2009. **16**(11): p. 1438-44.

262. West A. P., Khoury-Hanold W., Staron M., Tal M. C., Pineda C. M., Lang S. M., Bestwick M., Duguay B. A., Raimundo N., Macduff D. A., Kaech S. M., Smiley J. R., Means R. E., Iwasaki A. and Shadel G. S., *Mitochondrial DNA stress primes the antiviral innate immune response.* Nature, 2015. **520**(7548): p. 553-7.
263. Yipp B. G. and Kubes P., *NETosis: how vital is it?* Blood, 2013. **122**(16): p. 2784-94.
264. Kenny E. F., Herzig A., Kruger R., Muth A., Mondal S., Thompson P. R., Brinkmann V., Bernuth H. V. and Zychlinsky A., *Diverse stimuli engage different neutrophil extracellular trap pathways.* Elife, 2017. **6**.
265. Mereweather L. J., Constantinescu-Bercu A., Crawley J. T. B. and Salles Crawley, Ii, *Platelet-Neutrophil Crosstalk in Thrombosis.* Int J Mol Sci, 2023. **24**(2).
266. Kolaparthy L. K., Sanivarapu S., Swarna C. and Devulapalli N. S., *Neutrophil extracellular traps: Their role in periodontal disease.* J Indian Soc Periodontol, 2014. **18**(6): p. 693-7.
267. Agraz-Cibrian J. M., Giraldo D. M., Mary F. M. and Urcuqui-Inchima S., *Understanding the molecular mechanisms of NETs and their role in antiviral innate immunity.* Virus Res, 2017. **228**: p. 124-133.
268. Pieterse E., Rother N., Yanginlar C., Hilbrands L. B. and Van Der Vlag J., *Neutrophils Discriminate between Lipopolysaccharides of Different Bacterial Sources and Selectively Release Neutrophil Extracellular Traps.* Front Immunol, 2016. **7**: p. 484.
269. Pilsczek F. H., Salina D., Poon K. K., Fahey C., Yipp B. G., Sibley C. D., Robbins S. M., Green F. H., Surette M. G., Sugai M., Bowden M. G., Hussain M., Zhang K. and Kubes P., *A novel mechanism of rapid nuclear neutrophil extracellular trap formation in response to Staphylococcus aureus.* J Immunol, 2010. **185**(12): p. 7413-25.
270. Papayannopoulos V., *Neutrophil extracellular traps in immunity and disease.* Nat Rev Immunol, 2018. **18**(2): p. 134-147.
271. Zhao W., Fogg D. K. and Kaplan M. J., *A novel image-based quantitative method for the characterization of NETosis.* J Immunol Methods, 2015. **423**: p. 104-10.
272. Abrams S. T., Morton B., Alhamdi Y., Alsabani M., Lane S., Welters I. D., Wang G. and Toh C. H., *A Novel Assay for Neutrophil Extracellular Trap Formation Independently Predicts Disseminated Intravascular Coagulation and Mortality in Critically Ill Patients.* Am J Respir Crit Care Med, 2019. **200**(7): p. 869-880.
273. Nunnari J. and Suomalainen A., *Mitochondria: in sickness and in health.* Cell, 2012. **148**(6): p. 1145-59.
274. West A. P., Shadel G. S. and Ghosh S., *Mitochondria in innate immune responses.* Nat Rev Immunol, 2011. **11**(6): p. 389-402.
275. Protasoni M. and Zeviani M., *Mitochondrial Structure and Bioenergetics in Normal and Disease Conditions.* Int J Mol Sci, 2021. **22**(2).
276. Amini P., Stojkov D., Felser A., Jackson C. B., Courage C., Schaller A., Gelman L., Soriano M. E., Nuoffer J. M., Scorrano L., Benarafa C., Yousefi S. and Simon H. U., *Neutrophil extracellular trap formation requires OPA1-dependent glycolytic ATP production.* Nat Commun, 2018. **9**(1): p. 2958.
277. Amini P., Stojkov D., Wang X., Wicki S., Kaufmann T., Wong W. W., Simon H. U. and Yousefi S., *NET formation can occur independently of RIPK3 and MLKL signaling.* Eur J Immunol, 2016. **46**(1): p. 178-84.
278. Conceicao-Silva F., Reis C. S. M., De Luca P. M., Leite-Silva J., Santiago M. A., Morrot A. and Morgado F. N., *The Immune System Throws Its Traps: Cells and Their Extracellular Traps in Disease and Protection.* Cells, 2021. **10**(8).
279. Tan C., Aziz M. and Wang P., *The vitals of NETs.* J Leukoc Biol, 2021. **110**(4): p. 797-808.
280. Guillotin F., Fortier M., Portes M., Demattei C., Mousty E., Nouvellon E., Mercier E., Chea M., Letouzey V., Gris J. C. and Bouvier S., *Vital NETosis vs. suicidal NETosis during normal pregnancy and preeclampsia.* Front Cell Dev Biol, 2022. **10**: p. 1099038.

281. Feješ Andrej, Šebeková Katarína and Borbélyová Veronika, *Pathophysiological Role of Neutrophil Extracellular Traps in Diet-Induced Obesity and Metabolic Syndrome in Animal Models.* Nutrients, 2025. **17**(2).
282. Itagaki K., Kaczmarek E., Lee Y. T., Tang I. T., Isal B., Adibnia Y., Sandler N., Grimm M. J., Segal B. H., Otterbein L. E. and Hauser C. J., *Mitochondrial DNA released by trauma induces neutrophil extracellular traps.* PLoS One, 2015. **10**(3): p. e0120549.
283. Caielli S., Athale S., Domic B., Murat E., Chandra M., Banchereau R., Baisch J., Phelps K., Clayton S., Gong M., Wright T., Punaro M., Palucka K., Guiducci C., Banchereau J. and Pascual V., *Oxidized mitochondrial nucleoids released by neutrophils drive type I interferon production in human lupus.* J Exp Med, 2016. **213**(5): p. 697-713.
284. Lood C., Blanco L. P., Purmalek M. M., Carmona-Rivera C., De Ravin S. S., Smith C. K., Malech H. L., Ledbetter J. A., Elkon K. B. and Kaplan M. J., *Neutrophil extracellular traps enriched in oxidized mitochondrial DNA are interferogenic and contribute to lupus-like disease.* Nat Med, 2016. **22**(2): p. 146-53.
285. Bronkhorst A. J., Ungerer V., Oberhofer A., Gabriel S., Polatoglou E., Randeu H., Uhlig C., Pfister H., Mayer Z. and Holdenrieder S., *New Perspectives on the Importance of Cell-Free DNA Biology.* Diagnostics (Basel), 2022. **12**(9).
286. Fyodorov D. V., Zhou B. R., Skoultchi A. I. and Bai Y., *Emerging roles of linker histones in regulating chromatin structure and function.* Nat Rev Mol Cell Biol, 2018. **19**(3): p. 192-206.
287. Henneman B., Van Emmerik C., Van Ingen H. and Dame R. T., *Structure and function of archaeal histones.* PLoS Genet, 2018. **14**(9): p. e1007582.
288. Talbert P. B. and Henikoff S., *Histone variants--ancient wrap artists of the epigenome.* Nat Rev Mol Cell Biol, 2010. **11**(4): p. 264-75.
289. Katan A. J., Vlijm R., Lusser A. and Dekker C., *Dynamics of nucleosomal structures measured by high-speed atomic force microscopy.* Small, 2015. **11**(8): p. 976-84.
290. Zhou B. R., Feng H., Kato H., Dai L., Yang Y., Zhou Y. and Bai Y., *Structural insights into the histone H1-nucleosome complex.* Proc Natl Acad Sci U S A, 2013. **110**(48): p. 19390-5.
291. Allam R., Kumar S. V., Darisipudi M. N. and Anders H. J., *Extracellular histones in tissue injury and inflammation.* J Mol Med (Berl), 2014. **92**(5): p. 465-72.
292. Kawano H., Ito T., Yamada S., Hashiguchi T., Maruyama I., Hisatomi T., Nakamura M. and Sakamoto T., *Toxic effects of extracellular histones and their neutralization by vitreous in retinal detachment.* Lab Invest, 2014. **94**(5): p. 569-85.
293. Hamam H. J., Khan M. A. and Palaniyar N., *Histone Acetylation Promotes Neutrophil Extracellular Trap Formation.* Biomolecules, 2019. **9**(1).
294. Khan M. A. and Palaniyar N., *Transcriptional firing helps to drive NETosis.* Sci Rep, 2017. **7**: p. 41749.
295. Wang Y., Wysocka J., Sayegh J., Lee Y. H., Perlin J. R., Leonelli L., Sonbuchner L. S., Mcdonald C. H., Cook R. G., Dou Y., Roeder R. G., Clarke S., Stallcup M. R., Allis C. D. and Coonrod S. A., *Human PAD4 regulates histone arginine methylation levels via demethylimination.* Science, 2004. **306**(5694): p. 279-83.
296. Wang Y., Li M., Stadler S., Correll S., Li P., Wang D., Hayama R., Leonelli L., Han H., Grigoryev S. A., Allis C. D. and Coonrod S. A., *Histone hypercitrullination mediates chromatin decondensation and neutrophil extracellular trap formation.* J Cell Biol, 2009. **184**(2): p. 205-13.
297. Martinod K., Demers M., Fuchs T. A., Wong S. L., Brill A., Gallant M., Hu J., Wang Y. and Wagner D. D., *Neutrophil histone modification by peptidylarginine deiminase 4 is critical for deep vein thrombosis in mice.* Proc Natl Acad Sci U S A, 2013. **110**(21): p. 8674-9.
298. Abrams S. T., Zhang N., Dart C., Wang S. S., Thachil J., Guan Y., Wang G. and Toh C. H., *Human CRP defends against the toxicity of circulating histones.* J Immunol, 2013. **191**(5): p. 2495-502.

299. Xu J., Zhang X., Monestier M., Esmon N. L. and Esmon C. T., *Extracellular histones are mediators of death through TLR2 and TLR4 in mouse fatal liver injury.* J Immunol, 2011. **187**(5): p. 2626-31.
300. Huang H., Evankovich J., Yan W., Nace G., Zhang L., Ross M., Liao X., Billiar T., Xu J., Esmon C. T. and Tsung A., *Endogenous histones function as alarmins in sterile inflammatory liver injury through Toll-like receptor 9 in mice.* Hepatology, 2011. **54**(3): p. 999-1008.
301. Pos O., Biro O., Szemes T. and Nagy B., *Circulating cell-free nucleic acids: characteristics and applications.* Eur J Hum Genet, 2018. **26**(7): p. 937-945.
302. Gould T. J., Vu T. T., Stafford A. R., Dwivedi D. J., Kim P. Y., Fox-Robichaud A. E., Weitz J. I. and Liaw P. C., *Cell-Free DNA Modulates Clot Structure and Impairs Fibrinolysis in Sepsis.* Arterioscler Thromb Vasc Biol, 2015. **35**(12): p. 2544-53.
303. Meng W., Paunel-Gorgulu A., Flohe S., Witte I., Schadel-Hopfner M., Windolf J. and Logters T. T., *Deoxyribonuclease is a potential counter regulator of aberrant neutrophil extracellular traps formation after major trauma.* Mediators Inflamm, 2012. **2012**: p. 149560.
304. Tuboly Eszter, *The Role of Neutrophil Extracellular Traps in Post-Injury Inflammation*. 2017.
305. Cui B. B., Tan C. Y., Schorn C., Tang H. H., Liu Y. and Zhao Y., *Neutrophil extracellular traps in sterile inflammation: the story after dying?* Autoimmunity, 2012. **45**(8): p. 593-6.
306. Margraf S., Logters T., Reipen J., Altrichter J., Scholz M. and Windolf J., *Neutrophil-derived circulating free DNA (cf-DNA/NETs): a potential prognostic marker for posttraumatic development of inflammatory second hit and sepsis.* Shock, 2008. **30**(4): p. 352-8.
307. Yadav R., Momin A. and Godugu C., *DNase based therapeutic approaches for the treatment of NETosis related inflammatory diseases.* Int Immunopharmacol, 2023. **124**(Pt A): p. 110846.
308. Czaikoski P. G., Mota J. M., Nascimento D. C., Sonego F., Castanheira F. V., Melo P. H., Scortegagna G. T., Silva R. L., Barroso-Sousa R., Souto F. O., Pazin-Filho A., Figueiredo F., Alves-Filho J. C. and Cunha F. Q., *Neutrophil Extracellular Traps Induce Organ Damage during Experimental and Clinical Sepsis.* PLoS One, 2016. **11**(2): p. e0148142.
309. Demkow U., *Molecular Mechanisms of Neutrophil Extracellular Trap (NETs) Degradation.* Int J Mol Sci, 2023. **24**(5).
310. Kumar S., Gupta E., Kaushik S. and Jyoti A., *Neutrophil Extracellular Traps: Formation and Involvement in Disease Progression.* Iran J Allergy Asthma Immunol, 2018. **17**(3): p. 208-220.
311. Tanaka K., Koike Y., Shimura T., Okigami M., Ide S., Toiyama Y., Okugawa Y., Inoue Y., Araki T., Uchida K., Mohri Y., Mizoguchi A. and Kusunoki M., *In vivo characterization of neutrophil extracellular traps in various organs of a murine sepsis model.* PLoS One, 2014. **9**(11): p. e111888.
312. Boneschansker L., Inoue Y., Oklu R. and Irimia D., *Capillary plexuses are vulnerable to neutrophil extracellular traps.* Integr Biol (Camb), 2016. **8**(2): p. 149-55.
313. Otawara M., Roushan M., Wang X., Ellett F., Yu Y. M. and Irimia D., *Microfluidic Assay Measures Increased Neutrophil Extracellular Traps Circulating in Blood after Burn Injuries.* Sci Rep, 2018. **8**(1): p. 16983.
314. Sakuma M., Wang X., Ellett F., Edd J. F., Babatunde K. A., Viens A., Mansour M. K. and Irimia D., *Microfluidic capture of chromatin fibres measures neutrophil extracellular traps (NETs) released in a drop of human blood.* Lab Chip, 2022. **22**(5): p. 936-944.
315. Lisman T., *Platelet-neutrophil interactions as drivers of inflammatory and thrombotic disease.* Cell Tissue Res, 2018. **371**(3): p. 567-576.
316. Mandel J., Casari M., Stepanyan M., Martyanov A. and Deppermann C., *Beyond Hemostasis: Platelet Innate Immune Interactions and Thromboinflammation.* Int J Mol Sci, 2022. **23**(7).
317. Denorme F. and Campbell R. A., *Platelets net neutrophils during ALI.* Blood, 2023. **142**(17): p. 1409-1410.

318. Fuchs T. A., Brill A., Duerschmied D., Schatzberg D., Monestier M., Myers D. D., Jr., Wrobleski S. K., Wakefield T. W., Hartwig J. H. and Wagner D. D., *Extracellular DNA traps promote thrombosis.* Proc Natl Acad Sci U S A, 2010. **107**(36): p. 15880-5.
319. Savchenko A. S., Martinod K., Seidman M. A., Wong S. L., Borissoff J. I., Piazza G., Libby P., Goldhaber S. Z., Mitchell R. N. and Wagner D. D., *Neutrophil extracellular traps form predominantly during the organizing stage of human venous thromboembolism development.* J Thromb Haemost, 2014. **12**(6): p. 860-70.
320. Brill A., Fuchs T. A., Savchenko A. S., Thomas G. M., Martinod K., De Meyer S. F., Bhandari A. A. and Wagner D. D., *Neutrophil extracellular traps promote deep vein thrombosis in mice.* J Thromb Haemost, 2012. **10**(1): p. 136-44.
321. Jimenez-Alcazar M., Napirei M., Panda R., Kohler E. C., Kremer Hovinga J. A., Mannherz H. G., Peine S., Renne T., Lammle B. and Fuchs T. A., *Impaired DNase1-mediated degradation of neutrophil extracellular traps is associated with acute thrombotic microangiopathies.* J Thromb Haemost, 2015. **13**(5): p. 732-42.
322. Tilburg J., Adili R., Nair T. S., Hawley M. E., Tuk D. C., Jackson M., Spronk H. M., Versteeg H. H., Carey T. E., Van Vlijmen B. J. M., Maracle C. X. and Holinstat M., *Characterization of hemostasis in mice lacking the novel thrombosis susceptibility gene Slc44a2.* Thromb Res, 2018. **171**: p. 155-159.
323. Chen Q., Srivastava K., Ardinski S. C., Lam K., Huvard M. J., Schmid P. and Flegel W. A., *Full-length nucleotide sequences of 30 common SLC44A2 alleles encoding human neutrophil antigen-3.* Transfusion, 2016. **56**(3): p. 729-36.
324. Constantinescu-Bercu A., Salles Crawley, Ii and Crawley J. T. B., *SLC44A2 - A novel therapeutic target for venous thrombosis?* J Thromb Haemost, 2020. **18**(7): p. 1556-1558.
325. Kommareddi P., Nair T., Kakaraparthi B. N., Galano M. M., Miller D., Laczkovich I., Thomas T., Lu L., Rule K., Kabara L., Kanicki A., Hughes E. D., Jones J. M., Hoenerhoff M., Fisher S. G., Altschuler R. A., Dolan D., Kohrman D. C., Saunders T. L. and Carey T. E., *Hair Cell Loss, Spiral Ganglion Degeneration, and Progressive Sensorineural Hearing Loss in Mice with Targeted Deletion of Slc44a2/Ctl2.* J Assoc Res Otolaryngol, 2015. **16**(6): p. 695-712.
326. Zhi L., Feng W., Liang J., Zhong Q., Ren L., Ma J. and Yao S., *The Effect of Common Variants in SLC44A2 on the Contribution to the Risk of Deep Cein Thrombosis after Orthopedic Surgery.* J Atheroscler Thromb, 2020.
327. Tilburg J., Coenen D. M., Zirka G., Dolleman S., Van Oeveren-Rietdijk A. M., Karel M. F. A., De Boer H. C., Cosemans Jmem, Versteeg H. H., Morange P. E., Van Vlijmen B. J. M., Maracle C. X. and Thomas G. M., *SLC44A2 deficient mice have a reduced response in stenosis but not in hypercoagulability driven venous thrombosis.* J Thromb Haemost, 2020. **18**(7): p. 1714-1727.
328. Mehrbod M., Trisno S. and Mofrad M. R., *On the activation of integrin alphaIIbbeta3: outside-in and inside-out pathways.* Biophys J, 2013. **105**(6): p. 1304-15.
329. Jones M. L., Harper M. T., Aitken E. W., Williams C. M. and Poole A. W., *RGD-ligand mimetic antagonists of integrin alphaIIbbeta3 paradoxically enhance GPVI-induced human platelet activation.* J Thromb Haemost, 2010. **8**(3): p. 567-76.
330. Joo S. J., *Mechanisms of Platelet Activation and Integrin alphaIIbeta3.* Korean Circ J, 2012. **42**(5): p. 295-301.
331. Constantinescu-Bercu A., Grassi L., Frontini M., Salles Crawley, Ii, Woollard K. and Crawley J. T., *Activated alphaIIbbeta3 on platelets mediates flow-dependent NETosis via SLC44A2.* Elife, 2020. **9**.
332. Bennett J. A., Mastrangelo M. A., Ture S. K., Smith C. O., Loelius S. G., Berg R. A., Shi X., Burke R. M., Spinelli S. L., Cameron S. J., Carey T. E., Brookes P. S., Gerszten R. E., Sabater-Lleal M., De Vries P. S., Huffman J. E., Smith N. L., Morrell C. N. and Lowenstein C. J., *The choline transporter Slc44a2 controls platelet activation and thrombosis by regulating mitochondrial function.* Nat Commun, 2020. **11**(1): p. 3479.

333. Leffler J., Martin M., Gullstrand B., Tyden H., Lood C., Truedsson L., Bengtsson A. A. and Blom A. M., *Neutrophil extracellular traps that are not degraded in systemic lupus erythematosus activate complement exacerbating the disease.* J Immunol, 2012. **188**(7): p. 3522-31.
334. Buchanan J. T., Simpson A. J., Aziz R. K., Liu G. Y., Kristian S. A., Kotb M., Feramisco J. and Nizet V., *DNase expression allows the pathogen group A Streptococcus to escape killing in neutrophil extracellular traps.* Curr Biol, 2006. **16**(4): p. 396-400.
335. Hakkim A., Furnrohr B. G., Amann K., Laube B., Abed U. A., Brinkmann V., Herrmann M., Voll R. E. and Zychlinsky A., *Impairment of neutrophil extracellular trap degradation is associated with lupus nephritis.* Proc Natl Acad Sci U S A, 2010. **107**(21): p. 9813-8.
336. Boulares A. H., Zoltoski A. J., Contreras F. J., Yakovlev A. G., Yoshihara K. and Smulson M. E., *Regulation of DNAS1L3 endonuclease activity by poly(ADP-ribosyl)ation during etoposide-induced apoptosis. Role of poly(ADP-ribose) polymerase-1 cleavage in endonuclease activation.* J Biol Chem, 2002. **277**(1): p. 372-8.
337. Mccord J. J., Engavale M., Masoumzadeh E., Villarreal J., Mapp B., Latham M. P., Keyel P. A. and Sutton R. B., *Structural features of Dnase1L3 responsible for serum antigen clearance.* Commun Biol, 2022. **5**(1): p. 825.
338. Sisirak V., Sally B., D'agati V., Martinez-Ortiz W., Ozcakar Z. B., David J., Rashidfarrokhi A., Yeste A., Panea C., Chida A. S., Bogunovic M., Ivanov, Ii, Quintana F. J., Sanz I., Elkon K. B., Tekin M., Yalcinkaya F., Cardozo T. J., Clancy R. M., Buyon J. P. and Reizis B., *Digestion of Chromatin in Apoptotic Cell Microparticles Prevents Autoimmunity.* Cell, 2016. **166**(1): p. 88-101.
339. Lazzaretto B. and Fadeel B., *Intra- and Extracellular Degradation of Neutrophil Extracellular Traps by Macrophages and Dendritic Cells.* J Immunol, 2019. **203**(8): p. 2276-2290.
340. Jimenez-Alcazar M., Rangaswamy C., Panda R., Bitterling J., Simsek Y. J., Long A. T., Bilyy R., Krenn V., Renne C., Renne T., Kluge S., Panzer U., Mizuta R., Mannherz H. G., Kitamura D., Herrmann M., Napirei M. and Fuchs T. A., *Host DNases prevent vascular occlusion by neutrophil extracellular traps.* Science, 2017. **358**(6367): p. 1202-1206.
341. Haider P., Kral-Pointner J. B., Mayer J., Richter M., Kaun C., Brostjan C., Eilenberg W., Fischer M. B., Speidl W. S., Hengstenberg C., Huber K., Wojta J. and Hohensinner P., *Neutrophil Extracellular Trap Degradation by Differently Polarized Macrophage Subsets.* Arterioscler Thromb Vasc Biol, 2020. **40**(9): p. 2265-2278.
342. Wynn T. A., Chawla A. and Pollard J. W., *Macrophage biology in development, homeostasis and disease.* Nature, 2013. **496**(7446): p. 445-55.
343. Watanabe S., Alexander M., Misharin A. V. and Budinger G. R. S., *The role of macrophages in the resolution of inflammation.* J Clin Invest, 2019. **129**(7): p. 2619-2628.
344. Farrera C. and Fadeel B., *Macrophage clearance of neutrophil extracellular traps is a silent process.* J Immunol, 2013. **191**(5): p. 2647-56.
345. Laukova L., Konecna B., Janovicova L., Vlkova B. and Celec P., *Deoxyribonucleases and Their Applications in Biomedicine.* Biomolecules, 2020. **10**(7).
346. Winder S. J. and Ayscough K. R., *Actin-binding proteins.* J Cell Sci, 2005. **118**(Pt 4): p. 651-4.
347. Reisler E. and Egelman E. H., *Actin structure and function: what we still do not understand.* J Biol Chem, 2007. **282**(50): p. 36133-7.
348. Bareyre F. M., Raghupathi R., Saatman K. E. and Mcintosh T. K., *DNase I disinhibition is predominantly associated with actin hyperpolymerization after traumatic brain injury.* J Neurochem, 2001. **77**(1): p. 173-81.
349. Pollard T. D. and Cooper J. A., *Actin, a central player in cell shape and movement.* Science, 2009. **326**(5957): p. 1208-12.
350. Wegner A., *Head to tail polymerization of actin.* J Mol Biol, 1976. **108**(1): p. 139-50.
351. Lee W. M. and Galbraith R. M., *The extracellular actin-scavenger system and actin toxicity.* N Engl J Med, 1992. **326**(20): p. 1335-41.

352. Haddad J. G., Harper K. D., Guoth M., Pietra G. G. and Sanger J. W., *Angiopathic consequences of saturating the plasma scavenger system for actin.* Proc Natl Acad Sci U S A, 1990. **87**(4): p. 1381-5.
353. Dinsdale R. J., Hazeldine J., Al Tarrah K., Hampson P., Devi A., Ermogenous C., Bamford A. L., Bishop J., Watts S., Kirkman E., Dalle Lucca J. J., Midwinter M., Woolley T., Foster M., Lord J. M., Moiemen N. and Harrison P., *Dysregulation of the actin scavenging system and inhibition of DNase activity following severe thermal injury.* Br J Surg, 2020. **107**(4): p. 391-401.
354. Lazarides E. and Lindberg U., *Actin is the naturally occurring inhibitor of deoxyribonuclease I.* Proc Natl Acad Sci U S A, 1974. **71**(12): p. 4742-6.
355. Otterbein L. R., Cosio C., Graceffa P. and Dominguez R., *Crystal structures of the vitamin D-binding protein and its complex with actin: structural basis of the actin-scavenger system.* Proc Natl Acad Sci U S A, 2002. **99**(12): p. 8003-8.
356. Yin H. L. and Hartwig J. H., *The structure of the macrophage actin skeleton.* J Cell Sci Suppl, 1988. **9**: p. 169-84.
357. Ito H., Kambe H., Kimura Y., Nakamura H., Hayashi E., Kishimoto T., Kishimoto S. and Yamamoto H., *Depression of plasma gelsolin level during acute liver injury.* Gastroenterology, 1992. **102**(5): p. 1686-92.
358. Mounzer K. C., Moncure M., Smith Y. R. and Dinubile M. J., *Relationship of admission plasma gelsolin levels to clinical outcomes in patients after major trauma.* Am J Respir Crit Care Med, 1999. **160**(5 Pt 1): p. 1673-81.
359. Osborn T. M., Verdrengh M., Stossel T. P., Tarkowski A. and Bokarewa M., *Decreased levels of the gelsolin plasma isoform in patients with rheumatoid arthritis.* Arthritis Res Ther, 2008. **10**(5): p. R117.
360. Jorgensen C. S., Christiansen M., Norgaard-Pedersen B., Ostergaard E., Schiodt F. V., Laursen I. and Houen G., *Gc globulin (vitamin D-binding protein) levels: an inhibition ELISA assay for determination of the total concentration of Gc globulin in plasma and serum.* Scand J Clin Lab Invest, 2004. **64**(2): p. 157-66.
361. Freeman J., Wilson K., Spears R., Shalhoub V. and Sibley P., *Influence of Vitamin D Binding Protein on Accuracy of 25-Hydroxyvitamin D Measurement Using the ADVIA Centaur Vitamin D Total Assay.* Int J Endocrinol, 2014. **2014**: p. 691679.
362. Dahl B., Schiodt F. V., Ott P., Wians F., Lee W. M., Balko J. and O'keefe G. E., *Plasma concentration of Gc-globulin is associated with organ dysfunction and sepsis after injury.* Crit Care Med, 2003. **31**(1): p. 152-6.
363. Lee W. M., Emerson D. L., Werner P. A., Arnaud P., Goldschmidt-Clermont P. and Galbraith R. M., *Decreased serum group-specific component protein levels and complexes with actin in fulminant hepatic necrosis.* Hepatology, 1985. **5**(2): p. 271-5.
364. Kulakowska A., Ciccarelli N. J., Wen Q., Mroczko B., Drozdowski W., Szmitkowski M., Janmey P. A. and Bucki R., *Hypogelsolinemia, a disorder of the extracellular actin scavenger system, in patients with multiple sclerosis.* BMC Neurol, 2010. **10**: p. 107.
365. Dahl B., *The extracellular actin scavenger system in trauma and major surgery. Clinical and experimental studies.* Acta Orthop Suppl, 2005. **76**(317): p. 2 p preceding table of contents-24.
366. Periayah M. H., Halim A. S. and Mat Saad A. Z., *Mechanism Action of Platelets and Crucial Blood Coagulation Pathways in Hemostasis.* Int J Hematol Oncol Stem Cell Res, 2017. **11**(4): p. 319-327.
367. Opneja A., Kapoor S. and Stavrou E. X., *Contribution of platelets, the coagulation and fibrinolytic systems to cutaneous wound healing.* Thromb Res, 2019. **179**: p. 56-63.
368. Raziyeva K., Kim Y., Zharkinbekov Z., Kassymbek K., Jimi S. and Saparov A., *Immunology of Acute and Chronic Wound Healing.* Biomolecules, 2021. **11**(5).

369. Malik A., Rehman F. U., Shah K. U., Naz S. S. and Qaisar S., *Hemostatic strategies for uncontrolled bleeding: A comprehensive update.* J Biomed Mater Res B Appl Biomater, 2021. **109**(10): p. 1465-1477.
370. Janus-Bell E. and Mangin P. H., *The relative importance of platelet integrins in hemostasis, thrombosis and beyond.* Haematologica, 2023. **108**(7): p. 1734-1747.
371. Veuthey L., Aliotta A., Bertaggia Calderara D., Pereira Portela C. and Alberio L., *Mechanisms Underlying Dichotomous Procoagulant COAT Platelet Generation-A Conceptual Review Summarizing Current Knowledge.* Int J Mol Sci, 2022. **23**(5).
372. Angiolillo D. J., Capodanno D. and Goto S., *Platelet thrombin receptor antagonism and atherothrombosis.* Eur Heart J, 2010. **31**(1): p. 17-28.
373. Vulliamy P. and Armstrong P. C., *Platelets in Hemostasis, Thrombosis, and Inflammation After Major Trauma.* Arterioscler Thromb Vasc Biol, 2024. **44**(3): p. 545-557.
374. Johnson B. Z., Stevenson A. W., Barrett L. W., Fear M. W., Wood F. M. and Linden M. D., *Platelets after burn injury - hemostasis and beyond.* Platelets, 2022. **33**(5): p. 655-665.
375. Sloos P. H., Vulliamy P., Van 'T Veer C., Gupta A. S., Neal M. D., Brohi K., Juffermans N. P. and Kleinveld D. J. B., *Platelet dysfunction after trauma: From mechanisms to targeted treatment.* Transfusion, 2022. **62 Suppl 1**(Suppl 1): p. S281-S300.
376. Saillant N. N. and Sims C. A., *Platelet dysfunction in injured patients.* Mol Cell Ther, 2014. **2**: p. 37.
377. Kutcher M. E., Redick B. J., Mccreery R. C., Crane I. M., Greenberg M. D., Cachola L. M., Nelson M. F. and Cohen M. J., *Characterization of platelet dysfunction after trauma.* J Trauma Acute Care Surg, 2012. **73**(1): p. 13-9.
378. Rourke C., Curry N., Khan S., Taylor R., Raza I., Davenport R., Stanworth S. and Brohi K., *Fibrinogen levels during trauma hemorrhage, response to replacement therapy, and association with patient outcomes.* J Thromb Haemost, 2012. **10**(7): p. 1342-51.
379. Wu J., Heemskerk J. W. M. and Baaten Ccfmj, *Platelet Membrane Receptor Proteolysis: Implications for Platelet Function.* Front Cardiovasc Med, 2020. **7**: p. 608391.
380. Ebermeyer T., Cognasse F., Berthelot P., Mismetti P., Garraud O. and Hamzeh-Cognasse H., *Platelet Innate Immune Receptors and TLRs: A Double-Edged Sword.* Int J Mol Sci, 2021. **22**(15).
381. Levi M., *Pathogenesis and diagnosis of disseminated intravascular coagulation.* Int J Lab Hematol, 2018. **40 Suppl 1**: p. 15-20.
382. Duke J. M., Randall S. M., Fear M. W., O'halloran E., Boyd J. H., Rea S. and Wood F. M., *Long term cardiovascular impacts after burn and non-burn trauma: A comparative population-based study.* Burns, 2017. **43**(8): p. 1662-1672.
383. Moore E. E., Moore H. B., Kornblith L. Z., Neal M. D., Hoffman M., Mutch N. J., Schochl H., Hunt B. J. and Sauaia A., *Trauma-induced coagulopathy.* Nat Rev Dis Primers, 2021. **7**(1): p. 30.
384. Locatelli L., Colciago A., Castiglioni S. and Maier J. A., *Platelets in Wound Healing: What Happens in Space?* Front Bioeng Biotechnol, 2021. **9**: p. 716184.
385. Sun S., Urbanus R. T., Ten Cate H., De Groot P. G., De Laat B., Heemskerk J. W. M. and Roest M., *Platelet Activation Mechanisms and Consequences of Immune Thrombocytopenia.* Cells, 2021. **10**(12).
386. Neuenfeldt F. S., Weigand M. A. and Fischer D., *Coagulopathies in Intensive Care Medicine: Balancing Act between Thrombosis and Bleeding.* J Clin Med, 2021. **10**(22).
387. Bordeanu-Diaconescu E. M., Grosu-Bularda A., Frunza A., Grama S., Andrei M. C., Neagu T. P., Lascar I. and Hariga C. S., *Diagnostic and Prognostic Value of Thrombocytopenia in Severe Burn Injuries.* Diagnostics (Basel), 2024. **14**(6).
388. Cato L. D., Wearn C. M., Bishop J. R. B., Stone M. J., Harrison P. and Moiemen N., *Platelet count: A predictor of sepsis and mortality in severe burns.* Burns, 2018. **44**(2): p. 288-297.

389. Glas G. J., Levi M. and Schultz M. J., *Coagulopathy and its management in patients with severe burns.* J Thromb Haemost, 2016. **14**(5): p. 865-74.
390. Nikolaidou E., Kakagia D., Kaldoudi E., Stouras J., Sovatzidis A. and Tsaroucha A., *Coagulation Disorders And Mortality In Burn Injury: A Systematic Review.* Ann Burns Fire Disasters, 2022. **35**(2): p. 103-115.
391. Brohi K., Cohen M. J. and Davenport R. A., *Acute coagulopathy of trauma: mechanism, identification and effect.* Curr Opin Crit Care, 2007. **13**(6): p. 680-5.
392. Cohen M. J., *Acute traumatic coagulopathy: clinical characterization and mechanistic investigation.* Thromb Res, 2014. **133 Suppl 1**: p. S25-7.
393. Maegele M., Spinella P. C. and Schochl H., *The acute coagulopathy of trauma: mechanisms and tools for risk stratification.* Shock, 2012. **38**(5): p. 450-8.
394. Niles S. E., Mclaughlin D. F., Perkins J. G., Wade C. E., Li Y., Spinella P. C. and Holcomb J. B., *Increased mortality associated with the early coagulopathy of trauma in combat casualties.* J Trauma, 2008. **64**(6): p. 1459-63; discussion 1463-5.
395. Hess J. R., Brohi K., Dutton R. P., Hauser C. J., Holcomb J. B., Kluger Y., Mackway-Jones K., Parr M. J., Rizoli S. B., Yukioka T., Hoyt D. B. and Bouillon B., *The coagulopathy of trauma: a review of mechanisms.* J Trauma, 2008. **65**(4): p. 748-54.
396. Petros S., *Trauma-Induced Coagulopathy.* Hamostaseologie, 2019. **39**(1): p. 20-27.
397. Dobson G. P., Morris J. L. and Letson H. L., *Pathophysiology of severe burn injuries: new therapeutic opportunities from a systems perspective.* J Burn Care Res, 2024.
398. Hayakawa M., Gando S., Ono Y., Wada T., Yanagida Y. and Sawamura A., *Fibrinogen level deteriorates before other routine coagulation parameters and massive transfusion in the early phase of severe trauma: a retrospective observational study.* Semin Thromb Hemost, 2015. **41**(1): p. 35-42.
399. Huzar T. F., Martinez E., Love J., George T. C., Shah J., Baer L., Cross J. M., Wade C. E. and Cotton B. A., *Admission Rapid Thrombelastography (rTEG(R)) Values Predict Resuscitation Volumes and Patient Outcomes After Thermal Injury.* J Burn Care Res, 2018. **39**(3): p. 345-352.
400. Wiegele M., Schaden E., Koch S., Bauer D., Krall C. and Adelmann D., *Thrombin generation in patients with severe thermal injury.* Burns, 2019. **45**(1): p. 54-62.
401. Plautz W. E., Matthay Z. A., Rollins-Raval M. A., Raval J. S., Kornblith L. Z. and Neal M. D., *Von Willebrand factor as a thrombotic and inflammatory mediator in critical illness.* Transfusion, 2020. **60 Suppl 3**(Suppl 3): p. S158-S166.
402. Huang S., Ninivaggi M., Chayoua W. and De Laat B., *VWF, Platelets and the Antiphospholipid Syndrome.* Int J Mol Sci, 2021. **22**(8).
403. Macarthur T. A., Goswami J., Moon Tasson L., Tischer A., Bailey K. R., Spears G. M., Dong J. F., Auton M., Kozar R. and Park M. S., *Quantification of von Willebrand factor and ADAMTS-13 after traumatic injury: a pilot study.* Trauma Surg Acute Care Open, 2021. **6**(1): p. e000703.
404. Plautz W. E., Haldeman S. H., Dyer M. R., Sperry J. L., Guyette F. X., Loughran P. A., Alvikas J., Hassoune A., Hoteit L., Alsaadi N., Zuckerbraun B. S., Rollins-Raval M. A., Raval J. S., Mota R. I., Neal M. D. and Publication A. Tactic, *Reduced cleavage of von willebrand factor by ADAMTS13 is associated with microangiopathic acute kidney injury following trauma.* Blood Coagul Fibrinolysis, 2022. **33**(1): p. 14-24.
405. Takaya H., Namisaki T., Asada S., Iwai S., Kubo T., Suzuki J., Enomoto M., Tsuji Y., Fujinaga Y., Nishimura N., Sawada Y., Kaji K., Kawaratani H., Moriya K., Akahane T., Matsumoto M. and Yoshiji H., *ADAMTS13, VWF, and Endotoxin Are Interrelated and Associated with the Severity of Liver Cirrhosis via Hypercoagulability.* J Clin Med, 2022. **11**(7).
406. Hazeldine J., Mcgee K. C., Al-Tarrah K., Hassouna T., Patel K., Imran R., Bishop J. R. B., Bamford A., Barnes D., Wilson Y., Harrison P., Lord J. M. and Moiemen N. S., *Multicentre,*

longitudinal, observational cohort study to examine the relationship between neutrophil function and sepsis in adults and children with severe thermal injuries: a protocol for the Scientific Investigation of the Biological Pathways Following Thermal Injury-2 (SIFTI-2) study. BMJ Open, 2021. **11**(10): p. e052035.
407. Hazeldine J., Naumann D. N., Toman E., Davies D., Bishop J. R. B., Su Z., Hampson P., Dinsdale R. J., Crombie N., Duggal N. A., Harrison P., Belli A. and Lord J. M., *Prehospital immune responses and development of multiple organ dysfunction syndrome following traumatic injury: A prospective cohort study.* PLoS Med, 2017. **14**(7): p. e1002338.
408. Corporation Zacros. *T-TAS product information*. 2024 22 October 2024]; Available from: https://www.t-tas.info/product/index.html.
409. Goldshtein H., Hausmann M. J. and Douvdevani A., *A rapid direct fluorescent assay for cell-free DNA quantification in biological fluids.* Ann Clin Biochem, 2009. **46**(Pt 6): p. 488-94.
410. Ho J. W., Quan C., Gauger M. A., Alam H. B. and Li Y., *Role of Peptidylarginine Deiminase and Neutrophil Extracellular Traps in Injuries: Future Novel Diagnostics and Therapeutic Targets.* Shock, 2023. **59**(2): p. 247-255.
411. Schultz B. M., Acevedo O. A., Kalergis A. M. and Bueno S. M., *Role of Extracellular Trap Release During Bacterial and Viral Infection.* Front Microbiol, 2022. **13**: p. 798853.
412. Sobouti B., Ghavami Y., Asadifar B., Jafarzadeh M., Ghelman M. and Vaghardoost R., *Determination of Serum Levels of Interleukin-6, Interleukin-8, Interleukin-10, and Tumor Necrosis-Alpha and their Relationship With The Total Body Surface Area in Children.* J Burn Care Res, 2020. **41**(3): p. 539-543.
413. Wigerblad G. and Kaplan M. J., *Neutrophil extracellular traps in systemic autoimmune and autoinflammatory diseases.* Nat Rev Immunol, 2023. **23**(5): p. 274-288.
414. Andres C. M. C., Perez De La Lastra J. M., Juan C. A., Plou F. J. and Perez-Lebena E., *The Role of Reactive Species on Innate Immunity.* Vaccines (Basel), 2022. **10**(10).
415. Fetz A. E. and Bowlin G. L., *Neutrophil Extracellular Traps: Inflammation and Biomaterial Preconditioning for Tissue Engineering.* Tissue Eng Part B Rev, 2022. **28**(2): p. 437-450.
416. Song Y. H., Wang Z. J., Kang L., He Z. X., Zhao S. B., Fang X., Li Z. S., Wang S. L. and Bai Y., *PADs and NETs in digestive system: From physiology to pathology.* Front Immunol, 2023. **14**: p. 1077041.
417. Baz A. A., Hao H., Lan S., Li Z., Liu S., Chen S. and Chu Y., *Neutrophil extracellular traps in bacterial infections and evasion strategies.* Front Immunol, 2024. **15**: p. 1357967.
418. Zhao J. and Jin J., *Neutrophil extracellular traps: New players in cancer research.* Front Immunol, 2022. **13**: p. 937565.
419. Frade-Sosa B. and Sanmarti R., *Neutrophils, neutrophil extracellular traps, and rheumatoid arthritis: An updated review for clinicians.* Reumatol Clin (Engl Ed), 2023. **19**(9): p. 515-526.
420. Oliveira-Costa K. M., Menezes G. B. and Paula Neto H. A., *Neutrophil accumulation within tissues: A damage x healing dichotomy.* Biomed Pharmacother, 2022. **145**: p. 112422.
421. Korkmaz H. I., Ulrich M. M. W., Vogels S., De Wit T., Van Zuijlen P. P. M., Krijnen P. A. J. and Niessen H. W. M., *Neutrophil extracellular traps coincide with a pro-coagulant status of microcirculatory endothelium in burn wounds.* Wound Repair Regen, 2017. **25**(4): p. 609-617.
422. Narasaraju T., Yang E., Samy R. P., Ng H. H., Poh W. P., Liew A. A., Phoon M. C., Van Rooijen N. and Chow V. T., *Excessive neutrophils and neutrophil extracellular traps contribute to acute lung injury of influenza pneumonitis.* Am J Pathol, 2011. **179**(1): p. 199-210.
423. Unar A., Bertolino L., Patauner F., Gallo R. and Durante-Mangoni E., *Pathophysiology of Disseminated Intravascular Coagulation in Sepsis: A Clinically Focused Overview.* Cells, 2023. **12**(17).
424. Malickova K., Duricova D., Bortlik M., Hruskova Z., Svobodova B., Machkova N., Komarek V., Fucikova T., Janatkova I., Zima T. and Lukas M., *Impaired deoxyribonuclease I activity in patients with inflammatory bowel diseases.* Autoimmune Dis, 2011. **2011**: p. 945861.

425. Grabuschnig S., Bronkhorst A. J., Holdenrieder S., Rosales Rodriguez I., Schliep K. P., Schwendenwein D., Ungerer V. and Sensen C. W., *Putative Origins of Cell-Free DNA in Humans: A Review of Active and Passive Nucleic Acid Release Mechanisms.* Int J Mol Sci, 2020. **21**(21).
426. Lam N. Y., Rainer T. H., Chan L. Y., Joynt G. M. and Lo Y. M., *Time course of early and late changes in plasma DNA in trauma patients.* Clin Chem, 2003. **49**(8): p. 1286-91.
427. Wang H. C., Lin Y. J., Tsai N. W., Su B. Y., Kung C. T., Chen W. F., Kwan A. L. and Lu C. H., *Serial plasma deoxyribonucleic acid levels as predictors of outcome in acute traumatic brain injury.* J Neurotrauma, 2014. **31**(11): p. 1039-45.
428. Dwivedi D. J., Toltl L. J., Swystun L. L., Pogue J., Liaw K. L., Weitz J. I., Cook D. J., Fox-Robichaud A. E., Liaw P. C. and Canadian Critical Care Translational Biology Group, *Prognostic utility and characterization of cell-free DNA in patients with severe sepsis.* Crit Care, 2012. **16**(4): p. R151.
429. Yang X., Li L., Liu J., Lv B. and Chen F., *Extracellular histones induce tissue factor expression in vascular endothelial cells via TLR and activation of NF-kappaB and AP-1.* Thromb Res, 2016. **137**: p. 211-218.
430. Konishi S., Narita T., Hatakeyama S., Yoneyama T., Yoneyama M. S., Tobisawa Y., Noro D., Sato T., Togashi K., Okamoto T., Yamamoto H., Yoneyama T., Hashimoto Y. and Ohyama C., *Utility of total cell-free DNA levels for surgical damage evaluation in patients with urological surgeries.* Sci Rep, 2021. **11**(1): p. 22103.
431. Ungerer V., Bronkhorst A. J., Van Den Ackerveken P., Herzog M. and Holdenrieder S., *Serial profiling of cell-free DNA and nucleosome histone modifications in cell cultures.* Sci Rep, 2021. **11**(1): p. 9460.
432. Hiyama A., Sakai D., Nomura S., Katoh H. and Watanabe M., *Analysis of cell-free circulating DNA fragment size and level in patients with lumbar canal stenosis.* JOR Spine, 2022. **5**(2): p. e1189.
433. Zinkova A., Brynychova I., Svacina A., Jirkovska M. and Korabecna M., *Cell-free DNA from human plasma and serum differs in content of telomeric sequences and its ability to promote immune response.* Sci Rep, 2017. **7**(1): p. 2591.
434. Lee T. H., Montalvo L., Chrebtow V. and Busch M. P., *Quantitation of genomic DNA in plasma and serum samples: higher concentrations of genomic DNA found in serum than in plasma.* Transfusion, 2001. **41**(2): p. 276-82.
435. Lee J. S., Kim M., Seong M. W., Kim H. S., Lee Y. K. and Kang H. J., *Plasma vs. serum in circulating tumor DNA measurement: characterization by DNA fragment sizing and digital droplet polymerase chain reaction.* Clin Chem Lab Med, 2020. **58**(4): p. 527-532.
436. Meddeb R., Pisareva E. and Thierry A. R., *Guidelines for the Preanalytical Conditions for Analyzing Circulating Cell-Free DNA.* Clin Chem, 2019. **65**(5): p. 623-633.
437. Beutler E., Gelbart T. and Kuhl W., *Interference of heparin with the polymerase chain reaction.* Biotechniques, 1990. **9**(2): p. 166.
438. Alidousty C., Brandes D., Heydt C., Wagener S., Wittersheim M., Schafer S. C., Holz B., Merkelbach-Bruse S., Buttner R., Fassunke J. and Schultheis A. M., *Comparison of Blood Collection Tubes from Three Different Manufacturers for the Collection of Cell-Free DNA for Liquid Biopsy Mutation Testing.* J Mol Diagn, 2017. **19**(5): p. 801-804.
439. Kang Q., Henry N. L., Paoletti C., Jiang H., Vats P., Chinnaiyan A. M., Hayes D. F., Merajver S. D., Rae J. M. and Tewari M., *Comparative analysis of circulating tumor DNA stability In K(3)EDTA, Streck, and CellSave blood collection tubes.* Clin Biochem, 2016. **49**(18): p. 1354-1360.
440. Kaplan N., Moore I. K., Fondufe-Mittendorf Y., Gossett A. J., Tillo D., Field Y., Leproust E. M., Hughes T. R., Lieb J. D., Widom J. and Segal E., *The DNA-encoded nucleosome organization of a eukaryotic genome.* Nature, 2009. **458**(7236): p. 362-6.

441. Ren B., Liu F., Xu F., He J., Zhu H. and Zou G., *Is plasma cell-free DNA really a useful marker for diagnosis and treatment of trauma patients?* Clin Chim Acta, 2013. **424**: p. 109-13.
442. Kiwit A., Lu Y., Lenz M., Knopf J., Mohr C., Ledermann Y., Klinke-Petrowsky M., Pagerols Raluy L., Reinshagen K., Herrmann M., Boettcher M. and Elrod J., *The Dual Role of Neutrophil Extracellular Traps (NETs) in Sepsis and Ischemia-Reperfusion Injury: Comparative Analysis across Murine Models.* Int J Mol Sci, 2024. **25**(7).
443. Mutua V. and Gershwin L. J., *A Review of Neutrophil Extracellular Traps (NETs) in Disease: Potential Anti-NETs Therapeutics.* Clin Rev Allergy Immunol, 2021. **61**(2): p. 194-211.
444. Halpern D., Cohen A., Sharon N., Krieger Y., Silberstein E., Michael T., Douvdevani A. and Shoham Y., *Admission Circulating Cell-Free DNA Levels as a Prognostic Factor in Pediatric Burns.* Biomed Res Int, 2022. **2022**: p. 5004282.
445. Sundaram R. and Vasudevan D., *Structural Basis of Nucleosome Recognition and Modulation.* Bioessays, 2020. **42**(9): p. e1900234.
446. Li X., Ye Y., Peng K., Zeng Z., Chen L. and Zeng Y., *Histones: The critical players in innate immunity.* Front Immunol, 2022. **13**: p. 1030610.
447. Marsman G., Zeerleder S. and Luken B. M., *Extracellular histones, cell-free DNA, or nucleosomes: differences in immunostimulation.* Cell Death Dis, 2016. **7**(12): p. e2518.
448. Hansen J. C., Connolly M., Mcdonald C. J., Pan A., Pryamkova A., Ray K., Seidel E., Tamura S., Rogge R. and Maeshima K., *The 10-nm chromatin fiber and its relationship to interphase chromosome organization.* Biochem Soc Trans, 2018. **46**(1): p. 67-76.
449. Napirei M., Wulf S., Eulitz D., Mannherz H. G. and Kloeckl T., *Comparative characterization of rat deoxyribonuclease 1 (Dnase1) and murine deoxyribonuclease 1-like 3 (Dnase1l3).* Biochem J, 2005. **389**(Pt 2): p. 355-64.
450. Cato L. D., Bailiff B., Price J., Ermogeneous C., Hazeldine J., Lester W., Lowe G., Wearn C., Bishop J. R. B., Lord J. M., Moiemen N. and Harrison P., *Heparin resistance in severe thermal injury: A prospective cohort study.* Burns Trauma, 2021. **9**: p. tkab032.
451. Goswami J., Macarthur T., Bailey K., Spears G., Kozar R. A., Auton M., Dong J. F., Key N. S., Heller S., Loomis E., Hall N. W., Johnstone A. L. and Park M. S., *Neutrophil Extracellular Trap Formation and Syndecan-1 Shedding Are Increased After Trauma.* Shock, 2021. **56**(3): p. 433-439.
452. Xu X., Wu Y., Xu S., Yin Y., Ageno W., De Stefano V., Zhao Q. and Qi X., *Clinical significance of neutrophil extracellular traps biomarkers in thrombosis.* Thromb J, 2022. **20**(1): p. 63.
453. Ng H., Havervall S., Rosell A., Aguilera K., Parv K., Von Meijenfeldt F. A., Lisman T., Mackman N., Thalin C. and Phillipson M., *Circulating Markers of Neutrophil Extracellular Traps Are of Prognostic Value in Patients With COVID-19.* Arterioscler Thromb Vasc Biol, 2021. **41**(2): p. 988-994.
454. Fedorov K., Barouqa M., Yin D., Kushnir M., Billett H. H. and Reyes Gil M., *Identifying Neutrophil Extracellular Traps (NETs) in Blood Samples Using Peripheral Smear Autoanalyzers.* Life (Basel), 2023. **13**(3).
455. Rhodes A., Wort S. J., Thomas H., Collinson P. and Bennett E. D., *Plasma DNA concentration as a predictor of mortality and sepsis in critically ill patients.* Crit Care, 2006. **10**(2): p. R60.
456. Mccarthy C. G., Wenceslau C. F., Goulopoulou S., Ogbi S., Baban B., Sullivan J. C., Matsumoto T. and Webb R. C., *Circulating mitochondrial DNA and Toll-like receptor 9 are associated with vascular dysfunction in spontaneously hypertensive rats.* Cardiovasc Res, 2015. **107**(1): p. 119-30.
457. Muzes G., Bohusne Barta B., Szabo O., Horgas V. and Sipos F., *Cell-Free DNA in the Pathogenesis and Therapy of Non-Infectious Inflammations and Tumors.* Biomedicines, 2022. **10**(11).
458. Paunel-Gorgulu A., Wacker M., El Aita M., Hassan S., Schlachtenberger G., Deppe A., Choi Y. H., Kuhn E., Mehler T. O. and Wahlers T., *cfDNA correlates with endothelial damage after*

cardiac surgery with prolonged cardiopulmonary bypass and amplifies NETosis in an intracellular TLR9-independent manner. Sci Rep, 2017. **7**(1): p. 17421.
459. Abrams S. T., Zhang N., Manson J., Liu T., Dart C., Baluwa F., Wang S. S., Brohi K., Kipar A., Yu W., Wang G. and Toh C. H., *Circulating histones are mediators of trauma-associated lung injury.* Am J Respir Crit Care Med, 2013. **187**(2): p. 160-9.
460. Cheng Z., Abrams S. T., Alhamdi Y., Toh J., Yu W., Wang G. and Toh C. H., *Circulating Histones Are Major Mediators of Multiple Organ Dysfunction Syndrome in Acute Critical Illnesses.* Crit Care Med, 2019. **47**(8): p. e677-e684.
461. Medeiros S. K., Sharma N., Dwivedi D. and Liaw P. C., *Investigation of the Pathological Effects of Histones, DNA, and Nucleosomes in a Murine Model of Sepsis.* Shock, 2023. **60**(2): p. 291-297.
462. Huang J., Hong W., Wan M. and Zheng L., *Molecular mechanisms and therapeutic target of NETosis in diseases.* MedComm (2020), 2022. **3**(3): p. e162.
463. Boeltz S., Amini P., Anders H. J., Andrade F., Bilyy R., Chatfield S., Cichon I., Clancy D. M., Desai J., Dumych T., Dwivedi N., Gordon R. A., Hahn J., Hidalgo A., Hoffmann M. H., Kaplan M. J., Knight J. S., Kolaczkowska E., Kubes P., Leppkes M., Manfredi A. A., Martin S. J., Maueroder C., Maugeri N., Mitroulis I., Munoz L. E., Nakazawa D., Neeli I., Nizet V., Pieterse E., Radic M. Z., Reinwald C., Ritis K., Rovere-Querini P., Santocki M., Schauer C., Schett G., Shlomchik M. J., Simon H. U., Skendros P., Stojkov D., Vandenabeele P., Berghe T. V., Van Der Vlag J., Vitkov L., Von Kockritz-Blickwede M., Yousefi S., Zarbock A. and Herrmann M., *To NET or not to NET:current opinions and state of the science regarding the formation of neutrophil extracellular traps.* Cell Death Differ, 2019. **26**(3): p. 395-408.
464. Liu M. L., Lyu X. and Werth V. P., *Recent progress in the mechanistic understanding of NET formation in neutrophils.* FEBS J, 2022. **289**(14): p. 3954-3966.
465. Yang J., Wu Z., Long Q., Huang J., Hong T., Liu W. and Lin J., *Insights Into Immunothrombosis: The Interplay Among Neutrophil Extracellular Trap, von Willebrand Factor, and ADAMTS13.* Front Immunol, 2020. **11**: p. 610696.
466. Delabranche X., Stiel L., Severac F., Galoisy A. C., Mauvieux L., Zobairi F., Lavigne T., Toti F., Angles-Cano E., Meziani F. and Boisrame-Helms J., *Evidence of Netosis in Septic Shock-Induced Disseminated Intravascular Coagulation.* Shock, 2017. **47**(3): p. 313-317.
467. Stiel L., Mayeur-Rousse C., Helms J., Meziani F. and Mauvieux L., *First visualization of circulating neutrophil extracellular traps using cell fluorescence during human septic shock-induced disseminated intravascular coagulation.* Thromb Res, 2019. **183**: p. 153-158.
468. Cedervall J., Zhang Y., Huang H., Zhang L., Femel J., Dimberg A. and Olsson A. K., *Neutrophil Extracellular Traps Accumulate in Peripheral Blood Vessels and Compromise Organ Function in Tumor-Bearing Animals.* Cancer Res, 2015. **75**(13): p. 2653-62.
469. Hazeldine J., Dinsdale R. J., Naumann D. N., Acharjee A., Bishop J. R. B., Lord J. M. and Harrison P., *Traumatic injury is associated with reduced deoxyribonuclease activity and dysregulation of the actin scavenging system.* Burns Trauma, 2021. **9**: p. tkab001.
470. Laggner M., Lingitz M. T., Copic D., Direder M., Klas K., Bormann D., Gugerell A., Moser B., Radtke C., Hacker S., Mildner M., Ankersmit H. J. and Haider T., *Severity of thermal burn injury is associated with systemic neutrophil activation.* Sci Rep, 2022. **12**(1): p. 1654.
471. Kaplan M. J. and Radic M., *Neutrophil extracellular traps: double-edged swords of innate immunity.* J Immunol, 2012. **189**(6): p. 2689-95.
472. Apostolakis S., Vogiatzi K., Amanatidou V. and Spandidos D. A., *Interleukin 8 and cardiovascular disease.* Cardiovasc Res, 2009. **84**(3): p. 353-60.
473. Holmes W. E., Lee J., Kuang W. J., Rice G. C. and Wood W. I., *Structure and functional expression of a human interleukin-8 receptor.* Science, 1991. **253**(5025): p. 1278-80.

474. Wu L., Ruffing N., Shi X., Newman W., Soler D., Mackay C. R. and Qin S., *Discrete steps in binding and signaling of interleukin-8 with its receptor.* J Biol Chem, 1996. **271**(49): p. 31202-9.
475. Waugh D. J. and Wilson C., *The interleukin-8 pathway in cancer.* Clin Cancer Res, 2008. **14**(21): p. 6735-41.
476. Habanjar O., Bingula R., Decombat C., Diab-Assaf M., Caldefie-Chezet F. and Delort L., *Crosstalk of Inflammatory Cytokines within the Breast Tumor Microenvironment.* Int J Mol Sci, 2023. **24**(4).
477. Hann J., Bueb J. L., Tolle F. and Brechard S., *Calcium signaling and regulation of neutrophil functions: Still a long way to go.* J Leukoc Biol, 2020. **107**(2): p. 285-297.
478. Ha H., Debnath B. and Neamati N., *Role of the CXCL8-CXCR1/2 Axis in Cancer and Inflammatory Diseases.* Theranostics, 2017. **7**(6): p. 1543-1588.
479. Kaiser R., Leunig A., Pekayvaz K., Popp O., Joppich M., Polewka V., Escaig R., Anjum A., Hoffknecht M. L., Gold C., Brambs S., Engel A., Stockhausen S., Knottenberg V., Titova A., Haji M., Scherer C., Muenchhoff M., Hellmuth J. C., Saar K., Schubert B., Hilgendorff A., Schulz C., Kaab S., Zimmer R., Hubner N., Massberg S., Mertins P., Nicolai L. and Stark K., *Self-sustaining IL-8 loops drive a prothrombotic neutrophil phenotype in severe COVID-19.* JCI Insight, 2021. **6**(18).
480. Teijeira A., Garasa S., Ochoa M. D. C., Cirella A., Olivera I., Glez-Vaz J., Andueza M. P., Migueliz I., Alvarez M., Rodriguez-Ruiz M. E., Rouzaut A., Berraondo P., Sanmamed M. F., Perez Gracia J. L. and Melero I., *Differential Interleukin-8 thresholds for chemotaxis and netosis in human neutrophils.* Eur J Immunol, 2021. **51**(9): p. 2274-2280.
481. Nie M., Yang L., Bi X., Wang Y., Sun P., Yang H., Liu P., Li Z., Xia Y. and Jiang W., *Neutrophil Extracellular Traps Induced by IL8 Promote Diffuse Large B-cell Lymphoma Progression via the TLR9 Signaling.* Clin Cancer Res, 2019. **25**(6): p. 1867-1879.
482. Kilic Irfan Baki, Yasar Acelya, Yalim Camci Irem, Guzel Turkan, Karahasan Aysegul, Yagci Tamer, Cine Naci and Kandilci Ayten, *NETosis Induced by Serum of Patients with COVID-19 is Reduced with Reparixin or Antibodies Against DEK and IL-8.* Turkish Journal of Immunology, 2024: p. 127-135.
483. Piersanti G., Landoni G., Scquizzato T., Zangrillo A. and Piemonti L., *Reparixin improves survival in critically ill and transplant patients: A meta-analysis.* Eur J Clin Invest, 2023. **53**(10): p. e14015.
484. Sitaru S., Budke A., Bertini R. and Sperandio M., *Therapeutic inhibition of CXCR1/2: where do we stand?* Intern Emerg Med, 2023. **18**(6): p. 1647-1664.
485. Brinkmann V. and Zychlinsky A., *Beneficial suicide: why neutrophils die to make NETs.* Nat Rev Microbiol, 2007. **5**(8): p. 577-82.
486. Kraft R., Herndon D. N., Finnerty C. C., Cox R. A., Song J. and Jeschke M. G., *Predictive Value of IL-8 for Sepsis and Severe Infections After Burn Injury: A Clinical Study.* Shock, 2015. **43**(3): p. 222-7.
487. Yamada Y., Endo S. and Inada K., *Plasma cytokine levels in patients with severe burn injury--with reference to the relationship between infection and prognosis.* Burns, 1996. **22**(8): p. 587-93.
488. Vindenes H., Ulvestad E. and Bjerknes R., *Increased levels of circulating interleukin-8 in patients with large burns: relation to burn size and sepsis.* J Trauma, 1995. **39**(4): p. 635-40.
489. Al-Ani F. W. and Fahad H. M., *Detection of the Level of Interleukin-8 in the Serum of Burn Patients by ELISA Technique.* Arch Razi Inst, 2023. **78**(3): p. 1087-1093.
490. Matsumoto H., Ogura H., Shimizu K., Ikeda M., Hirose T., Matsuura H., Kang S., Takahashi K., Tanaka T. and Shimazu T., *The clinical importance of a cytokine network in the acute phase of sepsis.* Sci Rep, 2018. **8**(1): p. 13995.

491. Anderson B. J., Calfee C. S., Liu K. D., Reilly J. P., Kangelaris K. N., Shashaty M. G. S., Lazaar A. L., Bayliffe A. I., Gallop R. J., Miano T. A., Dunn T. G., Johansson E., Abbott J., Jauregui A., Deiss T., Vessel K., Belzer A., Zhuo H., Matthay M. A., Meyer N. J. and Christie J. D., *Plasma sTNFR1 and IL8 for prognostic enrichment in sepsis trials: a prospective cohort study.* Crit Care, 2019. **23**(1): p. 400.
492. Liu X. W., Ma T., Cai Q., Wang L., Song H. W. and Liu Z., *Elevation of Serum PARK7 and IL-8 Levels Is Associated With Acute Lung Injury in Patients With Severe Sepsis/Septic Shock.* J Intensive Care Med, 2019. **34**(8): p. 662-668.
493. Zhang Y., Chandra V., Riquelme Sanchez E., Dutta P., Quesada P. R., Rakoski A., Zoltan M., Arora N., Baydogan S., Horne W., Burks J., Xu H., Hussain P., Wang H., Gupta S., Maitra A., Bailey J. M., Moghaddam S. J., Banerjee S., Sahin I., Bhattacharya P. and Mcallister F., *Interleukin-17-induced neutrophil extracellular traps mediate resistance to checkpoint blockade in pancreatic cancer.* J Exp Med, 2020. **217**(12).
494. Van Avondt K., Schimmel M., Bulder I., Van Mierlo G., Nur E., Van Bruggen R., Biemond B. J., Luken B. M. and Zeerleder S., *Circulating Iron in Patients with Sickle Cell Disease Mediates the Release of Neutrophil Extracellular Traps.* Transfus Med Hemother, 2023. **50**(4): p. 321-329.
495. Miguel L. I., Leonardo F. C., Torres L. S., Garcia F., Mendonca R., Ferreira W. A., Jr., Gotardo E. M. F., Fabris F. C. Z., Brito P. L., Costa F. F. and Conran N., *Heme induces significant neutrophil adhesion in vitro via an NFkappaB and reactive oxygen species-dependent pathway.* Mol Cell Biochem, 2021. **476**(11): p. 3963-3974.
496. Teng H. W., Wang T. Y., Lin C. C., Tong Z. J., Cheng H. W. and Wang H. T., *Interferon gamma induces higher neutrophil extracellular traps leading to tumor-killing activity in microsatellite stable colorectal cancer.* Mol Cancer Ther, 2024.
497. Eulitz D. and Mannherz H. G., *Inhibition of deoxyribonuclease I by actin is to protect cells from premature cell death.* Apoptosis, 2007. **12**(8): p. 1511-21.
498. Belsky J. B., Morris D. C., Bouchebl R., Filbin M. R., Bobbitt K. R., Jaehne A. K. and Rivers E. P., *Plasma levels of F-actin and F:G-actin ratio as potential new biomarkers in patients with septic shock.* Biomarkers, 2016. **21**(2): p. 180-5.
499. Tullie S., Nicholson T., Bishop J. R. B., Mcgee K. C., Asiri A., Sullivan J., Chen Y. Y., Sardeli A. V., Belli A., Harrison P., Moiemen N. S., Lord J. M. and Hazeldine J., *Severe thermal and major traumatic injury results in elevated plasma concentrations of total heme that are associated with poor clinical outcomes and systemic immune suppression.* Front Immunol, 2024. **15**: p. 1416820.
500. Jeon K., Lee N., Jeong S., Park M. J. and Song W., *Immature granulocyte percentage for prediction of sepsis in severe burn patients: a machine leaning-based approach.* BMC Infect Dis, 2021. **21**(1): p. 1258.
501. Arneth B. M. and Menschikowki M., *Technology and new fluorescence flow cytometry parameters in hematological analyzers.* J Clin Lab Anal, 2015. **29**(3): p. 175-83.
502. Urrechaga E., *Reviewing the value of leukocytes cell population data (CPD) in the management of sepsis.* Ann Transl Med, 2020. **8**(15): p. 953.
503. Zhang W., Zhang Z., Pan S., Li J., Yang Y., Qi H., Xie J. and Qu J., *The clinical value of hematological neutrophil and monocyte parameters in the diagnosis and identification of sepsis.* Ann Transl Med, 2021. **9**(22): p. 1680.
504. Martens R. J. H., Van Adrichem A. J., Mattheij N. J. A., Brouwer C. G., Van Twist D. J. L., Broerse Jjcr, Magro-Checa C., Van Dongen C. M. P., Mostard R. L. M., Ramiro S., Landewe R. B. M. and Leers M. P. G., *Hemocytometric characteristics of COVID-19 patients with and without cytokine storm syndrome on the sysmex XN-10 hematology analyzer.* Clin Chem Lab Med, 2021. **59**(4): p. 783-793.

505. Garcia De Guadiana-Romualdo L., Diaz Lopez M. I., Crespo Alvarez E., Martinez Manzano A., Urrechaga E. and Orgaz Morales M. T., *Usefulness of the extended inflammatory parameters related to neutrophil activation reported on Sysmex XN-1000 haematology analyser as indicators of acute appendicitis: comparison with canonical inflammatory laboratory tests.* Scand J Clin Lab Invest, 2022. **82**(6): p. 492-494.
506. Urrechaga E., Mugertza G., Fernandez M., Espana P. P. and Aguirre U., *Leukocyte differential and reactive lymphocyte counts from Sysmex XN analyzer in the evaluation of SARS-CoV-2 infection.* Scand J Clin Lab Invest, 2021. **81**(5): p. 394-400.
507. Helms J., Meziani F., Mauvieux L. and Iba T., *The Detection of Neutrophil Activation by Automated Blood Cell Counter in Sepsis.* Juntendo Iji Zasshi, 2024. **70**(2): p. 114-117.
508. Kwiecien I., Rutkowska E., Gawronski K., Kulik K., Dudzik A., Zakrzewska A., Raniszewska A., Sawicki W. and Rzepecki P., *Usefulness of New Neutrophil-Related Hematologic Parameters in Patients with Myelodysplastic Syndrome.* Cancers (Basel), 2023. **15**(9).
509. Park S. H., Park C. J., Lee B. R., Nam K. S., Kim M. J., Han M. Y., Kim Y. J., Cho Y. U. and Jang S., *Sepsis affects most routine and cell population data (CPD) obtained using the Sysmex XN-2000 blood cell analyzer: neutrophil-related CPD NE-SFL and NE-WY provide useful information for detecting sepsis.* Int J Lab Hematol, 2015. **37**(2): p. 190-8.
510. Seo J. Y., Lee S. T. and Kim S. H., *Performance evaluation of the new hematology analyzer Sysmex XN-series.* Int J Lab Hematol, 2015. **37**(2): p. 155-64.
511. Mishra S., Chhabra G., Padhi S., Mohapatra S., Panigrahi A., Sable M. N. and Das P. K., *Usefulness of Leucocyte Cell Population Data by Sysmex XN1000 Hematology Analyzer in Rapid Identification of Acute Leukemia.* Indian J Hematol Blood Transfus, 2022. **38**(3): p. 499-507.
512. Johansson J., Sjogren F., Bodelsson M. and Sjoberg F., *Dynamics of leukocyte receptors after severe burns: an exploratory study.* Burns, 2011. **37**(2): p. 227-33.
513. Qiu L., Jin X., Wang J. J., Tang X. D., Fang X., Li S. J., Wang F. and Chen X. L., *Plasma Neutrophil-to-Lymphocyte Ratio on the Third Day Postburn is Associated with 90-Day Mortality Among Patients with Burns Over 30% of Total Body Surface Area in Two Chinese Burns Centers.* J Inflamm Res, 2021. **14**: p. 519-526.
514. Mulder P. P. G., Vlig M., Boekema Bkhl, Stoop M. M., Pijpe A., Van Zuijlen P. P. M., De Jong E., Van Cranenbroek B., Joosten I., Koenen Hjpm and Ulrich M. M. W., *Persistent Systemic Inflammation in Patients With Severe Burn Injury Is Accompanied by Influx of Immature Neutrophils and Shifts in T Cell Subsets and Cytokine Profiles.* Front Immunol, 2020. **11**: p. 621222.
515. Peter F. W., Schuschke D. A., Barker J. H., Fleishcher-Peter B., Pierangeli S., Vogt P. M. and Steinau H. U., *The effect of severe burn injury on proinflammatory cytokines and leukocyte behavior: its modulation with granulocyte colony-stimulating factor.* Burns, 1999. **25**(6): p. 477-86.
516. Prame Kumar K., Nicholls A. J. and Wong C. H. Y., *Partners in crime: neutrophils and monocytes/macrophages in inflammation and disease.* Cell Tissue Res, 2018. **371**(3): p. 551-565.
517. Kraus R. F. and Gruber M. A., *Neutrophils-From Bone Marrow to First-Line Defense of the Innate Immune System.* Front Immunol, 2021. **12**: p. 767175.
518. Sheats M. K., *A Comparative Review of Equine SIRS, Sepsis, and Neutrophils.* Front Vet Sci, 2019. **6**: p. 69.
519. V L., K K., E Y. and M S., *The Clinical Utility of Automated Immature Granulocyte Measurement in the Early Diagnosis of Bacteremia.* Cureus, 2024. **16**(2): p. e53660.
520. Williams H., Mack C., Baraz R., Marimuthu R., Naralashetty S., Li S. and Medbury H., *Monocyte Differentiation and Heterogeneity: Inter-Subset and Interindividual Differences.* Int J Mol Sci, 2023. **24**(10).

521. Bergmann C. B., Beckmann N., Salyer C. E., Hanschen M., Crisologo P. A. and Caldwell C. C., *Potential Targets to Mitigate Trauma- or Sepsis-Induced Immune Suppression.* Front Immunol, 2021. **12**: p. 622601.
522. Nourigheimasi S., Yazdani E., Ghaedi A., Khanzadeh M., Lucke-Wold B., Dioso E., Bazrgar A., Ebadi M. and Khanzadeh S., *Association of inflammatory biomarkers with overall survival in burn patients: a systematic review and meta-analysis.* BMC Emerg Med, 2024. **24**(1): p. 76.
523. Kremer V., Godon O., Bruhns P., Jonsson F. and De Chaisemartin L., *Isolation methods determine human neutrophil responses after stimulation.* Front Immunol, 2023. **14**: p. 1301183.
524. Luo Y., Lin J., Chen H., Zhang J., Peng S. and Kuang M., *Utility of neut-X, neut-Y and neut-Z parameters for rapidly assessing sepsis in tumor patients.* Clin Chim Acta, 2013. **422**: p. 5-9.
525. Stiel L., Delabranche X., Galoisy A. C., Severac F., Toti F., Mauvieux L., Meziani F. and Boisrame-Helms J., *Neutrophil Fluorescence: A New Indicator of Cell Activation During Septic Shock-Induced Disseminated Intravascular Coagulation.* Crit Care Med, 2016. **44**(11): p. e1132-e1136.
526. Cornet E., Boubaya M. and Troussard X., *Contribution of the new XN-1000 parameters NEUT-RI and NEUT-WY for managing patients with immature granulocytes.* Int J Lab Hematol, 2015. **37**(5): p. e123-6.
527. Rutkowska E., Kwiecien I., Kulik K., Chelstowska B., Klos K., Rzepecki P. and Chcialowski A., *Usefulness of the New Hematological Parameter: Reactive Lymphocytes RE-LYMP with Flow Cytometry Markers of Inflammation in COVID-19.* Cells, 2021. **10**(1).
528. Boomer J. S., To K., Chang K. C., Takasu O., Osborne D. F., Walton A. H., Bricker T. L., Jarman S. D., 2nd, Kreisel D., Krupnick A. S., Srivastava A., Swanson P. E., Green J. M. and Hotchkiss R. S., *Immunosuppression in patients who die of sepsis and multiple organ failure.* JAMA, 2011. **306**(23): p. 2594-605.
529. Ho S. F., Tan S. J., Mazlan M. Z., Iberahim S., Lee Y. X. and Hassan R., *Exploring Extended White Blood Cell Parameters for the Evaluation of Sepsis among Patients Admitted to Intensive Care Units.* Diagnostics (Basel), 2023. **13**(14).
530. Urrechaga E., Boveda O. and Aguirre U., *Improvement in detecting sepsis using leukocyte cell population data (CPD).* Clin Chem Lab Med, 2019. **57**(6): p. 918-926.
531. Gavillet M., Martinod K., Renella R., Harris C., Shapiro N. I., Wagner D. D. and Williams D. A., *Flow cytometric assay for direct quantification of neutrophil extracellular traps in blood samples.* Am J Hematol, 2015. **90**(12): p. 1155-8.
532. Fortier M., Chea M., Ain C., Loyens M., Boudemaghe T., Gris J. C. and Bouvier S., *Direct blood fluorescence signal intensity of neutrophils (NEU-SFL): A predictive marker of death in hospitalized COVID-19 patients?* Front Med (Lausanne), 2022. **9**: p. 1062112.
533. Yan C., Wu H., Fang X., He J. and Zhu F., *Platelet, a key regulator of innate and adaptive immunity.* Front Med (Lausanne), 2023. **10**: p. 1074878.
534. Smolle C., Cambiaso-Daniel J., Forbes A. A., Wurzer P., Hundeshagen G., Branski L. K., Huss F. and Kamolz L. P., *Recent trends in burn epidemiology worldwide: A systematic review.* Burns, 2017. **43**(2): p. 249-257.
535. Jeschke M. G., Van Baar M. E., Choudhry M. A., Chung K. K., Gibran N. S. and Logsetty S., *Burn injury.* Nat Rev Dis Primers, 2020. **6**(1): p. 11.
536. White J. G., *Effects of heat on platelet structure and function.* Blood, 1968. **32**(2): p. 324-35.
537. Rao G. H., Smith C. M., 2nd, Escolar G. and White J. G., *Influence of heat on platelet biochemistry, structure, and function.* J Lab Clin Med, 1993. **122**(4): p. 455-64.
538. Marck R. E., Montagne H. L., Tuinebreijer W. E. and Breederveld R. S., *Time course of thrombocytes in burn patients and its predictive value for outcome.* Burns, 2013. **39**(4): p. 714-22.

539. Huang X., Guo F., Zhou Z., Chang M., Wang F., Dou Y., Wang Z. and Huan J., *Relation between dynamic changes of platelet counts and 30-day mortality in severely burned patients.* Platelets, 2019. **30**(2): p. 158-163.
540. Guo F., Wang X., Huan J., Liang X., Chen B., Tang J. and Gao C., *Association of platelet counts decline and mortality in severely burnt patients.* J Crit Care, 2012. **27**(5): p. 529 e1-7.
541. Harrison P., *Platelet function analysis.* Blood Rev, 2005. **19**(2): p. 111-23.
542. Johnson B. Z., O'halloran E., Stevenson A. W., Wood F. M., Fear M. W. and Linden M. D., *Non-severe burn injury causes sustained platelet hyperreactivity.* Burns, 2024. **50**(3): p. 585-596.
543. Montague S. J., Delierneux C., Lecut C., Layios N., Dinsdale R. J., Lee C. S., Poulter N. S., Andrews R. K., Hampson P., Wearn C. M., Maes N., Bishop J., Bamford A., Gardiner C., Lee W. M., Iqbal T., Moiemen N., Watson S. P., Oury C., Harrison P. and Gardiner E. E., *Soluble GPVI is elevated in injured patients: shedding is mediated by fibrin activation of GPVI.* Blood Adv, 2018. **2**(3): p. 240-251.
544. Marck R. E., Van Der Bijl I., Korsten H., Lorinser J., De Korte D. and Middelkoop E., *Activation, function and content of platelets in burn patients.* Platelets, 2019. **30**(3): p. 396-402.
545. Lupia E., Bosco O., Mariano F., Dondi A. E., Goffi A., Spatola T., Cuccurullo A., Tizzani P., Brondino G., Stella M. and Montrucchio G., *Elevated thrombopoietin in plasma of burned patients without and with sepsis enhances platelet activation.* J Thromb Haemost, 2009. **7**(6): p. 1000-8.
546. Al Ghaithi R., Mori J., Nagy Z., Maclachlan A., Hardy L., Philippou H., Hethershaw E., Morgan N. V., Senis Y. A. and Harrison P., *Evaluation of the Total Thrombus-Formation System (T-TAS): application to human and mouse blood analysis.* Platelets, 2019. **30**(7): p. 893-900.
547. Zheng K. L., Wallen H., Aradi D., Godschalk T. C., Hackeng C. M., Dahlen J. R. and Ten Berg J. M., *The Total Thrombus Formation (T-TAS) platelet (PL) assay, a novel test that evaluates whole blood platelet thrombus formation under physiological conditions.* Platelets, 2022. **33**(2): p. 273-277.
548. Samanbar S., Pineyroa J. A., Moreno-Castano A. B., Pino M., Torramade-Moix S., Martinez-Sanchez J., Lozano M., Sanz C., Escolar G. and Diaz-Ricart M., *T-TAS((R)) 01 as a new tool for the evaluation of hemostasis in thrombocytopenic patients after platelet transfusion.* Blood Transfus, 2024. **22**(2): p. 166-175.
549. Posluszny J. A., Jr. and Gamelli R. L., *Anemia of thermal injury: combined acute blood loss anemia and anemia of critical illness.* J Burn Care Res, 2010. **31**(2): p. 229-42.
550. Randi A. M. and Laffan M. A., *Von Willebrand factor and angiogenesis: basic and applied issues.* J Thromb Haemost, 2017. **15**(1): p. 13-20.
551. Gragnano F., Sperlongano S., Golia E., Natale F., Bianchi R., Crisci M., Fimiani F., Pariggiano I., Diana V., Carbone A., Cesaro A., Concilio C., Limongelli G., Russo M. and Calabro P., *The Role of von Willebrand Factor in Vascular Inflammation: From Pathogenesis to Targeted Therapy.* Mediators Inflamm, 2017. **2017**: p. 5620314.
552. Lelas A., Greinix H. T., Wolff D., Eissner G., Pavletic S. Z. and Pulanic D., *Von Willebrand Factor, Factor VIII, and Other Acute Phase Reactants as Biomarkers of Inflammation and Endothelial Dysfunction in Chronic Graft-Versus-Host Disease.* Front Immunol, 2021. **12**: p. 676756.
553. Xu X., Kozar R., Zhang J. and Dong J. F., *Diverse activities of von Willebrand factor in traumatic brain injury and associated coagulopathy.* J Thromb Haemost, 2020. **18**(12): p. 3154-3162.
554. Plautz W. E., Raval J. S., Dyer M. R., Rollins-Raval M. A., Zuckerbraun B. S. and Neal M. D., *ADAMTS13: origins, applications, and prospects.* Transfusion, 2018. **58**(10): p. 2453-2462.

555. Cao W. J., Niiya M., Zheng X. W., Shang D. Z. and Zheng X. L., *Inflammatory cytokines inhibit ADAMTS13 synthesis in hepatic stellate cells and endothelial cells.* J Thromb Haemost, 2008. **6**(7): p. 1233-5.
556. Russell R. T., Mcdaniel J. K., Cao W., Shroyer M., Wagener B. M., Zheng X. L. and Pittet J. F., *Low Plasma ADAMTS13 Activity Is Associated with Coagulopathy, Endothelial Cell Damage and Mortality after Severe Paediatric Trauma.* Thromb Haemost, 2018. **118**(4): p. 676-687.
557. Matsumoto H., Takeba J., Umakoshi K., Kikuchi S., Ohshita M., Annen S., Moriyama N., Nakabayashi Y., Sato N. and Aibiki M., *ADAMTS13 activity decreases in the early phase of trauma associated with coagulopathy and systemic inflammation: a prospective observational study.* Thromb J, 2021. **19**(1): p. 17.
558. Ghirardello S., Lecchi A., Artoni A., Panigada M., Aliberti S., Scalambrino E., La Marca S., Boscarino M., Gramegna A., Properzi P., Abruzzese C., Blasi F., Grasselli G., Mosca F., Tripodi A. and Peyvandi F., *Assessment of Platelet Thrombus Formation under Flow Conditions in Adult Patients with COVID-19: An Observational Study.* Thromb Haemost, 2021. **121**(8): p. 1087-1096.
559. Ahmed A., Ahmed S. and Radegran G., *Plasma ADAMTS13 and von Willebrand factor in diagnosis and prediction of prognosis in pulmonary arterial hypertension.* Pulm Circ, 2021. **11**(4): p. 20458940211041500.
560. Grande Gutierrez N., Shankar K. N., Sinno T. and Diamond S. L., *Thrombosis and Hemodynamics: external and intrathrombus gradients.* Curr Opin Biomed Eng, 2021. **19**.
561. Giridharan G. A., Berg I. C., Ismail E., Nguyen K. T., Hecking J., Kirklin J. K., Cheng X. and Sethu P., *Loss of pulsatility with continuous-flow left ventricular assist devices and the significance of the arterial endothelium in von-Willebrand factor production and degradation.* Artif Organs, 2023. **47**(4): p. 640-648.
562. Arisz R. A., De Vries J. J., Schols S. E. M., Eikenboom J. C. J. and De Maat M. P. M., *Interaction of von Willebrand factor with blood cells in flow models: a systematic review.* Blood Adv, 2022. **6**(13): p. 3979-3990.
563. Meara C. H. O., Coupland L. A., Kordbacheh F., Quah B. J. C., Chang C. W., Simon Davis D. A., Bezos A., Browne A. M., Freeman C., Hammill D. J., Chopra P., Pipa G., Madge P. D., Gallant E., Segovis C., Dulhunty A. F., Arnolda L. F., Mitchell I., Khachigian L. M., Stephens R. W., Von Itzstein M. and Parish C. R., *Neutralizing the pathological effects of extracellular histones with small polyanions.* Nat Commun, 2020. **11**(1): p. 6408.

Appendix

Table 1: Neutrophil count in burns and HC									
	Medians			Sepsis .vs. Healthy Controls			No Sepsis .vs. Healthy Controls		
Day	Sepsis	No Sepsis	Healthy Controls	Estimate	95% CI	P-value	Estimate	95% CI	P-value
1	14.54	13.655	2.44	12.101	(9.31 to 14.45)	0	10.86	(7.76 to 13.95)	0
2	5.53	5.095	2.44	3.2	(1.76 to 5.29)	0	2.64	(1.16 to 4.61)	0
3	3.13	3.395	2.44	0.35	(-0.51 to 1.34)	0.546	0.722	(0.06 to 1.41)	0.028
4	2.96	2.84	2.44	0.3	(-0.54 to 1.33)	0.466	0.31	(-0.29 to 0.99)	0.316
5	3.755	3.385	2.44	1.174	(0.30 to 2.24)	0.011	0.866	(0.05 to 2.04)	0.032
6	4.475	4.955	2.44	1.897	(0.70 to 3.07)	0.002	2.133	(0.36 to 3.36)	0.01
7	8.24	6	2.44	5.309	(2.88 to 7.61)	0	3.36	(1.88 to 4.78)	0
14	8.625	7.71	2.44	5.978	(4.52 to 10.28)	0	5.311	(3.94 to 7.25)	0
28	8.415	4.55	2.44	6.069	(5.09 to 7.86)	0	1.93	(1.04 to 2.88)	0

Table 2: Neutrophil % in burns and HC									
	Medians			Sepsis .vs. Healthy Controls			No Sepsis .vs. Healthy Controls		
Day	Sepsis	No Sepsis	Healthy Controls	Estimate	95% CI	P-value	Estimate	95% CI	P-value
1	82.15	81.05	52.85	27.9	(24.4 to 31.8)	0	27.4	(23.2 to 31.6)	0
2	73.2	67.65	52.85	18.5	(11.3 to 23.9)	0	14	(9.1 to 19)	0
3	67.75	68.2	52.85	14.5	(7.4 to 20.4)	0	15.4	(10.5 to 21.3)	0
4	63.7	64.9	52.85	12.1	(4.9 to 19.8)	0.001	11.5	(6.5 to 16.6)	0
5	65.7	64	52.85	12.8	(7.7 to 18.2)	0	12.071	(5.9 to 18)	0
6	69.6	68.6	52.85	17.7	(12.8 to 24.5)	0	14.7	(9 to 19.5)	0
7	77.1	70.5	52.85	24.82	(19.9 to 29.8)	0	18.7	(14.7 to 24.3)	0
14	78.8	75.7	52.85	25.334	(21.4 to 29)	0	22.153	(17.9 to 25.6)	0
28	76.2	64.3	52.85	23.3	(18.7 to 27.9)	0	11.6	(6.2 to 17.6)	0

Table 3: Prognostic modelling of neutrophil counts for sepsis prediction in septic and non-septic burn							
Day	**Sepsis**		**Odds Ratio**		**AUROC**		**Brier Score**
	Yes	**No**	**OR**	**95% CI**	**AUROC**	**95% CI**	
1	42	40	1.026	(0.881 to 1.196)	0.533	(0.406 to 0.660)	0.250
2	37	32	1.179	(0.867 to 1.604)	0.540	(0.402 to 0.678)	0.245
3	40	38	1.049	(0.689 to 1.597)	0.539	(0.408 to 0.670)	0.250
4	37	31	1.064	(0.694 to 1.630)	0.481	(0.342 to 0.621)	0.248
5	40	32	1.126	(0.702 to 1.805)	0.516	(0.380 to 0.652)	0.246
6	34	30	1.243	(0.770 to 2.007)	0.483	(0.338 to 0.628)	0.246
7	37	31	1.379	(0.976 to 1.948)	0.618	(0.483 to 0.753)	0.234
14	34	29	1.340	(0.987 to 1.819)	0.594	(0.452 to 0.736)	0.235
28	26	23	2.452	(1.342 to 4.481)	0.776	(0.640 to 0.912)	0.192

Table 4: Lymphocyte count in burns and HC									
	Medians			**Sepsis .vs. Healthy Controls**			**No Sepsis .vs. Healthy Controls**		
Day	**Sepsis**	**No Sepsis**	**Healthy Controls**	**Estimate**	**95% CI**	**P-value**	**Estimate**	**95% CI**	**P-value**
1	1.62	1.385	1.74	-0.13	(-0.43 to 0.21)	0.416	-0.26	(-0.51 to 0.02)	0.066
2	1.4	1.29	1.74	-0.33	(-0.68 to 0.07)	0.108	-0.35	(-0.66 to 0.04)	0.077
3	0.865	0.855	1.74	-0.79	(-1 to -0.55)	0	-0.77	(-1 to -0.51)	0
4	0.78	0.95	1.74	-0.86	(-1.09 to -0.62)	0	-0.71	(-0.91 to -0.46)	0
5	0.875	1.07	1.74	-0.786	(-1.02 to -0.52)	0	-0.62	(-0.87 to -0.36)	0
6	0.75	0.97	1.74	-0.88	(-1.12 to -0.66)	0	-0.635	(-0.92 to -0.33)	0
7	1.06	1.04	1.74	-0.67	(-0.98 to -0.34)	0.001	-0.59	(-0.87 to -0.29)	0.001
14	1.6	1.67	1.74	-0.06	(-0.45 to 0.26)	0.663	-0.06	(-0.44 to 0.31)	0.732
28	1.57	1.83	1.74	-0.12	(-0.39 to 0.19)	0.469	0.08	(-0.24 to 0.47)	0.57

Table 5: Lymphocyte % in burns and HC									
	Medians			Sepsis .vs. Healthy Controls			No Sepsis .vs. Healthy Controls		
Day	Sepsis	No Sepsis	Healthy Controls	Estimate	95% CI	P-value	Estimate	95% CI	P-value
1	10.2	9	33.95	-24.4	(-27.4 to -21.2)	0	-24.3	(-27.1 to -21.2)	0
2	17.4	19.35	33.95	-16.4	(-21.6 to -10.9)	0	-15.22	(-19.5 to -10.8)	0
3	20	19.35	33.95	-14.2	(-18.6 to -9.7)	0	-14.9	(-19.1 to -9.6)	0
4	19.2	20.8	33.95	-15.071	(-21.1 to -8.7)	0	-13.611	(-18.2 to -8.7)	0
5	18.75	18.95	33.95	-16.876	(-20.6 to -12.7)	0	-15.2	(-19.2 to -11)	0
6	13.25	15.5	33.95	-20.5	(-24 to -16.4)	0	-17.543	(-20.9 to -13.4)	0
7	11.4	15.2	33.95	-22.7	(-26.2 to -19.7)	0	-19.347	(-23 to -15.8)	0
14	12.7	16.1	33.95	-20.9	(-24 to -17.6)	0	-18.508	(-21.7 to -15.2)	0
28	14.55	23.6	33.95	-20.091	(-24 to -16.7)	0	-10.112	(-14.1 to -5.6)	0

Table 6: Monocyte count in burns and HC									
	Medians			Sepsis .vs. Healthy Controls			No Sepsis .vs. Healthy Controls		
Day	Sepsis	No Sepsis	Healthy Controls	Estimate	95% CI	P-value	Estimate	95% CI	P-value
1	1.495	1.145	0.415	1.04	(0.69 to 1.34)	0	0.74	(0.56 to 1.02)	0
2	0.86	0.845	0.415	0.419	(0.19 to 0.61)	0	0.45	(0.29 to 0.68)	0
3	0.425	0.58	0.415	0.05	(-0.06 to 0.21)	0.457	0.17	(-0.01 to 0.4)	0.075
4	0.48	0.54	0.415	0.09	(-0.02 to 0.25)	0.1	0.17	(0.05 to 0.32)	0.005
5	0.575	0.66	0.415	0.2	(0.09 to 0.42)	0.001	0.24	(0.07 to 0.5)	0.002
6	0.63	0.74	0.415	0.24	(0.06 to 0.52)	0.017	0.33	(0.16 to 0.53)	0
7	0.74	0.82	0.415	0.32	(0.08 to 0.57)	0.006	0.375	(0.13 to 0.59)	0.001
14	0.72	0.84	0.415	0.29	(0.13 to 0.46)	0.001	0.35	(0.17 to 0.53)	0
28	0.73	0.58	0.415	0.33	(0.18 to 0.59)	0	0.16	(0.05 to 0.26)	0.005

Table 7: Prognostic modelling of monocyte counts for sepsis prediction in septic and non-septic burn							
Day	**Sepsis**		**Odds Ratio**		**AUROC**		**Brier Score**
	Yes	**No**	**OR**	**95% CI**	**AUROC**	**95% CI**	
1	42	40	1.004	(0.905 to 1.113)	0.564	(0.437 to 0.691)	0.250
2	37	32	0.913	(0.734 to 1.135)	0.442	(0.305 to 0.580)	0.246
3	40	38	0.85	(0.631 to 1.145)	0.568	(0.438 to 0.698)	0.246
4	37	31	0.933	(0.662 to 1.315)	0.567	(0.429 to 0.705)	0.248
5	40	32	1.028	(0.774 to 1.366)	0.495	(0.357 to 0.632)	0.247
6	34	30	0.945	(0.735 to 1.215)	0.550	(0.406 to 0.693)	0.248
7	37	31	1.013	(0.800 to 1.284)	0.507	(0.368 to 0.646)	0.248
14	34	29	1.076	(0.864 to 1.340)	0.510	(0.363 to 0.656)	0.244
28	26	23	1.991	(1.144 to 3.465)	0.696	(0.548 to 0.845)	0.216

Table 8: Monocyte % in burns and HC									
	Medians			**Sepsis .vs. Healthy Controls**			**No Sepsis .vs. Healthy Controls**		
Day	**Sepsis**	**No Sepsis**	**Healthy Controls**	**Estimate**	**95% CI**	**P-value**	**Estimate**	**95% CI**	**P-value**
1	7.45	7.95	7.75	-0.1	(-1.3 to 1.2)	0.91	0.1	(-1.3 to 1.4)	0.889
2	10.3	11.5	7.75	1.7	(-0.3 to 3.6)	0.101	3.6	(1.6 to 5.6)	0
3	9.7	11.6	7.75	1.775	(-0.1 to 3.8)	0.062	2.6	(0.3 to 5.1)	0.02
4	10.8	13	7.75	2.7	(0.9 to 4.2)	0.003	3.8	(1.3 to 6.5)	0.001
5	11.9	10.7	7.75	3.5	(1.3 to 5.8)	0.001	2.8	(0.6 to 5.4)	0.007
6	11.1	12.85	7.75	2.7	(0.4 to 4.6)	0.023	3.7	(1.4 to 6.6)	0.002
7	7.4	10	7.75	-0.5	(-2.3 to 1.4)	0.583	1.5	(-0.2 to 3.3)	0.095
14	6.25	7.4	7.75	-1.9	(-3.4 to -0.7)	0.004	-0.9	(-2.3 to 0.4)	0.183
28	6.9	7.7	7.75	-1.5	(-2.6 to -0.1)	0.031	-0.4	(-1.7 to 0.7)	0.517

Table 9: Eosinophil count in burns and HC									
	Medians			Sepsis .vs. Healthy Controls			No Sepsis .vs. Healthy Controls		
Day	Sepsis	No Sepsis	Healthy Controls	Estimate	95% CI	P-value	Estimate	95% CI	P-value
1	0.01	0.015	0.16	-0.14	(-0.19 to -0.1)	0	-0.13	(-0.17 to -0.09)	0
2	0.02	0.02	0.16	-0.13	(-0.18 to -0.09)	0	-0.13	(-0.19 to -0.09)	0
3	0.045	0.025	0.16	-0.11	(-0.16 to -0.05)	0	-0.13	(-0.19 to -0.09)	0
4	0.1	0.05	0.16	-0.06	(-0.13 to 0)	0.059	-0.1	(-0.16 to -0.05)	0
5	0.15	0.07	0.16	-0.05	(-0.11 to 0.03)	0.193	-0.08	(-0.14 to -0.02)	0.014
6	0.1	0.075	0.16	-0.07	(-0.13 to -0.02)	0.012	-0.08	(-0.14 to -0.03)	0.002
7	0.12	0.1	0.16	-0.06	(-0.12 to -0.01)	0.023	-0.06	(-0.13 to 0)	0.045
14	0.12	0.1	0.16	-0.05	(-0.12 to 0)	0.078	-0.06	(-0.12 to 0.01)	0.087
28	0.215	0.12	0.16	0.05	(-0.05 to 0.12)	0.3	-0.04	(-0.11 to 0.05)	0.351

Table 10: Eosinophil % in burns and HC									
	Medians			Sepsis .vs. Healthy Controls			No Sepsis .vs. Healthy Controls		
Day	Sepsis	No Sepsis	Healthy Controls	Estimate	95% CI	P-value	Estimate	95% CI	P-value
1	0.05	0.1	2.85	-2.6	(-3.2 to -2)	0	-2.6	(-3.2 to -2)	0
2	0.3	0.2	2.85	-2.4	(-3.2 to -1.8)	0	-2.4	(-3.2 to -1.8)	0
3	1.05	0.35	2.85	-1.801	(-2.7 to -1)	0	-2.2	(-3.1 to -1.7)	0
4	2.1	1.2	2.85	-0.856	(-1.8 to 0.3)	0.11	-1.7	(-2.7 to -1)	0
5	2.15	1.4	2.85	-0.8	(-1.7 to 0.4)	0.198	-1.3	(-2.3 to -0.4)	0.009
6	1.45	1.65	2.85	-1.2	(-2.1 to -0.3)	0.014	-1.3	(-2.3 to -0.3)	0.005
7	1.3	1.4	2.85	-1.7	(-2.6 to -0.9)	0	-1.4	(-2.5 to -0.6)	0.004
14	0.95	1.1	2.85	-1.9	(-2.8 to -1.1)	0	-1.7	(-2.6 to -0.9)	0
28	1.95	1.6	2.85	-0.9	(-2 to 0)	0.043	-1.1	(-2.1 to -0.1)	0.036

Table 11: IG count in burns and HC									
	Medians			Sepsis .vs. Healthy Controls			No Sepsis .vs. Healthy Controls		
Day	Sepsis	No Sepsis	Healthy Controls	Estimate	95% CI	P-value	Estimate	95% CI	P-value
1	0.14	0.1	0.03	0.11	(0.06 to 0.15)	0	0.07	(0.04 to 0.11)	0
2	0.04	0.03	0.03	0.01	(-0.01 to 0.03)	0.33	0	(-0.01 to 0.01)	0.823
3	0.025	0.02	0.03	0	(-0.01 to 0.02)	0.782	0	(-0.01 to 0)	0.245
4	0.06	0.04	0.03	0.03	(0 to 0.06)	0.013	0.01	(0 to 0.04)	0.044
5	0.165	0.09	0.03	0.14	(0.09 to 0.25)	0	0.06	(0.03 to 0.21)	0
6	0.27	0.165	0.03	0.24	(0.14 to 0.43)	0	0.14	(0.09 to 0.42)	0
7	0.51	0.22	0.03	0.48	(0.27 to 0.88)	0	0.19	(0.12 to 0.45)	0
14	0.57	0.14	0.03	0.54	(0.25 to 0.84)	0	0.12	(0.07 to 0.34)	0
28	0.175	0.04	0.03	0.145	(0.09 to 0.28)	0	0.02	(0 to 0.06)	0.01

Table 12: IG % in burns and HC									
	Medians			Sepsis .vs. Healthy Controls			No Sepsis .vs. Healthy Controls		
Day	Sepsis	No Sepsis	Healthy Controls	Estimate	95% CI	P-value	Estimate	95% CI	P-value
1	0.8	0.6	0.5	0.3	(0 to 0.5)	0.015	0	(-0.1 to 0.2)	0.544
2	0.5	0.3	0.5	-0.1	(-0.2 to 0.1)	0.459	-0.2	(-0.3 to -0.1)	0.003
3	0.6	0.4	0.5	0.1	(-0.1 to 0.3)	0.314	-0.1	(-0.2 to 0)	0.199
4	0.9	1	0.5	0.4	(0.2 to 1)	0.001	0.4	(0.1 to 0.8)	0.007
5	3.1	2.05	0.5	2.5	(1.7 to 4.7)	0	1.439	(0.7 to 3.1)	0
6	5.85	3.9	0.5	5.3	(2.4 to 6.2)	0	3.4	(1.4 to 5.7)	0
7	5.9	3.7	0.5	5.4	(3.5 to 7.2)	0	3.3	(1.4 to 5.1)	0
14	4.6	1.5	0.5	4.1	(2.8 to 6)	0	1	(0.5 to 3.7)	0
28	1.55	0.6	0.5	1.1	(0.4 to 2.2)	0	0.1	(-0.1 to 0.4)	0.17

Table 13: Prognostic modelling of IG count for sepsis prediction in septic and non-septic burn							
Day	**Sepsis**		**Odds Ratio**		**AUROC**		**Brier Score**
	Yes	**No**	**OR**	**95% CI**	**AUROC**	**95% CI**	
1	42	40	1.008	(0.899 to 1.130)	0.583	(0.458 to 0.708)	0.250
2	37	32	2.273	(0.854 to 6.050)	0.559	(0.423 to 0.695)	0.238
3	40	38	1.498	(0.551 to 4.076)	0.578	(0.450 to 0.705)	0.247
4	37	31	1.173	(0.755 to 1.822)	0.541	(0.402 to 0.680)	0.246
5	40	32	1.112	(0.942 to 1.312)	0.651	(0.517 to 0.785)	0.241
6	34	30	1.102	(0.963 to 1.261)	0.595	(0.453 to 0.736)	0.241
7	37	31	1.079	(0.995 to 1.170)	0.664	(0.533 to 0.795)	0.233
14	34	29	1.079	(0.996 to 1.168)	0.712	(0.582 to 0.843)	0.228
28	26	23	1.128	(0.941 to 1.353)	0.753	(0.610 to 0.895)	0.234

Table 14: Prognostic modelling of IG % for sepsis prediction in septic and non-septic burn							
Day	**Sepsis**		**Odds Ratio**		**AUROC**		**Brier Score**
	Yes	**No**	**OR**	**95% CI**	**AUROC**	**95% CI**	
1	42	40	1.331	(0.745 to 2.378)	0.628	(0.506 to 0.750)	0.246
2	37	32	7.765	(1.237 to 48.735)	0.632	(0.501 to 0.763)	0.231
3	40	38	2.587	(0.918 to 7.295)	0.645	(0.521 to 0.768)	0.237
4	37	31	1.105	(0.844 to 1.448)	0.459	(0.319 to 0.598)	0.246
5	40	32	1.072	(0.961 to 1.196)	0.626	(0.494 to 0.757)	0.240
6	34	30	1.106	(0.966 to 1.268)	0.613	(0.472 to 0.754)	0.241
7	37	31	1.117	(0.986 to 1.266)	0.643	(0.508 to 0.778)	0.236
14	34	29	1.193	(1.026 to 1.387)	0.699	(0.564 to 0.835)	0.223
28	26	23	1.186	(0.907 to 1.553)	0.707	(0.559 to 0.855)	0.236

Table 15: Neutrophil X in burns and HC									
	Medians			Sepsis .vs. Healthy Controls			No Sepsis .vs. Healthy Controls		
Day	Sepsis	No Sepsis	Healthy Controls	Estimate	95% CI	P-value	Estimate	95% CI	P-value
1	315.5	310	302	15	(8 to 22)	0	7	(1 to 14)	0.032
2	309	301.5	302	8	(2 to 15)	0.019	3	(-4 to 12)	0.383
3	302.5	299	302	0	(-10 to 11)	0.947	-1.596	(-8 to 6)	0.701
4	299	296	302	-3	(-9 to 4)	0.48	-1	(-9 to 6)	0.652
5	309	302	302	9	(0 to 19)	0.059	2	(-8 to 14)	0.628
6	323	320.5	302	25	(17 to 33)	0	21	(9 to 31)	0.001
7	331	318	302	30	(20 to 42)	0	20	(12 to 29)	0
14	355	335	302	56	(46 to 68)	0	35	(23 to 48)	0
28	323.5	323	302	22	(13 to 30)	0	23.359	(14 to 33)	0

Table 16: Prognostic modelling of neutrophil X for sepsis prediction in septic and non-septic burn							
Day	Sepsis		Odds Ratio		AUROC		Brier Score
	Yes	No	OR	95% CI	AUROC	95% CI	
1	42	40	2.010	(1.076 to 3.754)	0.657	(0.539 to 0.775)	0.233
2	37	32	1.380	(0.734 to 2.595)	0.580	(0.440 to 0.720)	0.245
3	40	38	1.084	(0.690 to 1.704)	0.522	(0.390 to 0.655)	0.249
4	37	31	0.941	(0.529 to 1.673)	0.493	(0.353 to 0.634)	0.248
5	40	32	1.186	(0.866 to 1.623)	0.579	(0.443 to 0.714)	0.241
6	34	30	1.208	(0.803 to 1.816)	0.575	(0.429 to 0.720)	0.245
7	37	31	1.476	(0.930 to 2.343)	0.627	(0.492 to 0.762)	0.237
14	34	29	1.574	(1.076 to 2.303)	0.700	(0.566 to 0.835)	0.222
28	26	23	0.816	(0.468 to 1.421)	0.476	(0.309 to 0.642)	0.246

Table 17: Neutrophil Y in burns and HC									
	Medians			Sepsis .vs. Healthy Controls			No Sepsis .vs. Healthy Controls		
Day	Sepsis	No Sepsis	Healthy Controls	Estimate	95% CI	P-value	Estimate	95% CI	P-value
1	727.5	717.5	600	120	(93 to 149)	0	111	(79 to 146)	0
2	762	725.5	600	144	(107 to 179)	0	132	(97 to 168)	0
3	799.5	721.5	600	190	(150 to 239)	0	127	(84 to 173)	0
4	754	700	600	166	(131 to 215)	0	103	(74 to 146)	0
5	822.5	696.5	600	223.742	(174 to 283)	0	110	(70 to 193)	0
6	924	792	600	315	(250 to 370)	0	190.499	(112 to 263)	0
7	830	747	600	229.5	(177 to 291)	0	132	(73 to 216)	0
14	789.5	710	600	200.256	(156 to 268)	0	101	(48 to 141)	0
28	665	629	600	52	(26 to 79)	0	33.788	(5 to 61)	0.018

Table 18: Prognostic modelling of neutrophil Y for sepsis prediction in septic and non-septic burn							
Day	Sepsis		Odds Ratio		AUROC		Brier Score
	Yes	No	OR	95% CI	AUROC	95% CI	
1	42	40	1.011	(0.737 to 1.385)	0.538	(0.410 to 0.666)	0.250
2	37	32	1.228	(0.789 to 1.912)	0.545	(0.406 to 0.684)	0.246
3	40	38	1.600	(1.126 to 2.273)	0.692	(0.574 to 0.811)	0.225
4	37	31	1.391	(0.976 to 1.984)	0.670	(0.535 to 0.805)	0.234
5	40	32	1.078	(0.931 to 1.248)	0.677	(0.545 to 0.809)	0.242
6	34	30	1.318	(1.055 to 1.647)	0.692	(0.560 to 0.823)	0.223
7	37	31	1.384	(1.049 to 1.827)	0.684	(0.551 to 0.818)	0.225
14	34	29	1.318	(1.028 to 1.689)	0.748	(0.621 to 0.876)	0.221
28	26	23	1.016	(0.643 to 1.605)	0.595	(0.428 to 0.762)	0.249

Table 19: Neutrophil Z in burns and HC									
	Medians			Sepsis .vs. Healthy Controls			No Sepsis .vs. Healthy Controls		
Day	Sepsis	No Sepsis	Healthy Controls	Estimate	95% CI	P-value	Estimate	95% CI	P-value
1	573	581.5	589.5	-4.946	(-29 to 22)	0.777	-7	(-25 to 12)	0.453
2	578	582	589.5	-2	(-26 to 25)	0.826	-1	(-26 to 21)	0.853
3	592	589.5	589.5	12	(-11 to 40)	0.27	2	(-14 to 26)	0.848
4	598	592	589.5	14.426	(-4 to 37)	0.138	2	(-16 to 26)	0.691
5	611.5	613.5	589.5	31	(6 to 68)	0.011	45	(11 to 76)	0.005
6	640	625	589.5	62	(36 to 91)	0	43	(13 to 73)	0.008
7	631	628	589.5	50	(25 to 75)	0	43	(18 to 68)	0.002
14	686.5	626	589.5	98	(67 to 141)	0	51	(20 to 88)	0.001
28	584.5	599	589.5	4	(-19 to 35)	0.634	16	(-6 to 41)	0.128

Table 20: Prognostic modelling of neutrophil Z for sepsis prediction in septic and non-septic burn							
Day	Sepsis		Odds Ratio		AUROC		Brier Score
	Yes	No	OR	95% CI	AUROC	95% CI	
1	42	40	1.151	(0.785 to 1.687)	0.497	(0.368 to 0.626)	0.248
2	37	32	0.941	(0.735 to 1.204)	0.492	(0.351 to 0.632)	0.248
3	40	38	1.166	(0.827 to 1.643)	0.540	(0.410 to 0.671)	0.247
4	37	31	1.553	(0.927 to 2.604)	0.589	(0.451 to 0.728)	0.238
5	40	32	0.983	(0.810 to 1.192)	0.520	(0.382 to 0.657)	0.247
6	34	30	1.219	(0.891 to 1.668)	0.601	(0.458 to 0.744)	0.242
7	37	31	1.138	(0.807 to 1.605)	0.547	(0.408 to 0.686)	0.246
14	34	29	1.334	(1.012 to 1.758)	0.652	(0.513 to 0.790)	0.231
28	26	23	0.793	(0.449 to 1.400)	0.578	(0.414 to 0.742)	0.246

Table 21: Neutrophil RI in burns and HC									
	Medians			Sepsis .vs. Healthy Controls			No Sepsis .vs. Healthy Controls		
Day	Sepsis	No Sepsis	Healthy Controls	Estimate	95% CI	P-value	Estimate	95% CI	P-value
1	50.6	50.8	47	4.053	(2.1 to 6.1)	0	4.137	(2.3 to 6)	0
2	60.2	58.9	47	12.938	(8.6 to 18)	0	11.6	(8.8 to 14.8)	0
3	66.45	63.7	47	18.9	(15.8 to 23)	0	17.5	(14.6 to 20.7)	0
4	71.7	67	47	24.049	(21.3 to 27.5)	0	20.2	(16.2 to 25.3)	0
5	72.5	63.9	47	25.7	(21.5 to 31.6)	0	18.58	(13.7 to 25.1)	0
6	79.4	70.2	47	32.15	(25.7 to 40.1)	0	22.219	(13.5 to 28.1)	0
7	80.4	61.75	47	33.6	(28.1 to 38)	0	16	(11.7 to 24.6)	0
14	65.05	53.4	47	18.2	(12.1 to 24)	0	5.9	(3 to 9.8)	0
28	54.8	48.7	47	7	(3.7 to 14)	0	2.1	(-0.4 to 5.9)	0.108

Table 22: Prognostic modelling of neutrophil RI for sepsis prediction in septic and non-septic burn							
Day	Sepsis		Odds Ratio		AUROC		Brier Score
	Yes	No	OR	95% CI	AUROC	95% CI	
1	35	34	0.913	(0.658 to 1.267)	0.500	(0.361 to 0.640)	0.247
2	34	30	0.998	(0.946 to 1.052)	0.543	(0.398 to 0.688)	0.249
3	36	33	1.522	(0.863 to 2.685)	0.572	(0.435 to 0.709)	0.242
4	35	29	0.968	(0.886 to 1.057)	0.619	(0.475 to 0.763)	0.245
5	36	27	2.063	(1.214 to 3.504)	0.703	(0.571 to 0.835)	0.212
6	33	29	1.823	(1.200 to 2.770)	0.718	(0.590 to 0.846)	0.215
7	33	26	1.999	(1.272 to 3.141)	0.771	(0.639 to 0.903)	0.192
14	30	24	2.444	(1.325 to 4.507)	0.742	(0.604 to 0.880)	0.202
28	22	19	1.875	(0.896 to 3.925)	0.682	(0.511 to 0.852)	0.231

Table 23: Neutrophil GI in burns and HC									
	Medians			Sepsis .vs. Healthy Controls			No Sepsis .vs. Healthy Controls		
Day	Sepsis	No Sepsis	Healthy Controls	Estimate	95% CI	P-value	Estimate	95% CI	P-value
1	156.3	157.75	153.5	3.3	(0.9 to 5.4)	0.008	4.058	(2 to 6)	0.001
2	157.4	158.55	153.5	4.3	(2.1 to 6.4)	0.001	5.3	(3.1 to 7.6)	0
3	157.35	158.4	153.5	4.8	(2.6 to 7.2)	0	5.383	(3.3 to 7.6)	0
4	158.4	157.7	153.5	4.8	(2.8 to 6.8)	0	4.6	(2.4 to 6.9)	0
5	155	153.6	153.5	1.9	(-0.2 to 4)	0.091	0.9	(-1.5 to 3.4)	0.507
6	156.4	154.8	153.5	2.7	(-0.2 to 4.7)	0.07	1.2	(-1.3 to 3.5)	0.332
7	155.9	155.15	153.5	2.5	(-0.1 to 5)	0.075	1.7	(-0.9 to 4.4)	0.175
14	154.65	157.05	153.5	1.7	(-1.2 to 4.1)	0.218	3.3	(0.3 to 5.6)	0.035
28	155.15	155.3	153.5	3.324	(0.3 to 6.5)	0.019	2.1	(-0.3 to 4.5)	0.082

Table 24: Lymphocyte RE count in burns and HC									
	Medians			Sepsis .vs. Healthy Controls			No Sepsis .vs. Healthy Controls		
Day	Sepsis	No Sepsis	Healthy Controls	Estimate	95% CI	P-value	Estimate	95% CI	P-value
1	0.06	0.05	0.06	0	(-0.02 to 0.04)	0.782	-0.01	(-0.02 to 0.01)	0.217
2	0.07	0.07	0.06	0.01	(-0.01 to 0.04)	0.457	0	(-0.018 to 0.02)	0.864
3	0.04	0.05	0.06	-0.02	(-0.04 to 0)	0.135	-0.02	(-0.04 to 0.01)	0.186
4	0.05	0.06	0.06	-0.02	(-0.03 to 0)	0.101	0	(-0.02 to 0.02)	1
5	0.09	0.07	0.06	0.022	(0 to 0.05)	0.029	0.01	(-0.01 to 0.04)	0.386
6	0.11	0.09	0.06	0.05	(0 to 0.12)	0.033	0.034	(0.01 to 0.07)	0.019
7	0.15	0.11	0.06	0.09	(0.01 to 0.19)	0.013	0.04	(0.01 to 0.1)	0.003
14	0.31	0.225	0.06	0.25	(0.17 to 0.33)	0	0.15	(0.09 to 0.24)	0
28	0.225	0.14	0.06	0.16	(0.11 to 0.21)	0	0.09	(0.04 to 0.19)	0

Table 25: Prognostic modelling of lymphocyte RE count for sepsis prediction in septic and non-septic burn							
Day	**Sepsis**		**Odds Ratio**		**AUROC**		**Brier Score**
	Yes	**No**	**OR**	**95% CI**	**AUROC**	**95% CI**	
1	33	32	1.266	(0.742 to 2.160)	0.570	(0.425 to 0.714)	0.247
2	29	25	1.586	(0.733 to 3.430)	0.541	(0.385 to 0.697)	0.243
3	23	25	1.567	(0.579 to 4.243)	0.503	(0.336 to 0.671)	0.246
4	21	22	0.888	(0.309 to 2.546)	0.628	(0.457 to 0.798)	0.250
5	30	23	1.488	(0.570 to 3.885)	0.570	(0.408 to 0.733)	0.243
6	27	25	1.015	(0.750 to 1.373)	0.549	(0.387 to 0.711)	0.250
7	25	23	1.115	(0.792 to 1.569)	0.543	(0.372 to 0.713)	0.247
14	26	24	1.149	(0.856 to 1.541)	0.599	(0.436 to 0.763)	0.245
28	20	18	1.223	(0.719 to 2.079)	0.621	(0.431 to 0.810)	0.245

Table 26: Lymphocyte RE% in burns and HC									
	Medians			**Sepsis .vs. Healthy Controls**			**No Sepsis .vs. Healthy Controls**		
Day	**Sepsis**	**No Sepsis**	**Healthy Controls**	**Estimate**	**95% CI**	**P-value**	**Estimate**	**95% CI**	**P-value**
1	0.4	0.3	1.3	-0.8	(-1 to -0.5)	0	-0.8	(-1.1 to -0.6)	0
2	0.8	0.6	1.3	-0.4	(-0.7 to 0)	0.054	-0.445	(-0.7 to -0.1)	0.013
3	0.7	0.9	1.3	-0.5	(-0.8 to -0.1)	0.016	-0.4	(-0.8 to 0)	0.049
4	0.8	1.1	1.3	-0.3	(-0.6 to 0)	0.073	-0.2	(-0.5 to 0.3)	0.495
5	1.4	1.2	1.3	0.1	(-0.2 to 0.6)	0.419	0	(-0.4 to 0.4)	0.927
6	1.7	1.7	1.3	0.4	(-0.2 to 0.9)	0.162	0.4	(-0.2 to 0.7)	0.155
7	1.5	1.5	1.3	0.293	(-0.3 to 1)	0.393	0.2	(-0.2 to 0.5)	0.374
14	2.25	2.55	1.3	1.1	(0.7 to 1.6)	0	1.374	(0.8 to 2)	0
28	1.85	2.25	1.3	0.6	(0.2 to 1.2)	0.009	0.9	(0.4 to 1.5)	0.001

Table 27: Monocyte X in burns and HC									
	Medians			Sepsis .vs. Healthy Controls			No Sepsis .vs. Healthy Controls		
Day	Sepsis	No Sepsis	Healthy Controls	Estimate	95% CI	P-value	Estimate	95% CI	P-value
1	120.15	120.4	118.9	1.3	(0.4 to 2.3)	0.003	1.306	(0.3 to 2.3)	0.016
2	123.3	123.25	118.9	4.3	(2.8 to 5.8)	0	4.274	(2.8 to 5.5)	0
3	125.55	123.9	118.9	6.4	(4.7 to 7.9)	0	5.2	(3.6 to 6.8)	0
4	126.6	125.4	118.9	7.1	(5 to 8.8)	0	6.2	(4.4 to 8.4)	0
5	125.95	123.1	118.9	6.9	(5.5 to 8.4)	0	4.3	(2.9 to 6.9)	0
6	125.7	124.25	118.9	7	(5.7 to 8.3)	0	5.1	(3.6 to 6.5)	0
7	125.4	122.6	118.9	6.3	(4.8 to 7.7)	0	4.3	(3 to 6)	0
14	123.95	122.1	118.9	4.837	(3.5 to 6)	0	3.385	(2.2 to 4.8)	0
28	122.45	121.6	118.9	3.471	(2.1 to 4.9)	0	2.6	(1.3 to 3.9)	0.002

Table 28: Prognostic modelling of monocyte X for sepsis prediction in septic and non-septic burn							
Day	Sepsis		Odds Ratio		AUROC		Brier Score
	Yes	No	OR	95% CI	AUROC	95% CI	
1	42	40	1.252	(0.771 to 2.032)	0.469	(0.341 to 0.597)	0.247
2	37	32	1.184	(0.805 to 1.740)	0.529	(0.390 to 0.668)	0.246
3	40	38	1.222	(0.914 to 1.633)	0.584	(0.456 to 0.712)	0.244
4	37	31	1.026	(0.735 to 1.433)	0.540	(0.400 to 0.679)	0.248
5	40	32	1.62	(1.111 to 2.360)	0.674	(0.547 to 0.801)	0.221
6	34	30	1.501	(1.005 to 2.240)	0.657	(0.519 to 0.794)	0.231
7	37	31	1.478	(0.991 to 2.205)	0.646	(0.512 to 0.780)	0.234
14	34	29	1.387	(0.925 to 2.080)	0.606	(0.463 to 0.749)	0.238
28	26	23	1.267	(0.790 to 2.033)	0.574	(0.407 to 0.740)	0.244

Table 29: Monocyte Y in burns and HC									
	Medians			Sepsis .vs. Healthy Controls			No Sepsis .vs. Healthy Controls		
Day	Sepsis	No Sepsis	Healthy Controls	Estimate	95% CI	P-value	Estimate	95% CI	P-value
1	108.05	112.55	115.4	-6.9	(-10 to -3.5)	0	-3.9	(-7.2 to -0.2)	0.035
2	119	122.5	115.4	4.4	(0.3 to 9.2)	0.033	6.417	(2.5 to 11.5)	0.004
3	126.9	127.4	115.4	11.199	(5.7 to 16.9)	0	10.726	(6 to 15.5)	0
4	131.6	130.7	115.4	17.6	(12.1 to 22.2)	0	16.358	(10.7 to 21.8)	0
5	129	123.8	115.4	13.6	(9.3 to 18.3)	0	7.3	(1.6 to 12.7)	0.01
6	123.8	117.25	115.4	9.85	(4.3 to 15.5)	0.001	2.8	(-1.5 to 7.8)	0.173
7	120	115.4	115.4	6.064	(1.4 to 11.8)	0.007	0.6	(-3.9 to 5.4)	0.787
14	117.2	114.4	115.4	2.449	(-2 to 6.9)	0.29	-2	(-6.4 to 3)	0.512
28	116.95	117.3	115.4	2.54	(-1.7 to 6.4)	0.242	2.2	(-1.6 to 6.3)	0.256

Table 30: Monocyte Z in burns and HC									
	Medians			Sepsis .vs. Healthy Controls			No Sepsis .vs. Healthy Controls		
Day	Sepsis	No Sepsis	Healthy Controls	Estimate	95% CI	P-value	Estimate	95% CI	P-value
1	70.05	69.15	68.5	1.6	(0.5 to 2.6)	0.005	0.9	(-0.2 to 2)	0.096
2	69.8	69.65	68.5	1.4	(0.2 to 2.6)	0.022	1.3	(0.2 to 2.4)	0.025
3	69.2	69.4	68.5	1	(-0.1 to 2.2)	0.07	0.7	(-0.4 to 1.9)	0.206
4	68.9	69.4	68.5	0.3	(-0.9 to 1.4)	0.594	0.8	(-0.5 to 2.1)	0.23
5	68.2	67.8	68.5	0	(-1.1 to 1.3)	0.953	-0.6	(-1.8 to 0.7)	0.36
6	67.15	68.7	68.5	-1.2	(-2.5 to 0)	0.055	0.1	(-1.5 to 1.8)	0.904
7	67.3	68.1	68.5	-0.9	(-2.3 to 0.4)	0.168	-0.4	(-1.8 to 0.8)	0.498
14	66.05	67	68.5	-2.553	(-4.1 to -1)	0.002	-1.9	(-3.9 to -0.1)	0.036
28	67.9	69.5	68.5	-0.6	(-2 to 0.9)	0.469	0.5	(-0.9 to 1.6)	0.532

Table 31: A compression between SIFTI2 and SIFTI1 in the combined model of cfDNA and IGs levels in sever thermal injuries.								
	SIFTI2				**SIFTI 1**			
	Sepsis		**AUROC**		**Sepsis**		**AUROC**	
Day	**Yes**	**No**	**AUROC**	**95% CI**	**Yes**	**No**	**AUROC**	**95% CI**
1	39	39	0.593	(0.465 to 0.721)	24	9	0.829	(0.684 to 0.973)
3	36	36	0.630	(0.499 to 0.762)	26	10	0.515	(0.297 to 0.734)
7	35	31	0.725	(0.600 to 0.851)	29	9	0.750	(0.551 to 0.949)
14	31	29	0.796	(0.679 to 0.914)	33	10	0.791	(0.609 to 0.974)

Table 32: Correlation between VWF and cfDNA levels in severe thermal injuries.					
	No.	**correlation (Y/N)**	**P value**	**R^2 value**	**Pearson r**
DAY 1	63	N	0.5408	0.006164	0.07851
DAY 2	58	N	0.9895	0.000003149	0.001774
DAY 3	57	N	0.1676	0.03433	0.1853
DAY 4	53	Y *	0.0212	0.09983	0.316
DAY 5	54	Y *	0.0125	0.114	0.3376
DAY 6	46	N	0.1002	0.06022	0.2454
DAY 7	46	Y **	0.0031	0.1826	0.4273
DAY 8	44	Y **	0.0032	0.1885	0.4342
DAY 9	45	Y **	0.0014	0.2135	0.4621
DAY 10	46	Y ****	<0.0001	0.294	0.5422
DAY 11	43	Y ****	<0.0001	0.4522	0.6725
DAY 12	41	Y **	0.0015	0.2294	0.479
DAY 13	39	Y **	0.0025	0.2211	0.4702
DAY 14	40	Y *	0.0293	0.119	0.3449
DAY 28	28	N	0.5568	0.01344	-0.1159
Overall	708	Y ****	<0.0001	0.04957	0.2226

Table 33: Correlation between VWF and neutrophil Y levels in severe thermal injuries.					
	No.	**correlation (Y/N)**	**P value**	**R^2 value**	**Pearson r**
DAY 1	63	N	0.3707	0.01316	0.1147
DAY 2	54	N	0.853	0.000667	0.02582
DAY 3	59	N	0.9154	0.0002	0.01413
DAY 4	48	N	0.5363	0.008369	-0.09148
DAY 5	53	N	0.5813	0.006006	0.0775
DAY 6	38	N	0.5629	0.009385	0.09688
DAY 7	46	Y *	0.0415	0.09108	0.3018
DAY 8	38	N	0.275	0.033	0.1817
DAY 9	40	Y **	0.0021	0.2236	0.4728
DAY 10	46	Y ***	0.0001	0.2862	0.535
DAY 11	37	Y ***	0.0001	0.3506	0.5921
DAY 12	41	Y **	0.0022	0.2153	0.464
DAY 13	33	Y **	0.0042	0.2355	0.4853
DAY 14	43	Y *	0.0351	0.1038	0.3222
DAY 28	31	N	0.9338	0.000242	-0.01555
Overall	680	Y ****	<0.0001	0.04607	0.2146

Table 34: Correlation between neutrophil ADAMTS13 and cfDNA levels in severe thermal injuries					
	No.	**correlation (Y/N)**	**P value**	**R^2 value**	**Pearson r**
DAY 1	62	N	0.3009	0.01782	0.1335
DAY 2	59	N	0.9027	0.0002645	0.01626
DAY 3	58	N	0.6414	0.0039	0.06245
DAY 4	54	N	0.8676	0.02019	0.02322
DAY 5	54	N	0.3054	0.114	-0.1421
DAY 6	46	Y *	0.0324	0.09982	-0.3159
DAY 7	45	N	0.1634	0.04467	-0.2114
DAY 8	42	N	0.2282	0.0361	-0.19
DAY 9	44	N	0.1862	0.04123	-0.203
DAY 10	46	N	0.6762	0.004003	-0.06327
DAY 11	42	N	0.056	0.08829	-0.2971
DAY 12	41	Y *	0.0146	0.1435	-0.3788
DAY 13	39	Y **	0.0056	0.1894	-0.4352
DAY 14	40	Y *	0.0496	0.09767	-0.3125
DAY 28	29	N	0.0921	0.1015	-0.3186
Overall	705	Y ****	<0.0001	0.03575	-0.1891

Table 35: Correlation between ADAMTS13 and neutrophil Y levels in severe thermal injuries					
	No.	**correlation (Y/N)**	**P value**	**R^2 value**	**Pearson r**
DAY 1	64	N	0.3657	0.01322	0.115
DAY 2	55	N	0.8461	0.000717	0.02678
DAY 3	60	N	0.128	0.03949	-0.1987
DAY 4	49	N	0.7541	0.002107	-0.0459
DAY 5	54	N	0.111	0.04813	-0.2194
DAY 6	39	N	0.5225	0.01114	0.1056
DAY 7	44	N	0.7983	0.001573	-0.03966
DAY 8	36	N	0.0533	0.1055	-0.3248
DAY 9	39	N	0.0811	0.07997	-0.2828
DAY 10	46	N	0.1388	0.04912	-0.2216
DAY 11	36	Y *	0.0439	0.1141	-0.3378
DAY 12	41	Y **	0.0044	0.1902	-0.4361
DAY 13	33	Y *	0.0291	0.1445	-0.3801
DAY 14	43	Y *	0.0299	0.1099	-0.3315
DAY 28	32	N	0.5229	0.01374	-0.1172
Overall	671	Y ****	<0.0001	0.03302	-0.1817